MICROPLASTIC DEBRIS TRANSPORT IN AN URBAN WATERSHED ACROSS MULTIPLE FLOW CONDITIONS AND ENVIRONMENTAL COMPARTMENTS

Natalie F. Hernandez, B.S.

A Dissertation Presented to the Graduate Faculty of
Saint Louis University in Partial Fulfillment
of the Requirements for the Degree of
Doctor of Philosophy

2025

COMMITTEE IN CHARGE OF CANDIDACY:

Associate Professor Elizabeth A. Hasenmueller,
Chairperson and Advisor

Professor Craig D. Adams

Associate Professor Amanda L. Cox

Professor Jason H. Knouft

John J. Sloan, Watershed Scientist, National Great Rivers Research and Education Center

ACKNOWLEDGEMENTS

I would first like to express my sincere thanks to my advisor Dr. Elizabeth Hasenmueller for her guidance throughout my doctoral research. Her enthusiasm for the research process helped sustain my motivation to keep pursuing new research ideas, and her insight and expectations fostered a deeper understanding of my research topic and strengthened my ability to weave complex datasets into broad, impactful research outcomes. I would also like to thank my dissertation committee members: Dr. Craig Adams, Dr. Amanda Cox, Dr. Jason Knouft, and Dr. John Sloan for supporting my learning through their courses and offering advice to improve my research projects over the past five years.

I am also extremely grateful to have worked with current and former graduate students in the Environmental Geochemistry Lab who taught me foundational field and laboratory skills and learned alongside me: Dr. Teresa Baraza, Dr. Carly Finegan-Dronchi, Emily Persinger, Siobhan Perry, and Luke Ungerer. Special thanks to Dr. Teresa Baraza and Dr. Carly Finegan-Dronchi for their consistent help with fieldwork and feedback on presentations throughout my time in the program and their continued friendship and support.

I greatly appreciate the help of many undergraduate students with field and laboratory work across these research projects. Several long days of field work would not have been possible without Nicole Baumgarten, Ethan Brewer, Hannah Buerk, Grace Dodge, Carly Sear, and Morgan Ward, in addition to Dr. Teresa Baraza, Dr. Carly Finegan-Dronchi, and Sofie Liang, who consistently filled in when others were unable to help. I thank Julia Thiesen for consistent and efficient help with the duplication of research methods. Without the guidance and training of Daisy Youmans from the Brander Lab at Oregon State University and Leo Schrader from the Precision Imaging Research Lab at Saint Louis University, the timely acquisition of

polymer data for this dissertation would not have been possible; I greatly value their expertise and training.

I thank James Faupel, Adam Rembert, and all the staff and volunteers at the Litzsinger Road Ecology Center for their assistance with the long-term field installations necessary for this research. Furthermore, I would like to thank the coordinators of outreach and education programs at the Litzsinger Road Ecology Center, Saint Louis University WATER Institute, Department of Earth, Environmental, and Geospatial Science, and Open Space Council, who consistently work to connect scientists with the local community and inspire environmental awareness and action. Sharing my research with community volunteers and future generations of scientists at these events has been a highlight of my experience in St. Louis and kept me hopeful for future solutions to issues that seem unsolvable today.

I appreciate and acknowledge the funding sources for my doctoral studies and the research presented in this dissertation: Diversity Fellowship awarded by Graduate Education, Saint Louis University (2020); Graduate Student Geoscience Grant #13039-21, awarded by the Geological Society of America and funded by the National Science Foundation Award #1949901 (2021); Graduate Student Geoscience Grant #13688-23, awarded by the Geological Society of America (2023); Small Research Grant, awarded by the Litzsinger Road Ecology Center (2023); Water Resources Research Act Grant #G21AP10582-03, awarded by the United States Geological Survey and administered by the Missouri Water Center (2023); and Dissertation Fellowship awarded by Graduate Education, Saint Louis University (2024). The School of Science and Engineering, WATER Institute, Department of Earth, Environmental, and Geospatial Science, and Graduate Student Association at Saint Louis University provided additional funding for invaluable experiences presenting this research to international audiences.

I would finally like to thank my family and friends, both near and far from the St. Louis area, for always believing in me. Thank you to John Jung for your encouragement during the final steps of this research process. Special thanks to Lynette, whose companionship provided comfort throughout my doctoral program.

TABLE OF CONTENTS

LIST OF TABLES

CHAPTER 2

CHAPTER 3

CHAPTER 4

CHAPTER 5

LIST OF FIGURES

CHAPTER 1

CHAPTER 2

CHAPTER 3

CHAPTER 4

CHAPTER 5

LIST OF ABBREVIATIONS

ABS	Acrylonitrile Butadiene Styrene
ASOS	Automated Surface Observing System
CSO	Combined Sewer Overflow
DEM	Digital Elevation Model
DDI	Distilled Deionized
GIS	Geographic Information System
LOD	Limit of Detection
MO	Missouri
MoDNR	Missouri Department of Natural Resources
MSDIS	Missouri Spatial Data Information Service
MSD	Metropolitan St. Louis Sewer District
NaCl	Sodium Chloride
NCES	National Center for Education Statistics
NLCD	National Land Cover Database
NPDES	National Pollutant Discharge Elimination System
NWS	National Weather Service
PA	Polyamide (nylon)
PE	Polyethylene
PEA	Poly(ethyl acrylate)
PET	Polyethylene Terephthalate
PEVA	Polyethylene Vinyl Acetate
PM	Particulate Matter
PP	Polypropylene
SAN	Styrene Acrylonitrile
SpC	Specific Conductivity
STL	St. Louis ASOS Station
TSS	Total Suspended Solids

USEPA	United States Environmental Protection Agency
USGS	United States Geological Survey
μ-FTIR	Micro-Fourier Transform Infrared

CHAPTER 1: INTRODUCTION

1.1. Background

In recent years, microplastics have become a global focus of research that aims to understand the potential human and ecological health implications of this widespread contaminant suite (Rochman, 2018). These small plastics (1 μm to 5 mm in size) have diverse origins, primary polymers, additives, morphologies, colors, and adsorbed ecotoxins (Frias and Nash, 2019; Rochman et al., 2019). Concerningly, microplastics are ingested by terrestrial and aquatic organisms and can cause both physical (e.g., blockages) and chemical (e.g., exposures to leached toxins, reduced growth, and behavioral changes) impacts (Jeong et al., 2024). In the human body, microplastics have been found in blood, lungs, and other organs (e.g., livers and kidneys) and estimates of exposure to humans via inhalation and ingestion are on the order of hundreds of thousands of these microparticles per year (Cox et al., 2019; Thompson et al., 2024). The footprint of microplastics has touched nearly every part of the planet, with these pollutants having been identified on every continent (Akanyange et al., 2022; Cunningham et al., 2022) and in environments ranging from deep sea sediment (Barrett et al., 2020) to the top of Mount Everest (Napper et al., 2020). Microplastics are therefore an alarming contaminant requiring proper regulation to protect human and ecological health. Researchers and policy makers accordingly need comprehensive evidence regarding the sourcing and transport of microplastics in the environment.

Marine habitats have the largest body of research on microplastic presence and movement due to the origins of the field in the global ocean (Carpenter and Smith, 1972; Rochman et al., 2018). Microplastic fate within freshwater and terrestrial environments is less understood (Rochman et al., 2018) despite freshwater environments acting as key pathways in moving microplastics from terrestrial to marine systems. While freshwater environments have

been increasingly prioritized in research, freshwater research has developed a "size bias" that targets larger rivers and lakes, leaving small-scale systems understudied (Büngener et al., 2024). However, modeling and preliminary field studies indicate that small headwater streams can have longer microplastic retention times than large rivers due to their comparatively low flow, leading to highly contaminated upstream environments (Büngener et al., 2024; Dikareva and Simon, 2019; Drummond et al., 2022). These small freshwater systems therefore warrant further study as longer retention times mean they could serve as a source of legacy contamination far into the future even if microplastic inputs cease.

In urban areas, freshwater systems also receive enhanced inputs of microplastics due to more abundant and potent sources. Higher populations result in more people wearing textiles that can release microfibers into the atmosphere during their wear and into wastewater effluent during their washing (De Falco et al., 2020; Hernandez et al., 2017). Heavily trafficked urban roadways can cause increased emissions of vehicle-related microparticles (e.g., tire wear; Goehler et al., 2022). The high waste generation of urban areas also facilitates the entry of macroplastics (plastics > 5 mm) into the environment both through intentional littering and unintentional mismanagement of waste (Rinasti et al., 2022). Moreover, increased areas of impervious surfaces in cities enhance runoff that can result in urban freshwater systems that have highly variable flow, including rapid (i.e., flashy) discharge responses to precipitation events (O'Driscoll et al., 2010). Macroplastics and microplastics might enter waterways more easily because of this enhanced runoff. Due to their proximity to concentrated sources of microplastic pollution, small urban watersheds serve as interfaces between the contaminant's sources and transport to downstream environments. These systems may also potentially function as both long-term sinks and sources of microplastics during varying flow conditions.

Our knowledge of microplastic contamination in small urban watersheds is nevertheless limited in several dimensions. First, studies are incomplete in their spatial assessments (typically prioritizing longitudinal gradients along single rivers) as well as their temporal assessments (typically considering only 1-2 seasons). They also rarely examine high resolution spatial and temporal scales simultaneously (Range et al., 2023; Talbot and Chang, 2022). Second, studies fail to thoroughly consider the impacts of rapidly changing flow conditions by evaluating systems at high enough temporal resolution to capture discharge peaks (Hitchcock, 2020; Talbot and Chang, 2022). Third, attempts to determine a freshwater bioindicator species for microplastics have thus far focused on larger freshwater systems or marine environments (Su et al., 2018). A bioindicator species could simultaneously indicate the contamination level of its surroundings (e.g., for water or sediment) and provide information about aquatic organism exposure. However, the extent to which proposed bioindicators might function in more variable, small freshwater systems is largely unknown. Fourth, atmospheric deposition is frequently mentioned as a potential influence on freshwater microplastic distribution, but analyses of atmospheric microplastics are rarely incorporated into studies of their dispersal in watersheds (Talbot and Chang, 2022).

The current body of knowledge on microplastic contamination in small urban watersheds is thus lacking, and additional studies that consider these knowledge gaps are needed. Further, microplastics exist within a suite of similar, but not fully plastic, "anthropogenic microparticles," which can include soot, paint flakes, tire and road wear (e.g., microrubbers), and modified fibers of natural origin (e.g., viscose and dyed cotton; Athey and Erdle, 2022; Mattsson et al., 2021). Though non-plastic anthropogenic microparticles are frequently understudied due to their lower environmental persistence compared to their plastic counterparts, these other anthropogenic microparticles can have similar effects on organism health and are frequently found at higher

quantities in a similar range of environments as microplastics (Athey and Erdle, 2022; Kim et al., 2021; Turner, 2021). Accordingly, calls are growing to expand the field by studying these other anthropogenic microparticles (in addition to their more well-known plastic counterparts) to avoid underestimating the true effects of anthropogenic microparticles through a limited focus on only plastics. Additional research is therefore urgently needed on the complex suite of anthropogenic microparticles in small urban watersheds. This research must specifically emphasize understanding multiple compartments and flow conditions across the fluctuating spatiotemporal gradients present in these highly variable freshwater systems.

1.2. Study Objectives

Although the prevalence and potential ecosystem threats of microplastics are well established in larger aquatic systems, more research is needed to advance our understanding of their spatial and temporal fluctuations in small urban watersheds. These variations are not currently understood for the full suite of anthropogenic microparticles (including microplastics, semi-synthetic and non-plastic microfibers, paint flakes, and tire and road wear materials) across multiple environmental compartments and through the highly variable flow conditions that are found in small urban freshwater systems. Thus, the objectives of this research are to (1) assess the partitioning of anthropogenic microparticle debris between sediment and water over the spatially and temporally variable conditions present in a small urban catchment, (2) determine the impacts of short-term flood events on the sourcing, extent, and timing of anthropogenic microplastic debris transport in the selected stream, (3) evaluate the potential of the Asian clam, *Corbicula fluminea* (*C. fluminea*), as a bioindicator of anthropogenic microparticle fluctuation in the urban stream environment, and (4) characterize anthropogenic microparticles in the atmospheric deposition of a humid subtropical city.

1.3. Study Area

The outlined objectives were completed in this dissertation through a series of studies in the Deer Creek watershed, which is located near St. Louis, Missouri, United States. Deer Creek is a 95.8 km^2 urban watershed, containing 99.8% developed land (Fig. 1.1.; Dewitz, 2023). The Deer Creek catchment drains into the Mississippi River via the River des Peres, with the system therefore having implications for pollutant transport downstream to the Gulf of Mexico. Moreover, the Deer Creek watershed has been the subject of remediation efforts following bacterial and Cl^- contamination from urban land uses, historic sewer overflows, and road salting efforts (MoDNR, 2022; MSD, 2025a; MSD, 2025b) as well as research concerning its dangerous flash flooding (Criss et al., 2022). Deer Creek is thus an ideal location to study anthropogenic microparticle fluxes in a small-scale watershed impacted by common concerns for urban freshwater environments.

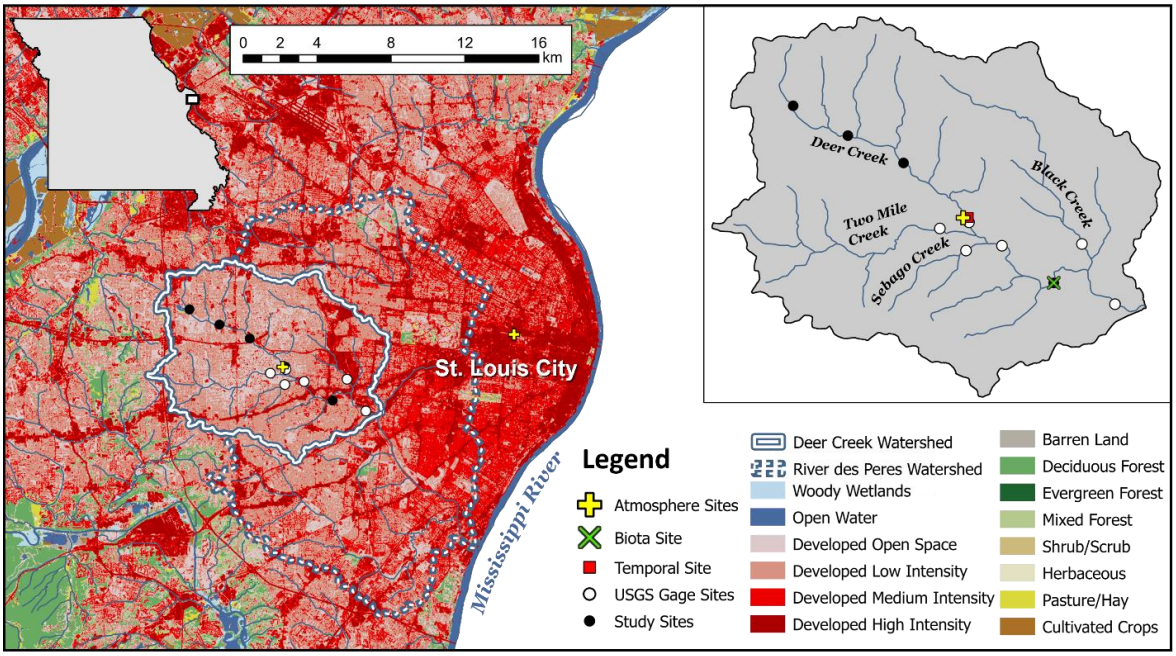

Figure 1.1. *The sampling sites for all the dissertation projects on a land cover map of the St. Louis, Missouri, United States, area (NLCD 2021; Dewitz, 2023). Note that the white filled circles indicate study sites that are collocated with United States Geological Survey (USGS) stage and discharge gage stations. One high resolution atmospheric sample site is located*

outside of the basin at Saint Louis University. The inset watershed map contains additional details about the high resolution spatial, temporal, biota, and atmosphere sample sites.

1.4. Outline of the Dissertation Chapters

The goal of this dissertation is to thoroughly characterize the transport of anthropogenic microparticle (including microplastic) debris in a small urban watershed across multiple environmental compartments (e.g., the water, sediment, biota, and atmosphere) and multiple flow conditions (from baseflow to flooding). This introductory chapter (Chapter 1) explained the background for the research focus, including the current body of work on microplastics in freshwater systems and the needs for further research. Chapter 2 characterizes spatial and temporal trends in anthropogenic microparticle fluctuations within the selected small urban watershed over a 1-year sampling campaign across 10 sites. Chapter 3 identifies the impacts of flow conditions in facilitating the export of anthropogenic microparticles from the small urban stream to downstream environments. Chapter 4 clarifies the efficacy of *C. fluminea* as a bioindicator for anthropogenic microparticles in the urban watershed. Chapter 5 quantifies the atmospheric deposition of anthropogenic microparticles in the surrounding urban environment over a 1-year period. Finally, Chapter 6 summarizes the key findings of this research and provides recommendations for further work.

1.5. References

Akanyange, S.N., Zhang, Y., Zhao, X., Adom-Asamoah, G, Ature, A.A., Anning, C., Tianpeng, C., Zhao, H., Lyu, X., Crittenden, J.C., 2022. A holistic assessment of microplastic ubiquitousness: Pathway for source identification in the environment. Sustain. Prod. Consum. 33, 113-145.

Athey, S.N., Erdle, L.M., 2022. Are we underestimating anthropogenic microfiber pollution? A critical review of occurrence, methods, and reporting. Environ. Toxicol. Chem. 41(4), 822-837.

Barrett, J., Chase, Z., Zhang, J., Holl, M.M.B., Willis, K., Williams, A., Hardesty, B.D., Wilcox, C., 2020. Microplastic pollution in deep-sea sediments from the Great Australian Bight. Front. Mar. Sci. 7, 576170.

Büngener, L., Schäffer, S., Schwarz, A., Shwalb, A., 2024. Microplastics in a small river: Occurrence and influencing factors along the river Oker, Northern Germany. J. Contam. Hydrol. 264, 104366.

Carpenter, E.J., Smith, K.L., 1972. Plastics on the Sargasso Sea surface. Science. 175(4027), 1240-1241.

Cox, K.D., Covernton, G.A., Davies, H.L., Dower, J.F., Juanes, F., Dudas, S.E., 2019. Human consumption of microplastics. Environ. Sci. Technol. 53, 7068-7074.

Criss, R.E., Stein, E.M., Nelson, D.L., 2022. Generation and propagation of an urban flash flood and our collective responsibilities. J. Earth Sci. 33(6), 1624-1628.

Cunningham, E.M., Seijo, N.R., Altieri, K.E., Audh, R.R., Burger, J.M., Bornman, T.G., Fawcett, S., Gwinnett, C.M.B., Osborne, A.O., Woodall, L.C., 2022. The transport and fate of microplastic fibres in the Antarctic: The role of multiple global processes. Front. Mar. Sci. 9:1056081.

De Falco, F., Cocca, M., Avella, M., Thompson, R.C., 2020. Microfiber release to water, via laundering, and to air, via everyday use: A comparison between polyester clothing with differing textile parameters. Environ. Sci. Technol. 54, 3288-3296.

Dewitz, J., 2023. National Land Cover Database (NLCD) 2021 Products: United States Geological Survey data release.

Dikareva, N., Simon, K.S., 2019. Microplastic pollution in streams spanning an urbanization gradient. Environ. Pollut. 250, 292-299.

Drummond, J.D., Schneidewind, U., Li, A., Hoellein, T.J., Krause, S., Packman, A.I., 2022. Microplastic accumulation in riverbed sediment via hyporheic exchange from headwaters to mainstems. Sci. Adv. 8, eabi9305.

Frias, J., Nash, R., 2019. Microplastics: Finding a consensus on the definition. Mar. Poll. Bull. 138, 145-147.

Goehler, L.O., Moruzzi, R.B., Da Conceiçao, F.T., Júnior, A.A.C., Speranza, L.G., Busquets, R., Campos, L.C., 2022. Relevance of tyre wear particles to the total content of microplastics transported by runoff in a high-imperviousness and intense vehicle traffic urban area. Environ. Pollut. 314, 120200.

Hernandez, E., Nowack, B., Mitrano, D.M., 2017. Polyester textiles as a source of microplastics from households: A mechanistic study to understand microfiber release during washing. Environ. Sci. Technol. 51, 7036-7046.

Hitchcock, J.N., 2020. Storm events as key moments of microplastic contamination in aquatic ecosystems. Sci. Total Environ. 734, 139436.

Jeong, E., Lee, J., Redwan, M., 2024. Animal exposure to microplastics and health effects: A review. Emerg. Contam. 10(4), 100369.

Kim, L., Kim, S.A., Kim, T.H., Kim, J., An, Y., 2021. Synthetic and natural microfibers induce gut damage in the brine shrimp *Artemia franciscana*. Aquat. Toxicol. 232, 105748.

Mattsson, K., Da Silva, V.H., Deonarine, A., Louie, S.M., Gondikas, A., 2021. Monitoring anthropogenic particles in the environment: Recent developments and remaining challenges at the forefront of analytical methods. Curr. Opin. Colloid Interface Sci. 56, 101513.

Metropolitan St. Louis Sewer District (MSD)., 2025a. "Deer Creek Sanitary Tunnel." Project Clear. https://msdprojectclear.org/projects/tunnels/deer-creek-sanitary-tunnel/. Accessed March 01, 2025.

Metropolitan St. Louis Sewer District (MSD)., 2025b. Sewer overflow locations map "sewer overflow locations as of June 30, 2018". https://msdprojectclear.org/customers/problems-tips/sewer-overflows/. Accessed March 01, 2025.

Missouri Department of Natural Resources (MoDNR), 2022. "2022 Section 303(d) listed waters: proposed list for public notice on October 13, 2022". https://dnr.mo.gov/document-search/2022-epa-approved-section-303d-listed-waters. Accessed April 03, 2025.

Napper, I.E., Davies, B.F.R., Clifford, H., Elvin, S., Koldewey, H.J., Mayewski, P.A., Miner, K.R., Potocki, M., Elmore, A.C., Gajurel, A.P., Thompson, R.C., 2020. Reaching new heights in plastic pollution—Preliminary findings of microplastics on Mount Everest. One Earth. 3, 621-630.

O'Driscoll, M., Clinton, S., Jefferson, A., Manda, A., McMillan, S., 2010. Urbanization effects on watershed hydrology and in-stream processes in the Southern United States. Water, 2(3), 605-648.

Range, D., Scherer, C., Stock. F., Ternes, T.A., Hoffmann, T.O., 2023. Hydro-geomorphic perspectives on microplastic distribution in freshwater river systems: A critical review. Water Res. 245, 120567.

Rinasti, A.N., Ibrahim, I.F., Gunasekara, K., Kottatep, T., Winijkul, E., 2022. Fate identification and management strategies of non-recyclable plastic waste through the integration of material flow analysis and leakage hotspot modeling. Nat. Sci. Rep. 12, 16298.

Rochman, C.M., 2018. Microplastics research — From source to sink in freshwater systems. Science, 360(6384), 28-29.

Rochman, C.M., Brookson, C., Bikker, J., Djuric, N., Earn, A., Bucci, K., Athey, S., Huntington, A., McIlwraith, H., Munno, K., De Frond, H., Kolomijeca, A., Erdle, L., Grbic, J., Bayoumi, M., Borrelle, S.B., Wu, T., Santoro, S., Werbowski, L.M., Zhu, X., Giles, R.K., Hamilton, B.M., Thaysen, C., Kaura, A., Klasios, N., Ead, L., Kim, J., Sherlock, C., Ho, A., Hung, C., 2019. Rethinking microplastics as a diverse contaminant suite. Environ. Toxicol. Chem. 38(4), 703-711.

Su, L., Huiwen, C., Kolandhasamy, P., Wu, C., Rochman, C.M., Shi, H., 2018. Using the Asian clam as an indicator of microplastic pollution in freshwater ecosystems. Environ. Pollut. 234, 347-355.

Talbot, R., Chang, H., 2022. Microplastics in freshwater: A global review of factors affecting spatial and temporal variations. Environ. Pollut. 292(B), 118393.

Thompson, R.C., Courtene-Jones, W., Boucher, J., Pahl, S., Raubenheimer, K., Koelmans, A.A., 2024. Twenty years of microplastic pollution research—What have we learned? Science, 386: eadl2746.

Turner, A., 2021. Paint particles in the marine environment: An overlooked component of microplastics. Water Res. X. 12, 100110.

CHAPTER 2: SPATIOTEMPORAL VARIATION OF ANTHROPOGENIC MICROPARTICLES (INCLUDING MICROPLASTICS) IN THE SEDIMENT OF A SMALL URBAN WATERSHED

2.1. Abstract

The drivers of spatiotemporal fluctuation in anthropogenic microparticles (including microplastics) remain poorly understood in small watersheds due to a historical research focus on marine environments and larger freshwater systems. Small urban streams are a key interface between urban sources of microplastics and downstream habitats. We thus assessed anthropogenic microparticle quantities and types in stream water and sediment across a small urban watershed in St. Louis, Missouri, United States, over 1 year. Most water samples (98%) had anthropogenic microparticle levels that were below our method detection limit, preventing our assessment of their spatial and temporal fluctuations in the stream water. In contrast, 92% of sediment samples from the streambed contained detectable quantities of anthropogenic microparticles that reached concentrations up to 188.6 counts/kg. Microfibers were the most common anthropogenic microparticle morphology in both sample types. The spatial attributes of the sampling sites, like the distance from the stream's outlet and number of nearby point sources of pollution, best explained the observed increases in sediment anthropogenic microparticle levels from upstream to downstream in the watershed. However, sediment samples collected in the summer months had unique spatial distributions across the watershed that generally demonstrated less variability among our sampling sites. No clear relationships were present between the observed sediment anthropogenic microparticle fluctuations over time and variations in the stream's hydrology or physicochemical characteristics. Our results suggest that the watershed's spatial attributes are stronger indicators of anthropogenic microparticle distribution in the bed sediment than fluctuating temporal conditions. Sampling anthropogenic microparticle

distributions across multiple seasons is nonetheless vital as the extrapolation of spatial patterns at a single point in time might be a poor representation of the overall drivers of their dispersal across a watershed.

2.2. Introduction

Microplastics (plastics < 5 mm) have gained notoriety in recent years as prevalent global contaminants with potentially harmful impacts on human and ecological health (Thompson et al., 2024). In freshwater systems, microplastics have historically been understudied due to the field's inception in and original focus on marine environments (Carpenter and Smith, 1972; Rochman, 2018). As the study of microplastics in freshwater systems has become more common, the research focus is still often narrowed to larger rivers and lakes (Dikareva and Simon, 2019; Rochman, 2018). However, both modeling and limited field studies suggest that retention time for microplastics might be higher in headwater streams, leading to highly polluted environments in these smaller hydrologic systems (Dikareva and Simon, 2019; Drummond et al., 2022; Kabir et al., 2022).

Correspondingly, small urban streams are both retention points and interfaces between highly populated landscapes (that may be major sources of microplastic emissions) and downstream freshwater systems. In high population areas, microfibers might be continuously released into the atmosphere from wearing textiles (De Falco et al., 2020) and into waterways from wastewater effluents that are rich in these microparticles due to textile laundering (Hernandez et al., 2017). Plastics enter and accumulate in the environment as litter or unintentionally leaked waste in cities, where they can subsequently degrade into smaller microplastics and nanoplastics (Alencar et al., 2022). Microplastics from vehicle wear can also be prevalent in major cities that are typically high traffic areas (Goehler et al., 2022).

Furthermore, higher levels of impervious surface area from urbanization can facilitate the entry of microplastics into waterways as decreased infiltration enhances surface runoff.

Despite their vital role as interfaces between pollution sources and downstream environments, smaller urban freshwater systems have rarely been the subject of detailed spatiotemporal assessments of microplastic pollution (Fan et al., 2022). Many studies focus on longitudinal gradients (i.e., upstream to downstream) or seasonal variations (e.g., examination of one sample per 2-4 seasons), but higher resolution spatial and temporal studies are both less common for freshwater catchments (Range et al., 2023). These long-term, higher resolution investigations may be less frequently conducted due to the time-consuming nature of microplastic analysis for large quantities of samples. However, improved understanding of spatiotemporal variation in microplastics across small urban headwater systems is necessary. Due to their upstream positioning and possible enhanced retention of pollutants, these smaller hydrologic settings might be key locations where implementation of filtration systems or other remediation efforts can have the greatest benefit to reduce downstream microplastic concentrations.

To improve our understanding of spatiotemporal microplastic variation in freshwater systems, a small urban watershed was investigated over a 1-year period in this study. In addition to microplastics, we examined other anthropogenic microparticles (e.g., modified cotton microfibers), which are common in the region (see Chapters 4 and 5) and have potential deleterious impacts on ecosystem health that are similar to microplastics (Athey and Erdle, 2022; Kim et al., 2021). We assessed these long-term spatiotemporal distributions of microplastics and other anthropogenic microparticles in both water and sediment across our selected watershed.

2.3. Materials and Methods

2.3.1. Study Area

Our selected study site was the Deer Creek watershed near St. Louis, Missouri, United States. Deer Creek drains 95.8 km^2 of 99.8% urban land into the Mississippi River via the River des Peres (Fig. 2.1. (A); Dewitz, 2023). Ten sites along Deer Creek and three of its tributaries were selected for representative sampling across the catchment (Fig. 2.1.). When possible, sampling sites were collocated with United States Geological Survey (USGS) gage stations to allow for the acquisition of discharge data for comparison to our measured anthropogenic microparticle quantities. The rest of the sites were evenly distributed along the remainder of the mainstem of Deer Creek. Some reaches of the stream fall along a border between limestone and shale lithology, resulting in historic (i.e., mostly filled) sinkholes along the main channel in the lower and middle portions of the watershed (Fig. 2.1. (B); MoDNR, 2020; MSDIS, 2019).

While the entire watershed features developed land, individual sites have unique land use characteristics (Fig. 2.1. (C)). These attributes include sites in largely industrial/commercial areas (sites A-C), a site bordering an active demolition landfill (site D), sites near lower intensity residential areas, parks, or schools (sites E, H-J), a site on a golf course (site F), and a site located in restored natural forest and prairie lands (site G; Fig. 2.1. (C)). Sewer overflows, which can be point sources of microplastic pollution, were historically prevalent along the Deer Creek mainstem and Black Creek tributary (MSD, 2025; Zhou et al., 2023). Many of these overflows have been removed, but outfalls for combined sewer overflows (CSOs), stormwater, and process water (largely from golf courses) are still present in the watershed, particularly along Black Creek and its tributaries (Fig. 2.1. (C)).

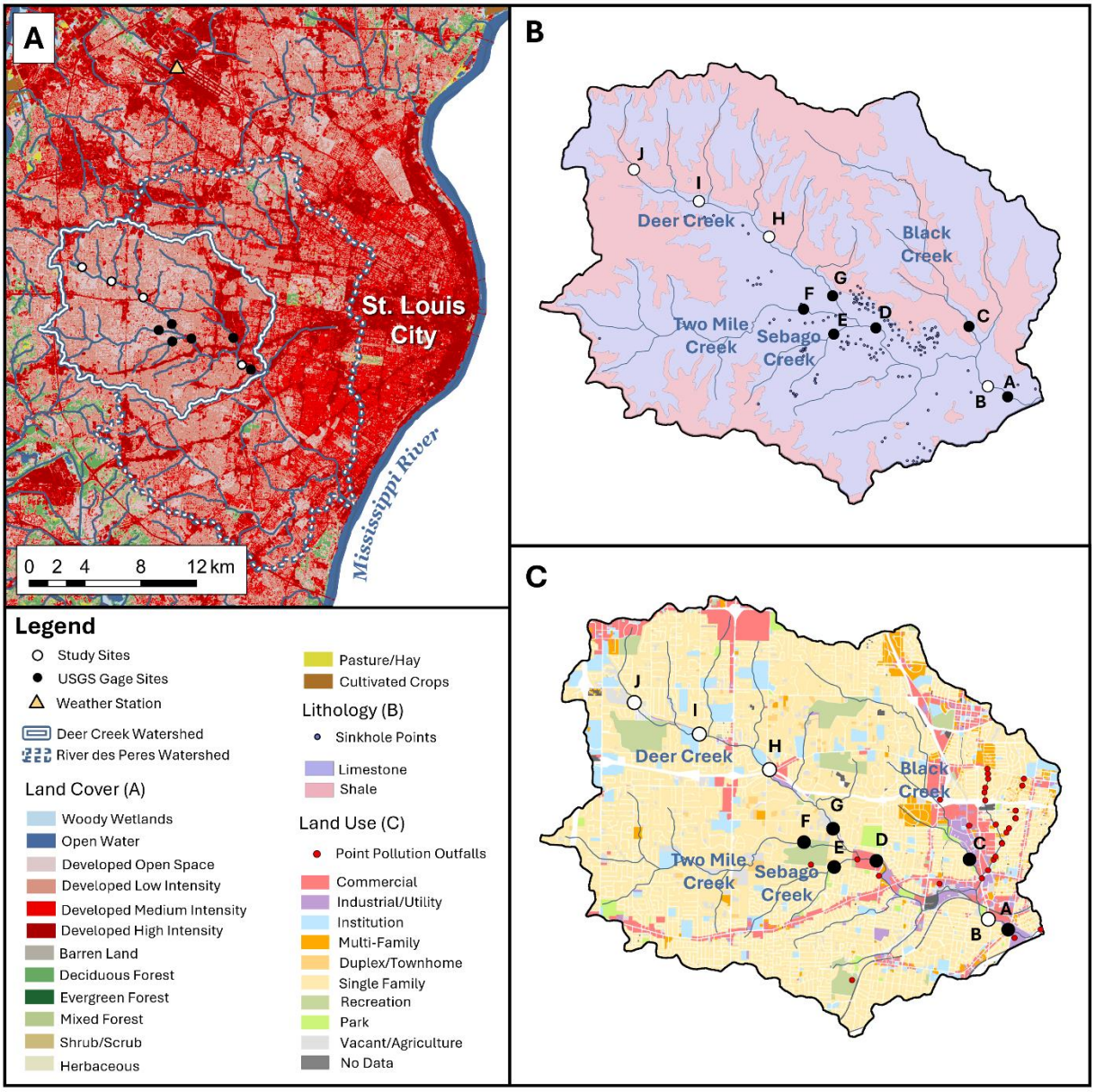

Figure 2.1. *(A) The Deer Creek watershed, our sampling sites (with those collocated with USGS gage sites indicated), and the weather station on a land cover map of the St. Louis region (Dewitz et al., 2023; IEM, 2025). (B) Lithology of the Deer Creek watershed, including suspected sinkhole locations and labelled study sites (MoDNR, 2020; MSDIS, 2019). (C) Land use within the Deer Creek watershed, including point data for outfalls from the United States Environmental Protection Agency's (USEPA) National Pollutant Discharge Elimination System (NPDES) permits (MoDNR, 2021; Saint Louis County GIS Service Center, 2021) and labelled study sites.*

2.3.2. Sample Collection

All ten sites in Deer Creek were visited monthly for 1 year (November 2021 through October 2022; see Table 2.S1. for the sample dates) during baseflow conditions (i.e., > 3 days since the last precipitation event) to collect water and sediment samples for anthropogenic microparticle analysis, with sample collection progressing from the downstream to upstream monitoring locations. Water grab samples (~ 2 L; n = 120) were obtained with two 1-L amber glass bottles that had been triple rinsed with filtered distilled deionized (DDI) water then triple rinsed with stream water before the water samples were attained. Sediment samples (~ 1 kg; n = 120) were collected from the streambed using a custom 74-80 µm mesh Hess sampler into 1-L glass jars (a detailed explanation of this method is provided in Hernandez and Hasenmueller, 2024). Each sediment sample was a homogenization of subsamples taken at three points evenly spaced across the channel width, which was performed to account for intra-site variability. The stream water depth was measured at each subsampling site.

Weekly water samples (n = 39) and biweekly sediment samples (n = 18) were collected throughout the study period using the same methods at a mid-watershed site (site G; Fig. 2.1.; see Table 2.S1. for the sample dates). This sampling regime at site G was used to assess variations in anthropogenic microparticles in the two environmental compartments at higher temporal resolution. The weekly sampling protocol had no strict requirement of baseflow discharge, though the samples were generally obtained at low flow conditions. Since site G was also visited during the monthly sampling events, we collected a total of 51 water samples and 30 sediment samples from the site throughout the year-long study period. On every sampling occasion, an additional sample of stream water was acquired for analysis of total suspended solids (TSS) using polyethylene (PE) bottles that were triple rinsed in filtered DDI water, then triple rinsed with stream water.

2.3.3. Anthropogenic Microparticle Characterization

2.3.3.1. Environmental samples

To characterize anthropogenic microparticles in our two environmental sample types, water samples were directly vacuum-filtered using an all-glass apparatus, while the sediment samples (~ 250 g subsets) were dried and density separated with a sodium chloride (NaCl) solution, then the supernatant was vacuum-filtered in the same manner as the water samples. The full density separation process for the sediment is described in Hasenmueller et al. (2023). Each filter was then visually inspected for humanmade microparticles, which were defined as "anthropogenic" if they had no organic structures, no tapering fibers, resistance to breakage, and synthetic colors (i.e., obviously dyed colors were presumed to be anthropogenic). These anthropogenic microparticles were photographed and characterized by their morphology (e.g., fiber, film, or fragment), size (i.e., length measured along their longest axis), and color. Because no further analysis of material type was performed, these microparticles are referred to as "anthropogenic microparticles", although microplastics are expected to comprise a portion of the total anthropogenic microparticles identified. Indeed, ~ 9% of the anthropogenic microparticles in sediment at site B (n = 37) were analyzed with micro-Fourier Transform Infrared (μ-FTIR) spectroscopy, and plastic material types made up 51% of the anthropogenic microparticles in this subsample (see Chapter 4).

2.3.3.2. Quality assurance and quality control measures

To avoid contamination of the environmental samples by ambient anthropogenic microparticles, several quality assurance and quality control practices were employed for our study. All surfaces in the laboratory were wiped down three times and glassware was triple rinsed with filtered DDI water before any sample handling. Glassware openings were covered with aluminum (Al) foil when samples were not actively being processed to avoid anthropogenic

microparticle contamination through deposition from the ambient air in the laboratory. The filtration and density processing steps for the environmental samples were performed inside a fume hood. Throughout sample processing, 100% cotton and bright-colored attire was worn to facilitate identification of contamination from clothing.

Field and laboratory blanks were collected and examined to account for contamination in the environmental samples. Field blanks were taken during 10 of the 12 monthly sampling events at site G (i.e., the mid-watershed site), except for one field blank taken at site H in July 2021. Field water blanks consisted of 2-L of filtered DDI water stored in two clean 1-L amber glass bottles poured into two new and clean 1-L amber glass bottles on-site. Laboratory blanks for water consisted of bottles of filtered DDI water that were processed through the vacuum-filtration system alongside field samples, with 10 laboratory water blanks collected throughout the project. Sediment laboratory blanks were obtained by processing the NaCl solution in the same series of separation and filtration steps as the sediment samples, with six laboratory sediment blanks collected throughout the project. From our full suite of blanks, a limit of detection (LOD) was calculated as the average of all blanks for a respective sample type plus three times the standard deviation of the blanks. The compartment LODs were calculated with total numbers of anthropogenic microparticles per sample and rounded to a whole number (see Table 2.S2.). Any sample with a total count of anthropogenic microparticles that was below the LOD value for that type of environmental compartment was reported as containing zero anthropogenic microparticles.

To assess the variability of the environmental samples, field replicates were taken during both the watershed-wide and high frequency sampling events. However, the data for the water replicates are unreported as all their values were below the LOD. For the sediment, we collected a second homogenization of the same three points across the stream channel that were obtained

for the first sample. In total, we collected 18 of these field sediment replicates, with 14 acquired during the monthly sampling across nine of the sites and four acquired during the biweekly sampling at site G. Field replicate results were averaged for the final value for samples that featured replication. If one replicate was above the LOD, but the average of both replicates resulted in a total anthropogenic microparticle number below the LOD, the reported sample value was corrected to zero anthropogenic microparticles.

To determine how well the homogenization of sediment at three points across the streambed represented cross-channel variation, separate (i.e., non-homogenized) sediment samples of ~ 1 kg at each of the three points across the stream channel were taken as cross-channel subsamples to compare to the homogenized sediment samples. These cross-channel subsamples were obtained on eight occasions during the monthly sampling campaigns at five of the sites (n = 24 subsamples) and three times during biweekly sampling campaigns at site G (n = 9 subsamples). These separate subsamples are not averaged into the reported values for their associated homogenized sediment samples.

2.3.4. Collection of Additional Physicochemical Data for the Stream

In situ monitoring of water physicochemical parameters (e.g., temperature, specific conductivity, and chloride (Cl^-)) was performed using a handheld YSI Professional Plus Multiparameter Instrument. Additional water samples were analyzed for total suspended solids (TSS) following United States Environmental Protection Agency (USEPA) Method 160.2 (USEPA, 1971). We analyzed sediment grain size (n = 120) for the monthly sediment samples across all the watershed sites using the sediment that remained after the ~ 250 g subsample for anthropogenic microplastic analysis had been removed (the grain size analysis method is described in detail in Hasenmueller et al., 2023). For the six sites collocated with USGS gaging stations (i.e., gage numbers 07010086, 07010075, 07010055, 07010082, 07010070, and

07010061), discharge data were collected throughout the study period (USGS, 2025). Hourly precipitation data were acquired from an Automated Surface Observing System unit located at the St. Louis Lambert International Airport. These precipitation data were downloaded from a historical data archive (Iowa Environmental Mesonet (IEM), 2025).

2.3.5. Data Analysis

The percentage of developed land for each subwatershed draining to a given sample site was calculated using the methods of Lockmiller et al. (2019) and data from the National Land Cover Database (Dewitz, 2023; NLCD, 2019). The number of point source pollution inputs in a 2-km radius buffer around each sampling site was calculated using data from the USEPA National Pollutant Discharge Elimination System (NPDES) permits (MoDNR, 2021). Since outfall remediation has been ongoing in the watershed, NPDES data might contain some historical outfalls that could have contributed to legacy pollution in addition to outfalls which were active at the time of sampling. Statistical relationships among the data were tested using nonparametric Spearman's rank correlations and pairwise Wilcoxon tests (with $\alpha = 0.05$). All statistical analyses were performed in R and Microsoft Excel. Figures were created using ArcGIS Pro Version 3.0.3, R, and Microsoft Excel.

2.4. Results

2.4.1. Sample Conditions and Representativeness

All the monthly spatial samples were taken from the watershed at least 3 days since the last rainfall event and thus reflected the seasonal baseflow discharge. Discharge at the mid-watershed site G for these monthly samples ranged 0.0-0.11 m^3/s (Table 2.S1.). The highest discharge during monthly sampling occurred in February 2022, when snowfall occurred 2 days prior to the sampling event and the stream's discharge was consequently elevated slightly from baseflow due to snowmelt (Table 2.S1.). For the higher temporal resolution samples at site G, some sampling dates occurred when precipitation had happened within the past 24 h, with the highest observed discharge of 0.80 m^3/s occurring in March 2022 (Table 2.S1.). While all the temporal samples were taken during relatively low flow conditions (i.e., < 1 m^3/s), they included sampling events during the return to low flow after high-magnitude discharge events (e.g., the record-breaking July 2022 flood event (Criss et al., 2022; Table 2.S1.). The water quality parameters varied most in winter months when road deicing activities elevated the stream's specific conductivity and TSS values (Table 2.S1.).

The field replicates that homogenized sediment across three points in the channel (Fig. 2.S1.; Fig. 2.S2.) and the separate subsamples (i.e., non-homogenized) that individually compared the three channel sampling points (Fig. 2.S2.; Fig. 2.S3.) were taken to determine the representativeness of the homogenized sediment sampling method. The average percentage difference between field replicates and the corresponding initial homogenized sediment samples was 32%, with the greatest differences occurring when one replicate was below the LOD and the other was above the LOD (which happened on three occasions). The average of the three individual (i.e., non-homogenized) sediment samples taken across the channel was within

30 counts/kg of the cooccurring homogenized composite sample, with one exception in February 2022 (Fig. 2.S2.; Fig. 2.S3.). Winter months (December through February) typically had the largest differences between the three individual samples across the channel and their corresponding homogenized samples (Fig. 2.S2.; Fig. 2.S3.).

The anthropogenic microparticle distribution across the stream channel did not seem to be related to the attributes of the channel's profile at a given site, with neither deeper nor shallower portions of the channel consistently exhibiting elevated anthropogenic microparticle levels (Fig. 2.S3.). The dominant anthropogenic microparticle make up (i.e., > 50% black, blue, and/or clear fibers) was typically comparable between the field replicates, but less common anthropogenic microparticle attributes (e.g., unique colors) were often not shared between the field replicates (Fig. 2.S1.). While the cross-channel variations of a particular sampling site cannot be accurately represented without more comprehensive sampling, we found that our homogenization approach represented the overall anthropogenic microparticle quantities and characteristics at a given site by smoothing differences across the stream channel.

2.4.2. Anthropogenic Microparticle Content in Stream Water and Sediment

Across the monthly watershed baseflow samples (n = 120 each for water and sediment), only 2% of water samples (n = 2) were above the LOD, while 92% of sediment samples had detectable anthropogenic microparticle levels (n = 110; Table 2.S3.). Monthly water samples had an average and standard deviation of 0.1 ± 0.5 counts/L, while monthly sediment samples were 61.9 ± 39.9 counts/kg (Table 2.S3.). None of the weekly site G (i.e., mid-watershed) water samples (n = 39) were above the LOD, even though these samples spanned a slightly wider range of hydrologic conditions than the monthly samples across the watershed. In contrast, 67% (n = 12) of the biweekly mid-watershed sediment samples (total n = 18) were above the LOD (Table 2.S1.). These biweekly sediment samples at site G contained 22.5 ± 23.2 counts/kg,

and, across all samples from site G (n = 30, including monthly samples), the sediment contained 35.6 ± 33.4 counts/kg (Table 2.S1.). The only site with anthropogenic microparticles above the LOD in water was site E (Sebago Creek) in December 2021 (which featured the maximum observed value of 4.1 counts/L) and September 2022. The maximum quantity of anthropogenic microparticles identified in sediment was 188.6 counts/kg at site B in February 2022 (Table 2.S3.).

Clear and blue fibers were consistently the most common anthropogenic microparticles identified in the baseflow spatial water samples (respectively 40% and 47% of n = 15 anthropogenic microparticles), watershed-wide sediment samples (respectively 50% and 30% of n = 1779 anthropogenic microparticles), and biweekly sediment samples taken at site G (respectively 35% and 27% of n = 99 anthropogenic microparticles, not including the monthly samples at site G; Fig. 2.2.). The average and standard deviation of the sediment anthropogenic microparticle sizes in the monthly samples across the watershed and biweekly samples at site G were 1352.4 ± 880.9 µm, while the average and standard deviation of the water anthropogenic microparticles sizes from monthly spatial samples across the watershed were 1166.2 ± 651.3 µm (the weekly water samples at site G were all below the LOD and thus were not included in this calculation).

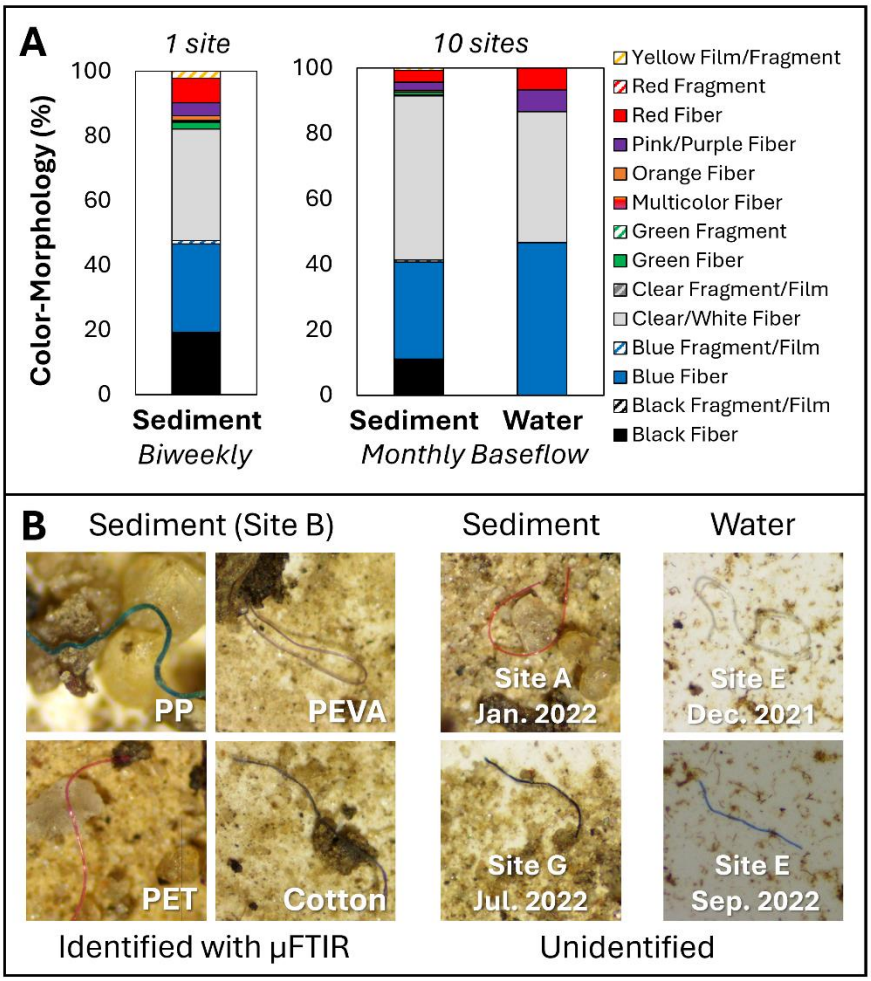

Figure 2.2. *(A) The characteristics of anthropogenic microparticles in biweekly mid-watershed sediment samples (left) and across the 10-site monthly watershed-wide samples in sediment (middle) and water (right). (B) Images of anthropogenic microparticles from site B sediment samples that were identified with μ-FTIR in Chapter 4 (left) and from site A and G sediment samples and site E water samples that have not been characterized for material types (right) are provided. The photo sizes are all 1 mm by 1 mm for scale.*

2.4.3. Spatial Trends in Anthropogenic Microparticles in Stream Sediment

Anthropogenic microparticle concentrations increased downstream in the watershed, having their highest averages at site A (92.6 ± 42.7 counts/kg), site B (85.0 ± 53.1 counts/kg), and site C (79.3 ± 32.5 counts/kg; Fig. 2.3.; Table 2.S3.). On a monthly basis, the highest anthropogenic microparticle level always occurred in one of the five downstream-most sites (most commonly at site A or site B; Table 2.S3.). Unique spatial profiles occurred in the spring

months (e.g., May 2022, when the highest anthropogenic microparticle levels occurred in mid-watershed site E) and summer months (e.g., in June 2022 and July 2022, when relatively low levels of anthropogenic microparticles were observed across all sites; Fig. 2.S4.). Via pairwise Wilcoxon tests, downstream site A, site B, site C, and site E had significantly higher anthropogenic microparticle content in the sediment than upstream site I and site J (Table 2.S4.).

The strongest explanatory variable for the spatial distribution of anthropogenic microparticles in Deer Creek sediment was river kilometer values (i.e., the distance from each site to the outlet), which were strongly, significantly, and negatively correlated with sediment anthropogenic microparticle values averaged by site (Spearman's ρ = -0.97; Fig. 2.3. (C)). The number of nearby point source pollution outfalls had a significant and positive correlation with sediment anthropogenic microparticles at each site (Spearman's ρ = 0.73; Fig. 2.3. (C)). However, the percentage of developed land in each subwatershed had no correlation with anthropogenic microparticle distribution in the sediment across the Deer Creek watershed. Anthropogenic microparticle content in sediment across the basin sites was typically higher when sediment grain sizes were smaller (which was assessed through d_{10}, d_{25}, and d_{50} values), but none of these trends were significant (Fig. 2.S5). We found no significant differences in the proportions of fiber versus non-fiber or colorless versus colored anthropogenic microparticles by site (Fig. 2.S6.) as anthropogenic microparticle characteristics in the sediment were similar across the watershed.

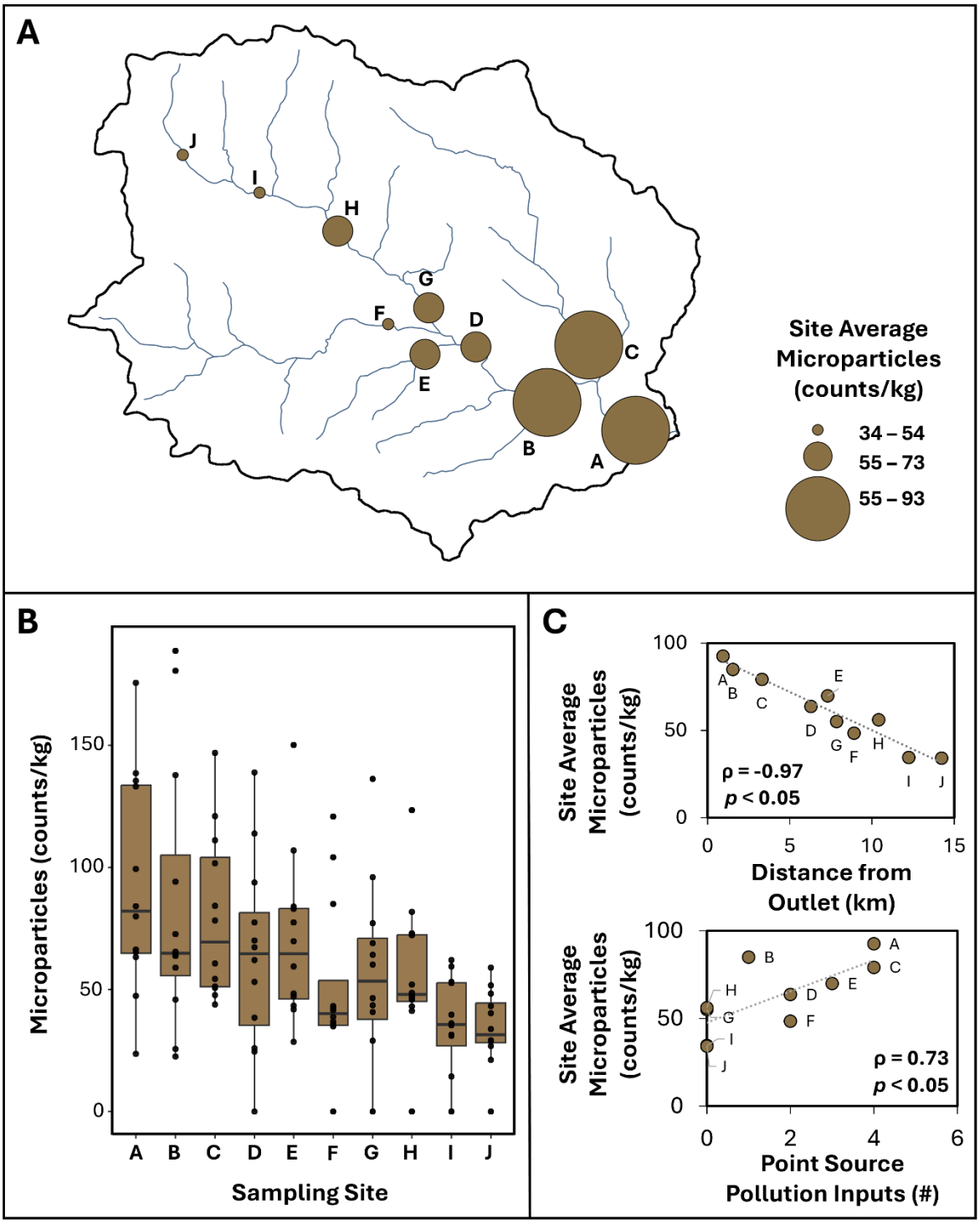

Figure 2.3. *(A) The average anthropogenic microparticle values for the monthly spatial sediment samples across Deer Creek on a watershed map. (B) The distribution of anthropogenic microparticle concentrations for the sediment samples at each site for the 12 monthly sampling events. (C) Comparisons of average anthropogenic microparticle content at each site with the site's distance from the outlet and point source pollution inputs.*

2.4.4. Temporal Trends in Anthropogenic Microparticles in Stream Sediment

Sediment anthropogenic microparticle concentrations and variability were highest across the 10 watershed sites in all the winter months and some spring months, but these values decreased in the late spring and early summer (Fig. 2.4.). Using pairwise Wilcoxon tests, we found that no month had significantly higher or lower levels of anthropogenic microparticles in the sediment than any other month. We also saw no significant differences in the proportions of fiber versus non-fiber or colorless versus colored anthropogenic microparticles by month (Fig. 2.S7.) as anthropogenic microparticle characteristics in the sediment were similar across the study period.

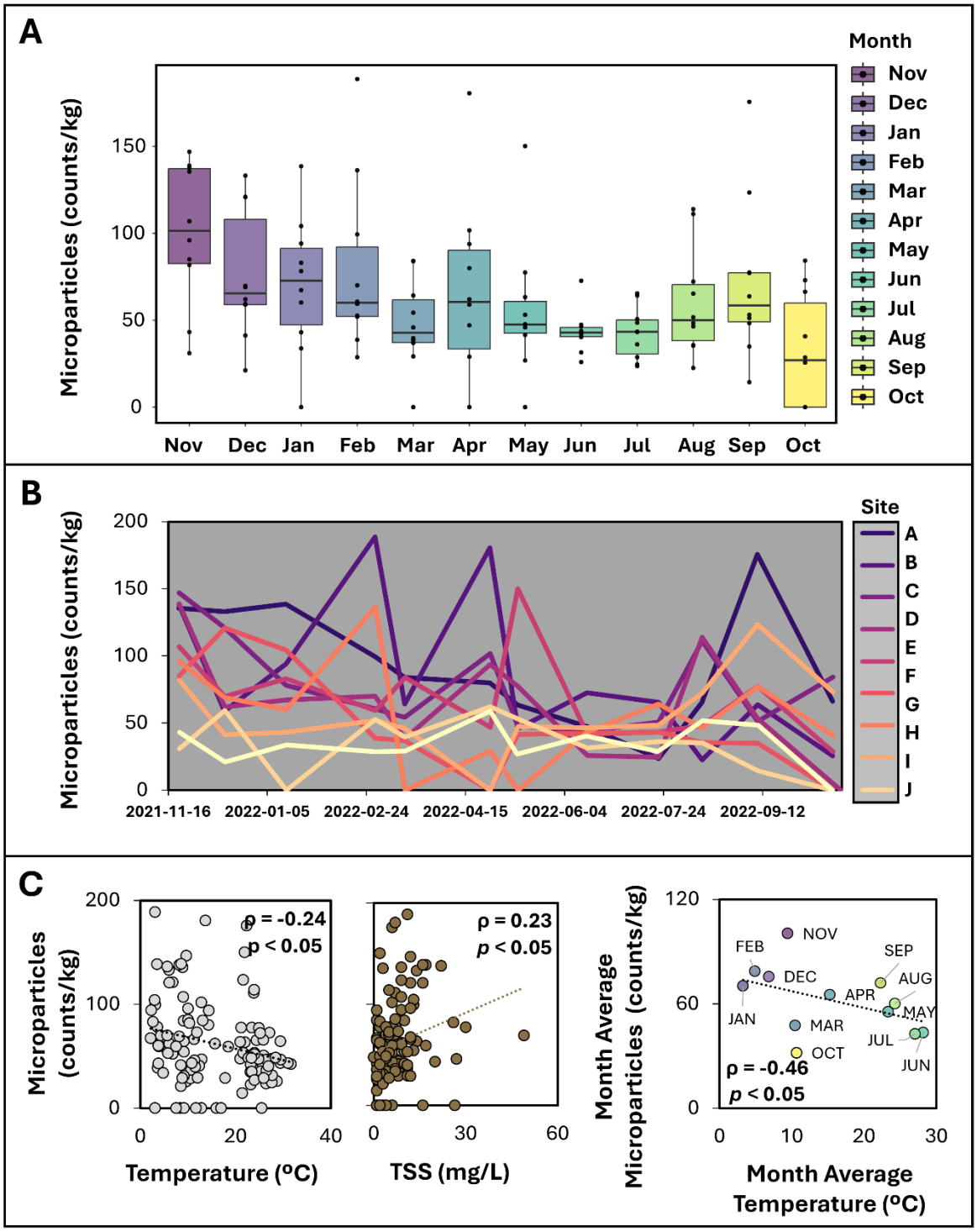

Figure 2.4. *(A) Boxplots for the sediment anthropogenic microparticle content across the 10 baseflow sampling sites each month. (B) The temporal behavior of anthropogenic microparticles in sediment at each site. (C) Comparisons of the sediment anthropogenic microparticle content with additional variables that featured significant relationships (i.e., water temperature and TSS).*

Though many temporally fluctuating variables were examined, including weather data (e.g., precipitation and wind speed), streamflow metrics (e.g., discharge during, 3 days before, 7 days before, and 20 days before each sampling event), and stream water physicochemical parameters (e.g., specific conductivity and Cl^-), only two parameters had minor significant trends with the sediment anthropogenic microparticle flux over time. Water temperature had a significant and negative correlation with the sediment anthropogenic microparticle content that was averaged for all sites for each month (Spearman's ρ = -0.46; Fig. 2.4. (C)). The same relationship was present for the entire dataset (i.e., when the data were not averaged by month; Spearman's ρ = -0.24; Fig. 2.4. (C)), but the strength of the correlation decreased. Across the complete dataset, anthropogenic microparticles in sediment also had a significant and positive relationship with TSS (Spearman's ρ = 0.23; Fig. 2.4. (C)).

The biweekly sediment samples were taken at mid-watershed site G to capture a higher temporal resolution dataset compared to the monthly watershed samples. However, they lacked a clear trend with time (Fig. 2.5.). Although these biweekly sediment samples encompassed the same range of stream temperature and TSS values across the year as the watershed-wide samples, these parameters had no trends with site G's sediment anthropogenic microparticle content. No correlations were present between anthropogenic microparticles in sediment at site G and discharge at or in the days leading up to sampling, despite the slightly larger range in discharge values during the collection of these samples (Fig. 2.5.; Table 2.S1.).

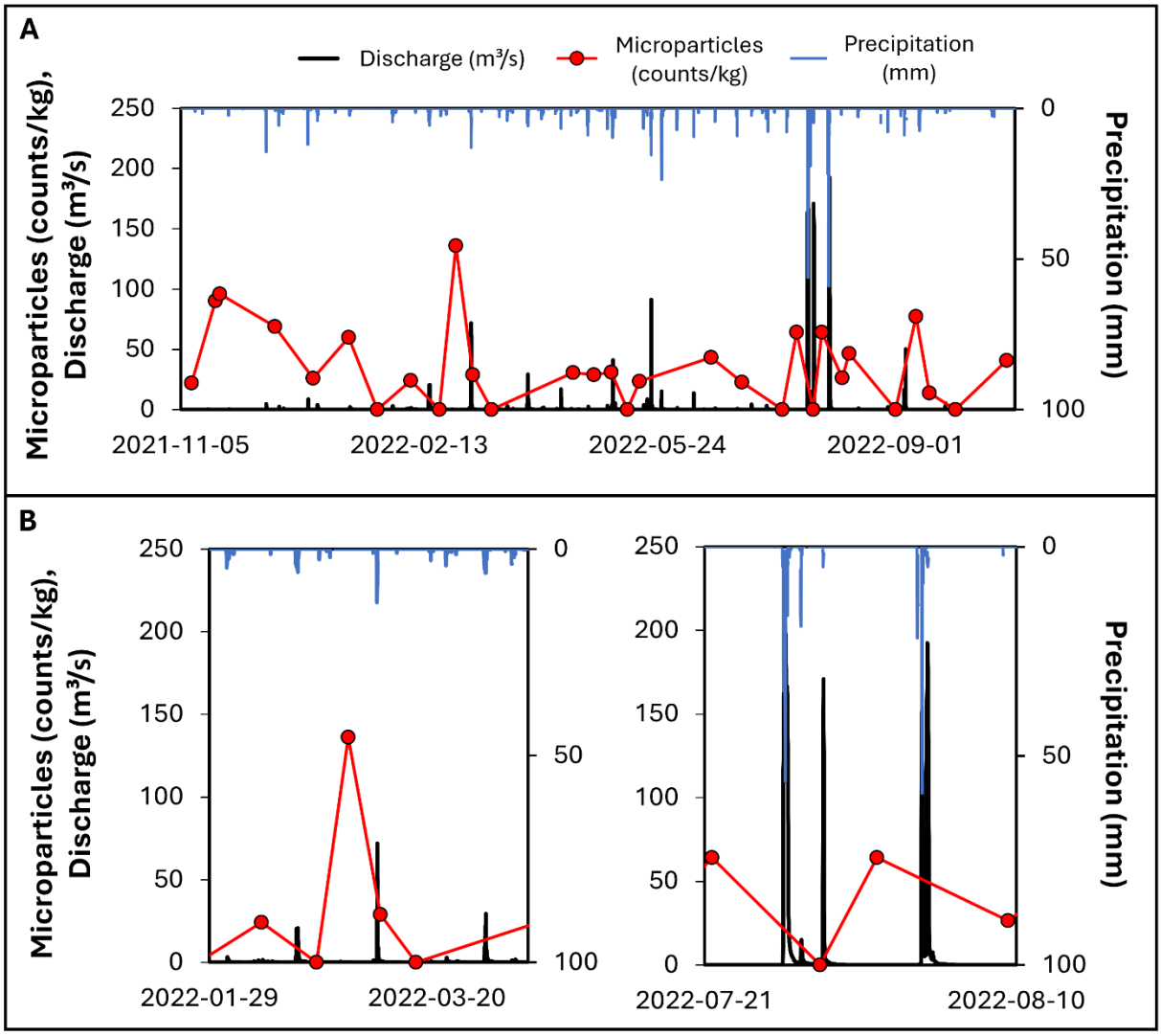

Figure 2.5. *(A) The full dataset for the higher resolution (i.e., biweekly and monthly) sediment samples taken at site G, with corresponding discharge and precipitation data shown. (B) A close view of the highest anthropogenic microparticle content found in the sediment in February 2022 (left) and the largest precipitation and discharge events in late July 2022 and early August 2022 (right).*

2.5. Discussion

2.5.1. Concentrations and Characteristics of Anthropogenic Microparticles in Urban Watersheds

The range of anthropogenic microparticle concentrations found in our sediment samples (0-188.6 counts/kg; Table 2.S3.) is comparable to other global studies of freshwater catchments. However, differences in the lower size limits for anthropogenic microparticle detection and sediment sampling methods complicate the comparison of totals among studies. Indeed, some studies that used methods that can detect anthropogenic microparticles of < 100 μm (which was our lower size limit) found concentrations of these microparticles in sediment that were orders of magnitude higher than those found in this study (Skalska et al., 2020). Our finding of low levels of anthropogenic microparticles in the water (0-4.1 counts/L) compared to the sediment is consistent with earlier research comparing the two compartments (e.g., Dahms et al., 2020; Scherer et al., 2020). Sampling higher volumes of water with a pump method (rather than the 2-L grab sampling technique we used) might allow for the detection of anthropogenic microparticles above the LOD and facilitate the spatiotemporal analysis of their variation in water, which was not possible with our dataset due to the low number of water samples with detectable anthropogenic microparticle levels.

The anthropogenic microparticle content reported in the bed sediment of Deer Creek is at higher levels than what prior research has found in the nearby but larger Meramec River (where a maximum of 8.3 counts/kg in sediment was observed; Baraza and Hernandez et al., 2022). Higher anthropogenic microparticle content in the sediment of small headwater stream systems compared to large rivers has been predicted by multiple prior modeling studies because of the potentially longer residence time and accumulation of these microparticles in the channel bed due to the lower flow conditions of headwater streams (De Arbeloa and Marzadri, 2024;

Drummond et al., 2022). Other field studies have also indicated higher microplastic content in headwater and tributary streams compared to larger mainstem waterways in both water and sediment (Feng et al., 2023; Luo et al., 2024). These potential retention and accumulation processes in headwater stream systems might therefore drive the difference between anthropogenic microparticle quantities in the sediment of these two proximal lotic systems. The long-term storage of anthropogenic microparticles in headwater stream sediment that can later be released to downstream environments (i.e., by flood events; Hurley et al., 2018) is a concerning implication of our study findings.

The predominance of fibers among the anthropogenic microparticles across various environmental compartments has been seen globally (Athey and Erdle, 2022). Other studies of water and sediment in both surface water and groundwater systems in the St. Louis region also found > 90% microfibers (Baraza and Hernandez et al., 2022; Hasenmueller et al., 2023; Hasenmueller and Ritter, 2024; Hernandez and Hasenmueller, 2024). Although only a portion of our study's anthropogenic microparticles from the sediment of a single site were analyzed for material types as part of a separate study (see Chapter 4) we can theorize that the 51% synthetic and 24% cotton materials found at site B might extend to other sites across the Deer Creek watershed. Among the synthetic materials identified in stream water and sediment samples, polyethylene terephthalate (PET) is the most common, not only in the preliminary subset of sediment anthropogenic microparticles analyzed at site B (see Chapter 4) but also in other regional studies of Mississippi River water (Rochman et al., 2022) and the St. Louis urban atmosphere (see Chapter 5). Prevalent microfibers of both synthetic (i.e., PET) and modified natural (i.e., cotton) materials are likely sourced from textile use (De Falco et al., 2020) in the highly populated St. Louis area.

2.5.2. Drivers of Spatiotemporal Anthropogenic Microparticle Distributions in Stream Sediment

Over the study period, the average anthropogenic microparticle content in our streambed sediment sampling locations increased from upstream to downstream in the Deer Creek watershed (Fig. 2.3.). This spatial pattern has been observed previously in surface water and sediment across catchments (Matjašič et al., 2022). However, prior research has also occasionally found the opposite longitudinal pattern in stream sediment, which has been attributed to dams or retaining walls that limit the flow of anthropogenic microparticles downstream (Scherer et al., 2020).

In the Deer Creek watershed, the longitudinal gradient (i.e., upstream to downstream) co-occurs with a transition from less dense residential neighborhoods to commercial and industrial land uses, including an increasing prevalence of outfall locations for various anthropogenic discharge types that might be point sources of microplastic pollution (Fig. 2.1. (C)). Relationships between land use elements (e.g., urbanization and point source pollution outfalls) and sediment microplastic concentrations have been found by various previous studies, independent of any longitudinal gradient (Baraza and Hernandez et al., 2022; de Carvalho et al., 2021). The observed spatial pattern in sediment anthropogenic microparticles might therefore be partially caused by the locations of development and point source pollution outfalls in the watershed. Implementation of filtration systems at point outfalls may accordingly be an effective management strategy to reduce further inputs of pollutants to the watershed.

Still, the strongest correlation occurred between anthropogenic microparticles and a given sample site's distance upstream of the mouth (Fig. 2.3. (C)). This outcome suggests that the erosion to deposition profile along the stream's longitudinal gradient is also a driving factor of the anthropogenic microparticle abundances in watershed sediment. Our hypothesis is further

supported by sediment grain size data demonstrating that depositional processes may be more prevalent at some of the downstream sites that feature finer grain sizes, which might therefore retain anthropogenic microparticles more readily (e.g., site A and site C; Fig. 2.S5.). Thus, historic anthropogenic microparticle inputs (e.g., from point outfalls such as sewer overflows) may have been distributed into the observed spatial pattern as these contaminants gradually moved downstream to settle in depositional environments near the mouth of the watershed over time.

Notably, some months (that mostly occurred in the summer) had spatial patterns with no clear longitudinal trend along Deer Creek (Fig. 2.S4.). This result suggests that the season in which sampling occurs might impact the observed spatial gradient, which is a crucial consideration for any study assessing the spatial distributions of microplastics. Our finding underscores the importance of long-term monitoring to identify broad patterns in microplastic distribution that might not be visible on short timescales or with single sampling events.

Unlike the more apparent spatial pattern observed in the sediment's anthropogenic microparticle distribution across the watershed, the temporal variation of this contaminant suite had no clear drivers. Difficulty explaining the temporal variation in sediment anthropogenic microparticle levels is not unique to this study, with various assessments of stream sediment finding conflicting information about their anthropogenic microparticle content in wet versus dry seasons (He et al., 2019; Skalska et al., 2020; Wu et al., 2019). Additionally, while prior studies often compare wet and dry seasons and discuss quantities of rainfall, the impacts of snowfall on watershed anthropogenic microparticles are understudied. Snow and ice have nevertheless been shown to release high volumes of these microparticles to water during melting (Chand et al., 2024; Karapetrova et al., 2024; Soininen et al., 2024). Indeed, the peak anthropogenic

microparticle content we saw after recent snowfall could be a result of short-term weather influences, but larger temporal trends are still obscure within the dataset (Fig. 2.4., Fig. 2.5.).

Minor correlations between sediment anthropogenic microparticle content and other stream physicochemical parameters (e.g., temperature and TSS; Fig. 2.4. (C)) may point to potential influences on the temporal flux of anthropogenic microparticles in sediment. The positive trend between sediment anthropogenic microparticle content and TSS is potential evidence that increased sediment transport in the stream's water column might lead to enhanced deposition of anthropogenic microparticles into the bed sediment (Mancini et al., 2023; Soler et al., 2025). However, the negative trend between sediment anthropogenic microparticles and temperature is less easily explained. Summer months with warmer temperatures might have lower microparticle content due to variable deposition rates (see Chapter 5), or interactions with biota that are more active in warmer weather. Further research of temporal anthropogenic microparticle fluxes across stream systems impacted by both winter weather (including snowfall) and warmer, drier summers is needed to better understand anthropogenic microparticle suspension and deposition processes.

Overall, the spatial patterns we observed in Deer Creek's sediment anthropogenic microparticle distribution over time were valuable to identify the broader longitudinal gradient present across the watershed (which was not always apparent from individual sampling campaigns). Nevertheless, the drivers of temporal trends in sediment anthropogenic microparticle levels in the catchment were not made clearer either through our focus on a single site that was sampled at higher frequency over the year-long study period or through our consideration of the entire watershed during baseflow conditions (which was intended to remove the influence of short-term events like floods). Further work is needed to better understand the drivers of the long-term temporal fluxes of anthropogenic microparticles to and from stream

sediment. Our findings that anthropogenic microparticle levels fluctuated from below our method LOD to nearly 200 counts/kg in the stream's bed sediment suggest that this environmental compartment can transition between a sink and source for these pollutants in small urban watersheds.

2.6. Conclusions

Stream systems are key interfaces between terrestrial sources of anthropogenic microparticles and downstream environments. However, our understanding of the spatiotemporal variation in anthropogenic microparticles (including microplastics) in small urban headwater streams is lacking. We showed that watershed-scale sampling of an urban stream over a 1-year period can reveal broader spatial patterns in anthropogenic microparticle deposition within the watershed as well as highlight the times of year with unique spatial profiles. The gradient of anthropogenic microparticle distribution across the watershed was best explained by basin attributes, particularly the distance from a given sampling site to the stream's outlet and the number of nearby point source pollution inputs. However, the temporal fluctuation in anthropogenic microparticle content in the sediment had unclear causes. Our understanding of the anthropogenic microparticle flux between stream sediment and water over space and time could be improved by a higher volume sampling method for the stream water that allows for improved anthropogenic microparticle detection in water samples with low concentrations of these pollutants. Nevertheless, our finding that anthropogenic microparticles are more prevalent at the stream's outlet is useful to land managers for considering how to target remediation efforts that have the highest potential to reduce downstream concentrations of this contaminant suite. In particular, the relationship between anthropogenic microparticles in sediment and pollution outfalls might reveal a point source of these contaminants that could be managed to reduce inputs.

2.7. Acknowledgments

This work was partially funded by a United States Geological Survey Water Resources Research Act Program grant, administered through the Missouri Water Center (Award: G21AP10582-03), and a Geological Society of America Graduate Student Research Grant (Award: 13039-21), funded by the National Science Foundation (Award: 1949901). We thank James Faupel and Adam Rembert for facilitating access to Deer Creek at the Litzsinger Road Ecology Center, and we appreciate all who helped with the field and laboratory work.

2.8. References

Alencar, M.V., Gimenez, B.G., Sasahara, C., Elliff, C.I., Rodrigues, L.S., Conti, L.A., Dias, S.L.F.G., Cetrulo, T.B., Scrich, V.M., Turra, A., 2022. How far are we from robust estimates of plastic litter leakage to the environment? J. Environ. Manage. 323, 116195.

Athey, S.N., Erdle, L.M., 2022. Are we underestimating anthropogenic microfiber pollution? A critical review of occurrence, methods, and reporting. Environ. Toxicol. Chem. 41(4), 822-837.

Baraza, T., Hernandez, N.F., Sebok, J.N., Wu, C., Hasenmueller, E.A., Knouft, J.H., 2022. Integrating land cover, point source pollution, and watershed hydrologic processes data to understand the distribution of microplastics in riverbed sediments. Environ. Pollut. 311, 119852.

Carpenter, E.J., Smith, K.L., 1972. Plastics on the Sargasso Sea surface. Science. 175(4027), 1240-1241.

Chand, R., Putna-Nimane, I., Vecmane, E., Lykkemark, J., Dencker, J., Nielsen, A.H., Vollertsen, J., Liu, F., 2024. Snow dumping station – A considerable source of tyre wear, microplastics, and heavy metal pollution. Environ. Int. 188, 108782.

Criss, R.E., Stein, E.M., Nelson, D.L., 2022. Generation and propagation of an urban flash flood and our collective responsibilities. J. Earth Sci. 33(6), 1624-1628.

Dahms, H.F.J., van Rensburg, G.J., Greenfield, R., 2020. The microplastic profile of an urban African stream. Sci. Total Environ. 731, 138893.

De Arbeloa, N.P., Marzadri, A., 2024. Modeling the transport of microplastics along river networks. Sci. Total Environ. 911, 168227.

De Carvalho, A.R., Garcia, F., Riem-Galliano, L., Tudesque, L., Albignac, M., ter Halle, A., Cucherousset, J., 2021. Urbanization and hydrological conditions drive the spatial and temporal variability of microplastic pollution in the Garonne River. Sci. Total Environ. 769, 144479.

De Falco, F., Cocca, M., Avella, M., Thompson, R.C., 2020. Microfiber release to water, via laundering, and to air, via everyday use: A comparison between polyester clothing with differing textile parameters. Environ. Sci. Technol. 54, 3288-3296.

Dewitz, J., 2023. National Land Cover Database (NLCD) 2021 Products: U.S. Geological Survey data release.

Dikareva, N., Simon, K.S., 2019. Microplastic pollution in streams spanning an urbanization gradient. Environ. Pollut. 250, 292-299.

Drummond, J.D., Schneidewind, U., Li, A., Hoellein, T.J., Krause, S., Packman, A.I., 2022. Microplastic accumulation in riverbed sediment via hyporheic exchange from headwaters to mainstems. Sci. Adv. 8, eabi9305.

Feng, S., Lu, H., Xue, Y., Yan, P., Sun, T., 2024. Fate, transport, and source of microplastics in the headwaters of the Yangtze River on the Tibetan Plateau. J. Hazard. Mater. 455, 131526.

Goehler, L.O., Moruzzi, R.B., da Conceicao, F.T., Couto, A.A.J., Speranza, L.G., Busquets, R., Campos, L.C., 2022. Relevance of tyre wear particles to the total content of microplastics transported by runoff in a high-imperviousness and intense vehicle traffic urban area. Environ. Pollut. 314, 120200.

Hasenmueller, E.A., Baraza, T., Hernandez, N.F., Finegan, C.R., 2023. Cave sediment sequesters anthropogenic microparticles (including microplastics and modified cellulose) in subsurface environments. Sci. Total Environ. 893, 164690.

Hasenmueller, E.A., Ritter, A.N. 2024. Microplastic chemostasis and homogeneity during a historic flood on the Mississippi River. Environ. Eng. Sci. 41(12), 563-573.

He, B., Goonetilleke, A., Ayoko, G., Rintoul, L., 2019. Abundance, distribution patterns, and identification of microplastics in Brisbane River sediments, Australia. Sci. Total Environ. 700, 134467.

Hernandez, E., Nowack, B., Mitrano, D.M., 2017. Polyester textiles as a source of microplastics from households: A mechanistic study to understand microfiber release during washing. Environ. Sci. Technol. 51, 7036-7046.

Hernandez, N.F., Hasenmueller, E.A., 2024. Anthropogenic macroscale and microscale debris (including plastics) have differing spatial distributions across a small urban watershed. Environ. Eng. Sci. 41(12), 509-519.

Hurley, R., Woodward, J., Rothwell, J.J., 2018. Microplastic contamination of river beds significantly reduced by catchment-wide flooding. Nat. Geosci. 11, 251-257.

Iowa Environmental Mesonet (IEM), 2025. ASOS Network "ASOS-AWOS-METAR data download". https://mesonet.agron.iastate.edu/ASOS/. Accessed March 01, 2025.

Kabir, A.H.M.E., Sekine, M., Imai, T., Yamamoto, K., Kanno, A., Higuchi, T., 2022. Microplastics in the sediments of small-scale Japanese rivers: Abundance and distribution, characterization, sources-to-sink, and ecological risks. Sci. Total Environ. 812, 152590.

Karapetrova, A., Cowger, W., Michell, A., Braun, A., Bair, E., Gray, A., Gan, J., 2024. Exploring microplastic distribution in Western North American snow. J. Hazard. Mater. 480, 136126.

Kim, L., Kim, S.A., Kim, T.H., Kim, J., An, Y., 2021. Synthetic and natural microfibers induce gut damage in the brine shrimp *Artemia franciscana.* Aquat. Toxicol. 232, 105748.

Lockmiller, K.A., Wang, K., Fike, D.A., Shaughnessy, A.R., Hasenmueller, E.A., 2019. Using multiple tracers (F−,B, δ11B, and optical brighteners) to distinguish between municipal drinking water and wastewater inputs to urban streams. Sci. Total Environ. 671, 1245-1256.

Luo, W., Fu, H., Lu, Q., Li, B., Cao, X., Chen, S., Liu, R., Tang, B., Yan, X., Zheng, J., 2024. Microplastic pollution differences in freshwater river according to stream order: Insights from spatial distribution, annual load, and ecological assessment. J. Environ. Manage. 366, 121836.

Mancini, M., Serra, T., Colomer, J., Solari, L., 2023. Suspended sediments mediate microplastic sedimentation in unidirectional flows. Sci. Total Environ. 890, 164363.

Matjašič, T., Mori, N., Hostnik, I., Bajt, O., Viršek, M.K., 2022. Microplastic pollution in small rivers along rural–urban gradients: Variations across catchments and between water column and sediments. Sci. Total Environ. 858(3), 160043.

Metropolitan St. Louis Sewer District (MSD)., 2025. Sewer overflow locations map "sewer overflow locations as of June 30, 2018". https://msdprojectclear.org/customers/problems-tips/sewer-overflows/. Accessed March 01, 2025.

Missouri Department of Natural Resources (MoDNR), 2020. Bedrock 24k. https://gis.dnr.mo.gov/host/rest/services/geology/bedrock_24k/MapServer/1. Accessed March 01, 2025.

Missouri Department of Natural Resources (MoDNR), 2021. MO NPDES Outfalls. https://services2.arcgis.com/kNS2ppBA4rwAQQZy/arcgis/rest/services/MO_NPDES_Outfalls/FeatureServer. Accessed March 01, 2025.

Missouri Spatial Data Information Service (MSDIS), 2019. MO 2018 Sinkholes. https://services2.arcgis.com/kNS2ppBA4rwAQQZy/arcgis/rest/services/MO_2018_Sinkholes/FeatureServer/0. Accessed March 01, 2025.

Rochman, C.M., 2018. Microplastics research — From source to sink in freshwater systems. Science. 360(6384), 28-29.

Rochman, C.M., Grbic, J., Earn, A., Helm, P.A., Hasenmueller, E.A., Trice, M., Munno, K., De Frond, H., Djuric, N., Santoro, S., Kaura, A., Denton, D., Teh, S., 2022., Local monitoring should inform local solutions: Morphological assemblages of microplastics are similar within a pathway, but relative total concentrations vary regionally. Environ. Sci. Technol. 56, 9367-9378.

Saint Louis County GIS Service Center and St. Louis County Assessor's Office, 2021. Parcels "Parcel Data Jurisdictions". https://www.arcgis.com/apps/webappviewer/index.html?id=4ac4f88eb26543afb04e643b9cba868c. Accessed March 01, 2025.

Scherer, C., Weber, A., Stock, F., Vurusic, S., Egerci, H., Kochleus, C., Arendt, N., Foeldi, C., Dierkes, G., Wagner, M., Brennholt, N., Reifferscheid, G., 2020. Comparative assessment of

microplastics in water and sediment of a large European river. Sci. Total Environ. 738, 139866.

Skalska, K., Ockelford, A., Ebdon, J.E., Cundy, A.B., 2020. Riverine microplastics: Behaviour, spatio-temporal variability, and recommendations for standardised sampling and monitoring. J. Water Process Eng. 38, 101600.

Soler, M., Colomer, J., Pohl, F., Serra, T., 2025. Transport and sedimentation of microplastics by turbidity currents: Dependence on suspended sediment concentration and grain size. Environ. Int. 195, 109271.

Soininen, T., Uurasjärvi, E., Sorvari, J., Saarni, S., Koistinen, A., 2024. Microplastic accumulation in one-year freshwater ice: A four-year monitoring study reveals winter dynamics of microplastics. Sci. Total Environ. 957, 177602.

Thompson, R.C., Courtene-Jones, W., Boucher, J., Pahl, S., Raubenheimer, K., Koelmans, A.A., 2024. Twenty years of microplastic pollution research—what have we learned? Science, 386, 395.

United States Geological Survey (USGS), 2025. National Water Information System data available on the World Wide Web "USGS water data for the nation". https://waterdata.usgs.gov/. Accessed February 19, 2025.

Wu, P., Tang, Y., Dang, M., Wang, S., Jin, H., Liu, Y., Jing, H., Zheng, C., Yi, S., Cai, Z., 2019. Spatial-temporal distribution of microplastics in surface water and sediments of Maozhou River within Guangdong-Hong Kong-Macao Greater Bay Area. Sci. Total Environ. 717, 135187.

Zhou, Y., Li, Y., Yan, Z., Wang, H., Chen, H., Zhao, S., Zhong, N., Cheng, Y., Acharya, K., 2023. Microplastics discharged from urban drainage system: Prominent contribution of sewer overflow pollution. Water Res. 236, 119976.

2.9. Supplementary Materials

2.9.1. Supplemental Tables

Table 2.S1. *Basic sampling information and stream physicochemical data for the high-resolution sampling campaign at site G.*

Date	Sampling Strategy	Days Since Last Rainfall	Discharge at 9 AM on the Sampling Date (m^3/s)	Discharge at the Time of the Site G Sample (m^3/s)	Sediment Anthropogenic Microparticles (counts/kg)	Temperature (°C)	Specific Conductivity (µS/cm)	TSS (mg/L)
2021-11-09	Site G	8	0.11	0.09	22.1	12.1	501.7	21.0
2021-11-19	Site G	5	0.04	0.00	90.2	7.7	546.2	15.5
2021-11-21	Full Watershed	7	0.01	0.01	95.9	10.0	676.6	12.0
2021-12-14	Full Watershed	4	0.00	0.00	69.0	8.2	743.0	49.0
2021-12-30	Site G	1	0.04	0.04	26.1	7.4	464.4	11.0
2022-01-14	Full Watershed	5	0.01	0.01	60.1	3.8	1812	9.0
2022-01-26	Site G	10*	0.03	0.01	0.0	2.8	1870	10.0
2022-02-09	Site G	6*	0.38	0.31	24.2	2.1	2500	10.0
2022-02-21	Site G	4*	0.17	0.20	0.0	8.9	1988	25.0
2022-02-28	Full Watershed	4*	0.11	0.11	136.2	5.7	4940	9.0
2022-03-07	Site G	1	1.41	0.80	28.9	7.9	1220	22.0
2022-03-15	Full Watershed	4	0.08	0.07	0.0	11.7	2576	16.0
2022-04-18	Site G	1	0.22	0.18	30.9	14.1	1010	6.0
2022-04-27	Full Watershed	6	0.08	0.08	29.0	17.8	1074	8.0
2022-05-04	Site G	1	0.11	0.09	31.2	16.0	799.0	3.5
2022-05-11	Full Watershed	5	0.10	0.09	0.0	25.5	1270	1.0
2022-05-16	Site G	10	0.04	0.05	23.6	25.7	1265	3.0
2022-06-15	Full Watershed	5	0.03	0.03	43.4	31.0	1020	5.0
2022-06-28	Site G	2	0.02	0.02	22.9	24.8	1170	6.0
2022-07-15	Site G	3	0.01	0.01	0.0	24.4	842.0	10.0
2022-07-21	Full Watershed	4	0.01	0.01	64.2	29.4	760.0	1.0
2022-07-28	Site G	1	0.38	0.33	0.0	23.5	1193	9.0
2022-08-01	Site G	4	0.02	0.02	64.2	29.8	858.0	12.0
2022-08-09	Site G	1	0.10	0.07	26.5	26.5	934.0	11.0
2022-08-12	Full Watershed	3	0.02	0.02	46.5	26.5	1000	4.0
2022-09-01	Site G	4	0.02	0.01	0.0	27.3	870.0	36.0

Table 2.S1. *Continued.*

Date	Sampling Strategy	Days Since Last Rainfall	Discharge at 9 AM on the Sampling Date (m^3/s)	Discharge at the Time of the Site G Sample (m^3/s)	Sediment Anthropogenic Microparticles (counts/kg)	Temperature (°C)	Specific Conductivity (µS/cm)	TSS (mg/L)
2022-09-09	Full Watershed	4	0.01	0.01	77.1	24.9	857.0	30.0
2022-09-15	Site G	4	0.01	0.01	14.0	24.9	1653	11.0
2022-09-26	Site G	3	0.01	0.01	0.0	19.9	846.0	9.0
2022-10-17	Full Watershed	5	0.01	0.00	40.7	12.4	462.7	8.0

*Indicates days when snowfall occurred more recently than rainfall.

Table 2.S2. *The data used to calculate the LOD for each sample type.*

Blank Type	Total (counts)	Black Fiber (counts)	Blue Fiber (counts)	Blue Fragment (counts)	Clear Fiber (counts)	Pink Fiber (counts)	Red Fiber (counts)
Water Processing Blank 1	3	0	1	0	2	0	0
Water Processing Blank 2	4	0	1	0	3	0	0
Water Processing Blank 3	3	0	2	0	0	0	0
Water Processing Blank 4	3	0	2	0	1	0	0
Water Processing Blank 5	2	0	1	0	1	0	0
Water Processing Blank 6	2	0	2	0	0	0	0
Water Processing Blank 7	1	0	0	1	0	0	0
Water Processing Blank 8	1	0	0	0	1	0	0
Water Processing Blank 9	4	1	1	0	1	0	1
Water Processing Blank 10	3	1	2	0	0	0	0
November 2021 Field Blank	3	0	0	0	2	1	0
December 2021 Field Blank	4	0	3	0	1	0	0
January 2022 Field Blank	5	0	2	0	2	1	0
February 2022 Field Blank	2	0	0	0	2	0	0
March 2022 Field Blank	3	0	2	0	1	0	0
May 2022 Field Blank	3	0	2	0	1	0	0
July 2022 Field Blank	3	0	2	0	1	0	0
August 2022 Field Blank	4	0	3	0	1	0	0
September 2022 Field Blank	3	0	2	0	0	1	0
October 2022 Field Blank	6	0	3	0	3	0	0
Average	3.10						
Standard Deviation	1.18						
Water LOD	7						
Sediment Processing Blank 1	4	1	1	0	2	0	0
Sediment Processing Blank 2	3	0	1	0	2	0	0
Sediment Processing Blank 3	3	0	2	0	1	0	0
Sediment Processing Blank 4	4	0	2	0	2	0	0
Sediment Processing Blank 5	3	0	0	0	3	0	0
Sediment Processing Blank 6	4	0	0	0	4	0	0
Average	3.50						
Standard Deviation	0.50						
Sediment LOD	5						

Table 2.S3. *The concentration data for anthropogenic microparticles in sediment at each site for each sampling month, with the averages and standard deviations for each month and site on the left and bottom of the matrix, respectively. The units are counts/kg for all anthropogenic microparticle values.*

	A	**B**	**C**	**D**	**E**	**F**	**G**	**H**	**I**	**J**	Month Averages and Standard Deviations
NOV	135.4	137.8	146.8	138.8	106.9	85.0	95.9	81.8	30.9	43.1	100.3 ± 38.7
DEC	133.0	58.9	121.0	62.0	69.8	120.8	69.0	41.2	59.4	21.1	75.6 ± 35.2
JAN	138.5	94.1	78.2	67.2	82.9	104.2	60.1	43.0	0.0	33.7	70.2 ± 37.1
FEB	99.4	188.6	60.6	70.0	59.4	38.7	136.2	52.0	52.7	28.7	78.6 ± 47.0
MAR	84.0	64.2	54.3	38.4	83.9	36.9	0.0	45.8	39.6	29.2	47.6 ± 24.2
APR	80.0	180.5	101.7	93.7	47.0	0.0	29.0	0.0	62.0	58.9	65.3 ± 50.8
MAY	63.3	45.9	47.6	77.4	150.1	41.5	0.0	47.3	53.1	26.9	55.3 ± 37.2
JUN	47.3	72.6	43.8	25.9	41.8	42.3	43.4	46.5	31.5	40.2	43.5 ± 11.6
JUL	23.6	65.5	50.6	24.6	43.3	43.2	64.2	48.5	36.1	28.8	42.8 ± 14.2
AUG	65.2	22.6	111.1	113.8	48.2	35.6	46.5	72.2	35.2	51.7	60.2 ± 29.5
SEP	175.5	63.7	51.3	53.1	77.4	34.9	77.1	123.4	14.4	48.3	70.5 ± 46.2
OCT	66.3	25.6	84.3	0.0	28.5	0.0	40.7	73.0	0.0	0.0	31.8 ± 31.3
Site Averages and Standard Deviations	92.6 ± 42.7	85.0 ± 53.1	79.3 ± 32.5	63.7 ± 37.7	69.9 ± 32.3	48.6 ± 35.4	55.2 ± 36.7	56.2 ± 28.3	33.4 ± 21.7	34.2 ± 15.0	

Table 2.S4. *The p values for pairwise Wilcoxon tests of the differences among sites across the watershed. Significant p values are in bold.*

Site	A	B	C	D	E	F	G	H	I
B	0.62								
C	0.55	0.98							
D	0.33	0.65	0.54						
E	0.36	0.79	0.52	0.76					
F	0.07	0.16	0.05	0.53	0.16				
G	0.14	0.39	0.21	0.70	0.48	0.55			
H	0.09	0.38	0.16	0.75	0.53	0.25	0.86		
I	**0.01**	**0.04**	**0.03**	0.15	**0.05**	0.54	0.23	0.16	
J	**0.01**	**0.03**	**0.01**	0.15	**0.03**	0.48	0.16	0.09	0.70

2.9.2. Supplemental Figures

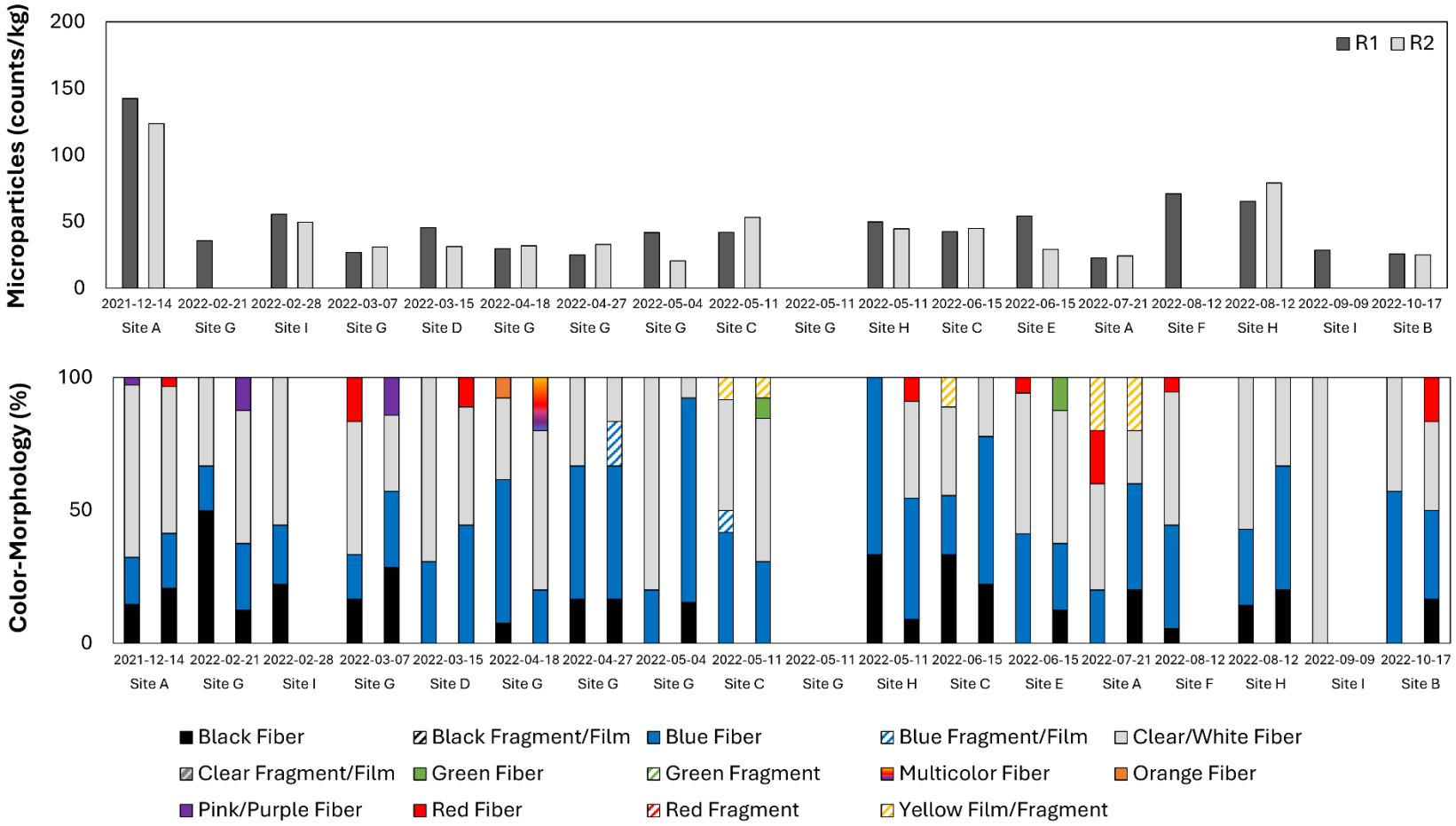

Figure 2.S1. *A comparison of the anthropogenic microparticle content and color-morphology proportions in sediment replicates. For both plots, each sample has two bars: the first replicate (R1, left) and the second replicate (R2, right).*

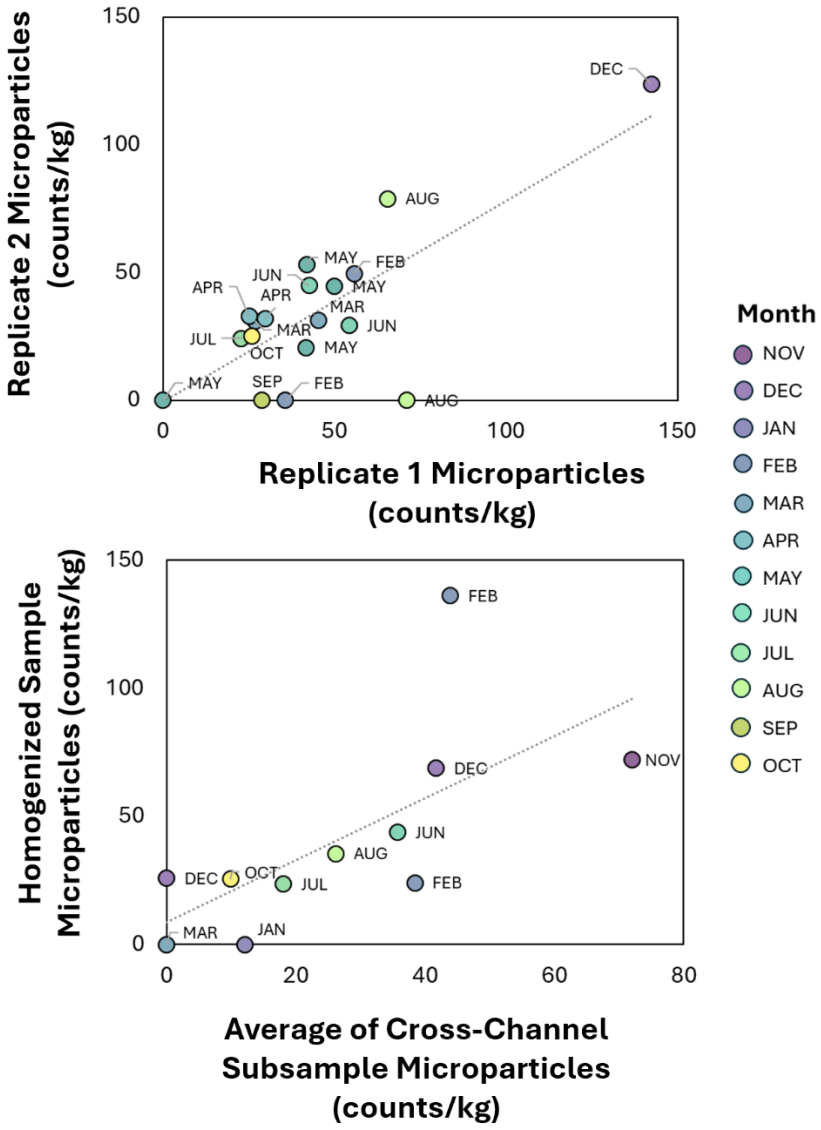

Figure 2.S2. *The relationships between the homogenized field replicates of sediment (top) and the homogenized sediment samples compared to the averages of individual sediment subsamples taken across the channel (bottom).*

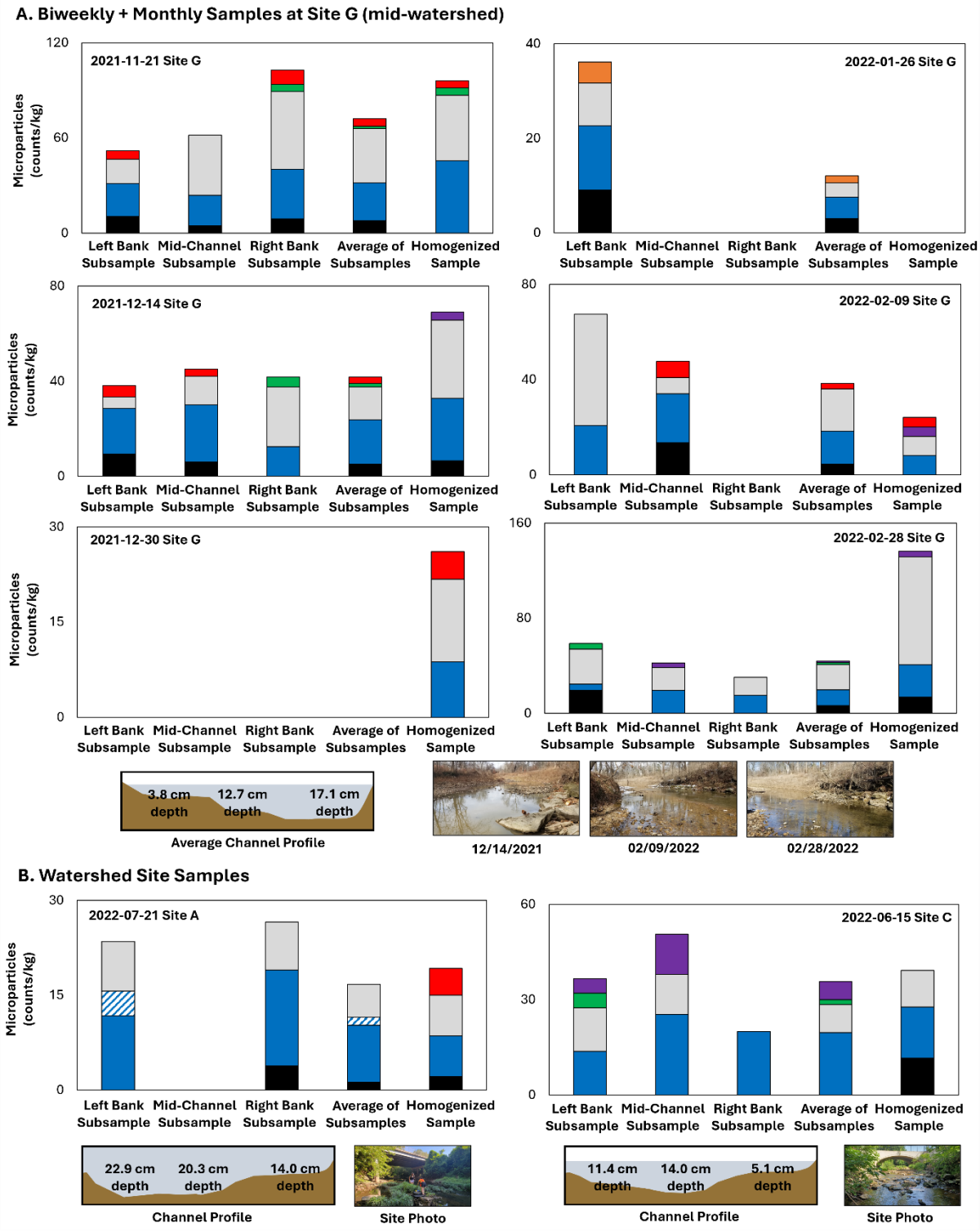
A. Biweekly + Monthly Samples at Site G (mid-watershed)
2021-11-21 Site G
2022-01-26 Site G
2021-12-14 Site G
2022-02-09 Site G
2021-12-30 Site G
2022-02-28 Site G
Microparticles (counts/kg)
Left Bank Subsample
Mid-Channel Subsample
Right Bank Subsample
Average of Subsamples
Homogenized Sample
3.8 cm depth
12.7 cm depth
17.1 cm depth
Average Channel Profile
12/14/2021
02/09/2022
02/28/2022
B. Watershed Site Samples
2022-07-21 Site A
2022-06-15 Site C
22.9 cm depth
20.3 cm depth
14.0 cm depth
Channel Profile
Site Photo
11.4 cm depth
14.0 cm depth
5.1 cm depth

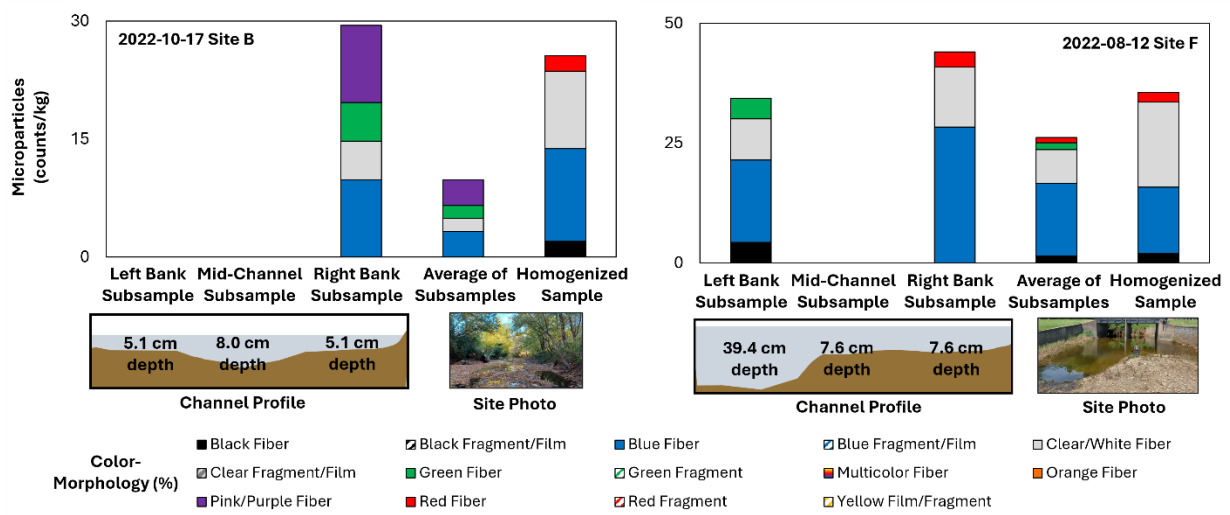

Figure 2.S3. *Individual subsamples of sediment from three points across the stream channel next to their average value and the corresponding value for a homogenized sediment sample for the (A) biweekly and monthly sampling at site G and (B) other sites across the watershed. The height of each bar indicates the anthropogenic microparticle concentration in each sediment sample and the percentage of each color-morphology type is indicated within the bar. On 15 March 2022, at site G, all three triplicate samples and the homogenized replicate were below the LOD. This data is shown in Figure 2.S2. but not visualized here.*

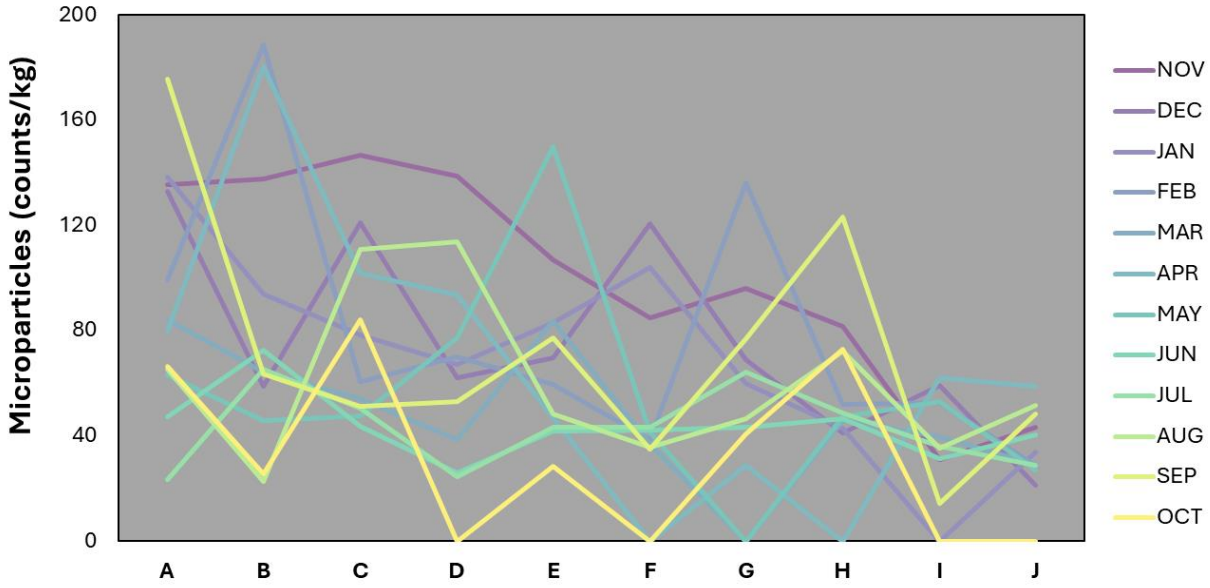

Figure 2.S4. *Spatial trends in sediment anthropogenic microparticle levels for downstream (A) to upstream (J) sites for each month of sampling across the Deer Creek basin.*

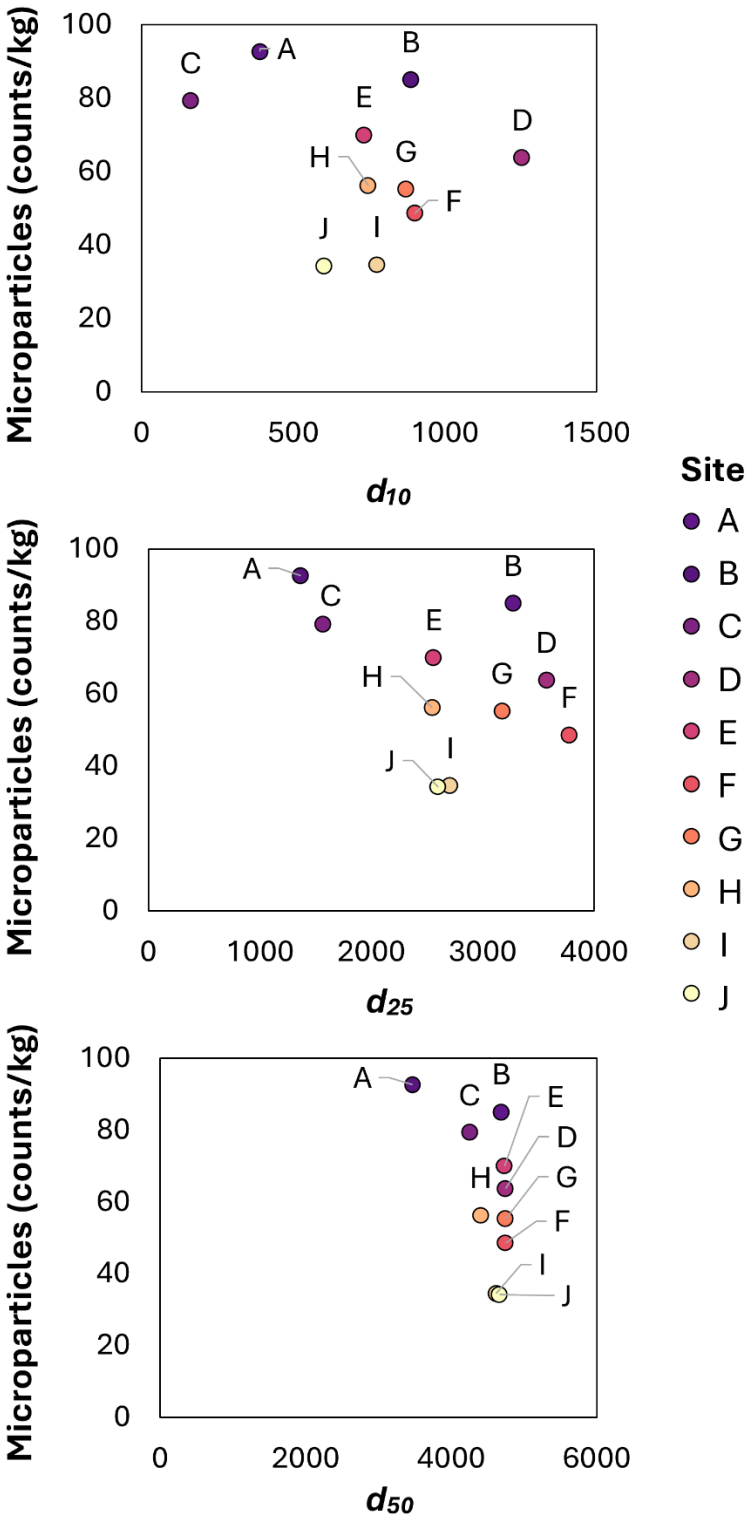

Figure 2.S5. *The relationships between the sediment's anthropogenic microparticle content and grain size attributes for each site. No significant trends were found.*

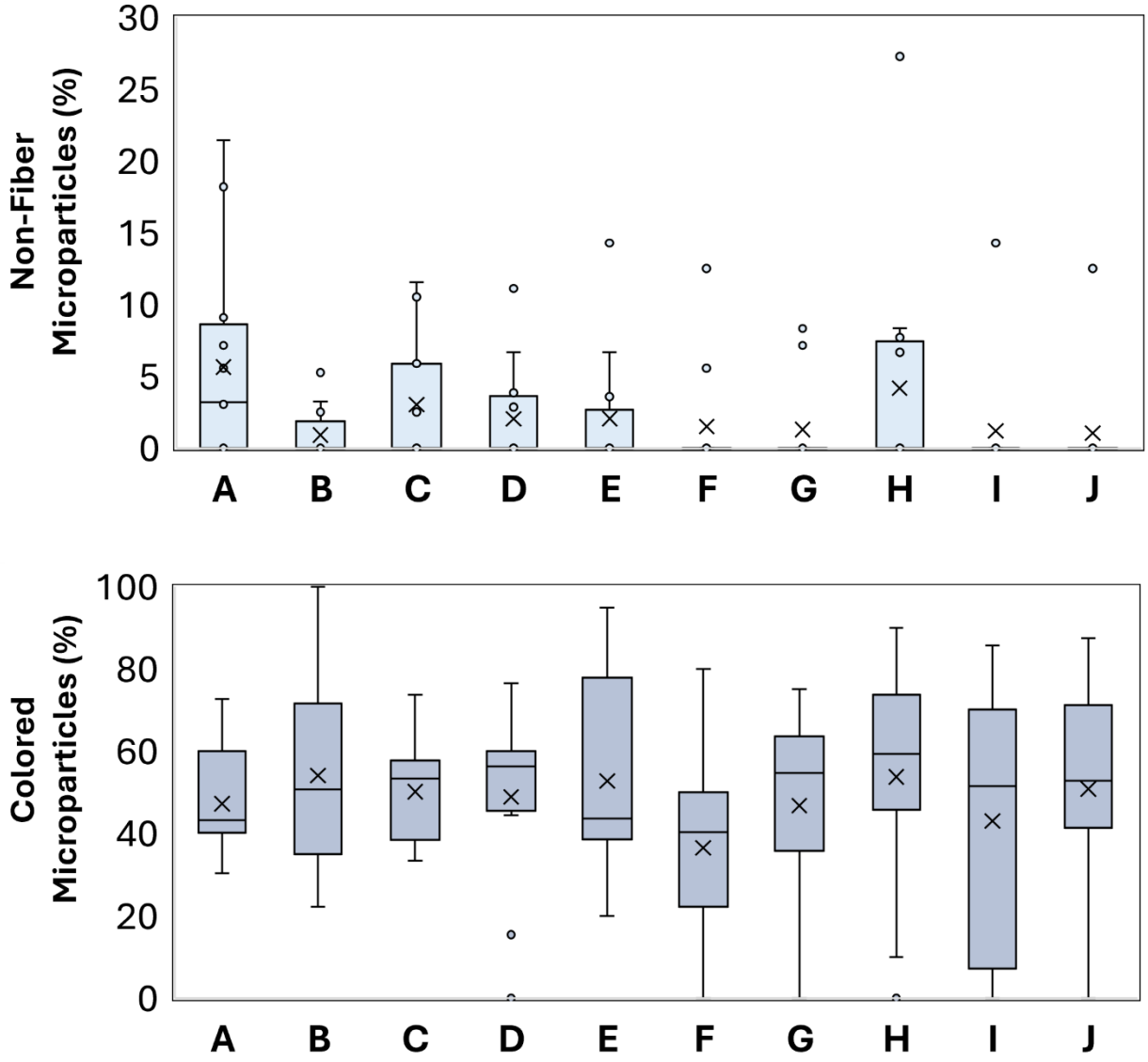

Figure 2.S6. *Boxplots of the percentages of less common anthropogenic microparticle attributes. The top boxplot demonstrates unique morphologies (i.e., films and fragments) and the bottom boxplot shows colored (i.e., non-clear) anthropogenic microparticles in the sediment by site.*

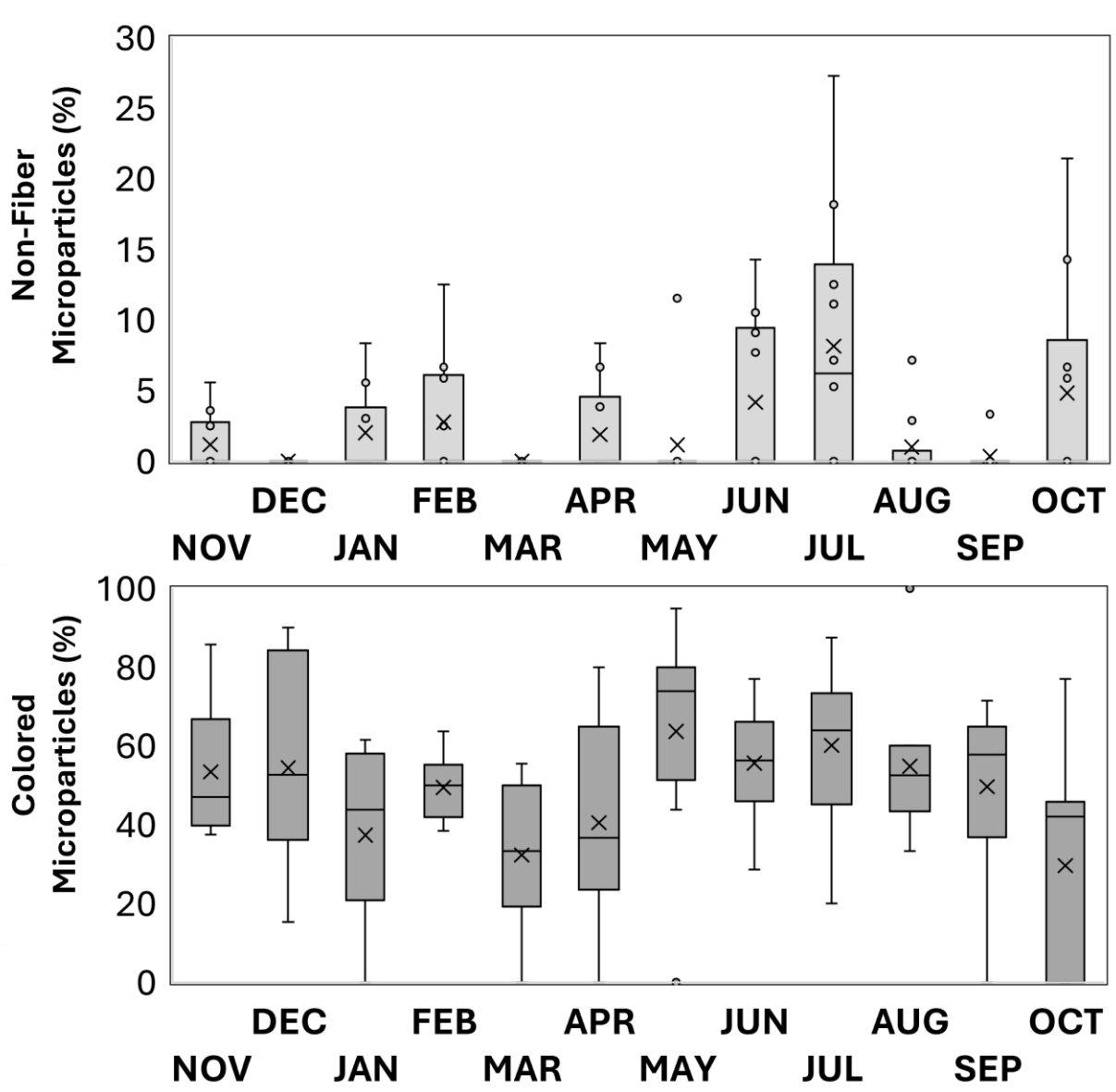

Figure 2.S7. *Boxplots of the percentages of less common anthropogenic microparticle attributes. The top boxplot demonstrates unique morphologies (i.e., films and fragments) and the bottom boxplot shows colored (i.e., non-clear) anthropogenic microparticles in the sediment by month.*

CHAPTER 3: FLOOD EVENTS ENHANCE URBAN STREAM MICROPLASTIC TRANSPORT VIA CONTRIBUTIONS FROM RAINFALL AND SEDIMENT RESUSPENSION

3.1. Abstract

Stream systems are major conveyers of microplastics (plastics < 5 mm) to downstream waterbodies. Flood events can mobilize these contaminants from storage compartments within watersheds, thereby increasing their transport to downstream habitats. In addition to microplastics, other harmful anthropogenic microparticles (e.g., dyed cotton fibers) can be moved at higher levels during flooding. Several sources are suspected of causing increased anthropogenic microparticle transport during flood events, including input from rainfall and road runoff as well as export from sediment storage. The goal of this study was therefore to examine the sourcing, timing, and extent of anthropogenic microparticle (including microplastic) transport during flood events in an urban stream (i.e., Deer Creek near St. Louis, Missouri, United States). High frequency samples of stream water were taken throughout four flood events. For each event, additional samples were collected for suspected sourcing components (e.g., rainfall, road runoff, and bed sediment before and after flooding). Anthropogenic microparticle concentrations increased from below the limit of detection (LOD) to detectable quantities during every flood peak, with the maximum anthropogenic microparticle content found in water at 17.4 counts/L. Anthropogenic microparticles were mostly fibers (96%) and plastics (84%) in the floodwaters and had significant and positive correlations with discharge and turbidity. High quantities of anthropogenic microparticles that were 99% fibers occurred in rainfall samples and in the floodwaters when the turbidity was low. Additionally, for every flood event, anthropogenic microparticles decreased from the pre-flood to the post-flood sediment samples obtained from the streambed (which were 97% fibers on average), suggesting that they could also be exported

from sediment storage and transported in turbid water during high flow. Given that the morphologies of the anthropogenic microparticles in floodwater were similar to the rainfall and sediment but not the road runoff (which was comprised of 63% fragments), our findings point to rainfall and export from bed sediment storage as the most likely sources of flood-transported anthropogenic microparticles. Our results confirm the significance of flood events as key movers of microplastics in urban streams.

3.2. Introduction

The global ubiquity of microplastics and concerns about their impacts on human and ecological health are well established. Improved understanding of the movement of microplastics through the environment is therefore vital to inform microplastic pollution prevention strategies (Akanyange et al., 2022; Rochman, 2018). Importantly, streams can serve as conveyers and reservoirs of both macro- (≥ 5 mm) and micro- (< 5 mm) sized plastics (Drummond et al., 2022; van Emmerik et al., 2022).

In stream systems, flood events may represent key moments that deliver new microplastics as runoff from land sources to the system as well as export microplastics out of burial in channel sediment storage when high flow mobilizes the bed material (Drummond et al., 2022). Early evidence for floods as transporters of microplastics include microplastic export from sediment storage in streams because of these discharge events (Hurley et al., 2018) as well as microplastic accumulation in coastal sediment downstream of fluvial systems after long flood periods (Veerasingan et al., 2016). More recent studies have also identified higher levels of microplastics in water samples following flood events, though these observations include samples collected after multi-month flood seasons (i.e., not after a single flood; Gündogdu et al., 2018; Lahon and Handique, 2024) and during the falling limb of individual flood events (e.g., de Carvalho et al., 2022).

Studies that employ high frequency sampling of microplastic fluctuations during floods that specifically capture discharge maxima have been uncommon but thus far demonstrate that microplastic content in water can peak and recede with discharge responses (Hitchcock, 2020; Baraza and Hasenmueller, 2023). However, research on large rivers has also identified alternate responses including dilution (i.e., lower levels of microplastics related to flooding; Scircle et al., 2020) and chemostasis (i.e., no change in microplastic levels during flooding; Hasenmueller and Ritter, 2024; Treilles et al., 2022). Improved understanding of microplastic sourcing, accumulation, and mobilization by flood events is thus still needed (Drummond et al., 2022).

Along with export of microplastics from sediment storage as a potential source into flood waters, flood events are accompanied by other key inputs of anthropogenic microparticles including wet atmospheric deposition and stormwater runoff (Abbasi, 2021; Sewwandi et al., 2024). The profile of anthropogenic microparticles throughout floods may vary as these unique sources move through a watershed. Urban stormwater runoff can also contain higher levels of harmful contaminants (e.g., heavy metals; Wei et al., 2010) that might enhance the toxicity of the anthropogenic microparticles transported with urban runoff due to the adsorption of chemical contaminants (Rochman et al., 2014). The sourcing and conveyance of microplastics in water during high flow periods are thus recognized as areas requiring further study and potential intervention to reduce export of harmful microplastics downstream (Koutnik et al., 2021; Sewwandi et al., 2024).

Microplastics comprise a portion of a larger suite of anthropogenic microparticles including environmentally prevalent semi-synthetic (e.g., rayon) and modified natural (e.g., dyed cotton) microfibers (Athey and Erdle, 2022; Finnegan et al., 2022). These non- or semi-synthetic microparticles are found to increase during peak flood conditions alongside microplastics (Baraza and Hasenmueller, 2023). Though microplastics are more frequently studied, non- or

semi-synthetic anthropogenic microparticles can also persist in the environment and impact organism health. We therefore need more holistic approaches to study the full suite of anthropogenic microparticles to accurately understand this group of contaminants (Adams et al., 2021; Kim et al., 2021; Park et al., 2004; Sait et al., 2021; Sanchez-Vidal et al., 2018).

Accordingly, the objective of our research is to clarify the sourcing and timing of anthropogenic microparticle conveyance by flood events. Anthropogenic microparticles (including microplastics and other humanmade materials that are < 5 mm) were quantified at high temporal resolution (< 1 h sampling increments) throughout four flood events in an urban stream near St. Louis, Missouri, United States. Flood events across multiple seasons and with varying peak discharge levels (~1-60 m^3/s) were assessed to determine the influence of flood characteristics on anthropogenic microparticle transport. Additional samples of suspected sourcing compartments were also obtained, such as wet atmospheric deposition (i.e., rain), urban runoff from roads, and bed sediment before and after the floods, to compare the characteristics of anthropogenic microparticles between high flow samples from the stream and potential source samples.

3.3. Materials and Methods

3.3.1. Sampling Site

Samples were collected from the Deer Creek watershed (Fig. 3.1.), which is located near St. Louis, Missouri, United States. Our sampling site was located in the middle of the catchment, ~ 150 m upstream from a United States Geological Survey (USGS) gaging station (07010055; Fig. 3.1.), from which we obtained discharge data for our study. The landscape draining to our sampling site largely consists of lower intensity developed areas (i.e., residential zones), but it is also crossed by a major interstate (I-64; Fig. 3.1.). At and immediately upstream of the sampling site, the stream is within a private, protected area consisting of restored native prairies and forest

managed by the Litzsinger Road Ecology Center (an affiliate of the Missouri Botanical Garden; Fig. 3.1.). Downstream from the site, Deer Creek drains into the River des Peres and subsequently the Mississippi River. Sample collection took place during four floods with unique antecedent moisture conditions and flow attributes in October 2022, February 2023, April 2024, and July 2024 (Table 3.1.).

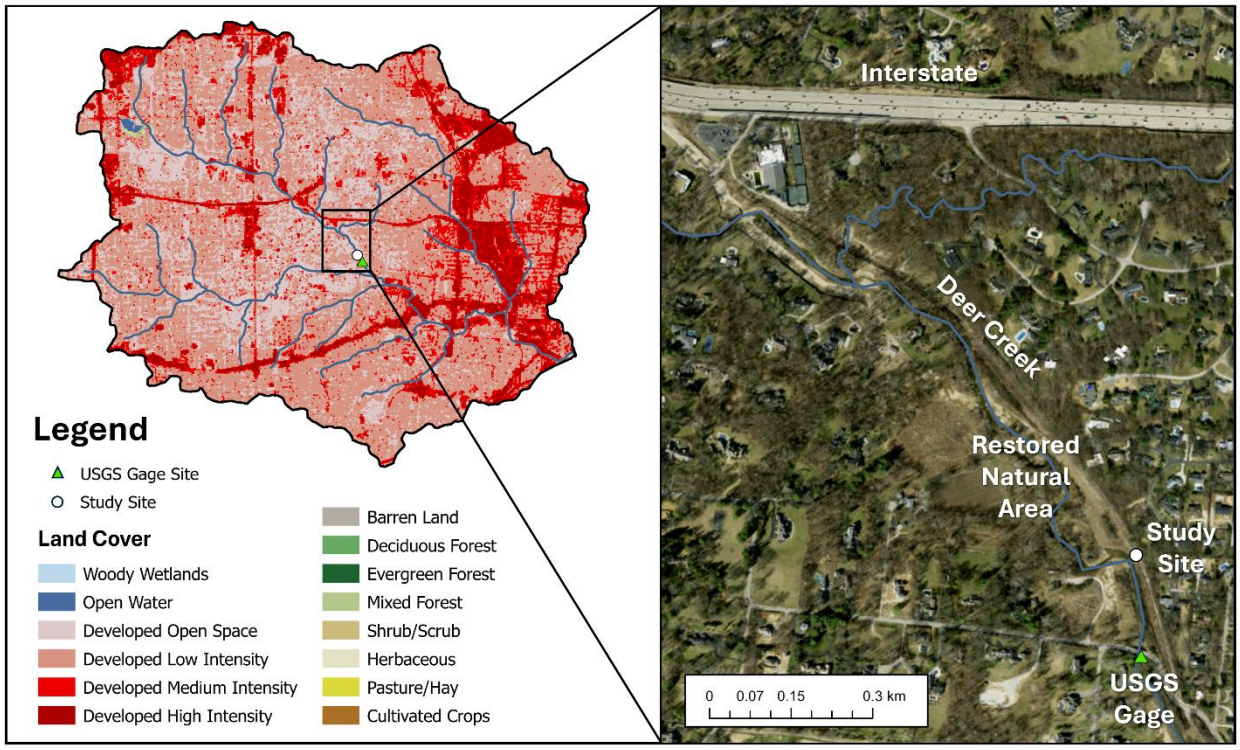

Figure 3.1. *The sampling site and USGS gage locations within the Deer Creek basin. The land use for the watershed is provided in the map (Dewitz, 2023). The inset map shows the location of the conservation area and interstate upstream of the sample site (Esri, 2024).*

3.3.2. Sample and Data Collection

3.3.2.1. Sample collection

Water and sediment samples were obtained from our Deer Creek monitoring site before, during, and following four flood events in October 2022, February 2023, April 2024, and July 2024 (Table 3.1.). Prior to the collection of high temporal resolution water samples during each flood event, single pre-flood samples for both water and sediment were acquired at baseflow conditions. We define baseflow as the stream's discharge level when precipitation had not been delivered to the basin for at least 3 days. Each baseflow water sample consisted of 2 L of water collected in two 1-L amber glass bottles that were pre-rinsed with filtered distilled deionized (DDI) water and the site water prior to sample collection. Each pre-flood sediment sample was taken by subsampling three evenly spaced points laterally across the channel using a custom Hess sampler with a 74-80 µm mesh. The three sediment subsamples were homogenized in a single 1-L glass mason jar to obtain a representative sample of the channel bed sediment prior to the flood event (see Hernandez and Hasenmueller, 2024, for additional method details).

Table 3.1. *Characteristics of each flood event.*

Attribute	October 2022	February 2023	April 2024	July 2024
Time since last discharge event (days)[a]	34	14	7	4
Event precipitation (mm)	61.7	23.1	25.1	52.1
Peak discharge (m^3/s)	13.0	15.3	1.7	61.7
Peak TSS (mg/L)	471	1111	23	663
Average baseflow water anthropogenic microparticle content (counts/L)	1.2	0.0	0.0	0.0
Peak water anthropogenic microparticle content (counts/L)	17.4	15.5	6.5	13.5
Average flood water anthropogenic microparticle content (counts/L)	5.5	1.2	0.6	2.3
Rainfall anthropogenic microparticle content (counts/m^2/h)[b]	164.5	355.8	6.0	233.0
Road runoff anthropogenic microparticle content (counts/L)	16.2	0.0	n/a	0.0
Anthropogenic microparticle loss from the sediment (counts/kg)[c]	122.8	23.9	19.1	54.8

[a]Days since the last flood with a discharge response of > 1 m^3/s.
[b]The methodologies for sampling atmospheric deposition varied over the study period, convoluting comparisons among floods. For the July 2024 flood, an average of two samples is presented.
[c]Calculated by subtracting the post-flood sediment anthropogenic microparticle content from the pre-flood sediment anthropogenic microparticle content.

Following the pre-flood water and sediment sampling, an atmospheric deposition sampler that consisted of a funnel connected to a bottle (see Dris et al., 2016) was deployed at our site. The atmospheric sampling method varied slightly among our selected flood events. In October 2022 and February 2023, atmospheric deposition samples were respectively taken using a plastic funnel and glass funnel, and we did not rinse any material deposited on the funnels into the glass sample collection bottles. In April 2024 and July 2024, a stainless-steel funnel and glass bottle were used for the atmospheric deposition sampling. We also used 100-mL of filtered DDI water to rinse anthropogenic microparticles from the funnel into the bottle before sample collection according to the method in Chapter 5. These varying techniques confound the comparison of anthropogenic microparticle quantities collected from atmospheric deposition across flood events. Atmospheric deposition samples were typically collected for at least 24 h, including dry deposition periods before and after rainfall. In July 2024, the 1-L glass bottle was full of rainfall after the first 5 h of sampling and a second bottle was placed out for the remainder of the event (Fig. 3.S1.).

High frequency sampling of stream water during the flood events was performed using an automatic sampler (i.e., a Teledyne ISCO 6712 Full-Size Portable Sampler) with semi-opaque white polypropylene (PP) bottles (that had been triple rinsed with DDI) and clear polyvinyl chloride (PVC) tubing. The autosampler was programmed to rinse the entire tubing length before and after each sample collection with site water. These 1-L water samples were collected at < 1 h frequency during the rising limb and peak of the flood hydrographs, and the more protracted falling limb responses were captured with > 1 h frequency samples (Fig. 3.S1.). A total of 206 water samples (including both the hand-collected and autosampler samples) were obtained across the four floods. For each flood sample, approximately 120 mL was removed from the bulk sample for geochemical analyses. We analyzed 95 of the floodwater samples that

captured key moments throughout each discharge event for anthropogenic microparticles using the remaining ~ 880 mL (Fig. 3.S1.).

During each flood event, a road runoff sample was collected from a storm drain near a bridge over Deer Creek that is downstream of the flood sampling site but located immediately next to the USGS gaging station (Fig. 3.1.). Each runoff sample was obtained in a 1-L amber glass bottle that was pre-rinsed three times with DDI water and runoff water prior to sample collection. During the smallest captured flood event in April 2024, the flow of water from the road was not sufficient to collect a runoff sample. Finally, the post-flood baseflow water and sediment samples were hand-collected with the same methodology as the pre-flood baseflow samples. The detailed timing of each sample type for the four floods as well as which in-flood samples were selected for anthropogenic microparticle analysis are presented in Fig. 3.S1.

3.3.2.2. Water and sediment physicochemical data and analysis

Water quality data (e.g., temperature, specific conductivity, and turbidity) were monitored at 5-minute intervals for each flood with a YSI EXO2 Multiparameter Sonde collocated with the autosampler. These continuous water quality data were drift-corrected using the R package driftR (Shaughnessy et al., 2019). The corrected specific conductivity data were used to perform hydrograph separations for each flood event (see Baraza and Hasenmueller, 2023, and Hasenmueller et al., 2017, for the full hydrograph separation method; Fig. 3.S2.). Turbidity measurements obtained with a Hach 2100Q Portable Turbidimeter for all hand- and autosampler-collected water samples were used rather than the continuous data from the sonde for comparisons with the anthropogenic microparticle content. Water samples were analyzed for total suspended solids (TSS) in the laboratory following United States Environmental Protection Agency (USEPA) Method 160.2 (USEPA 1971). Pre- and post-flood sediment samples were

assessed for sediment grain sizes in the laboratory using the sieving method described in Hasenmueller et al. (2023).

In October 2022, the in situ sonde stopped recording part-way through the flood, and specific conductivity and turbidity data had to be obtained in the laboratory from the water samples that were collected by the autosampler for the remainder of the flood (respectively using a Fisherbrand Accumet XL200 Benchtop pH/Conductivity Meter and Hach 2100Q Portable Turbidimeter). When we measured specific conductivity for samples collected while the sonde was still recording, we found that the field and laboratory results were comparable (Fig. 3.S3.). However, since the units for turbidity were not the same between the sonde (i.e., FNU) and turbidimeter (i.e., NTU), we used the more complete turbidimeter dataset to plot turbidity for the October 2022 flood for which the continuous data were incomplete (Fig. 3.S3.).

Discharge data were collected from the nearby USGS gauge 07010055 at 5-minute intervals for each flood event (USGS, 2025). Hourly precipitation data were acquired from an Automated Surface Observing System unit located at the St. Louis Lambert International Airport. These precipitation data were downloaded from a historical data archive (Iowa Environmental Mesonet (IEM), 2025).

3.3.3. Anthropogenic Microparticle Characterization

3.3.3.1. Environmental samples

To isolate anthropogenic microparticles from our environmental samples, water samples were filtered using an all-glass filtration system. Sediment samples were dried at 55 °C, then a subset of ~ 250 g was removed for a density separation technique that employed a prefiltered 1.20 kg/L NaCl solution (additional method details can be found in Hasenmueller et al., 2023). After the density separation was complete, the supernatant was filtered with the same filtration system as the water samples. The resulting filters for both the water and sediment samples were

visually inspected for suspected anthropogenic microparticles, which were identified by their lack of cellular/organic structures, color, and malleability/resistance to breakage. The suspected anthropogenic microparticles were photographed, categorized by their color and morphology, and measured along their longest axis. Suspected anthropogenic microparticles were then removed from the filters and stored in prefiltered 10% ethanol until further analysis. White fragments that had a similar appearance to shed pieces from the autosampler bottle lids were not counted in the total quantity of anthropogenic microparticles for any samples (see Baraza and Hasenmueller, 2023).

A ~ 8% subset (n = 15) of all visually identified and detectable anthropogenic microparticles (see Section 3.3.3.2. for details about our method detection limits) from stream water (n = 197) were analyzed for material type using a custom-built confocal Raman Spectroscopy system. The system includes a BX41 Olympus Raman Microscope, solid-state laser (λ = 532 nm beam that maintains a 1.50 mm diameter Gaussian profile), iHR550 spectrometer (0.55 m optical length) with diffraction grating of 1800 gr/mm, and a Synapse CCD that maintained a constant operating temperature of - 70 °C. A front slit width of 200 µm, pinhole diameter of 400 µm, power of 15-50 mW, spectral range of 250-3500 cm^{-1}, and acquisition times of 20-200 s were used for analysis. Horiba LabSpec software's baseline noise correction method was applied to all spectra.

The resulting spectra were uploaded to Open Specy to check for matches with publicly available anthropogenic microparticle libraries, employing automatic preprocessing steps of min-max normalization, smoothing, and wavenumber conformation using linear interpolation (Cowger et al., 2021). If the Open Specy match value was > 0.6 and the top two matches were for the same material type, these matches were accepted. The match rate averaged at 0.79. All

particles that matched with cellulosic material (including both cellulose and cotton matches) were dyed with humanmade colors and were therefore called “anthropogenic cellulose”.

3.3.3.2. Quality assurance and quality control measures

Steps to reduce the possible contamination of our environmental samples by ambient anthropogenic microparticles were taken throughout sample processing and included wearing 100% cotton and bright colored clothing when handling samples, prefiltering all working solutions, triple rinsing glassware before use, and filtering samples within a fume hood. To assess potential contamination from the autosampler, two autosampler field blanks were collected using the onsite installation which consisted of pumping prefiltered DDI water from an amber glass bottle at stream level up to the autosampler location and into one of the PP autosampler bottles. Two laboratory autosampler blanks were also obtained, again with prefiltered DDI water pumped through the autosampler tubing into a PP bottle. For each autosampler blank, a 1-L bottle of prefiltered DDI water was used to rinse the tubing (during the pre-programmed rinse cycle used for all autosampler samples). The tube was then transferred into a new 1-L bottle of prefiltered DDI water for the collection of the blank.

Procedural blanks for processing the water and sediment samples respectively consisted of taking pre-filtered DDI water or pre-filtered NaCl solution through the same processing steps as the environmental samples. Blank data were used to calculate a limit of detection (LOD) for each environmental sample type. The DDI water blanks were used for the rainfall, runoff, and flood water sample LOD calculations, while the NaCl solution blanks were used for the bed sediment sample LOD calculations. For each blank type, the LOD was equal to the average of the anthropogenic microparticles found in each blank plus three times the standard deviation. The LOD for each sample type was rounded to a whole number and any environmental sample with a total anthropogenic microparticle quantity below the LOD value was corrected to zero

prior to other data analyses. Samples that were corrected to zero were not considered detectable for the anthropogenic microparticle material type analyses described in Section 3.3.3.1. Blank information and LOD calculations for each sample type are provided in Table 3.S1.

3.3.4. Data Analysis

All statistical analyses were performed in R and Microsoft Excel. Nonparametric Spearman's correlation analyses were used to test relationships among the data (with $\alpha = 0.05$). Figures were created using ArcGIS Pro Version 3.0.3, R, and Microsoft Excel.

3.4. Results

3.4.1. Flood Event Hydrologic and Physicochemical Responses

The four sampled flood events had unique antecedent moisture conditions and discharge responses (Table 3.1.; Fig. 3.2.). The October 2022 flood event followed the longest dry period and had the largest amount of rainfall, though the rainfall was spread over a longer period than any other event (Table 3.1.; Fig. 3.2.). These pulses of rain led to a long series of relatively small discharge peaks during the October 2022 flooding. The February 2023 flood took place after snowfall and road salting that elevated specific conductivity levels in the stream (Fig. 3.S2.). This event also featured ~ 2.5× higher peak TSS values compared to the October 2022 flood that had a similar peak discharge value (Table 3.1.). The April 2024 flood event featured the lowest peak discharge at 1.7 m^3/s, despite having similar total precipitation to the February 2023 flood. Finally, the July 2024 flood was the largest sampled discharge event with peak flow of 61.7 m^3/s, even though it had a lower precipitation total than the October 2022 flood and a lower peak TSS value than the February 2023 flood (Table 3.1.). While turbidity and TSS typically increased near discharge maxima during the flood events, the long October 2022 flood featured a discharge peak towards the end of the event that was not accompanied by high turbidity or TSS (Fig. 3.2.).

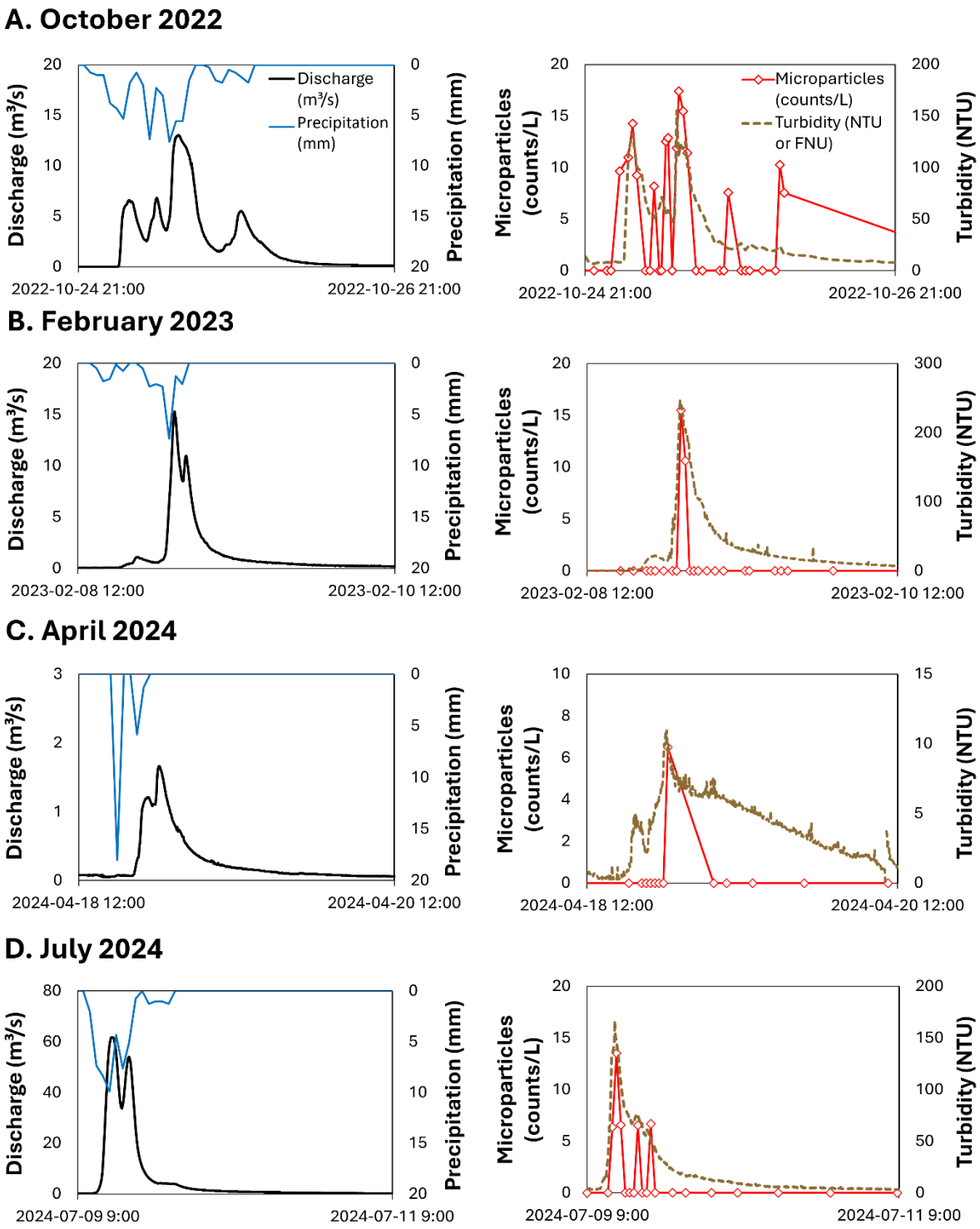

Figure 3.2. *Discharge and precipitation (left) and anthropogenic microparticle content and turbidity (right) for the (A) October 2022, (B) February 2023, (C) April 2024, and (D) July 2024 flood events. The turbidity for the October 2022 flooding response is from point measurements rather than continuous data and consequently has different units (see section 3.3.2.2.).*

3.4.2. Anthropogenic Microparticle Content and Characteristics in Stream Water

Anthropogenic microparticles were found above the LOD in only 23% of water samples (n = 22), all but one of which were samples taken during high flow conditions. The October 2022 flood event had the highest peak anthropogenic microparticle content (17.4 counts/L), highest average and standard deviation for anthropogenic microparticles across the non-baseflow samples (5.5 ± 6.1 counts/L), and the only baseflow sample with detectable anthropogenic microparticles, which occurred between the first rainfall and the onset of the discharge response (Table 3.1., Fig. 3.2.). While most samples with anthropogenic microparticle abundances above the LOD were collected during discharge and turbidity peaks, some samples with detectable anthropogenic microparticles were obtained on the rising or falling limbs of the respectively longer and larger discharge events in October 2022 and July 2024 (Fig. 3.2.).

Most anthropogenic microparticles in the stream water samples were fibers (96% of the total anthropogenic microparticles detected; n = 197), and the most common fiber colors were clear, blue, and black (Fig. 3.3.; Fig. 3.4.). Anthropogenic microparticle lengths in the water had an average and standard deviation of 1127.5 ± 870.5 μm (Fig. 3.4.). Color-morphology combinations of the anthropogenic microparticles were most similar between the October 2022 and April 2024 floods (i.e., a predominance of fibers that were clear and blue) and February 2023 and July 2024 floods (i.e., more black fibers, red fibers, and yellow fragments; Fig. 3.3.). The subset of anthropogenic microparticles analyzed with Raman spectroscopy (n = 15) were 78% polyethylene terephthalate (PET; matches also included polyester), 16% anthropogenic cellulose, and 6% PP (Fig. 3.3.). While PET was found during every flood event, PP was found only during the February 2023 flood, and anthropogenic cellulose was found only during the October 2022 and July 2024 flood events (Fig. 3.3.).

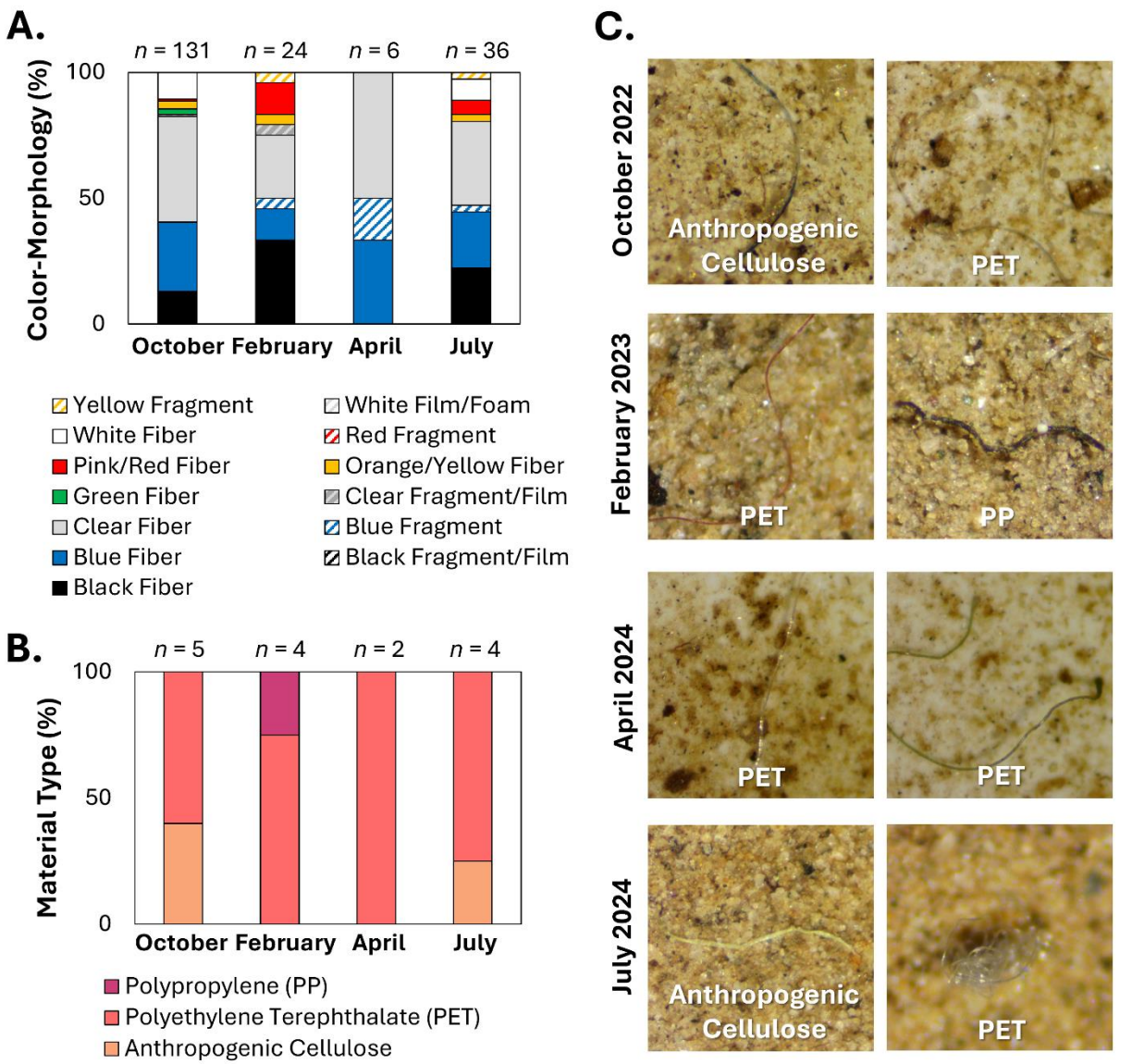

Figure 3.3. *The percentage of each (A) color-morphology combination for the total anthropogenic microparticle content for water samples above the LOD and (B) material type found in the subset of anthropogenic microparticles analyzed with Raman spectroscopy for each flood event (sample numbers as n values are provided for both plots). (C) Example photos of anthropogenic microparticles with identified material types for each flood event, with the photo size being 1 mm by 1 mm for scale.*

3.4.3. Anthropogenic Microparticles in Potential Source Compartments

Of the sourcing compartments that we assessed, rainfall typically had the highest potential for contributing anthropogenic microparticles to the stream during a given flood event since it averaged 189.8 counts/m^2/h across all four sampled discharge events. The attributes of

deposited anthropogenic microparticles from rainfall were similar to those found in the stream water samples, with mostly clear (61%) and blue (26%) fibers (Fig. 3.4.). The anthropogenic microparticle sizes in rainfall (878.3 ± 583.6 μm) were typically smaller than those in the stream water samples (average 1127.5 ± 870.5 μm; Fig. 3.4.). However, the differences in methodologies between the October 2022 and February 2023 versus the April 2024 and July 2024 flood events affected the sizing distributions (Fig. 3.S4.). For the latter rainfall samples that were collected with a standard methodology, the average and standard deviation of anthropogenic microparticle size was significantly larger (974.5 ± 660.5 μm) than those collected earlier in our study (814.0 ± 516.0 μm; Fig. 3.S4.). During the July 2024 flood event, when two separate samples of atmospheric deposition were collected due to the high quantity of rainfall, the first sample had deposition rates almost twice as high (303.6 counts/m^2/h) as the second sample (162.5 counts/m^2/h).

The quantities and characteristics of anthropogenic microparticles in the pre- and post-flood sediment samples varied by flood. Though anthropogenic microparticle abundances and sizes always decreased between the pre- and post-flood sediment samples, the differences were not significant (Fig. 3.S5.; Fig. 3.S6.). The majority of anthropogenic microparticles in the sediment samples were clear fibers (45%), followed by blue fibers (33%; Fig. 3.4.), and these color-morphology combinations were similar before and after the flood events as well as to the stream water samples. Anthropogenic microparticles in sediment had significantly (pairwise Wilcoxon with $p < 0.05$) larger sizes than those in the rain, runoff, and stream water, averaging 1296.3 ± 867.4 μm (Fig. 3.4.). The October 2022 flood had both the highest amount of anthropogenic microparticles present in the pre-flood sediment (226.1 counts/kg) and the largest amount of anthropogenic microparticles lost from the sediment when the post-flood sample

content was subtracted from the pre-flood sample content (122.8 counts/kg; Table 3.1.; Fig. 3.S6.).

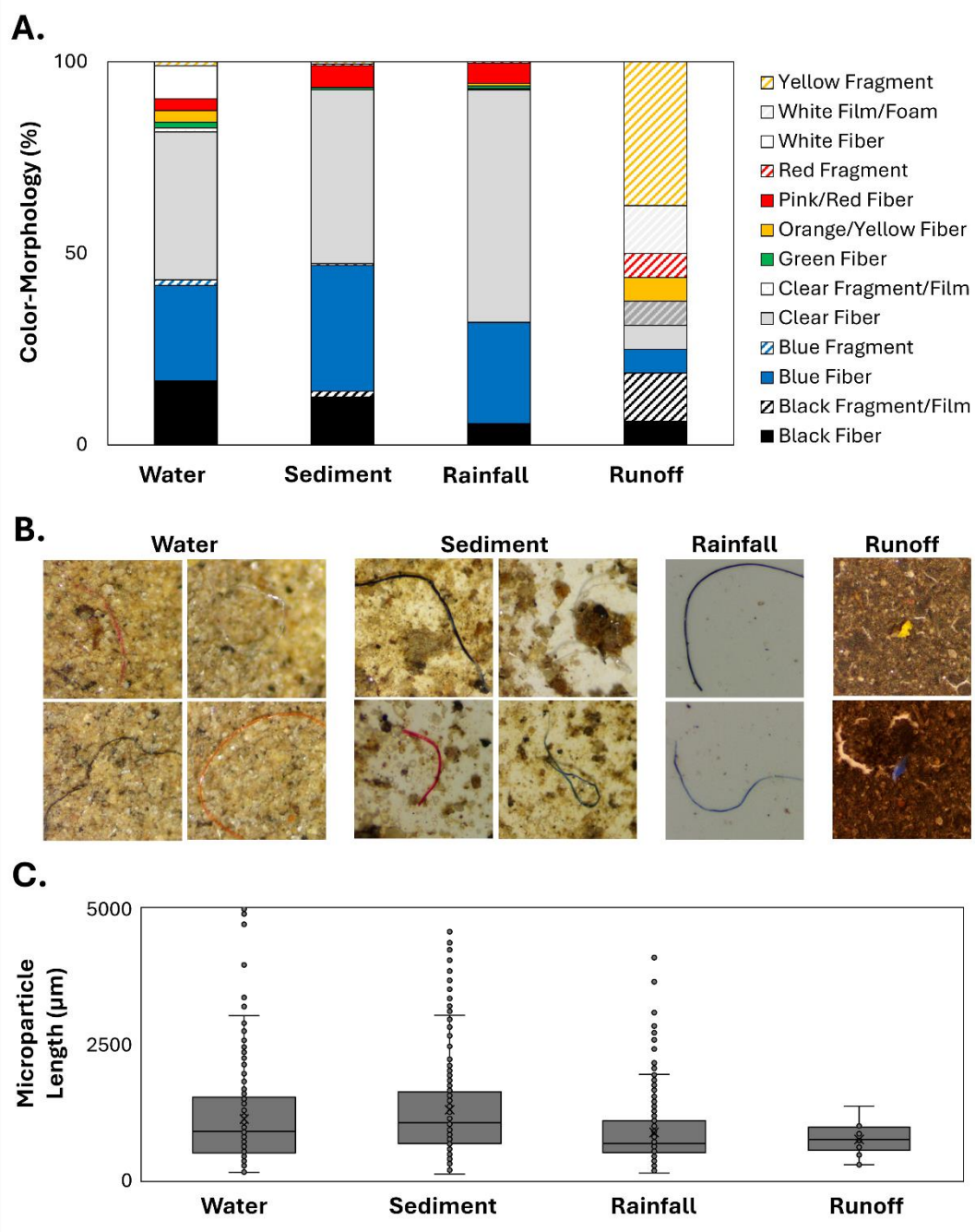

Figure 3.4. *(A) The percentage of each color-morphology combination for anthropogenic microparticles above the LOD in all compartments across all four floods, (B) example photos of common anthropogenic microparticle types in each compartment, with photo size being 1 mm by 1 mm for scale, and (C) comparison of the anthropogenic microparticle sizing among the compartments across all four floods.*

Road runoff had the lowest anthropogenic microparticle content of all the sources that were examined, with only one sample above the LOD (at 16.2 counts/L) that was collected during the October 2022 flood event. The majority of the anthropogenic microparticles in the runoff were fragments (63%; Fig. 3.4.). The prevalence of this anthropogenic microparticle morphology was unique compared to the other compartments, which were > 95% fibers. The average and standard deviation of the road runoff anthropogenic microparticle size was 749.7 ± 276.3 µm (Fig. 3.4.).

3.4.4. Relationships among Stream Physicochemical Parameters and Anthropogenic Microparticle Content and Attributes in the Water and Sediment

Anthropogenic microparticle concentrations in the stream water during all flood events correlated significantly and positively with discharge, the fraction of event water, TSS, and turbidity. The February 2023 and April 2024 floods had too few data points above the LOD to assess correlations for these events individually, but the October 2022 and July 2024 floods had at least five samples above the LOD that allowed for their individual assessments (Fig. 3.5.). In October 2022, significant and positive correlations occurred between anthropogenic microparticle concentrations and TSS as well as turbidity, while the significant relationships present in the July 2024 flood were positive correlations between anthropogenic microparticle concentrations and the fraction of event water as well as TSS (Fig. 3.5.). Specific conductivity had no relationship to anthropogenic microparticle content for individual floods or across the entire dataset. We found significant and positive relationships between the average size of anthropogenic microparticles in the stream samples and TSS for both the full dataset and the July 2024 flood, but we did not see a correlation between these parameters for the October 2022 flood event (Fig. 3.5. (D)).

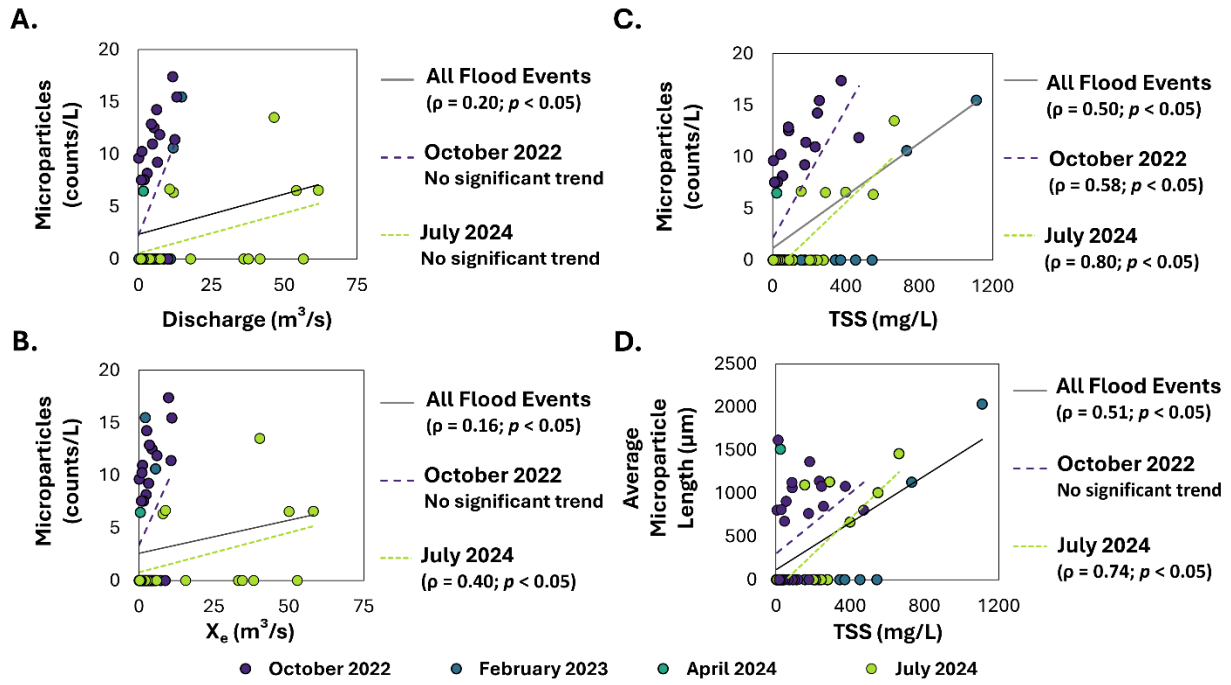

Figure 3.5. *Correlations between anthropogenic microparticle content and (A) discharge, (B) the fraction of event water (X_e), and (C) TSS. (D) Average anthropogenic microparticle sizes and TSS for the stream water samples. Trends for the data from all four floods are shown with solid lines, while trends for individual flood events with at least five data points (i.e., those in October 2022 and July 2024) are shown with dashed lines.*

The anthropogenic microparticle content in pre- and post-flood sediment samples and the sediment grain sizes of each respective sample exhibited no obvious relationships across the four floods (Fig. 3.S6.). The flood events with the greatest loss of anthropogenic microparticles from the sediment (i.e., in October 2022 and July 2024; Table 3.1.; Fig. 3.S6.) both showed a decrease in their d_{10} values. In contrast, the February 2023 and April 2024 flood events saw relatively smaller losses of anthropogenic microparticles from sediment (< 25 counts/kg) and had notable losses of finer grained sediment from the streambed (i.e., increased d_{10} values) following flooding (Fig. 3.S6.).

3.5. Discussion

3.5.1. The Extent of Anthropogenic Microparticle Transport in Stream Water during Flood Events

Though we observed consistent increases in anthropogenic microparticle content in the flood waters of Deer Creek during each event regardless of the discharge maxima (Fig. 3.2.), the peak quantities of these microparticles present during high flow were often lower than those observed during peak discharge in prior studies. During peak discharge in a flood on the Cooks River catchment, Australia, water contained 17383 microplastics/m^3 (equating to ~ 17.4 counts/L; Hitchcock, 2020), much like our sample of peak flow during the highest rainfall event in October 2022 (Table 3.1.; Fig. 3.2.). However, for a karst spring issuing from Cliff Cave (which is located in the St. Louis region ~ 20 km southeast of our Deer Creek site), much higher levels of anthropogenic microparticles were present at peak flow when the spring was in flood (up to 81.3 counts/L; Baraza and Hasenmueller, 2023), even for precipitation events with lower rainfall levels than those we observed in this study. Although few studies have peak flood flow anthropogenic microparticle data to compare to our results, this discrepancy could indicate that flood transport of anthropogenic microparticles in surface water systems is distinct compared to groundwater-fed springs.

However, 100% of anthropogenic microparticles assessed for material type in the Australian study of one flood event were synthetic (Hitchcock, 2020), while 84% of the subset of anthropogenic microparticles analyzed across four events in our study were synthetic, and only 23% of the Cliff Cave anthropogenic microparticles across four events were synthetic (Baraza and Hasenmueller). Accordingly, considering only synthetic microparticles, the highest reported flood microplastic content present at Cliff Cave (17.1 counts/L; Baraza and Hasenmueller, 2023) is very similar to the peak concentrations in both this study and the prior Australian study

(Hitchcock, 2020). Higher anthropogenic microparticle concentrations at the cave site are therefore largely due to high quantities of non-synthetic material types that were identified in this groundwater system but not the surface water systems. This material type discrepancy with the Australian study was influenced by Hitchcock's (2020) methodological differences and intention to exclude non-synthetic anthropogenic microparticles. Nevertheless, similar criteria were used to identify anthropogenic microparticles (including plastics and other material types) for the studies of Deer Creek (the present work) and Cliff Cave (Baraza and Hasenmueller, 2023), which were both conducted in the St. Louis region, suggesting a true difference between microparticle types present in the two types of hydrologic systems.

Higher quantities of non-synthetic anthropogenic microparticles in groundwater may be a result of the slower degradation of cellulose fibers in subsurface environments compared to surface settings. Indeed, cellulose fibers have been found to persist in some cave systems for thousands of years (Muller et al., 2007), though in surface conditions they are typically expected to biodegrade (Li et al., 2010). Studies of non-synthetic anthropogenic microparticles in karst systems are limited, but a comparison of anthropogenic microparticle content in the sediment of Cliff Cave (average 842.7 counts/kg at 29% synthetic; Hasenmueller et al., 2023) and Deer Creek (average 79.7 counts/kg at 51% synthetic; see Chapter 4) as well as findings from an Italian cave (163.5 counts/L at 15% synthetic in water and 4776.7 counts/kg at 8% synthetic in sediment; Balestra et al., 2024) support the hypothesis that high quantities of non-synthetic anthropogenic microparticles occur in subsurface environments compared to surface environments across multiple environmental compartments.

One prior study with flood samples at upstream and downstream river sites found higher anthropogenic microparticle concentrations in flood water occurred at the downstream site (de Carvalho et al., 2022). This observation raises the possibility that our mid-watershed Deer Creek

site might also collect lower peak flood anthropogenic microparticle concentrations than the Cliff Cave Spring outlet due to its more upstream location in the broader drainage pattern of the system. However, springs as outlets for the recharge areas of karst systems and surface water catchment outlets are not necessarily analogous. Regardless of this comparison, the prior surface water study by de Carvalho et al. (2022) suggests that the peak concentrations reported during flood events for our mid-watershed site on Deer Creek are likely lower than would be found at the watershed's outlet.

Across the four discharge events that we compared, flood characteristics and quantities of anthropogenic microparticles transported at peak flow were not obviously linked, which is a similar result to prior comparisons of multiple floods at Cliff Cave (Baraza and Hasenmueller, 2023). Antecedent moisture conditions (e.g., long dry periods that may have enhanced the potential for anthropogenic microparticle accumulation in the Deer Creek system prior to the October 2022 and February 2023 flood events) as well as large magnitude discharge responses (i.e., 61.7 m^3/s in July 2024) resulted in peak anthropogenic microparticle content within a similar range of 13.5-17.4 counts/L (Table 3.1.). The April 2024 event, which was by far the smallest at 1.7 m^3/s for its peak discharge, was unique in having only one sample above the LOD with 6.5 counts/L present (Table 3.1.). These findings suggest a potential response threshold for the quantity of anthropogenic microparticles transported in flood waters that is based on the frequency and size of discharge events.

3.5.2. The Sourcing and Timing of Anthropogenic Microparticle Transport in Stream Water during Flood Events

The comparison of anthropogenic microparticles in flood water samples to their potential origins during each discharge event demonstrates the complexity of the sourcing of these contaminants to waterways. Each flood event featured unique timing of anthropogenic microparticle transport (Fig. 3.2.) as well as distinctive assemblages of their colors, morphologies, and material types (Fig. 3.3.). Given the similarities in amounts and types of anthropogenic microparticles in the flood water compared to those in the rain and sediment (Fig. 3.4.), atmospheric deposition and sediment storage seem to be the most likely sourcing compartments for the anthropogenic microparticles present in the sampled flood events. Higher deposition rates in the first rainfall sample of the July 2024 flood event compared to a subsequent sample suggests a potential initial flush of anthropogenic microparticles from the atmosphere in the early hours of the rainfall event. This wash out effect has been documented in prior studies (Abbasi, 2021). Flushing of anthropogenic microparticles from sediment storage is evidenced by the consistent decreases in anthropogenic microparticle levels between the pre- and post-flood sediment samples (Fig. 3.S5., Fig. 3.S6.) as well as the significant and positive relationships between water anthropogenic microparticle content and TSS and turbidity (Fig. 3.5.).

Although we only analyzed material types for the anthropogenic microparticles in the stream water during our selected flood events (finding 78% PET, 16% anthropogenic cellulose, and 6% PP; Fig. 3.3.), we can compare to prior studies of anthropogenic microparticles in the local atmosphere (where 45% cotton and 27% PET were found, see Chapter 5) and Deer Creek sediment (where 30% PET, 24% cotton, and 11% PP were found, see Chapter 4). These material type results confirm that the atmosphere and sediment are potential sources for the flood transported anthropogenic microparticles. Though road runoff material types remain unknown,

the low concentrations of anthropogenic microparticles present in this compartment (i.e., only one sample above the LOD) that are of unique morphologies (i.e., mostly non-fibers; Fig. 3.4.) compared to the flood water anthropogenic microparticles suggest that road runoff is not a major source of these pollutants to Deer Creek during flood events.

The observed fluctuation of anthropogenic microparticle content during floods aligned with increasing and decreasing discharge and sediment transport (evidenced by significant and positive relationships between the anthropogenic microparticle abundances and discharge, event water, TSS, and turbidity; Fig. 3.5.) and is consistent with the observations of the two prior studies that featured high temporal resolution sampling throughout flood events (Baraza and Hasenmueller, 2023; Hitchcock, 2020). Although significant and positive relationships were found between anthropogenic microparticle levels and both discharge and sediment transport metrics (i.e., TSS and turbidity) in our dataset (Fig. 3.5.), the timings and thresholds at which anthropogenic microparticles became detectable were unique to each flooding event (Fig. 3.2.). For example, in the February 2023 and July 2024 flood events, high quantities of suspended solids were moved before anthropogenic microparticles were transported at levels above the detection limit in water (Fig. 3.2.). However, in the other flooding events, a similarly high threshold was not required.

Decoupled relationships between water anthropogenic microparticle content and sediment transport parameters suggest both sourcing from non-sediment compartments (via high anthropogenic microparticle concentrations when TSS values were low) and the movement of sediment that did not contain high levels of anthropogenic microparticles (via high TSS values when anthropogenic microparticle concentrations were low). Though studies on sediment anthropogenic microparticle presence across stream channels are limited, research has suggested that, in net erosional environments (e.g., exposed floodplains only covered by water during high

flow events), low microplastic levels are likely due to erosion inhibiting their deposition in the sediment (Gonzalez-Inca et al., 2018; Van Daele et al., 2024). Sediment erosion during large floods (e.g., during our July 2024 flood event) or snowmelt-related bank erosion (e.g., during our February 2023 flood event) would then theoretically introduce high quantities of sediment with low anthropogenic microparticle content and may have caused the observed elevated sediment transport variables (i.e., TSS and turbidity) that outpaced anthropogenic microparticle increases in the flood waters for these two events.

Unique instances of anthropogenic microparticle presence before the onset of the discharge and turbidity responses as well as in samples on the falling limb of the hydrograph that likely followed the exhaustion of sediment sourcing occurred in the October 2022 flood (Fig. 3.2.). The behavior of these samples is unexplained by any relationship to discharge or sediment transport increases but might be related to atmospheric deposition of anthropogenic microparticles to the stream. Indeed, prior to a discharge response beginning, first rainfall could enhance anthropogenic microparticle deposition from the atmosphere. Likewise, following flood events, dry deposition rates can still be quite high in the watershed (see Chapter 5). Although only the July 2024 flood event had more than one temporal rainfall sample, higher anthropogenic microparticle levels in the first sample suggest that an initial flush of these microparticles from the atmosphere could be possible when rainfall begins. However, these deposited anthropogenic microparticles may not always be incorporated into stream water samples taken with the autosampler, which does not target the stream's surface.

More field studies examining high resolution temporal samples throughout flood events in other systems are necessary to determine whether the currently identified patterns of microplastic flux throughout flood events hold across other stream systems. Future work should also continue to compare potential sources of anthropogenic microparticles during flood events

(i.e., rainfall, road runoff, export from sediment storage, and other sources as they are relevant to a given system, such as sewer overflows) since studies which examine only one potential source might draw conclusions about its importance while missing another key input to the system. Thorough understanding of the most impactful sources of microplastics and other anthropogenic microparticles into a hydrologic system during high transport periods (like flood events) can help identify where management efforts could be focused to reduce the largest inputs of these contaminants to waterbodies.

3.6. Conclusions

Our findings join the growing body of evidence that flood events can elevate microplastic transport in stream systems. High levels of anthropogenic microparticles (including microplastics) in rainfall, which shared similar characteristics with the flood water anthropogenic microparticles, demonstrate the influence of atmospheric fallout as a source of these pollutants to the stream during flood events. Likewise, anthropogenic microparticles within our stream water samples typically increased alongside discharge and sediment transport during flood events and had similar characteristics and material types to anthropogenic microparticles in the stream's sediment. These findings suggest that export out of sediment storage is also a key source of microplastics into the stream water during flood events. The extent and timing of microplastic export by flooding depends on antecedent moisture conditions such as prior dry periods that may enhance sediment microplastic storage as well as in-flood conditions such as the quantity of rainfall and the erosive impacts of snowmelt. Further research using high frequency sampling throughout flood events is needed to improve our understanding of the complex set of hydrologic conditions and potential sources controlling microplastic transport during flooding.

3.7. Acknowledgements

This work was supported by a United States Geological Survey Water Resources Research Act Program grant administered through the Missouri Water Center (Award: G21AP10582-03). We thank James Faupel and Adam Rembert for their help coordinating field sampling and long-term deployment of sampling equipment at Deer Creek at the Litzsinger Road Ecology Center as well as those who helped with laboratory and field work. We also appreciate Dr. Gregory Triplett and Leo Schrader for facilitating the use of Raman spectroscopy instrumentation at the Precision Imaging Research Lab.

3.8. References

Abbasi, S., 2021. Microplastics washout from the atmosphere during a monsoon rain event. J. Hazard. Mater. Adv. 4, 100035.

Adams, J.K., Dean, B.Y., Athey, S.N., Jantunen, L.M., Bernstein, S., Stern, G., Diamond, M.L., Finkelstein, S.A., 2021. Anthropogenic particles (including microfibers and microplastics) in marine sediments of the Canadian Arctic. Sci. Total Environ. 784, 147155.

Akanyange, S.N., Zhang, Y., Zhao, X., Adom-Asamoah, G., Ature, A.A., Anning, C., Tianpeng, C., Zhao, H., Lyu, X., Crittenden, J.C., 2022. A holistic assessment of microplastic ubiquitousness: Pathway for source identification in the environment. Sustain. Prod. Consum. 33, 113-145.

Athey, S.N., Erdle, L.M., 2022. Are we underestimating anthropogenic microfiber pollution? A critical review of occurrence, methods, and reporting. Environ. Toxicol. Chem. 41(4), 822-837.

Balestra, V., Galbiati, M., Lapadula, S., Barzaghi, B., Manenti, R., Ficetola, G.F., Bellopede, R., 2024. The problem of anthropogenic microfibres in karst systems: Assessment of water and submerged sediments. Chemosphere. 363, 142811.

Baraza, T., Hasenmueller, E.A., 2023. Floods enhance the abundance and diversity of anthropogenic microparticles (including microplastics and treated cellulose) transported through karst systems. Water Res. 242, 120204.

Cowger, W., Steinmetz, Z., Gray, A., Munno, K., Lynch, J., Hapich, H., Primpke, S., De Frond, H., Rochman, C., Herodotou, O., 2021. Microplastic spectral classification needs an open source community: Open Specy to the rescue! Anal. Chem. 93(21), 7543-7548.

De Carvalho, A.R., Riem-Galliano, L., ter Halle, A., Cucherousset, J., 2022. Interactive effect of urbanization and flood in modulating microplastic pollution in rivers. Environ. Pollut. 309, 119760.

Dewitz, J., 2023. National Land Cover Database (NLCD) 2021 Products: U.S. Geological Survey data release.

Dris, R., Gasperi, J., Saad, M., Mirande, C., Tassin, B., 2016. Synthetic fibers in atmospheric fallout: A source of microplastics in the environment? Mar. Poll. Bull. 104(1-2), 290-293.

Drummond, J.D., Schneidewind, U., Li, A., Hoellein, T.J., Krause, S., Packman, A.I., 2022. Microplastic accumulation in riverbed sediment via hyporheic exchange from headwaters to mainstems. Sci. Adv. 8(2), eabi9305.

Esri., 2024. "World Imagery" [basemap]. https://www.arcgis.com/home/item.html?id=10df2279f9684e4a9f6a7f08febac2a9. Accessed January 03, 2025.

Finnegan, A.M.D., Susserott, R., Gabbott, S.E., Gouramanis, C., 2022. Man-made natural and regenerated cellulosic fibres greatly outnumber microplastic fibres in the atmosphere. Environ. Pollut. 310, 119808.

Gonzalez-Inca, C., Valkama, P., Lill, J., Slotte, J., Hietaharju, E., Uusitalo, R., 2018. Spatial modeling of sediment transfer and identification of sediment sources during snowmelt in an agricultural watershed in boreal climate. Sci. Total Environ. 612, 303-312.

Gündogdu, S., Cevik, C., Ayat, B., Aydogan, B., Karaka, S., 2018. How microplastics quantities increase with flood events? An example from Mersin Bay NE Levantine coast of Turkey. Environ. Pollut. 239, 342-350.

Hasenmueller, E.A., Baraza, T., Hernandez, N.F., Finegan, C.R., 2023. Cave sediment sequesters anthropogenic microparticles (including microplastics and modified cellulose) in subsurface environments. Sci. Total Environ. 893, 164690.

Hasenmueller, E.A., Criss, R.E., Winston, W.E., Shaughnessy, A.R., 2017. Stream hydrology and geochemistry along a rural to urban land use gradient. Appl. Geochem. 83, 136-149.

Hasenmueller, E.A., Ritter, A.N. 2024. Microplastic chemostasis and homogeneity during a historic flood on the Mississippi River. Environ. Eng. Sci. 41(12), 563-573.

He, B., Wijesiri, B., Ayoko, G.A., Egodawatta, P., Rintoul, L., Goonetilleke, A., 2020. Influential factors on microplastics occurrence in river sediments. Sci. Total Environ. 738, 139901.

Hernandez, N.F., Hasenmueller, E.A., 2024. Anthropogenic macroscale and microscale debris (including plastics) have differing spatial distributions across a small urban watershed. Environ. Eng. Sci. 41(12), 509-519.

Hitchcock, J.N., 2020. Storm events as key moments of microplastic contamination in aquatic ecosystems. Sci. Total Environ. 734, 139436.

Hurley, R., Woodward, J., Rothwell, J.J., 2018. Microplastic contamination of river beds significantly reduced by catchment-wide flooding. Nat. Geosci. 11, 251-257.

Iowa Environmental Mesonet (IEM), 2025. ASOS Network "ASOS-AWOS-METAR data download". https://mesonet.agron.iastate.edu/ASOS/. Accessed March 01, 2025.

Kim, L., Kim, S.A., Kim, T.H., Kim, J., An, Y. 2021. Synthetic and natural microfibers induce gut damage in the brine shrimp *Artemia franciscana*. Aquat. Toxicol. 232, 105748.

Koutnik, V.S., Leonard, J.L., Alkidim, S., DePrima, F.J., Ravi, S., Hoek, E.M.V., Mohanty, S.K., 2021. Distribution of microplastics in soil and freshwater environments: Global analysis and framework for transport modeling. Environ. Pollut. 274, 116552.

Lahon, J., Handique, S., 2024. Flood-induced variation and source apportionment of microplastics in Jia Bharali River of mid-Brahmaputra Valley, India. Environ. Monit. Assess. 196:1236.

Li, L., Frey, M., Browning, K.J., 2010. Biodegradability study on cotton and polyester fabrics. J. Eng. Fiber. Fabr. 5(4).

Muller, M., Murphy, B., Burghammer, M., Riekel, C., Pantos, E., Gunneweg, J., 2007. Ageing of native cellulose fibres under archaeological conditions: textiles from the Dead Sea region studied using synchrotron X-ray microdiffraction. Appl. Phys. A – Mater. 89, 877-881.

Park, C.H., Kang, Y.K., Im, S.S. Biodegradability of cellulose fabrics., 2004. J. Appl. Polym. Sci. 94(1), 248-253.

Rochman, C.M., Hentschel, B.T., Teh, S.J., 2014. Long-term sorption of metals is similar among plastic types: Implications for plastic debris in aquatic environments. PLOS One 9(1), e85433.

Rochman, C.M., 2018. Microplastics research — From source to sink in freshwater systems. Science 360(6384), 28-29.

Sait, S.T.L., Sorensen, L., Kubowicz, S., Vike-Jonas, K., Gonzalez, S.V., Asimakopoulos, A.G., Booth, A.M., 2021. Microplastic fibres from synthetic textiles: Environmental degradation and additive chemical content. Environ. Pollut. 268, 115745.

Sanchez-Vidal, A., Thompson, R.C., Canals, M., de Haan, W.P., 2018. The imprint of microfibres in southern European deep seas. PLoS ONE 13(11), e0207033.

Scircle, A., Cizdziel, J.V., Tisinger, L., Anumol, T., Robey, D., 2020. Occurrence of microplastic pollution at oyster reefs and other coastal sites in the Mississippi Sound, USA: Impacts of freshwater inflows from flooding. Toxics 8(2), 35.

Sewwandi, M., Kumar, A., Pallewatta, S., Vithanage, M., 2024. Microplastics in urban stormwater sediments and runoff: An essential component in the microplastic cycle. Trends Anal. Chem. 178, 117824.

Treilles, R., Gasperi, J., Tramoy, R., Dris, R., Gallard, A., Partibane, C., Tassin, B., 2022. Microplastic and microfiber fluxes in the Seine River: Flood events versus dry periods. Sci. Total Environ. 805, 150123.

United States Geological Survey (USGS), 2025. National Water Information System data available on the World Wide Web (USGS Water Data for the Nation). https://waterdata.usgs.gov/monitoring-location/07010086. Accessed February 19, 2025.

Van Daele, M., Van Bastelaere, B., De Clercq, J., Meyer, I., Vercauteren, M., Asselman, J., 2024. Mud and organic content are strongly correlated with microplastic contamination in a meandering riverbed. Commun. Earth Environ. 5, 453.

Van Emmerik, T., Mellink, Y., Hauk, R., Waldschlager, K., Schreyers, L., 2022. Rivers as plastic reservoirs. Front. Water 3, 786936.

Veerasingan, S., Mugilarasan, M., Venkatachalapathy, R., Vethamony, P., 2016. Influence of 2015 flood on the distribution and occurrence of microplastic pellets along the Chennai coast, India. Mar. Poll. Bull. 109(1), 196-204.

Wei, Q., Zhu, G., Wu, P., Cui, L., Zhang, K., Zhou, J., Zhang, W., 2010. Distributions of typical contaminant species in urban short-term storm runoff and their fates during rain events: A case of Xiamen City. J. Environ. Sci. 22(4), 533-539.

3.9. Supplementary Materials

3.9.1. Supplemental Tables

Table 3.S1. *Anthropogenic microparticles found in each blank and the calculation of the LOD for each sample type (i.e., water or sediment).*

Blank Type	Total (counts)	Black Fiber (counts)	Blue Fiber (counts)	Clear Fiber (counts)	Red Fiber (counts)
Autosampler Field Blank 1	1	0	1	0	0
Autosampler Field Blank 2	3	0	1	2	0
Autosampler Laboratory Blank 1	2	0	1	1	0
Autosampler Laboratory Blank 2	3	0	2	1	0
Water Processing Blank 1	4	1	1	1	1
Water Processing Blank 2	3	1	2	0	0
Water Processing Blank 3	0	0	0	0	0
Water Processing Blank 4	3	0	2	1	0
Average	2.38				
Standard Deviation	1.22				
Water LOD	6 counts				
Sediment Processing Blank 1	4	1	1	2	0
Sediment Processing Blank 2	3	0	1	2	0
Sediment Processing Blank 3	3	0	2	1	0
Sediment Processing Blank 4	4	0	2	2	0
Sediment Processing Blank 5	3	0	0	3	0
Sediment Processing Blank 6	4	0	0	4	0
Sediment Processing Blank 7	3	0	1	2	0
Average	3.43				
Standard Deviation	0.50				
Sediment LOD	5 counts				

3.9.2. Supplemental Figures

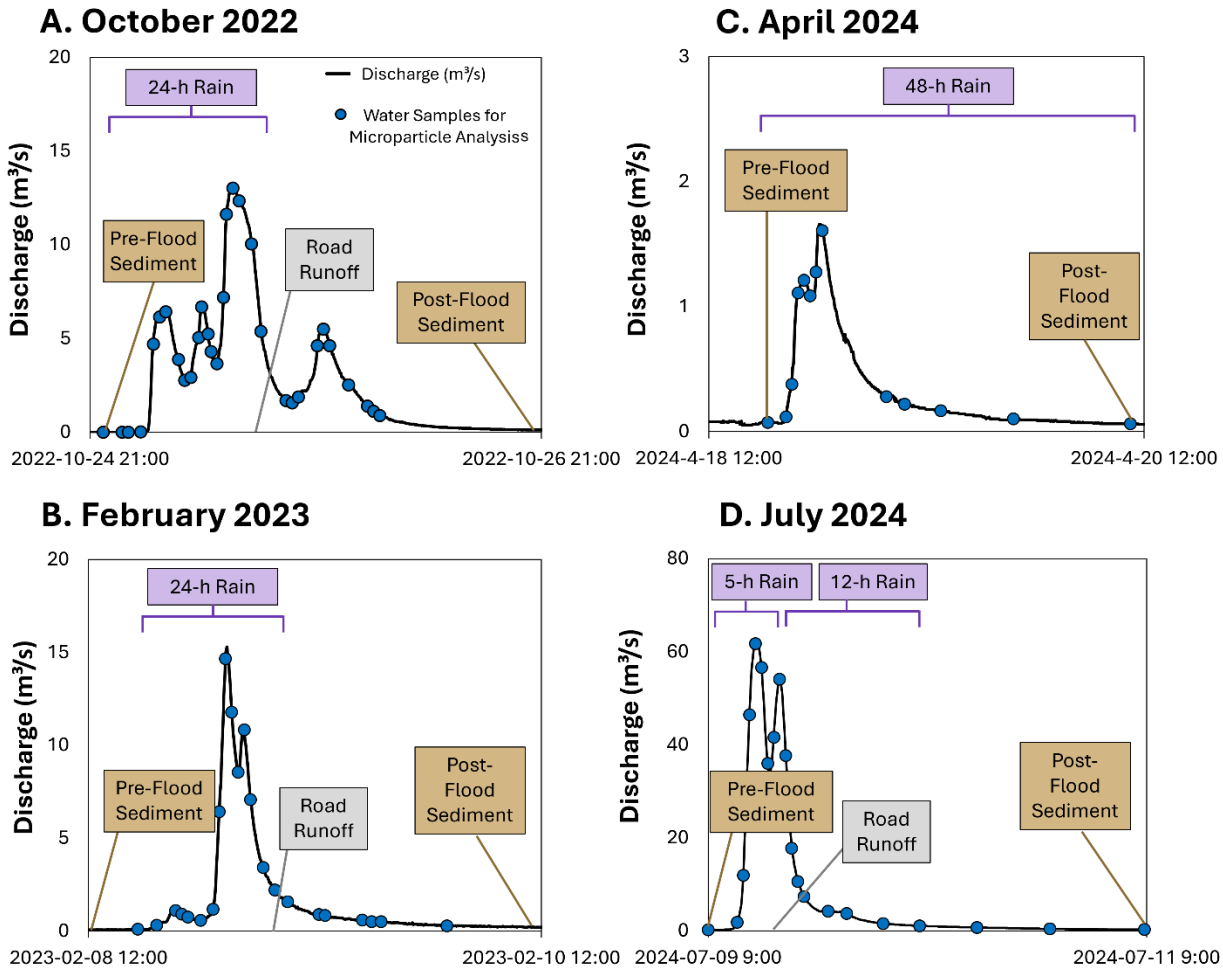

Figure 3.S1. *The timing of each sample type that was collected and analyzed for anthropogenic microparticles throughout each of the four selected flood events.*

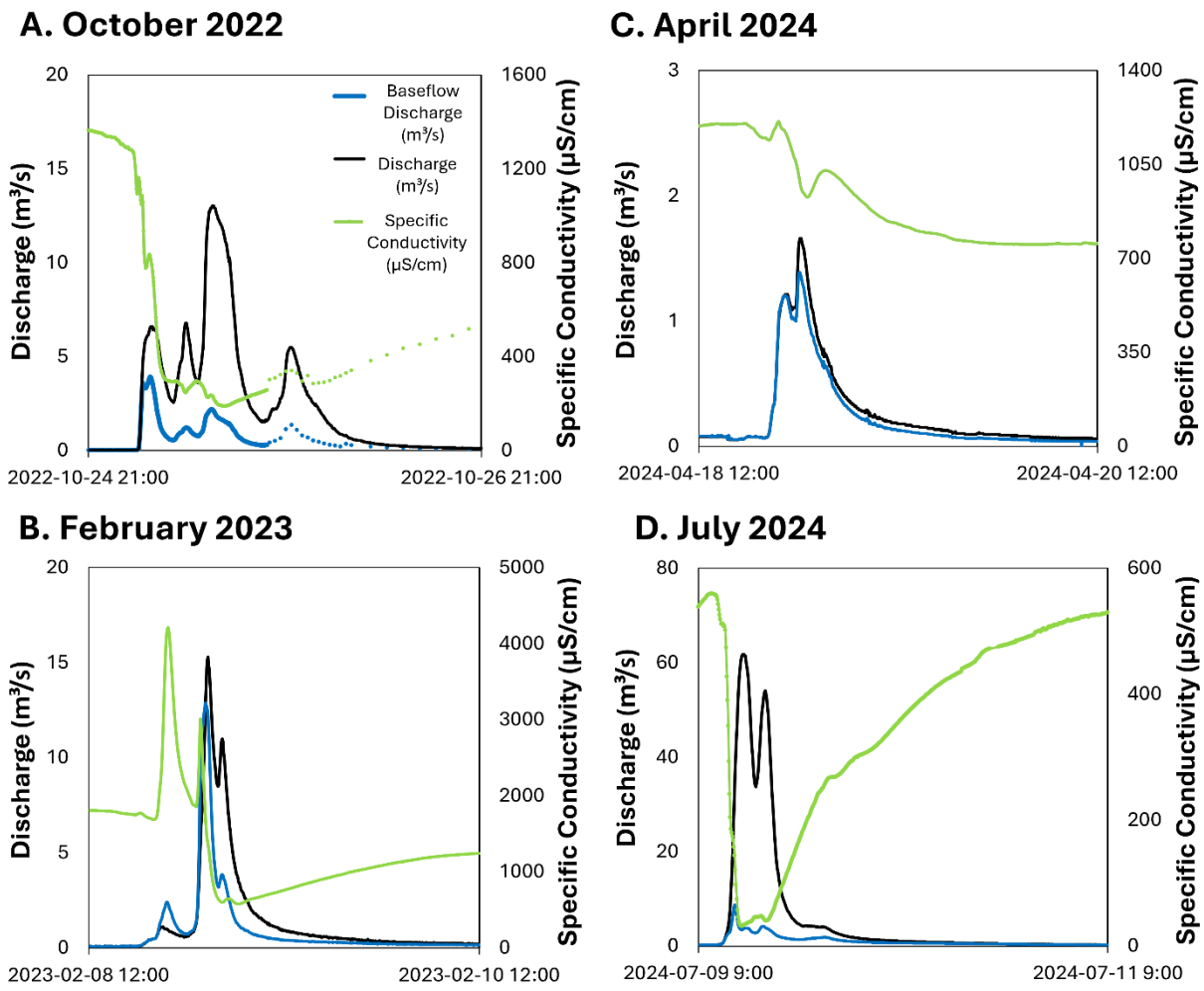

Figure 3.S2. *Hydrograph separations using specific conductivity data for each flood event. Note that the February 2023 flood shows baseflow levels that are higher than the recorded discharge values due to road salt applications elevating the specific conductivity signature.*

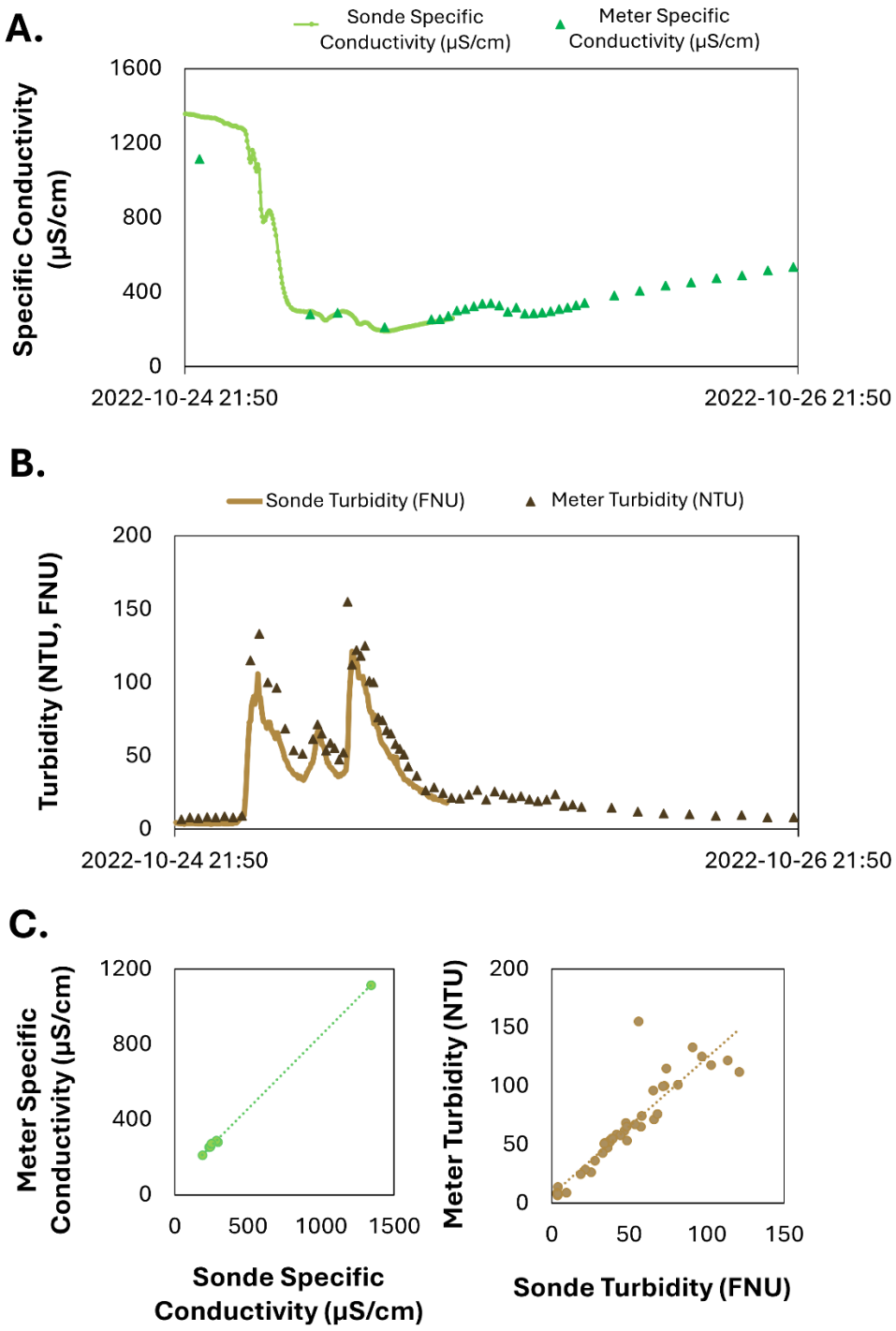

Figure 3.S3. *Comparisons of the sonde and benchtop or handheld water quality meter data for the October 2022 flood event when the in situ sonde stopped recording water quality data during the flood. We show the (A) in situ continuous and ex situ point measurements for specific conductivity, (B) in situ continuous and ex situ point measurements for turbidity, and (C) relationships between samples with both in situ continuous and ex situ point data.*

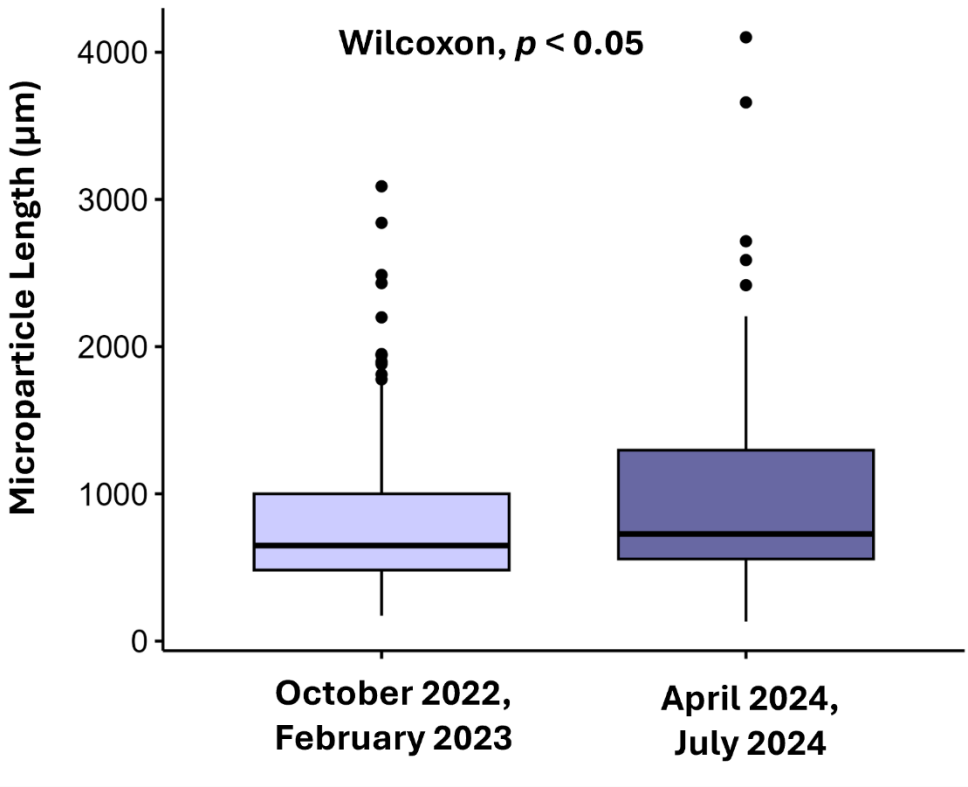

Figure 3.S4. *A comparison of the anthropogenic microparticle sizes in rainfall samples for the first two flood events (when non-standard methods were used to collect atmospheric deposition) versus the final two flood events (when a standard method was used to collect atmospheric deposition).*

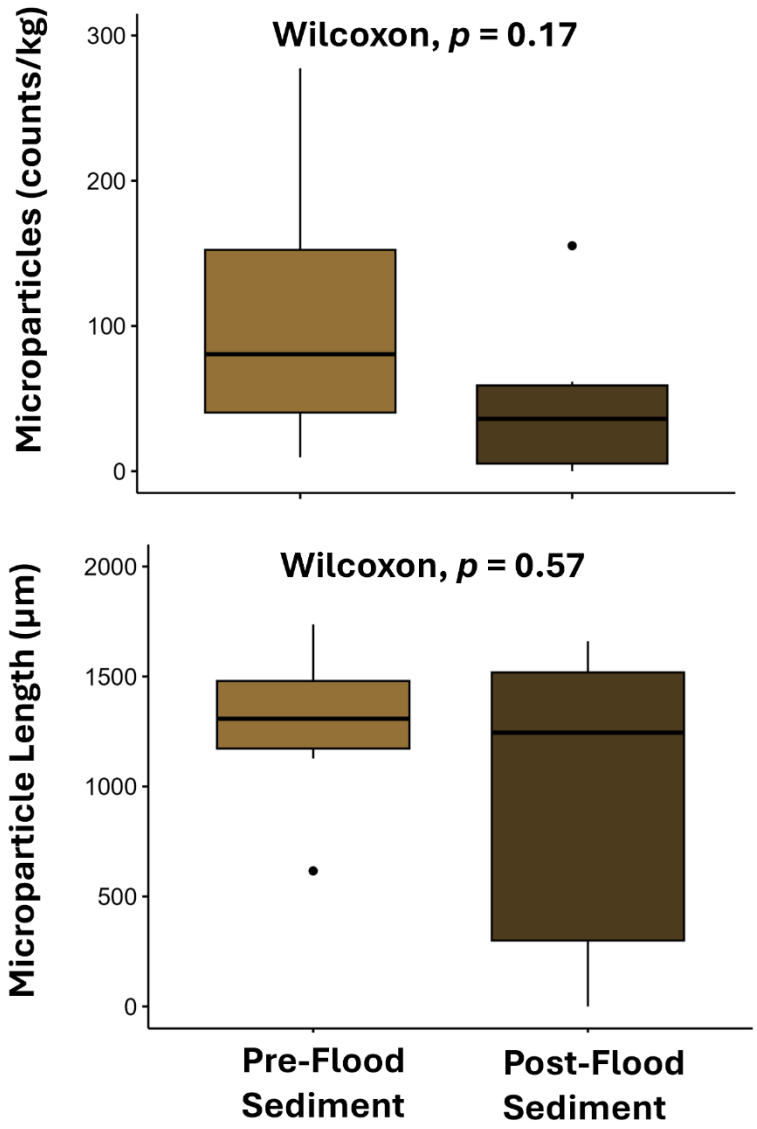

Figure 3.S5. *A comparison of the anthropogenic microparticle content (top) and sizing (bottom) in the pre- and post-flood sediment samples for all floods.*

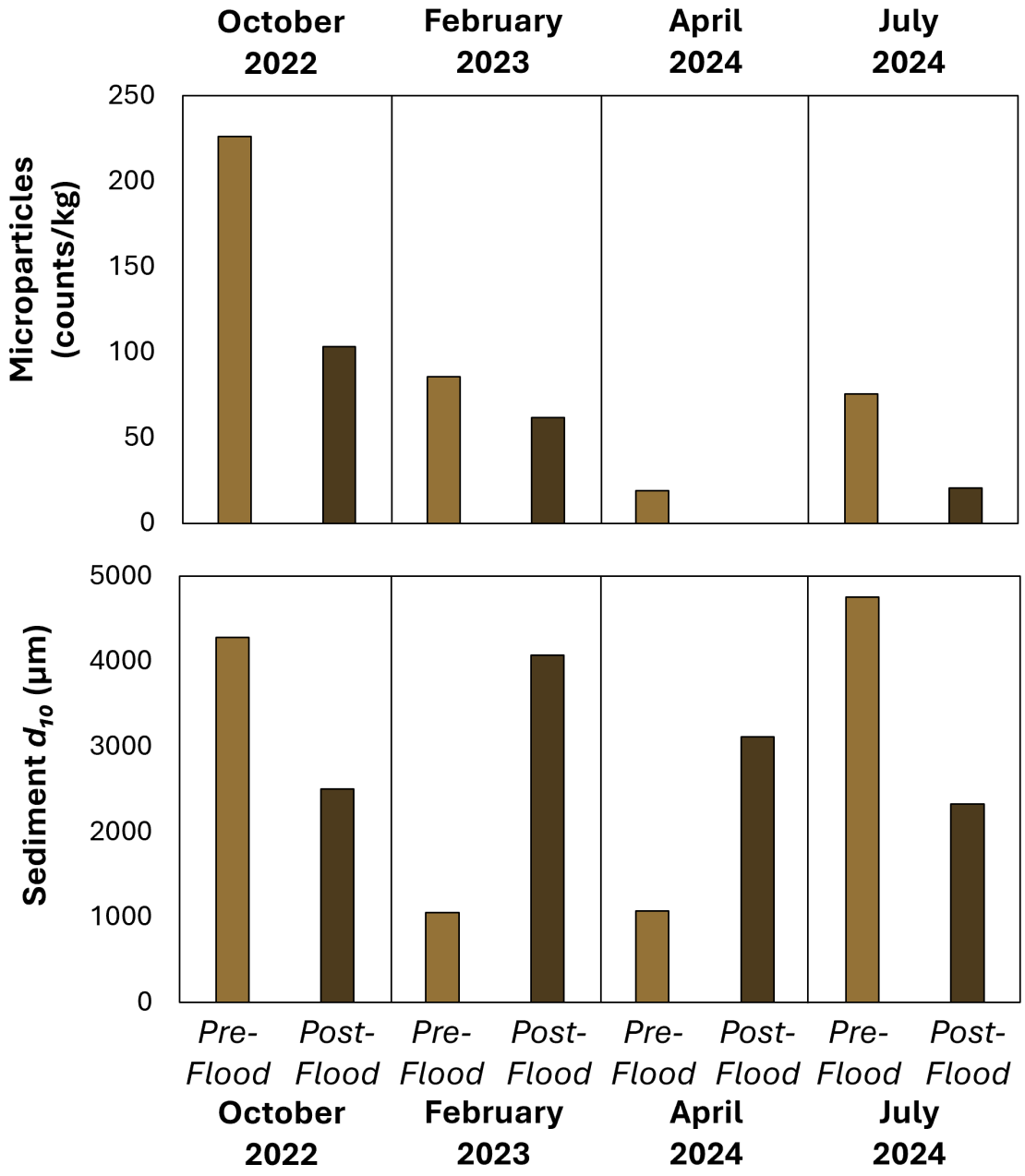

Figure 3.S6. *Comparisons of the pre- and post-flood anthropogenic microparticle content (top) and sediment grain sizes (represented by d_{10} values; bottom) for all four floods.*

CHAPTER 4: THE EFFICACY OF *C. FLUMINEA* AS A BIOINDICATOR OF MICROPLASTICS AND OTHER ANTHROPOGENIC MICROPARTICLES IN A SEASONALLY VARIABLE URBAN STREAM

4.1. Abstract

Bioindicator species for anthropogenic microparticles (including microplastics and other types of human-derived microparticles) are valuable to improve monitoring and the comparison of the uptake of these microparticles by organisms globally. *Corbicula fluminea* (*C. fluminea*) is an ideal freshwater bioindicator species because the bivalve is a widespread, abundant, and non-selective feeder, but a strong correlation between anthropogenic microparticles in *C. fluminea* and its surrounding environment (i.e., water and sediment) has only been identified in one system. Here, we assess anthropogenic microparticles in water, sediment, and clams (*C. fluminea*) monthly across a year of seasonal variation in an urban stream in St. Louis, Missouri, United States. No anthropogenic microparticles were present above the limit of detection (LOD) in the stream's water, and anthropogenic microparticles in *C. fluminea* ranged from below the LOD (81%) to 31.4 counts/g. In sediment, samples ranged from below the LOD (4%) to 188.6 counts/kg. The majority of the anthropogenic microparticles in sediment were microplastics (51%), while clam anthropogenic microparticles were largely cotton fibers (54%), with only 39% identified as plastic. No significant trend was observed between anthropogenic microparticle amounts in sediment and *C. fluminea*, but sediment anthropogenic microparticles were significantly and negatively correlated to sediment grain size. Clam anthropogenic microparticles were significantly and positively correlated to water suspended solid concentrations, which we suspect may indicate filtration activity. *C. fluminea* took up the most common types of anthropogenic microparticles from its surrounding environment (i.e., cotton and polyethylene terephthalate (PET) fibers), but did not ingest the full spectrum of diverse anthropogenic

microparticles in the sediment. Ultimately, *C. fluminea* has utility to compare systems globally, identify prominent contamination types (e.g., microfibers), and indicate key moments of anthropogenic microparticle fluctuation (i.e., seasonal extremes). However, a persistently strong relationship between the clam's and its surrounding environment's anthropogenic microparticle content is unlikely in highly variable freshwater environments.

4.2. Introduction

Microplastics are ubiquitous contaminants that can impact both human and ecological health (Akanyange et al., 2022; Rochman, 2018). These small (< 5 mm) plastics have diverse combinations of polymers, additives, and morphologies, and exist within a larger suite of prevalent anthropogenic microparticles including non-plastic materials with similar morphologies and potential toxicities (e.g., treated natural textile fibers; Athey and Erdle, 2022; Rochman et al., 2019). Both plastic and non-plastic microparticles with anthropogenic modifications can accumulate and persist in the environment (Adams et al., 2021; Park et al., 2004; Sait et al., 2021; Sanchez-Vidal et al., 2018). While many studies exclude non-synthetic anthropogenic microparticles (e.g., Su et al., 2018), when included, cellulosic microfibers are frequently the most common anthropogenic microparticle type found across atmospheric, water, sediment, and biota samples (e.g., Adams et al., 2021; González-Aravena et al., 2024; Macieira et al., 2021; Sanchez-Vidal et al., 2018; Stanton et al., 2019). Preliminary research has also suggested that cellulosic fibers, like plastic fibers, can cause physical harm when ingested (e.g., gut damage; Kim et al., 2021), though less is known about chemical effects from cellulosic fiber treatments or additives (Athey and Erdle, 2022). To fully assess and address the risk of these pollutants, monitoring and management strategies should consider non-plastic, but human-derived, microparticles in addition to microplastics, which is the approach used in our study.

A bioindicator species for microplastics and other anthropogenic microparticles could improve monitoring of this contaminant suite and comparison across multiple systems while simultaneously providing information about the ingestion of these pollutants and their spread across food webs (Wesch et al., 2016). An ideal bioindicator species would be a widespread, abundant, and non-selective feeder (Wesch et al., 2016). Proposed bioindicators for microplastics in freshwater systems to date have included bivalves (Su et al., 2018), gastropods (Akindele et al., 2019), crayfish (Pastorino et al., 2023), and fish (Koutsikos et al., 2023), though many of these examined species do not meet ideal indication criteria. Additionally, none of these studies consider non-plastic anthropogenic microparticles, either directly excluding them or not specifying material type.

The Asian clam, *Corbicula fluminea* (*C. fluminea*), is a globally distributed and abundant species with well-known ecology and an extensive history of use as a bioindicator (Sousa et al., 2008), including for various other contaminants such as fecal bacteria (Miller et al., 2005) and per- and polyfluoroalkyl substances (PFAS; Koban et al., 2024). *C. fluminea* is easily maintained in the laboratory and has already been used for laboratory studies examining how polymer type affects uptake and toxicity of microplastics alone and in combination with other contaminants (Fu et al., 2022; Guilhermino et al., 2018; Guo et al., 2021; Li et al., 2019; Oliveira et al., 2018). The species thus meets the criteria to be an ideal bioindicator of anthropogenic microparticles in freshwater systems. Early work using *C. fluminea* as a bioindicator species for microplastics has yielded variable results, with a negative correlation between sediment microplastics and the clam concentration factor (i.e., the level of accumulation) in one early study (Su et al., 2016) but a positive correlation between microplastics in the bivalves and sediment in a subsequent study of rivers, lakes, and estuaries (Su et al., 2018). Despite its potential as a bioindicator species, the

efficacy of *C. fluminea* remains unclear due to the limited quantity of systems and conditions across which its bioindication has been tested.

Thus, the objective of our research is to assess the effectiveness of *C. fluminea* as a bioindicator of both microplastics and other anthropogenic microparticles in an urban stream that experiences highly variable seasonal conditions (e.g., extremely low flow, flash flooding, and winter snowfall). Our study compared anthropogenic microparticle quantities and compositions in *C. fluminea*, water, and sediment samples in an urban stream over one year of monthly samples.

4.3. Materials and Methods

4.3.1. Study Area

Deer Creek is a 95.8-km^2 urban stream in St. Louis, Missouri, United States, which is connected to the Mississippi River via the River des Peres (Fig. 4.1). The system undergoes extreme changes in flow from low discharge in the late summer to flash flooding events that occur most frequently in the spring but have been recorded at all times of year (Criss et al., 2022; USGS, 2025). The watershed also has a history of wastewater contamination issues due to outdated infrastructure such as combined sewer overflows (CSOs), sanitary sewer overflows (SSOs), and leaking pipes (Finegan and Hasenmueller, 2024). These overflow sites had been mostly removed at the time of sampling for our study (MSD, 2024), but their past presence in the watershed might have introduced legacy contamination issues. In winter months, the stream also faces Cl^- pollution from road salt applications (Finegan and Hasenmueller, 2023). The selected sample site is near the outlet of the watershed, which collects water from locations with historical sewer overflow outfalls as well as current commercial areas (Fig. 4.1; Hasenmueller et al., 2017). The sampling site is ~ 550 m upstream of a United States Geological Survey discharge monitoring site (gauge 07010086; Fig. 4.1), which recorded an average discharge of 1.5 m^3/s in

2022 (USGS, 2025). The site was chosen for its consistently high populations of *C. fluminea*. Upstream and downstream sites occasionally also had individuals present, but not the similarly large populations required for the planned sampling.

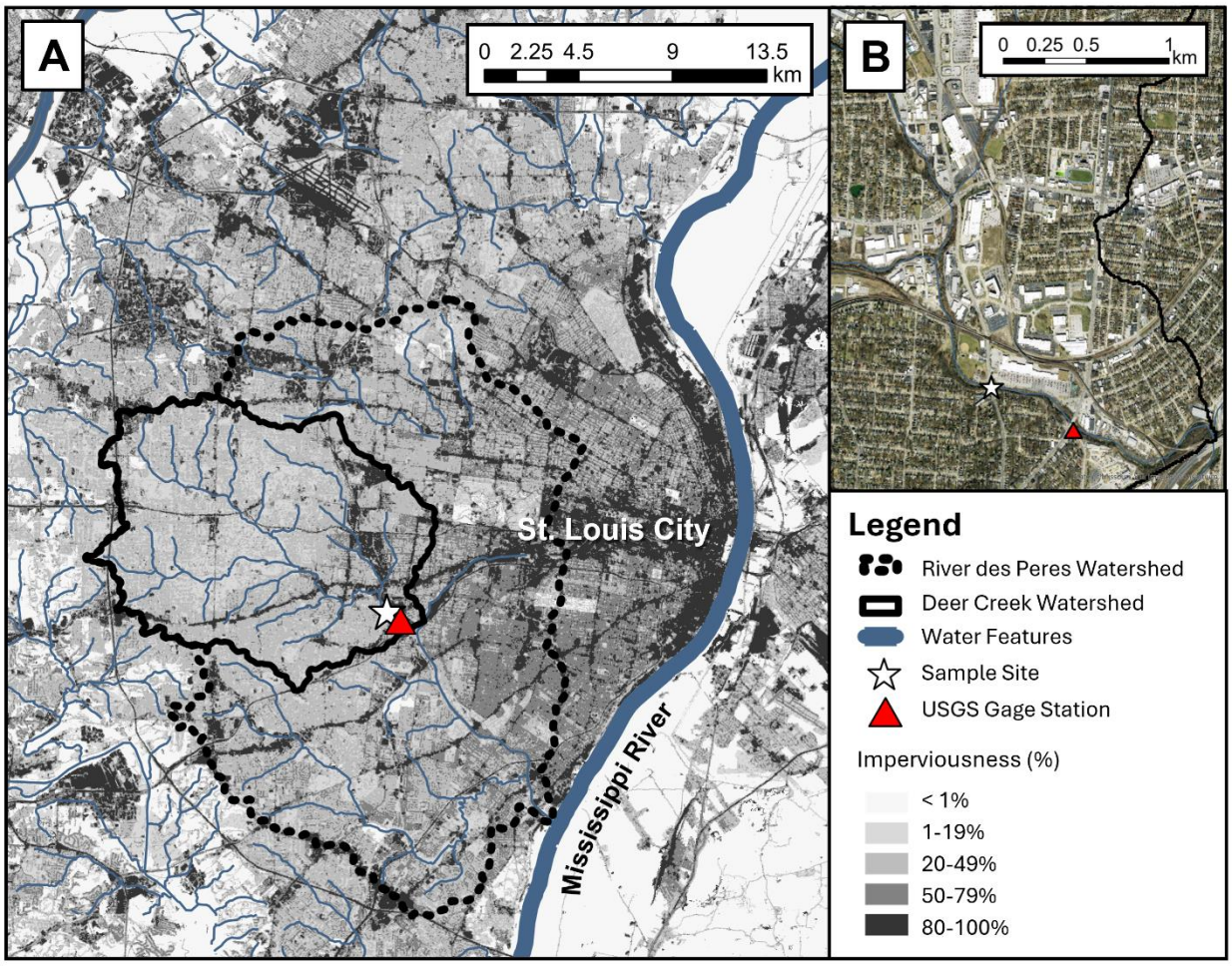

Figure 4.1. *The selected sampling site (A) on an imperviousness map (Dewitz, 2021) and (B) with a view of the nearby industrial area (Esri, 2025a).*

4.3.2. Anthropogenic Microparticle Sample Collection

Samples of the stream's *C. fluminea*, water, and bed sediment were collected monthly at our outlet site from November 2021 to October 2022 to analyze their anthropogenic microparticle content. Samples were taken at baseflow when possible, which we define as no precipitation events having occurred in the preceding 3 days. However, in February 2022, snowfall occurred 2 days prior to sampling, causing a small impact on stream discharge (Table 4.S1.; USGS, 2025). During each sampling event, we first collected 2 L of water into two 1-L amber glass jars that had been triple rinsed with filtered distilled deionized (DDI) water in the laboratory and then triple rinsed with site water before sample collection. Water samples were stored at room temperature until analysis. After the water sample was obtained, the sediment sample (~ 1 kg) was collected with a custom Hess sampler into a 1-L glass mason jar that had also been triple rinsed with filtered DDI water in the laboratory. The sediment sample consisted of a homogenization of sediment collected at three points spread evenly across the channel, resulting in a single combined sample per site and sampling date. Detailed steps for the sediment collection methods are described in Hernandez and Hasenmueller (2024) and the depths of the three sampling points are provided in Table 4.S2. All sediment samples were refrigerated until analysis.

Bivalve samples were taken upstream from the water and sediment samples by removing armoring rocks and digging into the sediment to locate the clams. Adult *C. fluminea* (shell length > 15 mm) were kept, while smaller bivalves were returned to the stream. Each month, the goal was to collect at least 10 adult bivalves, but, for some months, the population was too small to meet this criterion. At other times, the population was unhealthy such that most of the bivalves that were collected were shells filled with compacted sediment rather than living individuals (e.g., the August 2022 sampling event, which occurred after a damaging flood; see Tables 4.S1.-

4.S2.). In May 2022 and October 2020, we sought to collect at least 50 adult bivalves to compare spring and fall seasonal anthropogenic microparticle levels using a larger sample size. However, the clam totals ultimately fell to 30-40 individuals collected for these two months once shells filled with compacted sediment were removed from the collection totals during sample processing (Table 4.S2.). Bivalves were wrapped individually in Al foil at the field site and frozen until analysis. A portion of bivalves experienced a freezer thaw prior to analysis. The impact of thawing on measured tissue mass for these individuals was assessed and corrected (see Supplemental Method 4.S1. and Figs. 4.S1.-4.S3.).

4.3.3. Anthropogenic Microparticle Characterization

4.3.3.1. Environmental samples

To extract the anthropogenic microparticles from our sample types, water samples were vacuum-filtered, while ~ 250 g subsets of sediment samples were dried, density separated with a NaCl solution, and the supernatant vacuum-filtered (Hasenmueller et al., 2023). Bivalve samples were thawed for 24 h, then the shell length, total mass (i.e., shell and tissue), and tissue mass were recorded for each individual. The tissue removed from each individual was placed into an Erlenmeyer flask and ~ 50 mL of filtered 30% H_2O_2 was then added. The flask opening was covered with Al foil, and the flask was placed in an oscillation incubator at 60 ℃ and 80 rpm for 48 h to be digested and then vacuum-filtered. This method is adapted from prior studies of anthropogenic microparticles in *C. fluminea* (Su et al., 2018). The resulting filters from each sample type were examined for anthropogenic microparticles, which were photographed and characterized by their color, morphology, and size. The lower limit for this visual detection of anthropogenic microparticles was 100 µm. Criteria including color, tapering, and resistance to breakage were used to distinguish anthropogenic materials from organic matter (Hernandez and Hasenmueller, 2024).

Once the visual examination was complete, a subset of the anthropogenic microparticles were removed from the filters and placed into small containers with filtered 10% ethanol solution until further material type analysis. Material types were analyzed for 19% of the detectable clam anthropogenic microparticles (n = 41), 9% of the detectable sediment anthropogenic microparticles (n = 37), and two anthropogenic microparticles from the water samples (none of which had detectable microparticles; see Section 4.3.3.2.). The microparticles were mounted on Al foil-covered slides and analyzed with Micro-Fourier Transform Infrared (μ-FTIR) spectroscopy using a Thermo Fisher Scientific Nicolet iN5 μ-FTIR. Attenuated total reflectance was measured across wavenumbers 4000-650 nm using a Ge crystal. The resulting spectra were corrected with atmospheric suppression and compared to a series of libraries commonly used for microplastics research (e.g., Primpke et al., 2018; FLOPP from De Frond et al., 2021) in the μ-FTIR OMNIC software, which provides a correlation-based match value for each top match within the libraries. Only matches above 70% were accepted, and anything lower was considered "undefined". Our average match percentage was 90%.

4.3.3.2. Quality assurance and quality control measures

Throughout the sample processing steps, common quality assurance and quality control methods were employed to decrease and account for possible contamination of the samples with anthropogenic microparticles. To reduce the potential for contamination, we prefiltered working solutions, triple rinsed glassware, and covered samples and equipment when they were not in use, among other efforts (see Hernandez and Hasenmueller, 2024, and references therein, for a full list of protocols). As contamination cannot be completely avoided, blanks were used to account for anthropogenic microparticles that might have been introduced during the processing steps for each sample type. Water blanks consisted of 1-L of prefiltered DDI water, sediment blanks were ~ 300 mL of prefiltered NaCl solution that was treated with the same separation

steps as the sediment, and clam blanks were ~ 50 mL of prefiltered 30% H_2O_2 treated with the same digestion steps as the clams. Each blank type was filtered alongside the corresponding environmental sample category. These laboratory blanks were used to calculate the limit of detection (LOD) for each sample type (Table 4.S3.). The LOD for each environmental sample type was calculated as the mean of the blank values plus three standard deviations (Dawson et al., 2023). When anthropogenic microparticle quantities in a sample were below the calculated LOD, we report the sample to contain zero anthropogenic microparticles. Since these microparticles were corrected at the totals stage (i.e., before normalizing with the sample mass), the LOD was rounded to a whole number for our correction. Subsets of microparticles from each blank type were analyzed on μ-FTIR to understand contamination material types.

A series of replication procedures were employed to assess variability in field and laboratory processing steps, which are discussed in Supplemental Method 4.S2. These steps included field and laboratory replicates, samples assessing cross-channel variation in sediment, and replication of the visual identification process (Supplemental Method 4.S2.; Figs. 4.S4.-4.S7.). Individual *C. fluminea* replicates (i.e., individual clams, from $n = 4$ to $n = 43$ per month; see Table 4.S2.) each month were averaged into monthly clam anthropogenic microparticle totals, though individual data are still reported for maximum anthropogenic microparticle content in *C. fluminea*. Laboratory replicates for sediment ($n = 2$ per month) were also averaged into monthly sediment anthropogenic microparticle totals, though, again, individual replicate data are still reported for minimum and maximum sediment anthropogenic microparticle content.

4.3.4. Additional Physicochemical Analyses of Water and Sediment

Specific conductivity, Cl^-, and temperature were measured in situ for the water during site visits using a YSI Professional Plus Multiparameter Instrument. We also analyzed total suspended solids (TSS) concentrations ex situ from water samples following United States

Environmental Protection Agency (USEPA) Method 160.2 (USEPA, 1971). Sediment samples were analyzed ex situ for grain size distribution via sieving (see Hasenmueller et al., 2023, for the full method details). Physicochemical data are presented for comparison to the anthropogenic microparticle data in Table 4.S2.

4.3.5. Data Analysis

For analysis of the full clam dataset (n = 199 individuals), parametric tests (i.e., Welch's t test and Pearson's correlation) were used due to the size of the dataset (with $\alpha = 0.05$). However, small sample sizes for clam and sediment replicates when summarized by month (i.e., into one average for each of the 12 months; $n = 12$) prevented the assumption of normality when assessing relationships among summarized variables. Statistical relationships involving data summarized by month (including the anthropogenic microparticle data) were therefore tested using non-parametric Spearman's rank correlations (with $\alpha = 0.05$), though linear regressions for the original data are provided as visualizations. Differences in anthropogenic microparticle levels by month were examined using the Kruskal-Wallis test followed by pairwise Wilcoxon tests, and the differences in sizes of these microparticles were analyzed with a Wilcoxon test. All statistical analyses were performed in R and Microsoft Excel. Figures were created using ArcGIS Pro Version 3.0.3, R, and Microsoft Excel.

4.4. Results

4.4.1. Anthropogenic Microparticle Characterization

4.4.1.1. Quality assurance and quality control measures

Blanks for the clam, water, and sediment lab processing steps had 0-4 particles identified per individual blank, resulting in respective calculated LODs of 4, 6, and 5 counts (Table 4.S3.). The subset of anthropogenic microparticles from blank samples that were analyzed with μ-FTIR consisted of mainly cotton fibers (n = 3 for clam, n = 5 for sediment, and n = 2 for water) and some polyethylene terephthalate (PET; n = 1 in clam and n = 1 in sediment).

4.4.1.2. Anthropogenic microparticle content in Asian clam

Anthropogenic microparticles were found above the LOD in 37 sampled clams (19%), while the rest contained either no anthropogenic microparticles (19%; n = 38) or anthropogenic microparticles below the LOD (62%; n = 124). The total number of suspected anthropogenic microparticles identified above the LOD in *C. fluminea* samples was 218, with an average of 2.6 ± 6.4 counts/g. The highest average monthly anthropogenic microparticle level was found in November 2021 (11.4 ± 9.0 counts/g), which had significantly higher abundances compared to most other months except for December 2021, February 2022, March 2022, and September 2022 (Fig. 4.2.; Table 4.S4.). The highest quantity found in a single individual was also in November 2021, at 31.4 counts/g. August 2022 was the only month for which we found no anthropogenic microparticles above the LOD in any clam (Fig. 4.2.). This sampling event followed an extreme flood that featured a peak discharge of 216.34 m^3/s, which exceeded the National Weather Service flood stage for Deer Creek and was almost twice the peak discharge observed in any other floods that occurred during the year-long period we were sampling (Table 4.S1.; USGS, 2025).

The majority of the anthropogenic microparticles above the LOD in clam samples were fibers (> 99%), with only one fragment identified in November 2021. Of the total anthropogenic microparticles found in the clams, 75% were clear fibers, 18% were blue fibers, and the remaining color-morphology combinations made up < 10% of the total (Fig. 4.S8.). The anthropogenic microparticle sizes ranged 147.3-4474.9 µm, with an average of 752.6 ± 631.3 µm. The *C. fluminea* contained 61% non-synthetic and 39% synthetic materials (Fig. 4.3.). Cotton was the most common microparticle type at 54%, followed by PET (which included polyethylene terephthalate and polyester matches) at 37%. Every synthetic microparticle found in the clams was PET except for one fragment made of poly(ethyl acrylate) (PEA; Fig. 4.3.).

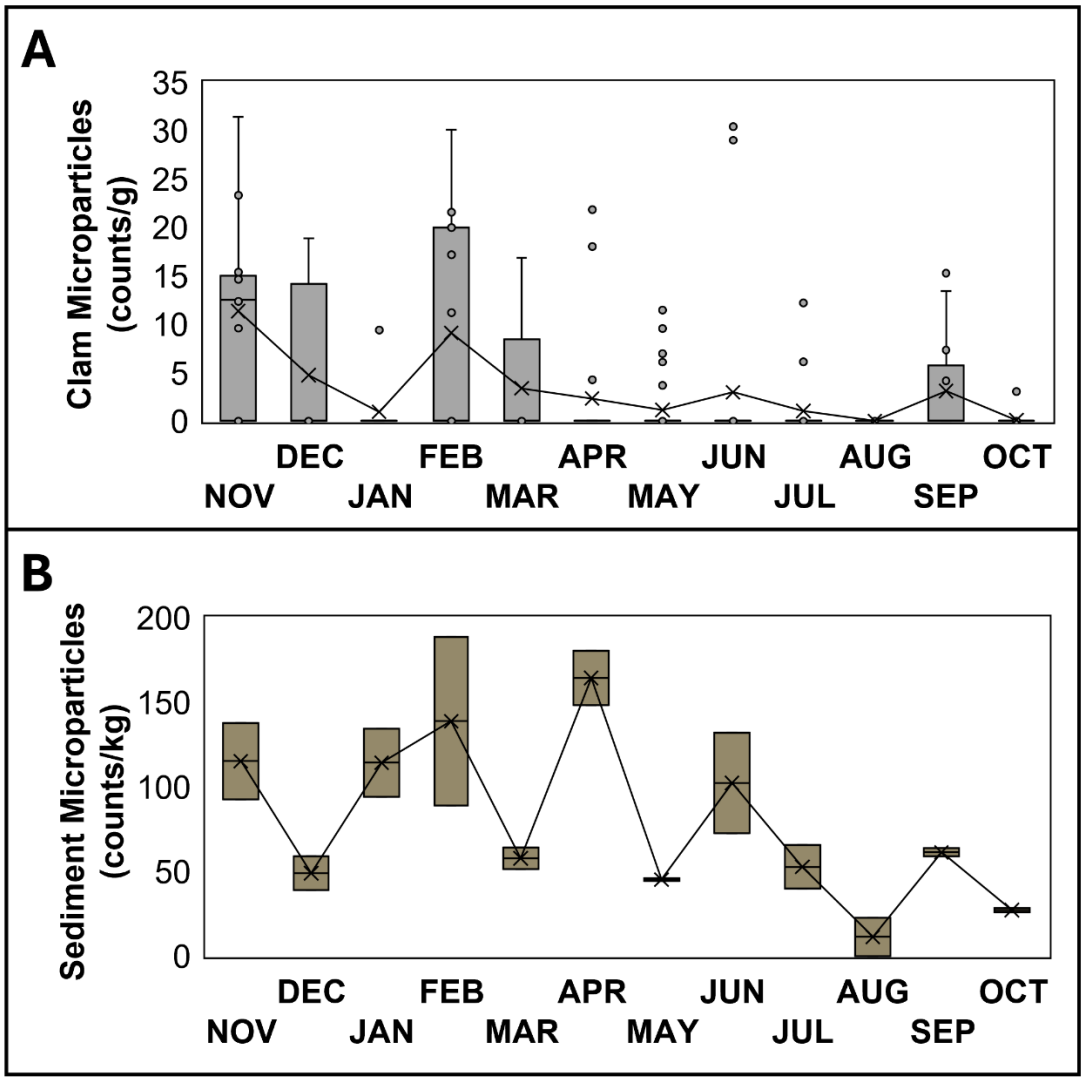

Figure 4.2. *Anthropogenic microparticle content in (A) clam (n values are from 4-43 per month) and (B) sediment (n = 2 per month) replicates for each month of sampling. The monthly means are shown with cross symbols and have been connected with an interpolation line. Anthropogenic microparticle data for the water samples are not shown because they were below the LOD.*

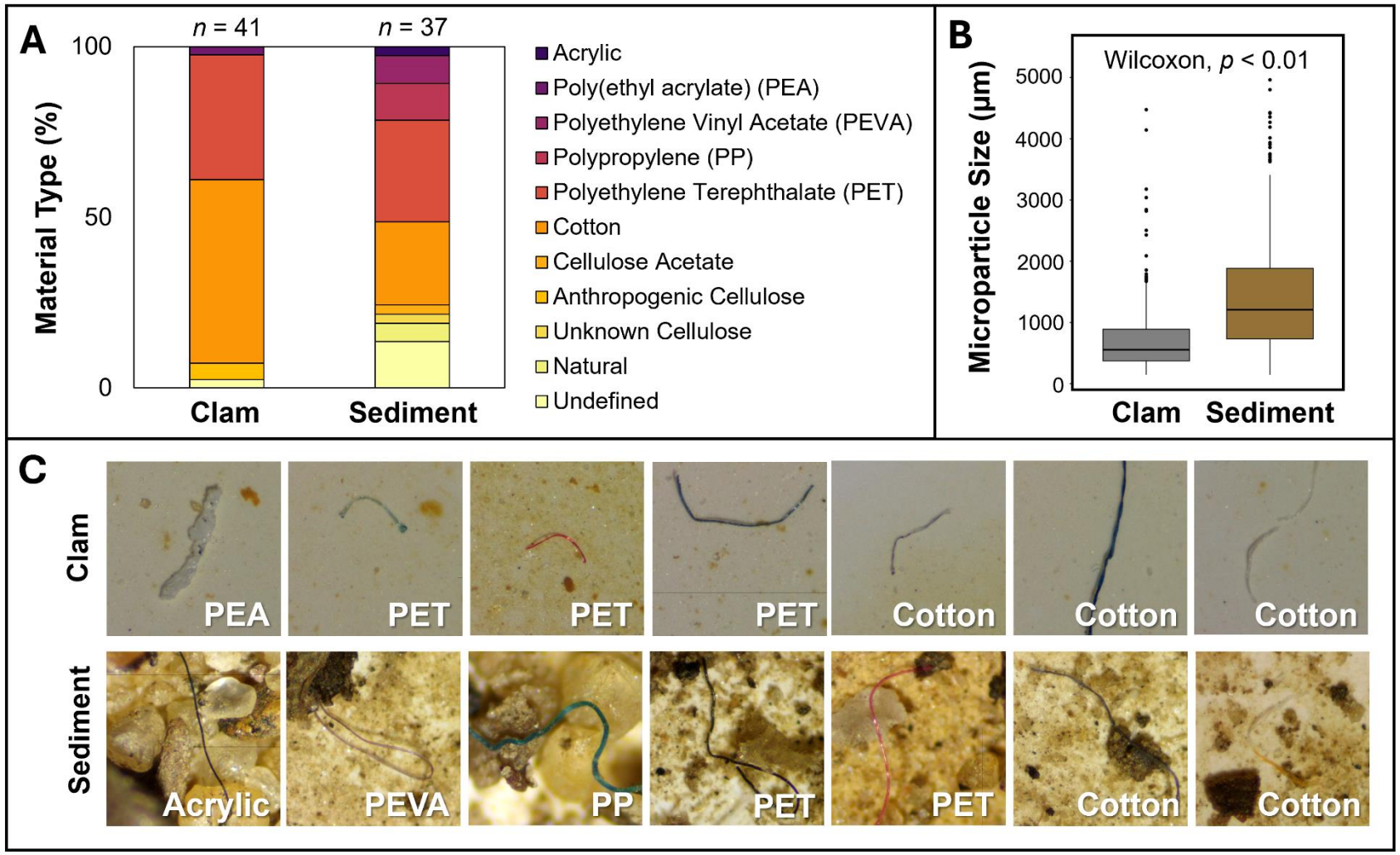

Figure 4.3. *Comparisons of clam and sediment anthropogenic microparticle (A) material types and (B) sizes. Example photos of various anthropogenic microparticle types found in clam (top) and sediment (bottom) are provided in (C), with the photo sizes being 1 mm by 1 mm for scale.*

4.4.1.3. Anthropogenic microparticle content in water and sediment

No anthropogenic microparticles were found above the LOD in water samples. However, 23 of the 24 sediment replicates (i.e., $n = 2$ per month over the year-long sampling period) had anthropogenic microparticle levels above the LOD, with a total anthropogenic microparticle number of 414 and average of 78.2 ± 49.8 counts/kg found in the sediment samples. The highest monthly average quantity of anthropogenic microparticles in sediment was found in April 2022 (164.3 ± 16.2 counts/kg), while, similar to the results for *C. fluminea*, the lowest quantity of anthropogenic microparticles in sediment was found in August 2022 (11.3 ± 11.3 counts/kg), with one sample containing no anthropogenic microparticles above the LOD (Fig. 4.2.). The highest quantity of any individual sediment replicate was 188.6 counts/kg in February 2022. We found no significant differences in anthropogenic microparticle content per month in sediment.

The anthropogenic microparticles in sediment were dominated by fibers (96%), and clear fibers (49%) and blue fibers (20%) were the most common color-morphology combinations (Fig. 4.S8.). The sediment anthropogenic microparticles were nearly twice as large as those in the clams, averaging 1402.3 ± 893.7 µm and ranging 145.9-4961.8 µm in size (Fig. 4.3 (B)). The majority of the anthropogenic microparticles in sediment were synthetic (~51%), with these microplastics mostly comprised of PET (30%), followed by polypropylene (PP; 11%), polyethylene vinyl acetate (PEVA; 8%), and acrylic (3%; Fig. 4.3. (C)). Cotton was also common in sediment, making up 24% of the analyzed anthropogenic microparticles (Fig. 4.3. (C)). Though the anthropogenic microparticle levels in water samples were below the LOD, the water microparticles analyzed for material type with µ-FTIR were both cotton.

4.4.2. Relationships between Anthropogenic Microparticles in Asian Clam and Sediment

The concentrations of anthropogenic microparticles in clams and sediment had a positive (Spearman's $\rho = 0.44$), though insignificant ($p = 0.15$), trend (Fig. 4.4.). The variability (defined by the standard deviation) of the clam replicates (whose numbers varied by month due to population size; see Table 4.S2.) as well as the sediment laboratory replicates (two per month) had strong significant positive relationships with their respective average anthropogenic microparticle concentrations (Fig. 4.4.). February 2022 had the highest replicate variability for both the clams and sediment (Fig. 4.2.; Fig. 4.4.). More variable anthropogenic microparticle content in sediment was also strongly significantly correlated with more variable anthropogenic microparticle content in clams (Fig. 4.4.).

Additionally, the clam samples had significantly smaller anthropogenic microparticle sizes than the sediment samples (Fig. 4.3. (B)). They also featured a greater percentage of clear fibers and a lower variety of other anthropogenic microparticle morphologies compared to the sediment samples (Fig. 4.S8.). Though both compartments had relatively high abundances of cotton and PET microparticles, material types were less diverse in *C. fluminea* compared to the sediment (Fig. 4.3. (C); Fig. 4.S8.).

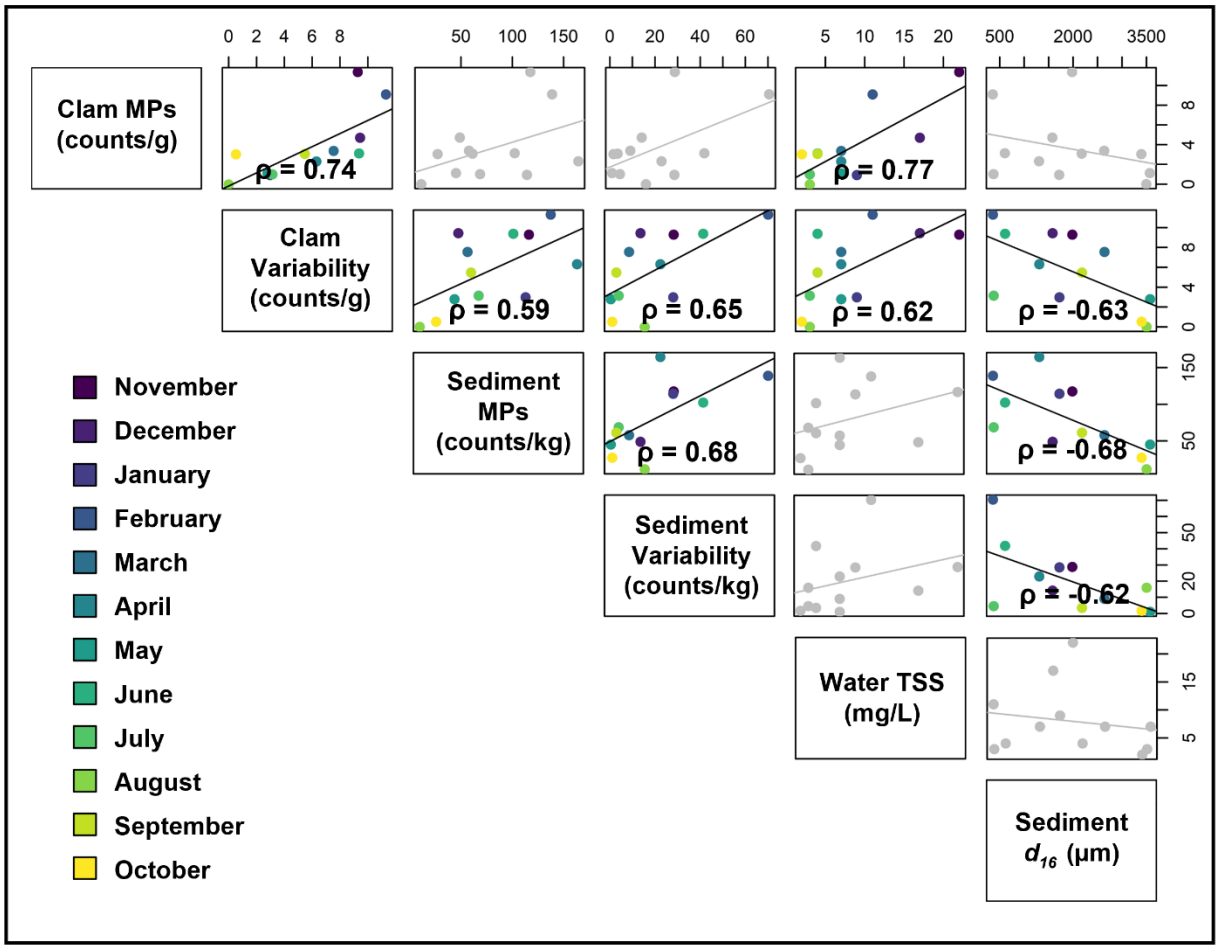

Figure 4.4. *The relationships among clam and sediment anthropogenic microparticle concentrations, clam and sediment anthropogenic microparticle variability (as the standard deviation of sample replicates), and selected physicochemical parameters (i.e., water TSS and sediment d_{16}). Significant correlations are shown in color with their Spearman's ρ values, while insignificant relationships are grayed.*

4.4.3. Relationships between Anthropogenic Microparticles and the Physicochemical Properties of Water and Sediment

The physicochemical data for water across the sampling dates exhibited large ranges including extremes in flow (Table 4.S1.) and elevated specific conductivity and Cl^- levels due to winter road salt applications (e.g., in February 2022; Table 4.S2.). The sediment grain size assemblages were consistently dominated by large rocks (i.e., d_{50} > 4.75 mm), so we used sediment d_{16} values for correlation analysis. Most of the physicochemical parameters we

assessed, including peak flow for the most recent flood event before sampling, discharge at the time of sample collection, average discharge for the 20 days prior to sampling, water temperature, water specific conductivity, and water Cl^-, had no significant relationships with the anthropogenic microparticles in the sediment or clam samples.

However, the strongest relationships for *C. fluminea* were between the clams' anthropogenic microparticle concentrations and water TSS values (Spearman's $\rho = 0.77$; $p < 0.05$; Fig. 4.4.). Sediment anthropogenic microparticle concentrations had their strongest significant and negative correlation with the sediment d_{16} grain size fraction (Spearman's $\rho = -0.68$; $p < 0.05$; Fig. 4.4.). We also found that water TSS concentrations were significantly and negatively correlated with temperature (Spearman's $\rho = -0.60$; $p < 0.05$), though temperature did not significantly correlate with clam anthropogenic microparticles. Nonetheless, the four months with the highest abundances and variability for clam anthropogenic microparticles occurred when water temperatures were at their lowest (Fig. 4.S9.).

4.5. Discussion

4.5.1. Anthropogenic Microparticle Quantities and Characteristics in Environmental Media

Our range of anthropogenic microparticles in the clams each month overlapped with those reported in other studies of anthropogenic microparticle content in *C. fluminea* (Table 4.S5.). Only two studies report higher levels of anthropogenic microparticles per individual (i.e., > 20 counts/individual) than our observations for Deer Creek (Table 4.S5.). McCoy et al. (2020) attributed the higher levels of anthropogenic microparticles in *C. fluminea* of the River Thames to a proximal sewer overflow, and Stankovic et al. (2024) cited plastic pollution as the reason for high *C. fluminea* anthropogenic microparticle levels in the Danube Basin. The predominance of

microfibers has been noted in most other studies of *C. fluminea*, though the proportions of observed synthetic and non-synthetic materials as well as the specific material types that have been identified vary globally (Fig. 4.5.; Table 4.S5.). In three prior studies of *C. fluminea*, PET was the most common microplastic type found, and laboratory exposure experiments suggest that PET might be preferentially taken up by the clam compared to other polymer types (Giarratano et al., 2024; Li et al., 2019; Stankovic et al., 2024; Su et al., 2018). The uptake of anthropogenic microparticles by the clams might also be higher for small size ranges (Li et al., 2019). These selection processes may explain why we observed that the anthropogenic microparticles in sediment were more diverse and larger than those found in *C. fluminea* (Fig. 4.3.).

Only three previous studies have assessed human-sourced microparticles in clam and sediment samples and discussed the bioindication potential of *C. fluminea* (Su et al., 2016; Su et al., 2018; Vidal et al., 2023). The strongest bioindication evidence was a significant linear relationship between *C. fluminea* microparticles and those in water and sediment in Su et al. (2018). The range of anthropogenic microparticles found in sediment samples in the Su et al. (2018) study (15.0-160.0 counts/kg) was similar to our studied system (0-188.6 counts/kg; see Table 4.S5.). Though our water samples were all below the LOD and we thus corrected their values to 0 counts/L for analysis purposes, the observed concentration range prior to our correction step was 0-2.7 counts/L, which overlaps with the 0.5-3.1 counts/L range observed in Su et al. (2018). Additionally, although the blank level reported in Su et al. (2018) is comparable to our blank values, no blank correction was performed for their study. In contrast, the Loire River study by Vidal et al. (2023) found much higher levels of anthropogenic microparticles in clam, water, and sediment even after a blank subtraction correction method. The Loire River work is also the only study of *C. fluminea* anthropogenic microparticle levels that found a

predominance of fragments instead of fibers in the samples, suggesting that the contamination types and levels at their study site are fundamentally different from other systems (Fig. 4.5.; Table 4.S5.).

Despite the similarities in anthropogenic microparticle ranges and characteristics across compartments between our study and the prior studies in China that demonstrated evidence of bioindication by *C. fluminea* (Su et al., 2016; Su et al., 2018), our data showed no significant relationship between clam and sediment anthropogenic microparticle content (Fig. 4.4). Similar anthropogenic microparticle types and quantities between these studies indicate that the failure of *C. fluminea* to act as a bioindicator in our system is not related to the abundance or type of human-sourced microparticles in the environment. Instead, seasonal fluctuations in clam and sediment anthropogenic microparticles may be controlled by unique factors influencing their bioindication potential as these prior studies have not examined temporal variation of anthropogenic microparticle bioindication over the extent of seasonal variation found in our dataset. Our conservative LOD correction method, if applied to prior bioindication studies, might also have weakened the perceived relationship between *C. fluminea* and sediment anthropogenic microparticle concentrations. That only one study (i.e., Su et al., 2018) has found a strong linear relationship between microplastics in *C. fluminea* and sediment also implies that such a straightforward relationship may not hold across most systems.

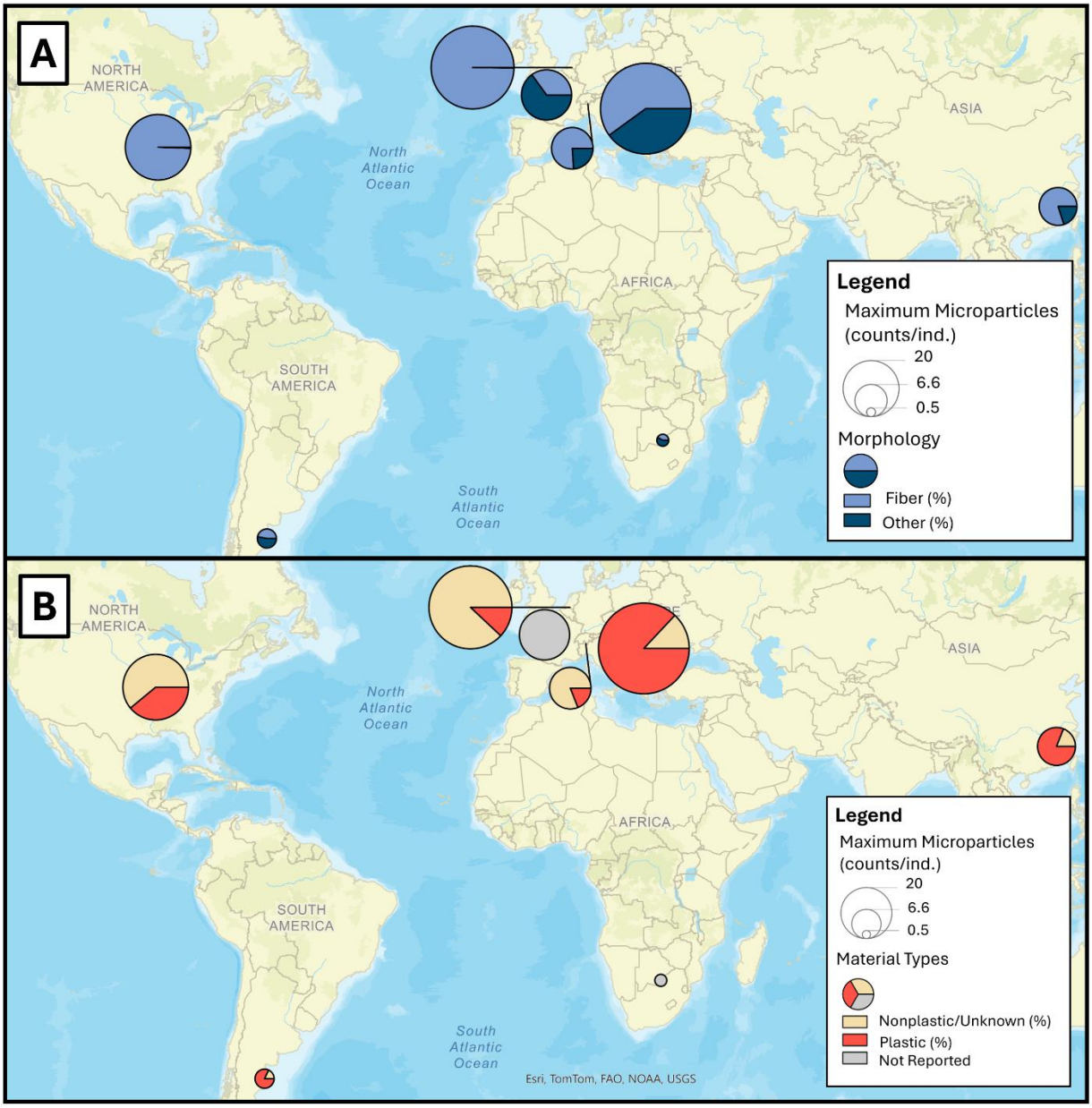

Figure 4.5. *The anthropogenic microparticle levels that have been observed in C. fluminea globally (basemap by Esri, 2025b), with the maximum content per individual represented by the circle sizes in both (A) and (B). The percentages of (A) fibers versus other morphologies (e.g., fragments, films, and spheres) and (B) plastic versus non-plastic materials are shown as pie charts within the circles. The designation of "not reported" in (B) refers to studies that either did not report any material types or only reported plastic types (thus preventing an estimate of non-plastic materials in C. fluminea). Table 4.S5. provides more details from the studies compiled for this visualization.*

4.5.2. Temporal Fluctuations of Anthropogenic Microparticles in Environmental Compartments Relative to the Physicochemical Properties of Stream Water and Sediment

Though we observed a positive but insignificant trend between *C. fluminea* and sediment anthropogenic microparticle concentrations, their strong relationships with unique physicochemical parameters for water and sediment (Fig. 4.4.) indicate that different mechanisms might drive the temporal fluctuations of anthropogenic microparticles in the two compartments. When fine sediment was more common in the < 4.75 mm grain size fraction (i.e., when d_{16} values were low), sediment anthropogenic microparticle content was higher (Fig. 4.4.). Both the ability of finer sediment grain sizes to better retain anthropogenic microparticles (seen in laboratory experiments; Li et al., 2024) as well as similar correlations between sediment particle sizes and microplastic abundance (seen in other field studies; e.g., He et al., 2020) have been demonstrated in prior research, with the physical explanation for this trend being that the reduced pore sizes that occur when sediment grains are small inhibit anthropogenic microparticle transport (Li et al., 2024).

However, neither clam anthropogenic microparticle abundance nor its correlated physicochemical parameter, water TSS, had significant relationships with sediment microparticle content or d_{16} (Fig. 4.4.). Instead, TSS had a significant and negative correlation with temperature. Filtration by *C. fluminea* can directly impact suspended solids in water, causing increased water clarity by decreasing suspended solid concentrations (Beaver et al., 1991; Rong et al., 2021). If this explanation alone is taken as reason for the varying TSS levels each month, summer months would result in low TSS due to high filtration by *C. fluminea* while winter months would have high TSS due to low filtration by the clams. Lower filtration by *C. fluminea* has been seen in winter months below 8 ºC (Lauritsen, 1986), along with behavior changes like

variable shell closure. In our study, low winter temperatures also corresponded with elevated salinity levels in the stream from road deicer applications (Table 4.S2.), which can similarly cause valve closure (Roden, 2018). Coinciding high TSS and high anthropogenic microparticle variability in the clams during the four months with water temperature near or below 8 ºC (Fig. 4.4.; Fig. 4.S9.) might therefore be explained by reduced filtration (elevating TSS) and variable valve and shell closure (leading to high variability in individual clam's anthropogenic microparticle content), with both caused by cold temperatures.

From this filtration explanation, we can further speculate that the clams might be concentrating the signature of anthropogenic microparticles present in water and drawing anthropogenic and other suspended materials down to the sediment-water interface where they are buried. This behavior would also result in anthropogenic microparticles within *C. fluminea* that more closely resemble the water's anthropogenic microparticle compositions than those in the sediment. Though we were ultimately unable to constrain anthropogenic microparticle content in the water, anthropogenic microparticles below the LOD from water samples analyzed for material type were cotton, which was a prevalent material type in the *C. fluminea* samples. Further work with higher volume water samples could clarify any similarities in anthropogenic microparticle compositions between water and *C. fluminea* samples.

The reason for higher average anthropogenic microparticle content in the clams during the winter months when the sediment anthropogenic microparticle storage was not similarly elevated (e.g., December 2021 and March 2022; Fig. 4.2.) remains uncertain. The influence of water anthropogenic microparticle content is one unknown that could be partially responsible for this difference. Additionally, researchers have not yet examined whether anthropogenic microparticle retention might be enhanced if valve closure occurs in bivalves (i.e., in winter months regardless of the sediment anthropogenic microparticle storage), though studies of other

types of contaminants suggest that accumulation potentially occurs during valve closure (e.g., Cd in Nan et al., 2016). The level of anthropogenic microparticles present in *C. fluminea* throughout the year-long study period seems to be impacted by a combination of bivalve behavior that could change seasonally (e.g., valve closure, variable filtration rates, and preferential selection of certain microparticles) and the available anthropogenic microparticles in the surrounding environment. Selective uptake might also be a reason for clam anthropogenic microparticle levels that sometimes seem temporally decoupled from the levels in sediment storage.

Though we did not observe a significant linear relationship between clam and sediment anthropogenic microparticle content in our samples (Fig. 4.4.), we detected similar patterns between the two compartments, specifically through two key examples. February 2022 featured the most variable clam and sediment anthropogenic microparticle amounts in replicates (Fig. 4.2.) and was the only month with both recent snowfall and elevated salinity (Table 4.S2.). Prior research has identified snowfall as a source of microplastics (Bergmann et al., 2019). Variable interaction with snowmelt by *C. fluminea* or mixing of snowmelt into sediment might therefore have impacted sample variability if recent snowfall was a major point source of anthropogenic microparticles on this sampling date. In contrast, in August 2022, an extreme flood occurred prior to sampling (Table 4.S1.) that led to prolonged high flow, turbid water, and channel geomorphological changes. August 2022 was the only month that no clam samples were above the LOD, and only one sediment replicate sample was above the LOD (Fig. 4.2.). The clam population was also lower, leading to difficulty collecting a sufficient number of healthy samples (Table 4.S2.). These August 2022 samples likely demonstrate a large-scale flushing of anthropogenic microparticles from the system as well as a die-off of the *C. fluminea* population (via the large proportion of discarded individuals to the quantity sampled; Table 4.S2.). In the cases of both February 2022 and August 2022, unusual water delivery to the stream may have

led to the respectively high and low anthropogenic microparticle content in both clam and sediment samples. Thus, while quantitative biomonitoring may be unsuccessful between the two compartments, qualitative indication of the extremes in anthropogenic microparticle fluctuation (i.e., exceptionally high or low levels of these microparticles) might still be feasible even in a highly variable environment.

4.5.3. The Potential of C. fluminea as a Bioindicator of Anthropogenic Microparticles in the Environment

The first direct proposal of *C. fluminea* as a bioindicator used significant and positive linear relationships between anthropogenic microparticle content in the clams and sediment or water samples as evidence of their bioindication potential (Su et al., 2018). Considering these correlations as requirements, bioindication would be unsuccessful across our sample set, which is likely due to the temporal variability of the urban stream we studied. Nonetheless, *C. fluminea* is the only species present in our study system that allows us to compare findings in the same organism for 16 countries spanning five continents (Fig. 4.5.; Table 4.S5.). Across these studies, the preferential uptake of microfibers is remarkably consistent and includes both plastic and non-plastic materials of human origin (Fig. 4.5.; Table 4.S5.). Although seasonal controls could affect how reliably *C. fluminea* demonstrates high resolution temporal changes in anthropogenic microparticle content and preferential selection of these microparticles might lead to higher levels of specific materials (e.g., PET), we found that *C. fluminea* still indicates the most common type of anthropogenic microparticle contamination (i.e., microfibers) in the surrounding environment. As an organism available across widespread freshwater hydrologic systems, *C. fluminea* can therefore be readily used to identify the most prevalent sources of microplastic pollution and global-scale commonalities or differences in anthropogenic microparticle

contamination sourcing. The findings of *C. fluminea* uptake are also relevant for understanding the entry of anthropogenic microparticles into aquatic and terrestrial food webs.

One element that inhibited thorough comparison of our results across studies was differences in reporting for anthropogenic microparticle content in samples and blanks as well as inconsistencies in background correction methods. Regardless of whether blank correction is used, reporting the quantities of anthropogenic microparticles in the blanks that are needed to correct data or calculate the LOD should be standard. For studies with *C. fluminea*, reporting of both counts by individual and per gram of tissue mass is necessary. Where conservative blank correction methods like the LOD are used, larger sample sizes might be required to ensure anthropogenic microparticle content can be detected even if a population has variable rates of contamination (i.e., it features individuals both above and below the LOD) that are potentially linked to behavior and filtration rates. The major remaining question that would aid our understanding of the efficacy of *C. fluminea* as a bioindicator is how anthropogenic microparticle uptake and retention in this species might be affected by changes in surrounding water properties (specifically low temperatures and high salinity).

4.6. Conclusions

After sampling human-sourced microparticles in an urban stream's *C. fluminea*, water, and sediment over a one-year period, we found that the clam species did not effectively bioindicate the temporal fluctuations or diversity of anthropogenic microparticles in its surrounding environment. Though the two compartments shared a positive trend, sediment anthropogenic microparticle content was more strongly controlled by sediment grain size, while clam anthropogenic microparticle content was most likely influenced by the connections between water quality and clam behavior. *C. fluminea* also might have selectively taken up anthropogenic microparticles, leading to smaller size ranges and a predominance of cotton and

PET microparticles compared to the assemblages found in the sediment. However, clams still indicated key moments of extreme variation in sediment anthropogenic microparticle content, like the high concentrations and variability during snowy conditions in February 2022 and the low concentrations after a severe flood in August 2022. Moreover, *C. fluminea* facilitated comparison and identification of the most prevalent contamination type in this stream environment (microfibers) and how this morphology may be a shared concern across global freshwater systems.

4.7. Acknowledgements

This work was funded by research grants from the United States Geological Survey Water Resources Research Act Program grant (Award: G21AP10582-03), awarded through the Missouri Water Center to Elizabeth A. Hasenmueller, and the Geological Society of America Graduate Student Research Grants program awarded to Natalie F. Hernandez (Award 13039-21, which was funded by the National Science Foundation Award 1949901 and Award 13688-23). We appreciate all who helped with field and laboratory work, but we are particularly grateful to Dr. Susanne Brander and her team for facilitating the use of μ-FTIR instrumentation at Oregon State University and Julia Thiesen for her assistance with replication of the anthropogenic microparticle visual identification process for a subset of samples.

4.8. References

Adams, J.K., Dean, B.Y., Athey, S.N., Jantunen, L.M., Bernstein, S., Stern, G., Diamond, M.L., Finkelstein, S.A., 2021. Anthropogenic particles (including microfibers and microplastics) in marine sediments of the Canadian Arctic. Sci. Total Environ. 784, 147155.

Akanyange, S.N., Zhang, Y., Zhao, X., Adom-Asamoah, G., Ature, A.A., Anning, C., Tianpeng, C., Zhao, H., Lyu, X., Crittenden, J.C., 2022. A holistic assessment of microplastic ubiquitousness: Pathway for source identification in the environment. Sustain. Prod. Consum. 33, 113-145.

Akindele, E.O., Ehlers, S.M., Koop, J.H.E., 2019. First empirical study of freshwater microplastics in West Africa using gastropods from Nigeria as bioindicators. Limnologica 78, 125708.

Athey, S.N., Erdle, L.M., 2022. Are we underestimating anthropogenic microfiber pollution? A critical review of occurrence, methods, and reporting. Environ. Toxicol. Chem. 41(4), 822-837.

Beaver, J.R., Crisman, T.L., Brock, R.J., 1991. Grazing effects of an exotic bivalve (*Corbicula fluminea)* on hypereutrophic lake water. LRM 7(1).

Bergmann, M., Mutzel, S., Primpke, S., Tekman, M.B., Trachsel, J., Gerdts, G., 2019. White and wonderful? Microplastics prevail in snow from the Alps to the Arctic. Sci. Adv. 5(8).

Criss, R.E., Stein, E.M., Nelson, D.L., 2022. Generation and propagation of an urban flash flood and our collective responsibilities. J. Earth Sci. 33(6), 1624-1628.

Dawson, A.L., Santana, M.F.M., Nelis, J.L.D., Motti, C.A., 2023. Taking control of microplastics data: A comparison of control and blank data correction methods. J. Hazard. Mater. 443A, 130218.

De Frond, H., Rubinovitz, R., Rochman, C.M., 2021. μATR-FTIR spectral libraries of plastic particles (FLOPP and FLOPP-e) for the analysis of microplastics. Anal. Chem. 93(48), 15878-15885.

Della Torre, C., Riccardi, N., Magni, S., Modesto, V., Fossati, M., Binelli, A., 2023. First comparative assessment of contamination by plastics and non-synthetic particles in three bivalve species from an Italian sub-alpine lake. Environ. Pollut. 330, 121752.

Dewitz, J., 2021. National Land Cover Database (NLCD) 2019 Impervious Products: U.S. Geological Survey data release.

Ditlhakanyane, B.C., Ultra Jr., V.U., Mokgosi, M.S., Mokopasetso, T., 2023. Microplastic abundance in the surface water, clams (*Corbicula fluminea*) and fish species (*Oreochromis niloticus* and *Coregonus kiyi*) from the Gaborone Dam, Botswana. Water Air Soil Pollut. 234:602.

Esri, DigitalGlobe, GeoEye, i-cubed, USDA FSA, USGS, AEX, Getmapping, Aerogrid, IGN, IGP, swisstopo, GIS User Community, 2025a. “World Imagery” [basemap]. https://services.arcgisonline.com/ArcGIS/rest/services/World_Imagery/MapServer. Accessed February 20, 2025.

Esri, TomTom, FAO, NOAA, USGS, 2025b. “World Street Map” [basemap]. https://basemaps.arcgis.com/arcgis/rest/services/World_Basemap_v2/VectorTileServer. Accessed February 24, 2025.

Finegan-Dronchi, C.R., Hasenmueller, E.A., 2023. Winter road salt retention is enhanced in watersheds dominated by silicate rocks compared to carbonate rocks. AGU Fall Meeting Abstracts, 2057, H33U-2057.

Finegan-Dronchi, C.R., Hasenmueller, E.A., 2024. Municipal water exchanges between surface water and groundwater resources in an urban catchment. Geological Society of America Abstracts, 56, 402924.

Fu, L., Xi, M., Nicholaus, R., Wang, Z., Wang, X., Kong, F., Yu, Z., 2022. Behaviors and biochemical responses of macroinvertebrate *Corbicula fluminea* to polystyrene microplastics. Sci. Total Environ. 813, 152617.

Giarratano, E., Trovant, B., Hernandez-Moresino, R.D., 2024. Asian clam *Corbicula fluminea* as potential bioindicator of microplastics and metal(oid)s in a Patagonian River. Mar. Environ. Res. 198, 106548.

González-Aravena, M., Rotunno, C., Cárdenas, C.A., Torres, M., Morley, S.A., Hurley, J., Caro-Lara, L., Pozo, K., Galban, C., Rondon, R., 2024. Detection of plastic, cellulosic micro-fragments and microfibers in *Laternula elliptica* from King George Island (Maritime Antarctica). Mar. Poll. Bull. 201, 116257.

Guilhermino, L., Vieira, L.R., Riveiro, D., Tavares, A.S., Cardoso, V., Alves, A., Almeida, J.M., 2018. Uptake and effects of the antimicrobial florfenicol, microplastics and their mixtures on freshwater exotic invasive bivalve *Corbicula fluminea*. Sci. Total Environ. 622-623, 1131-1142.

Guo, X., Cai, Y., Ma, C., Han, L., Yang, Z., 2021. Combined toxicity of micro/nano scale polystyrene plastics and ciprofloxacin to *Corbicula fluminea* in freshwater sediments. Sci. Total Environ. 789, 147887.

Hasenmueller, E.A., Criss, R.E., Winston, W.E., Shaughnessy, A.R., 2017. Stream hydrology and geochemistry along a rural to urban land use gradient. Appl. Geochem. 83, 136-149.

Hasenmueller, E.A., Baraza, T., Hernandez, N.F., Finegan, C.R., 2023. Cave sediment sequesters anthropogenic microparticles (including microplastics and modified cellulose) in subsurface environments. Sci. Total Environ. 893, 164690.

He, B., Wijesiri, B., Ayoko, G.A., Egodawatta, P., Rintoul, L., Goonetilleke, A., 2020. Influential factors on microplastics occurrence in river sediments. Sci. Total Environ. 738, 139901.

Hernandez, N.F., Hasenmueller, E.A., 2024. Anthropogenic macroscale and microscale debris (including plastics) have differing spatial distributions across a small urban watershed. Environ. Eng. Sci. 41(12), 509-519.

Kim, L., Kim, S.A., Kim, T.H., Kim, J., An, Y., 2021. Synthetic and natural microfibers induce gut damage in the brine shrimp *Artemia franciscana*. Aquat. Toxicol. 232, 105748.

Koban, L.A., King, T., Huff, T.B., Furst, K.E., Nelson, T.R., Pfluger, A.R., Kuppa, M.M., Fowler, A.E., 2024. Passive biomonitoring for per- and polyfluoroalkyl substances using invasive clams, *C. fluminea.* J. Hazard. Mater. 472, 134463.

Koutsikos, N., Koi, A.M., Zeri, C., Tsangaris, C., Dimitriou, Kalantzi, O., 2023. Exploring microplastic pollution in a Mediterranean river: The role of introduced species as bioindicators. Heliyon 9(4), e15069.

Lauritsen, D.D., 1986. Filter-Feeding in *Corbicula fluminea* and its effect on seston removal. J. N. Am. Benthol. Soc. 5(3).

Li, L., Su, L., Cai, H., Rochman, C.M., Li, Q., Kolandhasamy, P., Peng, J., Shi, H., 2019. The uptake of microfibers by freshwater Asian clams (*Corbicula fluminea*) varies based upon physicochemical properties. Chemosphere 221, 107-114.

Li, W., Brunetti, G., Zafiu, C., Kunaschk, M., Debreczeby, M., Stumpp, C., 2024. Experimental and simulated microplastics transport in saturated natural sediments: Impact of grain size and particle size. J. Hazard. Mater. 468, 133772.

Macieira, R.M., Oliveira, L.A.S., Cardozo-Ferreira, G.C., Pimental, C.R., Andrades, R., Gasparini, J.L., Sarti, F., Chelazzi, D., Cincinelli, A., Gomes, L.C., Giarrizzo, T., 2021. Microplastic and artificial cellulose microfibers ingestion by reef fishes in the Guarapari Islands, southwestern Atlantic. Mar. Poll. Bull. 167, 112371.

McCoy, K.A., Hodgson, D.J., Clark, P.F., Morritt, D., 2020. The effects of wet wipe pollution on the Asian clam, *Corbicula fluminea* (Mollusca: Bivalvia) in the River Thames, London. Environ. Pollut. 264, 114577.

Metropolitan Saint Louis Sewer District (MSD), 2024. Sewer Overflows, MSD Project Clear Web page. https://msdprojectclear.org/customers/problems-tips/sewer-overflows/. Accessed February 01, 2025.

Miller, W.A., Atwill, E.R., Gardner, I.A., Miller, M.A., Fritz, H.M., Hedrick, R.P., Melli, A.C., Barnes, N.M., Conrad, P.A., 2005. Clams (*Corbicula fluminea*) as bioindicators of fecal contamination with Cryptosporidium and Giardia spp. in freshwater ecosystems in California. IJP-PAW 35(6), 673-684.

Nan, G., Peigang, W., Chao, W., Jun, H., Jin, Q., Lingzhan, M., 2016. Mechanisms of cadmium accumulation (adsorption and absorption) by the freshwater bivalve *Corbicula fluminea* under hydrodynamic conditions. Environ. Pollut. 212, 550-558.

Park, C.H., Kang, Y.K., Im, S.S. Biodegradability of cellulose fabrics., 2004. J. Appl. Polym. Sci. 94(1), 248-253.

Pastorino, P., Anselmi, S., Zanoli, A., Esposito, G., Bondavalli, F., Dondo, A., Pucci, A., Pizzul, E., Faggio, C., Barcelo, D., Renzi, M., Prearo, M., 2023. The invasive red swamp crayfish (*Procambarus clarkii*) as a bioindicator of microplastic pollution: Insights from Lake Candia (northwestern Italy). Ecol. Indic. 150, 110200.

Primpke, S., Wirth, M., Lorenz, C., Gerdts, G., 2018. Reference database design for the automated analysis of microplastic samples based on Fourier transform infrared (FTIR) spectroscopy. Anal. Bioanal. Chem. 410, 5131-5141.

Rochman, C.M., 2018. Microplastics research — From source to sink in freshwater systems. Science 360(6384), 28-29.

Rochman, C.M., Brookson, C., Bikker, J., Djuric, N., Earn, A., Bucci, K., Athey, S., Huntington, A., McIlwraith, H., Munno, K., De Frond, H., Kolomijeca, A., Erdle, L., Grbic, J., Bayoumi, M., Borrelle, S.B., Wu, T., Santoro, S., Werbowski, L.M., Zhu, X., Giles, R.K., Hamilton, B.M., Thaysen, C., Kaura, A., Klasios, N., Ead, L., Kim, J., Sherlock, C., Ho, A., Hung, C., 2019. Rethinking microplastics as a diverse contaminant suite. Environ. Toxicol. Chem. 38(4), 703-711.

Roden, J., 2018. Determining the physiological and behavioral aspects of salinity tolerance in the Asian clam, *Corbicula fluminea*. Undergraduate Honors Theses, 443.

Rong, Y., Tang, Y., Ren, L., Taylor, W.D., Razlutskij, V., Naselli-Flores, L., Liu, Z., Zhang, X., 2021. Effects of the filter-feeding benthic bivalve *Corbicula fluminea* on plankton community and water quality in aquatic ecosystems: A mesocosm study. Water 13(13), 1827.

Sait, S.T.L., Sorensen, L., Kubowicz, S., Vike-Jonas, K., Gonzalez, S.V., Asimakopoulos, A.G., Booth, A.M., 2021. Microplastic fibres from synthetic textiles: Environmental degradation and additive chemical content. Environ. Pollut. 268, 115745.

Sanchez-Vidal, A., Thompson, R.C., Canals, M., de Haan, W.P., 2018. The imprint of microfibres in southern European deep seas. PLoS ONE 13(11): e0207033.

Sousa, R., Antunes, C., Fuilhermino, L., 2008. Ecology of the invasive Asian clam *Corbicula fluminea* (Müller, 1774) in aquatic ecosystems: an overview. Ann. Limnol.-Int. J. 44 (2), 85-94.

Stankovic, J., Milosevic, D., Paunovic, M., Jovanovic, B., Popovic, N., Tomovic, J., Atanackovic, A., Radulovic, K., Loncarevic, D., Rakovic, M., 2024. Microplastics in the Danube River and its main tributaries—ingestion by freshwater macroinvertebrates. Water 16, 962.

Stanton, T., Johnson, M., Nathanail, P., MacNaughtan, W., Gomes, R., 2019. Freshwater and airborne textile fibre populations are dominated by 'natural', not microplastic, fibres. Sci. Total Environ. 666, 377-389.

Su, L., Xue, Y., Li, L., Yang, D., Kolandhasamy, P., Li, D., Shi, H., 2016. Microplastics in Taihu Lake, China. Env. Pollut., 216, 711-719.

Su, L., Huiwen, C., Kolandhasamy, P., Wu, C., Rochman, C.M., Shi, H., 2018. Using the Asian clam as an indicator of microplastic pollution in freshwater ecosystems. Environ. Pollut. 234, 347-355.

United States Geological Survey (USGS), 2025. National Water Information System data available on the World Wide Web (USGS Water Data for the Nation). https://waterdata.usgs.gov/monitoring-location/07010086. Accessed February 19, 2025.

Vidal, A., Phuong, N., Metais, I., Gasperi, J., Chatel, A., 2023. Assessment of microplastic contamination in the Loire River (France) throughout analysis of different biotic and abiotic freshwater matrices. Environ. Pollut. 334, 122167.

Wesch, C., Bredimus, K., Paulus, M., Klein, R., 2016. Towards the suitable monitoring of ingestion of microplastics by marine biota: A review. Environ. Pollut. 218, 1200-1208.

4.9. Supplementary Materials

4.9.1. Supplemental Methods

4.9.1.1. Method 4.S1. Correction for thawed bivalve samples

A portion of the bivalve samples (50%; $n = 99$) experienced a freezer thaw event and lost water mass from their Al foil pouches before analysis was completed. We found a significant loss of both total and tissue masses for the samples that were thawed (Fig. 4.S1.). To assess the potential impacts to anthropogenic microparticle levels in these samples, we examined samples from a 3-month period (from April 2022, May 2022, and June 2022; $n = 82$) in which individual bivalve samples both did and did not experience the thaw event. For these samples, we observed no significant change to the monthly anthropogenic microparticle levels due to thawing both when the total number and the total number normalized to the unaffected shell length were compared (Fig. 4.S2.). Though liquid and its associated mass might have been lost from the closed clam shells during thawing, we suspect that anthropogenic microparticles were unlikely to be lost in this process. These comparisons were performed prior to any blank correction for anthropogenic microparticle quantities (see Section 4.3.3.2.).To determine a realistic tissue mass for the clam samples that were impacted by the thaw event, we used the significant and positive linear relationship between shell length and bivalve mass present in the samples that were unaffected by the thaw event ($n = 100$) to calculate the expected mass for shell length for the samples that experienced the thaw event (Fig. 4.S3.). These estimated masses were used to normalize the anthropogenic microparticle levels for clam samples that experienced the thawing event, both to account for how bivalve size could influence anthropogenic microparticle uptake as well as facilitate the comparison of our results to other studies that typically report anthropogenic microparticle levels in quantities per tissue mass (Su et al., 2018; Wu et al., 2022).

4.9.1.2. Method 4.S2. Replication procedures

4.9.1.2.1. 4.S2.1. Replicate samples

To understand the reproducibility of field sampling procedures, field replicates were taken for water and sediment in October 2022. The water field replicate consisted of a second 2 L of water collected alongside the first water sample. The sediment field replicate consisted of a second 1-L jar filled with a ~ 1 kg homogenization of sediment subsamples from the same three points across the channel as the original sample. Field replicates for both water and sediment in October 2022 had similar anthropogenic microparticle content (with both being below the LOD in the water and a < 5% difference occurring between the field replicates in the sediment; see Hernandez and Hasenmueller, 2024, for additional details). As we only have one field replicate collected during one sampling event, this information is reported here but the sediment field replicate's value is not averaged into the total microparticle levels reported for sediment in October 2022.

We analyzed 4-43 individual clams per sampling event, which were also considered replicates and were averaged together to quantify a given month's anthropogenic microparticle content in *C. fluminea* (Table 4.S2.). The full range of anthropogenic microparticle content reported for *C. fluminea* (i.e., minimum to maximum values) still includes data from individual clams. The variability of the clam replicates ranged ± 0.0 counts/g to ± 10.8 counts/g. For the subset of clam replicates with sufficient quantities of anthropogenic microparticles ($n > 2$ per individual) to be analyzed on µ-FTIR, we found consistency in the identified material types between replicates (all cotton and PET), though this outcome might relate to consistent color-morphology combinations in the clam replicates analyzed with µ-FTIR (Fig. 4.S4.).

Two sediment laboratory replicates were processed from each month's homogenized sample jar to account for any variability in the homogenized sample that might not be captured by a single ~ 250 g subset. Each month's anthropogenic microparticle content in sediment is

therefore an average of the two laboratory replicates taken from the single homogenized sample jar, though the minimum to maximum values reported in sediment still include individual replicate data. The variability of laboratory sediment replicates ranged ± 0.7 counts/kg to ± 49.8 counts/kg, showing that some sample jars may have had more heterogeneous anthropogenic microparticle distributions than others, despite the sample homogenization. The most variable month (i.e., the highest standard deviation) for both clam and sediment replicates was February 2022.

Typically, the color and morphology of the anthropogenic microparticles were similar between sediment replicates (Fig. 4.S5. (A)). However, anthropogenic microparticle material types analyzed with μ-FTIR were different between the subset of sediment replicates that featured sufficient quantities of anthropogenic microparticles ($n > 2$ per replicate) such that they could be analyzed for material type (Fig. 4.S5. (B)). These differences might relate to the more diverse color-morphology combinations randomly chosen for analysis with μ-FTIR, which often were not similar between the analyzed sediment replicates (Fig. 4.S5. (C)).

4.9.1.2.2. 4.S2.2. Cross-channel sampling

To determine how well the homogenization of three points across the channel represented a summary of the cross-channel variation, we collected three separate (i.e., non-homogenized) samples of ~ 1 kg each at each of the three subsampling points to compare to the co-collected homogenized original sample jar. These three non-homogenized subsamples were collected during the October 2022 sampling event. However, the average anthropogenic microparticle quantities found in the three non-homogenized cross-channel sediment subsamples were lower than what was found in the homogenized sediment sample average, though, notably, two of the cross-channel subsamples were below the LOD (Fig. 4.S6.). Additionally, though major anthropogenic microparticle types were similar between the non-homogenized cross-channel

sediment subsamples and the co-occurring homogenized sediment sample (i.e., blue and clear fibers), less common anthropogenic microparticles were different between the two sample types (Fig. 4.S6.).

4.9.1.2.3. 4.S2.3. Visual identification replication

We assessed the variability of our anthropogenic microparticle visual identification results depending on laboratory technician for ~ 10% of the clam samples (n = 27) by having a second worker repeat the count for the selected sample subset. These samples included clams collected in November 2021, February 2022, April 2022, June 2022, and July 2022. The second laboratory technician typically found fewer anthropogenic microparticles than the first laboratory technician (i.e., the average difference from the first to the second count was -0.7 total counts and -2.0 counts/g), which we assume is related to experience level and the potential loss of anthropogenic microparticles from the filters during the first visual inspection. These data are presented in Fig. 4.S7.

4.9.2. Supplemental Tables

Table 4.S1. *Discharge data for the sampling dates (data are summarized from USGS gauge 07010086; USGS, 2025).*

Date	Discharge[a] (m^3/s)	Prior 20-Day Discharge Average[b] (m^3/s)	Days Since Last Flood[c] (days)	Discharge Peak of Last Flood[c] (m^3/s)
2021-11-21	0.09	0.12	24	7.33
2021-12-14	0.03	0.20	4	6.97
2022-01-14	0.15	0.59	13	10.45
2022-02-28	0.39	1.81	6	3.65
2022-03-14	0.17	1.61	9	124.31
2022-04-27	0.27	1.12	2	5.58
2022-05-11	0.33	1.88	6	83.25
2022-06-15	0.11	0.59	6	16.71
2022-07-21	0.07	0.45	4	6.99
2022-08-12	0.23	12.14	8	216.34
2022-09-09	0.12	1.19	4	50.12
2022-10-17	0.02	0.07	5	2.76

[a]The discharge value recorded at 09:00 on the sample date.
[b]The discharge was averaged for the 20-day period leading up to each sampling date (e.g., 1 November 2021 to 21 November 2021 for the 21 November 2021 sampling date).
[c]The last flood is defined as the most recent flood event that reached discharge values > 2 m^3/s.

Table 4.S2. *Sampling information[a] and stream physicochemical data for each of the sampling dates.*

Date and Time	Total Sampled Bivalves	Discarded Bivalves[b]	Processed Bivalves	TSS (mg/L)	Water Temperature (°C)	Specific Conductivity (µS/cm)	Channel Width (m)	Point 1 Water Depth (cm)	Point 2 Water Depth (cm)	Point 3 Water Depth (cm)
2021-11-21 9:15	20	6	14	22	8.2	563.2	15.5	5.1	3.8	0.0
2021-12-14 9:10	5	1	4	17	5.1	667.5	13.5	6.4	10.2	0.0
2022-01-14 9:10	10	0	10	9	2.3	1388.0	12.5	17.8	15.2	0.0
2022-02-28 9:05	13	2	11	11	3.1	5170.0	12.0	15.2	15.2	12.7
2022-03-15 9:05	8	3	5	7	9.2	1740.0	13.5	12.7	12.7	0.0
2022-04-27 8:46	21	2	19	7	13.7	901.0	8.5	12.7	10.2	11.4
2022-05-11 9:16	60	17	43	7	23.1	1182.0	13.0	5.1	12.7	16.5
2022-06-15 9:25	22	2	20	4	27.1	1027.0	8.5	14.0	15.2	16.5
2022-07-21 9:30	21	3	18	3	25.8	728.0	8.5	19.1	15.2	12.7
2022-08-12 9:15	23	15	8	3	23.2	1055.0	9.0	24.1	5.1	8.9
2022-09-09 9:50	19	6	13	4	21.0	890.0	9.0	5.1	5.1	5.1
2022-10-17 9:15	53	19	34	2	9.7	459.8	9.0	15.2	3.8	5.1

[a]Sampling information for the sediment subsamples (that were taken at three points spread evenly across each site's entire channel width) are included in the table.
[b]Some bivalves were discarded due to their small size (< 15 mm) or their shells being filled with sand.

Table 4.S3. *Anthropogenic microparticle amounts and types found in blanks and the calculated LOD for each sample type.*

Blank Type	Total (counts)	Black Fiber (counts)	Blue Fiber (counts)	Blue Fragment (counts)	Clear Fiber (counts)	Pink Fiber (counts)	Red Fiber (counts)
Water Blank 1	4	0	2	0	2	0	0
Water Blank 2	4	0	1	0	3	0	0
Water Blank 3	3	0	2	0	0	0	0
Water Blank 4	3	0	2	0	1	0	0
Water Blank 5	2	0	1	0	1	0	0
Water Blank 6	2	0	2	0	0	0	0
Water Blank 7	1	0	0	1	0	0	0
Water Blank 8	4	0	0	0	1	0	0
Water Blank 9	3	1	1	0	1	0	1
Water Blank 10	3	1	2	0	0	0	0
Average	2.71						
Standard Deviation	1.10						
Water LOD	6 counts						
Sediment Blank 1	4	1	1	0	2	0	0
Sediment Blank 2	3	0	1	0	2	0	0
Sediment Blank 3	3	0	2	0	1	0	0
Sediment Blank 4	4	0	2	0	2	0	0
Sediment Blank 5	3	0	0	0	3	0	0
Sediment Blank 6	4	0	0	0	4	0	0
Average	3.50						
Standard Deviation	0.50						
Sediment LOD	5 counts						
Clam Blank 1	2	0	0	0	2	0	0
Clam Blank 2	0	0	0	0	0	0	0
Clam Blank 3	0	0	0	0	0	0	0
Clam Blank 4	3	0	0	0	3	0	0
Clam Blank 5	1	0	0	0	1	0	0
Clam Blank 6	1	0	0	0	1	0	0
Clam Blank 7	0	0	0	0	0	0	0
Clam Blank 8	1	0	0	0	1	0	0
Average	1.00						
Standard Deviation	1.00						
Clam LOD	4 counts						

Table 4.S4. *The p values for comparisons between each month's anthropogenic microparticle levels in clam using pairwise Wilcoxon tests. Significant differences are bolded.*

Month	NOV	DEC	JAN	FEB	MAR	APR	MAY	JUN	JUL	AUG	SEP
DEC	0.56										
JAN	**0.03**	0.76									
FEB	0.80	0.78	0.24								
MAR	0.49	0.97	0.80	0.56							
APR	**0.03**	0.80	0.80	0.28	0.99						
MAY	**0.00**	0.80	0.80	0.08	0.82	1.00					
JUN	**0.02**	0.80	1.00	0.23	0.80	0.82	0.80				
JUL	**0.00**	0.70	1.00	0.14	0.80	0.80	0.80	1.00			
AUG	**0.03**	0.53	0.70	0.19	0.54	0.54	0.53	0.68	0.66		
SEP	0.12	1.00	0.54	0.53	0.99	0.70	0.52	0.53	0.50	0.34	
OCT	**0.00**	0.25	0.65	**0.00**	0.35	0.30	0.23	0.54	0.53	0.80	**0.04**

Table 4.S5. *Comparison of anthropogenic microparticle content in C. fluminea, water, and sediment for prior studies as well as our work (last row).*

Study	Location	Range in *C. fluminea*[a]	Range in Sediment	Range in Water	Most Common Morphology in *C. fluminea*	Most Common Materials in *C. fluminea*	Blank Levels	Correction
Su et al. (2016)[b]	Taihu Lake, China	0.2-12.5 counts/g	11.0-234.6 counts/kg	3.4-25.8 counts/L	Fibers (> 50%)	Cellophane (31%), non-plastic (31%), PET (19%)	Not reported	None
Su et al. (2018)	Yangtze River Basin, China	0.3-4.9 counts/g; 0.4-5.0 counts/ind.	15.0-160.0 counts/kg	0.5-3.1 counts/L	Fibers (> 60%)	PET (33%), PP (19%), non-plastic (19%)	0-3.0 microparticles	None
McCoy et al. (2020)	River Thames, United Kingdom	0-24.0 counts/ind.			Fibers (> 99%)	Organic (40%), semi-synthetic (38%), PP (7%)	Not quantified in text	Subtraction
Della Torre et al. (2023)	Lake Maggiore, Italy	0-6.0 counts/ind.			Fibers (86%)	Cellulose (~50%), natural polyamide (31%)	Not quantified in text	None
Ditlhakanyane et al. (2023)	Gaborone Dam, Botswana	0.2-0.5 counts/ind.[c]		36.0-76.0 counts/L	Fibers (42%)	Not reported	Not reported	None
Giarratano et al. (2024)	Chubut River, Argentina	0.2-2.9 items/g; 0.2-12.5 counts/ind.			Fibers (47%)	PET (45%), indigo blue (27%), cotton (18%)	3.2 microparticles	Subtraction
Stankovic et al. (2024)[d]	Danube River, EU (DE, AT, HU, SK, HR, RS, BA, RO, BG)	3.9-28.7 counts/ind.			Fibers (60%)	PET (48%), polycarbonate (26%)	6.0 microparticles	Excluded fibers from further analysis
Vidal et al. (2023)	Loire River, France	1.3-24.6 counts/g; 1.1-8.8 counts/ind.	142.1-800.0 counts/kg	0-29.0 counts/L	Fragments (65%)	Polyethylene (> 60%)	0-4.0 microparticles	Subtraction
This Chapter	Deer Creek, United States	0-31.4 counts/g; 0-15.0 counts/ind.	0-188.6 counts/kg	< LOD [0-2.7 counts/L]	Fiber (> 99%)	Cotton (54%) [all non-plastic: 61%], PET (37%)	0-3.0 microparticles	Removed microparticles below LOD of 4.0

[a]Counts per individual are abbreviated as "counts/ind.".
[b]The Su et al. (2016) study is not used in the global map (Fig. 4.5.) because it does not report counts per individual.
[c]The data were reported as 3.2-8.0 counts/site, but 16 individuals were collected per site.
[d]Fibers and fragments were reported as separate counts but were combined here for comparison to other data.

4.9.3. Supplemental Figures

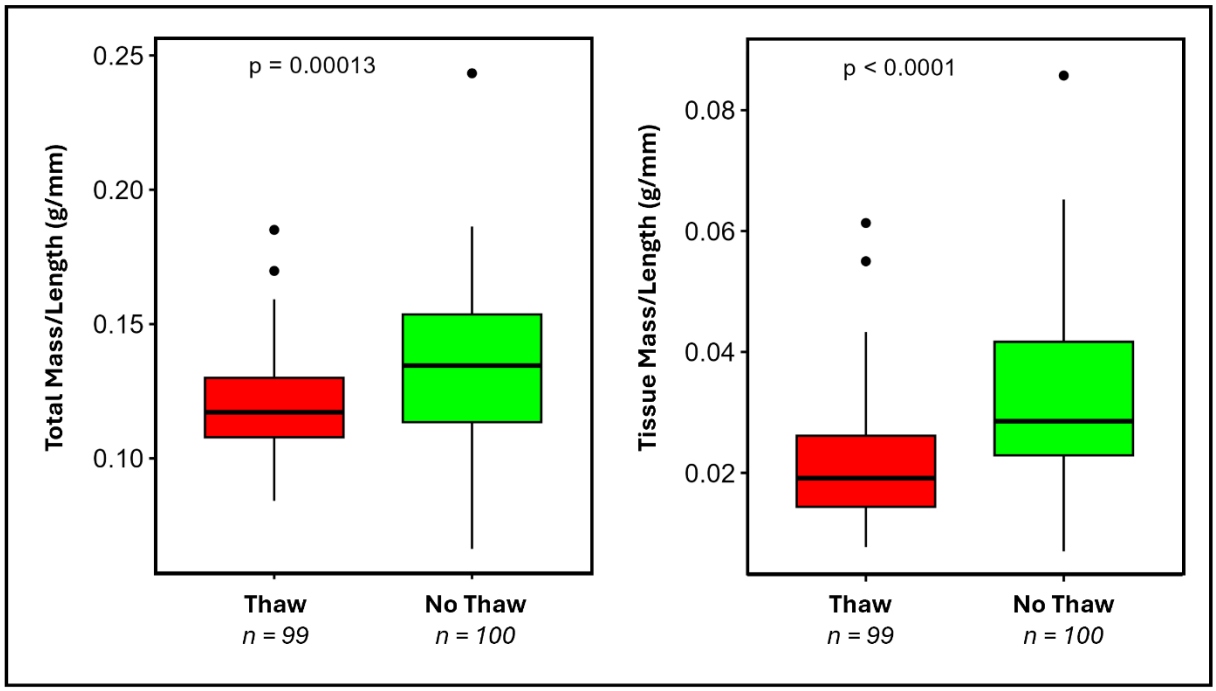

Figure 4.S1. *A comparison of the clams' total mass (tissue + shell) to shell length ratio (left) and the clams' tissue mass to shell length ratio (right) for samples that did and did not experience the thaw event. The p values for Welch's t test are provided above the plots.*

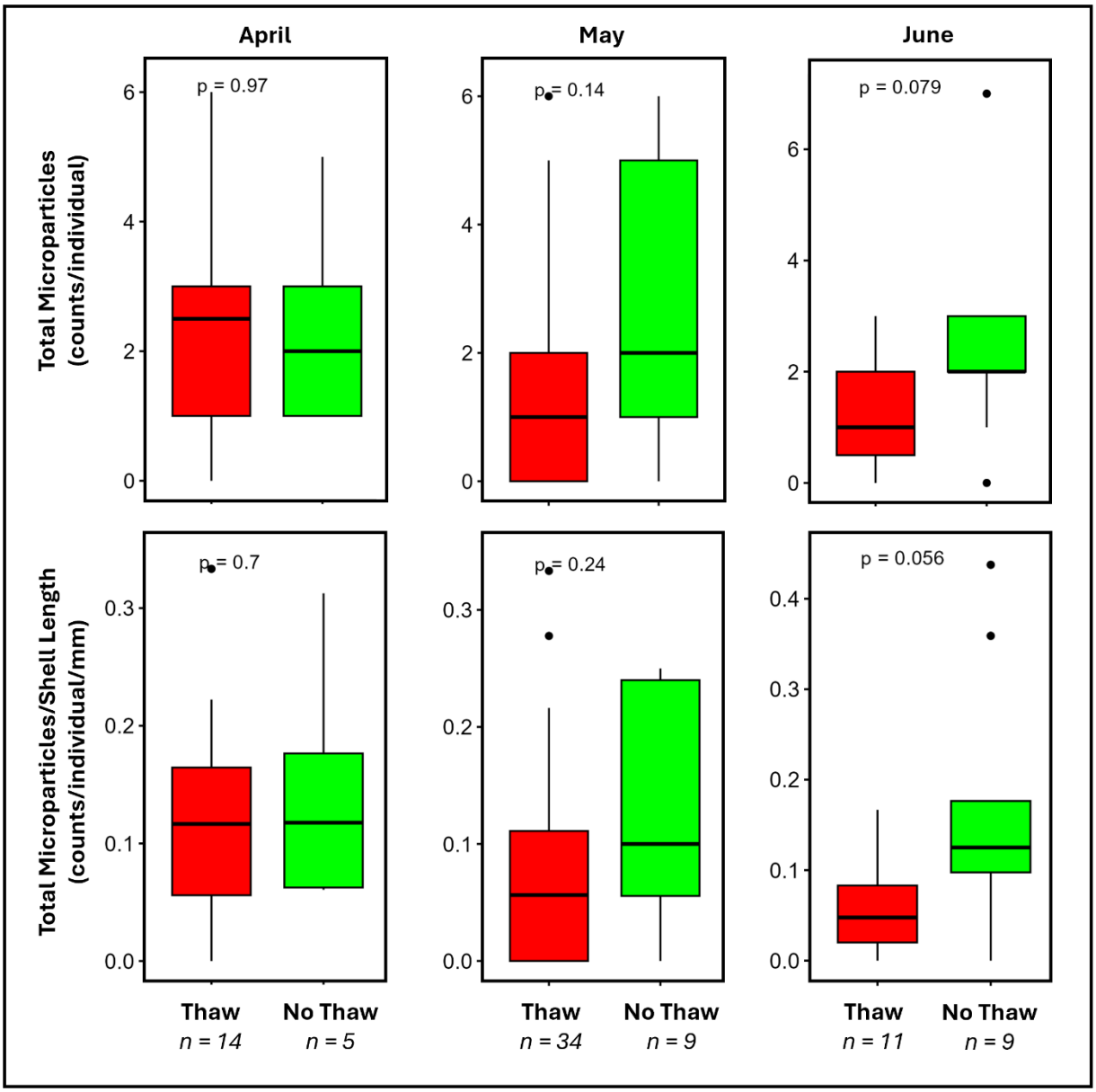

Figure 4.S2. *A comparison of the total anthropogenic microparticles per individual (top) and the total anthropogenic microparticles normalized to shell length (bottom) for sets of individual clams that did and did not experience the thawing event. Data for the April 2022, May 2022, and June 2022 (left to right) sampling events are presented. The p values for Welch's t test are provided above the plots.*

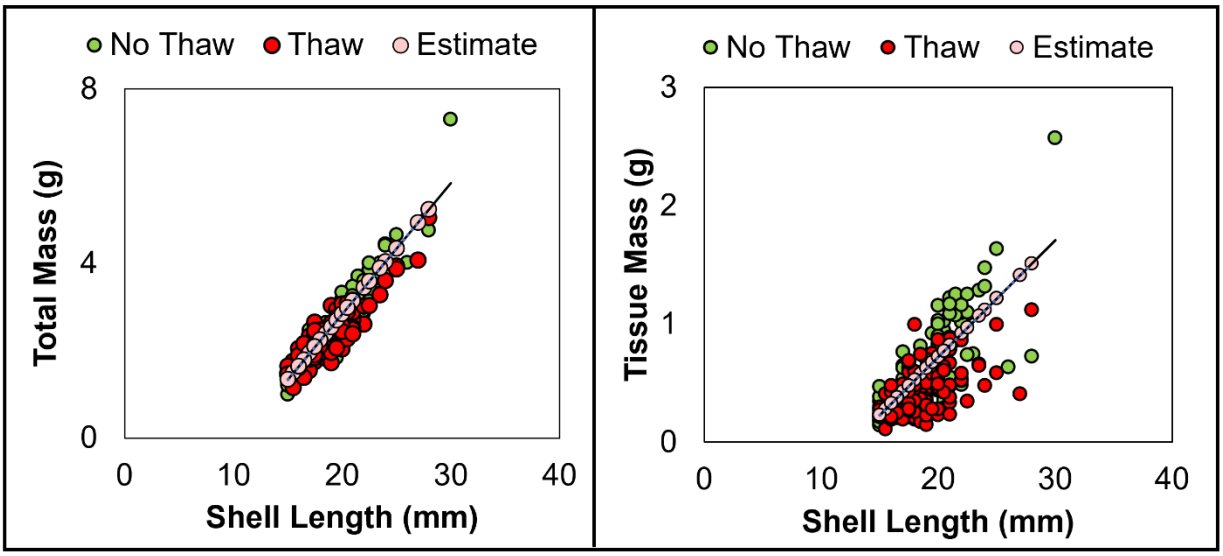

Figure 4.S3. *The relationship between the total mass and shell length (left) as well as the tissue mass and shell length (right) for the bivalve samples. Individuals that did (red circles) and did not (green circles) experience the thawing event are shown. We also estimated the pre-thaw masses of the thawed individuals from the relationship between masses and shell lengths for samples that did not experience the thawing event. These estimated original masses are shown as light red circles.*

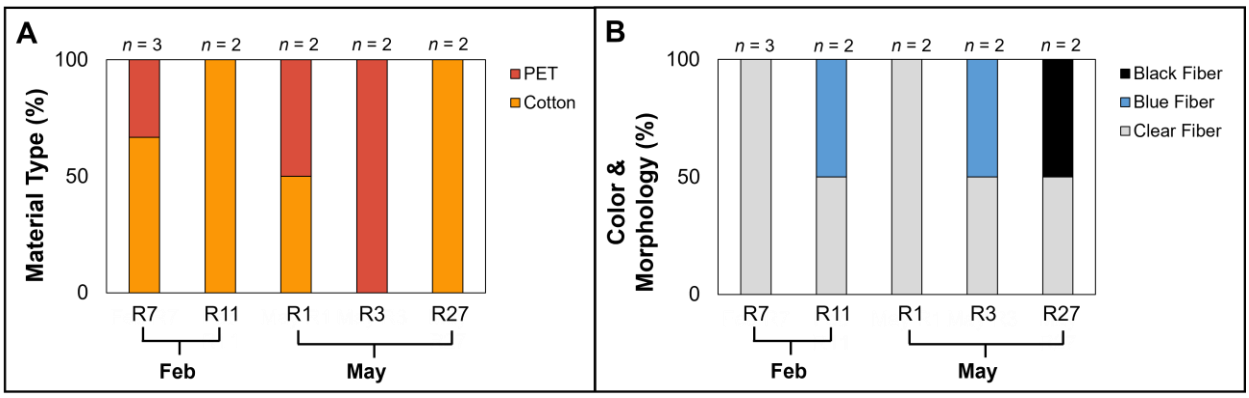

Figure 4.S4. *(A) A comparison of material types between clam replicate subsets (n = 5 from February 2022 and May 2022) where at least two anthropogenic microparticles from each replicate were analyzed using μ-FTIR (with the n value for the analyzed anthropogenic microparticles above each bar). (B) The color and morphology characteristics of the subset of clam anthropogenic microparticles run for material types in (A).*

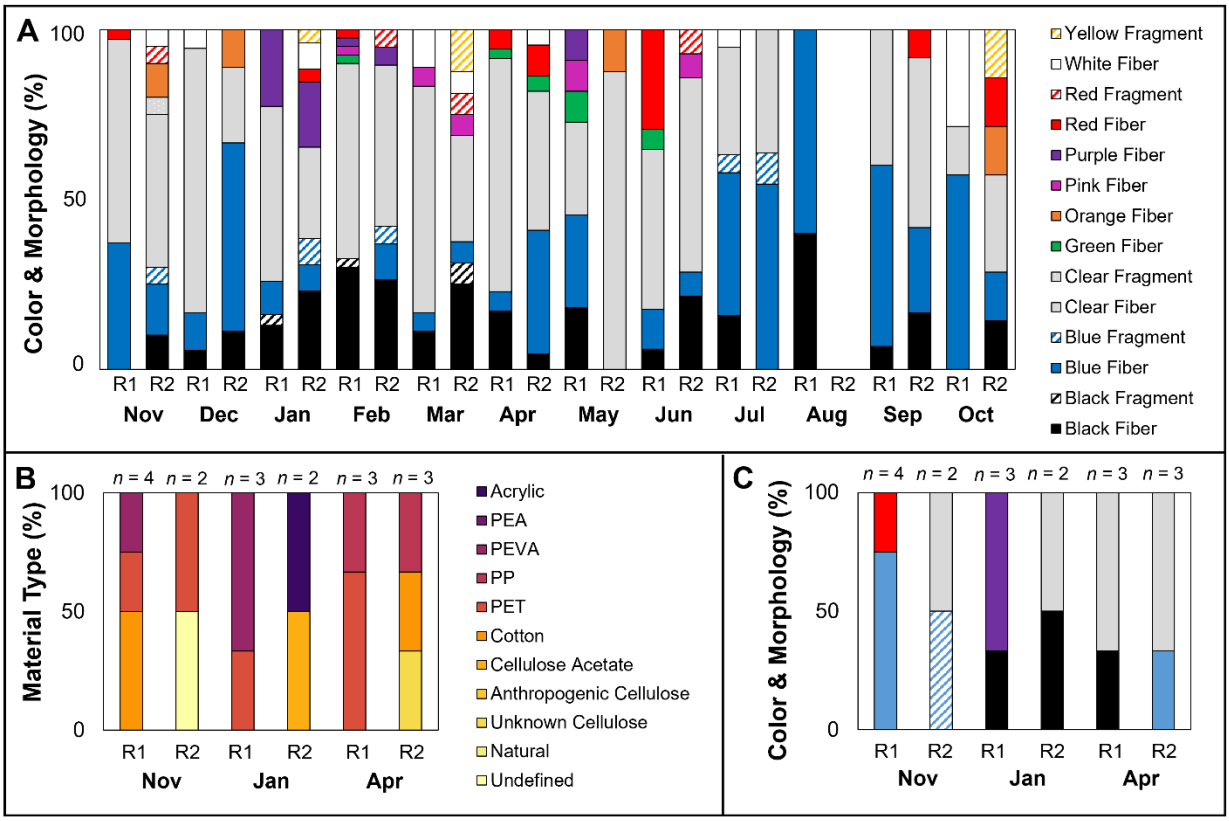

Figure 4.S5. *(A) A comparison of the color and morphology attributes of the anthropogenic microparticles in sediment laboratory replicates for every month (n = 24). For each month, the left column is the first replicate (R1), and the right column is the second replicate (R2). (B) A comparison of material types between sediment laboratory replicates for a subset of the replicates (n = 6 including November 2021, January 2022, and April 2022) where at least two anthropogenic microparticles from each replicate were analyzed using μ-FTIR (with the n value for the analyzed anthropogenic microparticles above each bar). For each month, the left column is the first replicate (R1), and the right column is the second replicate (R2). (C) The color and morphology characteristics of the subset of sediment anthropogenic microparticles run for material types in (B). For interpretation of the anthropogenic microparticle types seen in (C), reference the legend in (A).*

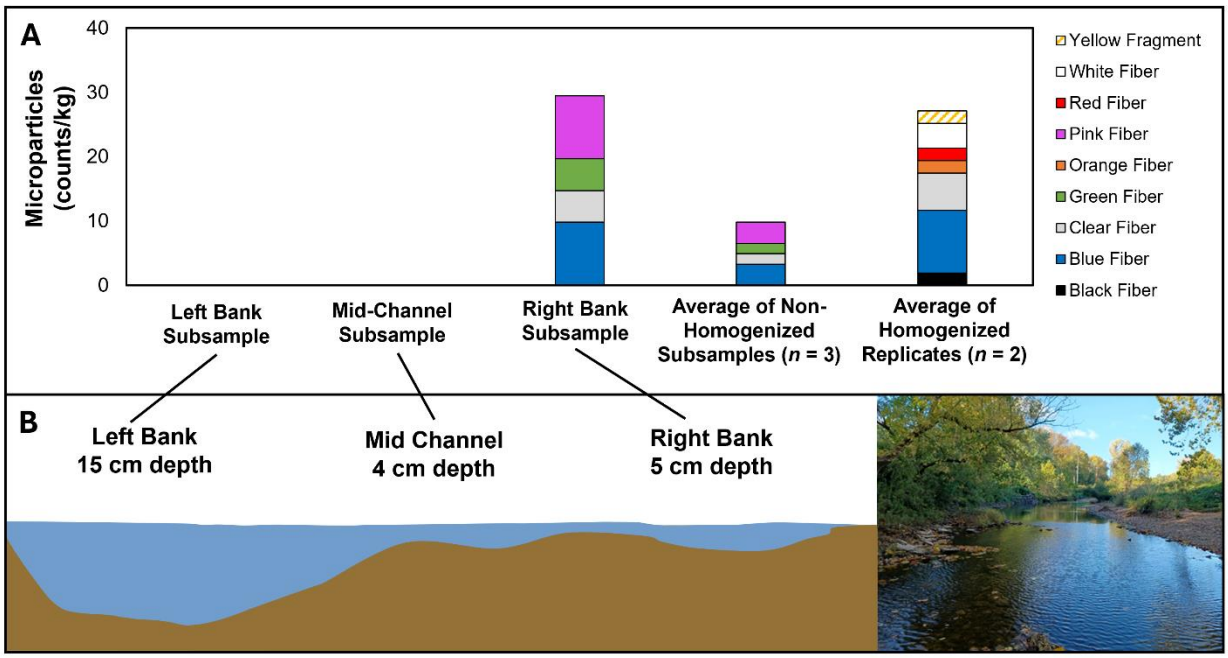

Figure 4.S6. *The cross-channel sediment anthropogenic microparticle data from the October 2022 sampling event. (A) The colors and morphologies found in each of the three, non-homogenized sediment subsamples, the averaged data for the three, non-homogenized sediment subsamples, and the homogenized sample and its laboratory replicate. (B) A visualization of the three subsampling locations across the channel with the depth of each point (left) and an image of the site in October 2022 (right).*

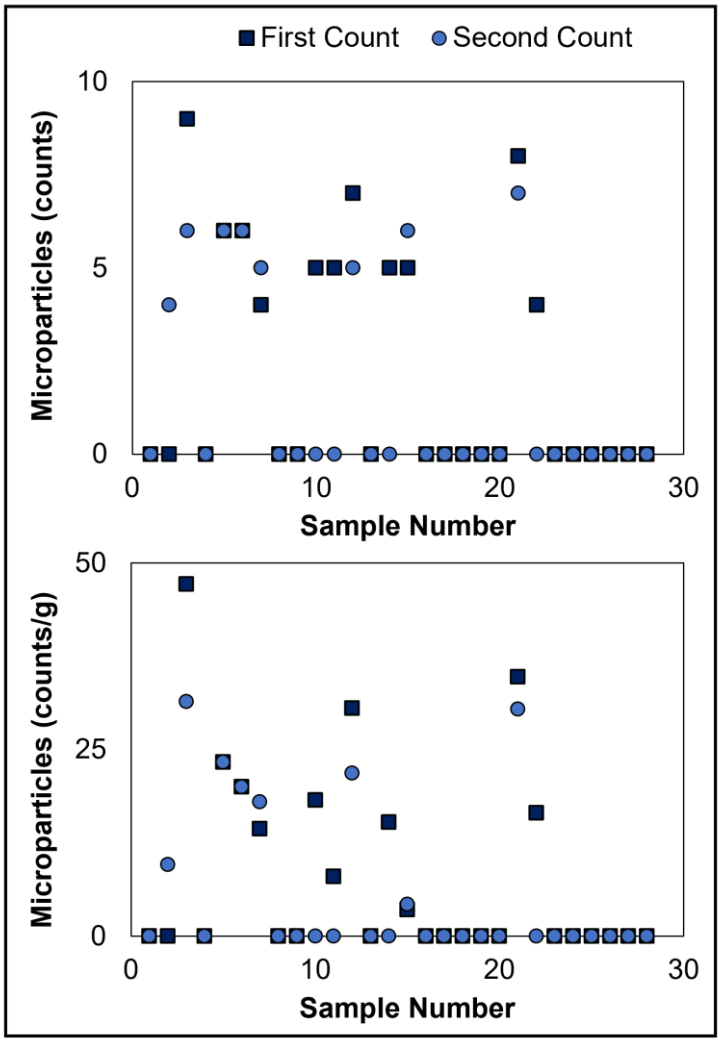

Figure 4.S7. *The LOD-corrected data from clam samples counted by two laboratory technicians. The total number of anthropogenic microparticles found by each worker per replicate (top) as well as the count normalized to tissue mass (bottom) are shown.*

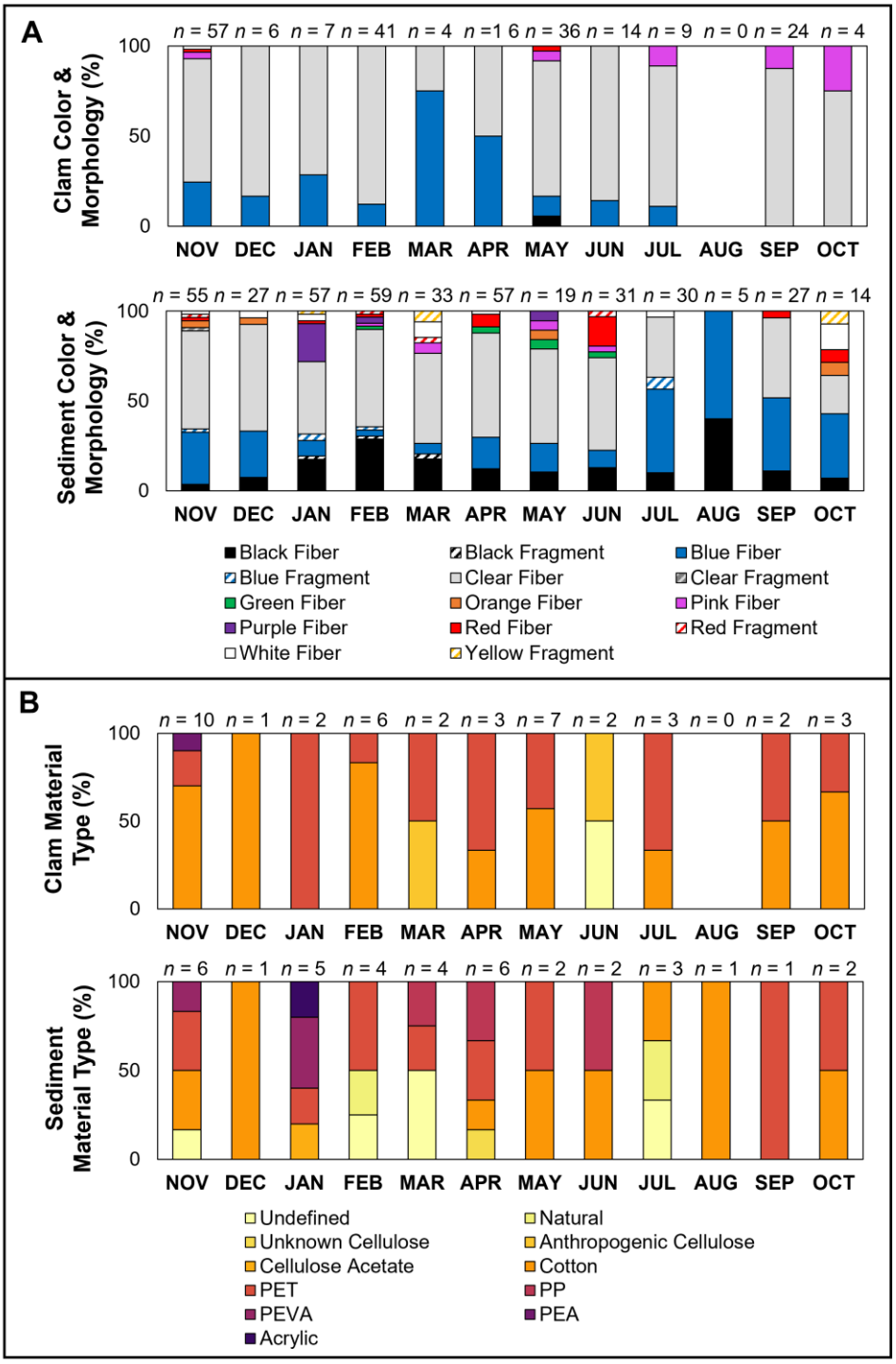

Figure 4.S8. *(A) The percentages of anthropogenic microparticle colors and morphologies for each month in all the clam replicates (sample n = 4-43 per month) and sediment laboratory replicates (sample n = 2 per month) that were above the LOD (the anthropogenic microparticle n values per month are shown above the plots). (B) The percentages of anthropogenic microparticle material types for each month in the subset of clam and sediment replicates that were analyzed with μ-FTIR (the anthropogenic microparticle n values per month are shown above the plots).*

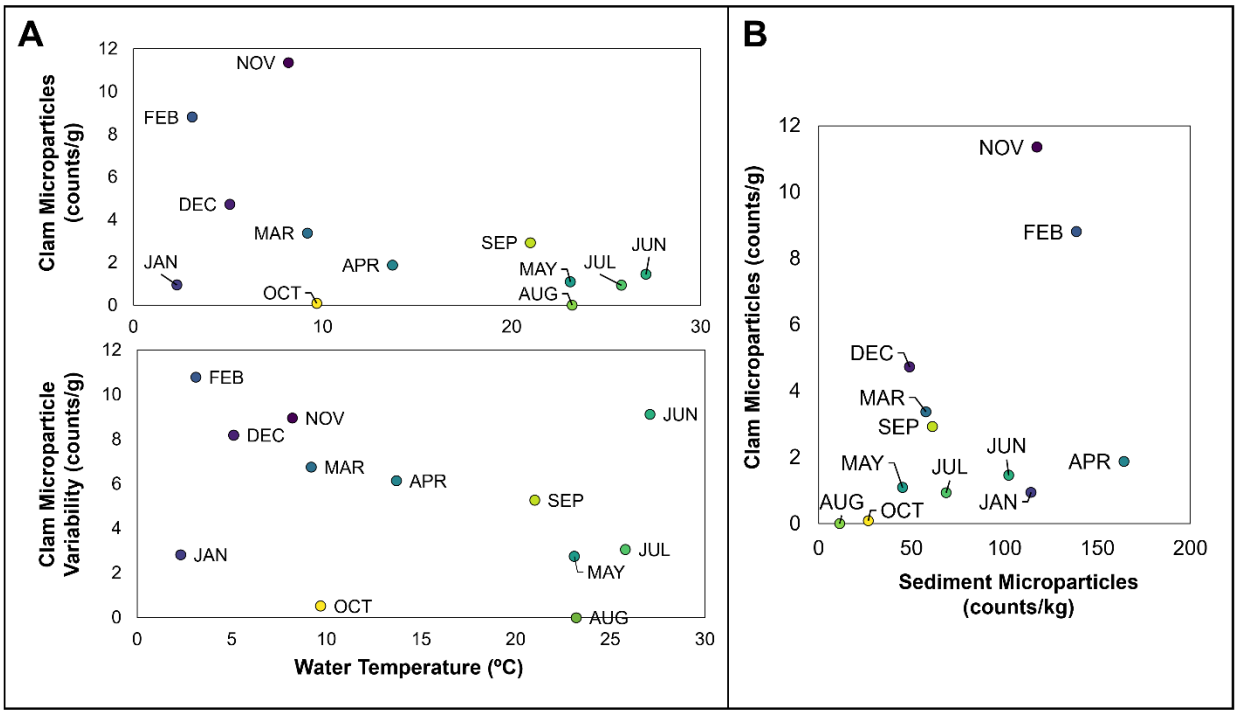

Figure 4.S9. *(A) Anthropogenic microparticle concentrations and their variability in clams each month compared to water temperature. (B) Anthropogenic microparticle abundances in clams compared to sediment, where each point is labeled with the month when the data were collected.*

4.9.4. Supplemental References

Hernandez, N.F., Hasenmueller, E.A., 2024. Anthropogenic macroscale and microscale debris (including plastics) have differing spatial distributions across a small urban watershed. Environ. Eng. Sci. 41(12), 509-519.

Su, L., Huiwen, C., Kolandhasamy, P., Wu, C., Rochman, C.M., Shi, H., 2018. Using the Asian clam as an indicator of microplastic pollution in freshwater ecosystems. Environ. Pollut. 234, 347-355.

Wu, Y., Yang, J., Li, Z., He, H., Wang, Y., Wu, H., Xie, L., Chen, D., Wang, L., 2022. How does bivalve size influence microplastics accumulation? Environ. Res. 113847.

CHAPTER 5: URBANIZATION AND HUMIDITY IMPACT ATMOSPHERIC DEPOSITION OF ANTHROPOGENIC MICROPARTICLES (INCLUDING MICROPLASTICS) IN A HUMID SUBTROPICAL CITY

5.1. Abstract

The fate of anthropogenic microparticles (i.e., microplastics as well as other natural and semi-synthetic materials of < 5 mm) that have been suspended in and transported through the atmosphere remains understudied. Though early work suggests high levels of microplastic deposition from the atmosphere in humid subtropical megacities, atmospheric anthropogenic microparticle deposition has not been assessed in the comparatively less-populated humid subtropical region of the central United States. Our study thus analyzes atmospheric deposition samples for anthropogenic microparticles (including microplastics) at an urban and suburban site in the St. Louis, Missouri, United States, metropolitan area over 1 year. Anthropogenic microparticles in atmospheric fallout samples were found from below our limit of detection (LOD) up to 312.9 particles/m^2/day. The urban site had a significantly higher 101.7 particles/m^2/day average deposition rate compared to the suburban site's average deposition rate of 43.3 particles/m^2/day. At both sites, microfibers were the most common anthropogenic microparticles that we found, and microplastics (i.e., fully synthetic substances) made up 41% and 49% of the material types that were analyzed for the suburban and urban sites, respectively. Cotton and polyethylene terephthalate (PET) were the most prevalent material types that we identified. Higher relative humidity enhanced anthropogenic microparticle deposition and was a key factor impacting the temporal fluctuation in anthropogenic microparticle deposition rates throughout the year of sampling. In comparison to research globally, anthropogenic microparticle deposition in the St. Louis region was comparable in quantities and types to the previously studied humid subtropical megacities despite large population

differences. Thus, climate might be a stronger driver of atmospheric anthropogenic microparticle deposition dynamics than population size.

5.2. Introduction

Though microplastics are a well-known and widespread contaminant, the study of atmospheric microplastics is an emerging subfield that has only been explored in the past decade (Zhang et al., 2020). Since the first publication on microplastic deposition from the atmosphere in 2015, research in recent years has found that both microplastics and other anthropogenic microparticles (especially cellulosic microfibers) are ubiquitously present and transported in the global atmosphere (Dris et al., 2015; Evangeliou et al., 2020; Finnegan et al., 2022; O'Brien et al., 2023; Zhang et al., 2020). Anthropogenic microparticle deposition (assessed via passively collected samples of fallout materials) or presence (assessed via actively pumped samples of suspended materials) has been found in a vast range of environments including remote locations (e.g., ocean and Antarctic settings; Trainic et al., 2020; Illuminati et al., 2024), sparsely to densely populated areas (e.g., suburban areas and megacities; Shruti et al., 2022; Jia et al., 2022), and across a range of altitudes up to the troposphere (Allen et al., 2021; Napper et al., 2020).

The deposition of anthropogenic microparticles can be as low as < 10 particles/m^2/day and as high as > 10,000 particles/m^2/day (Jia et al., 2022; O'Brien et al., 2023; Stanton et al., 2019; Welsh et al., 2022). These deposition rates have been found to vary independently of population size and land use and can feature opposite relationships in different locations (e.g., rural areas found with relatively higher deposition levels in Klein and Fischer, 2019, compared to urban areas found with relatively higher deposition levels in Kernchen et al., 2022, and O'Brien et al., 2023). Globally, current research suggests that climate may play a more important role in long-term deposition rate differences compared to land use, though land use can have noticeable effects in local studies of anthropogenic microparticle deposition (Leonard et al., 2024). In

addition to long-term climate and location attributes (e.g., altitude or land use), short-term weather fluctuations (e.g., precipitation events) and changing activity levels in populated areas might also affect the anthropogenic microparticle deposition trends (Abbasi, 2021; Beaurepaire et al., 2024).

Despite the recent growth in research on atmospheric microplastics, the consensus is that further work is required because the atmosphere is one of the least studied environmental compartments for these pollutants (Abbasi et al., 2023; Wright et al., 2020; Zhang et al., 2020). Additionally, only a few studies have assessed atmospheric microplastics in temperate or arid locations within the United States, and a knowledge gap persists on microplastic deposition in the country's humid subtropical region (i.e., in the central and southeastern United States; Allen et al., 2022; Brahney et al., 2020; Chandrakanthan et al., 2023; Yao et al., 2022). Globally, other studies of atmospheric microplastic deposition under humid subtropical climatic conditions have taken place in heavily populated megacities (e.g., Guangzhou, China in Huang et al., 2021, and São Paulo, Brazil in Amato-Lourenço et al., 2022; defined as > 10 million people via United Nations (UN), 2014), leaving unanswered questions about the relative influences of climate, population size, and local sourcing on the atmospheric deposition of microplastics and other anthropogenic microparticles. Prior studies also vary in their inclusion or exclusion of semi-synthetic and non-synthetic microfiber data when reporting deposition rates, despite these types of microfibers having similar negative impacts on ecological health compared to fully synthetic anthropogenic microparticles (Athey and Erdle, 2022; Finnegan et al., 2022; Kim et al., 2021).

Therefore, the objective of our study is to characterize anthropogenic microparticles (including microplastics, tire and road wear, and modified natural (e.g., cotton) or semi-synthetic (e.g., viscose) fibers) in atmospheric deposition in the St. Louis metropolitan area, which is located in the central United States and features a humid subtropical climate. We sampled

atmospheric deposition approximately weekly over a year-long period at two sites (in urban and suburban settings), assessing spatial and temporal controls on anthropogenic microparticle fallout variation over time.

5.3. Materials and Methods

5.3.1. Study Area

The metropolitan St. Louis area, located at the confluence of the Mississippi River and Missouri River in the central United States, has a population of ~ 2.8 million people and is therefore classified as a large city using the National Center for Education Statistics (NCES) classification (i.e., a population > 250,000; East-West Gateway, 2024; Geverdt, 2019). St. Louis has a humid subtropical climate according to the Köppen-Geiger climate classification, with four distinct seasons including drier winters with snowfall as well as rainy conditions in spring months (NWS, 2024). Several air quality monitoring stations across the city provide air quality data such as PM-2.5, PM-10, and O_3 values, and weather stations provide local meteorologic data (see Fig. 5.1.; USEPA, 2024).

We examined atmospheric deposition of anthropogenic microparticles at two sites, including an urban site in St. Louis City and a suburban site in St. Louis County (Fig. 5.1.). The two sites were selected to examine potential differences between urban and suburban anthropogenic microparticle deposition and because they both have prohibited public access, which avoids direct interference with our samplers. In detail, the urban site is a private, three-story rooftop access on Saint Louis University's campus in St. Louis' Midtown neighborhood and the suburban site is a gated field research center that features a stream system, restored native prairies and forests, and a nearby residential community. We were unable to identify a suburban site with a similar elevation to the rooftop of the building in urban St. Louis. Elevation differences therefore exist between the sites that could potentially influence deposition rates

(Table 5.1.). The suburban site also had slightly more trees nearby than the urban site, though in both cases the nearest tree was > 10 m away from the samplers (i.e., trees did not cover our sampling apparatuses).

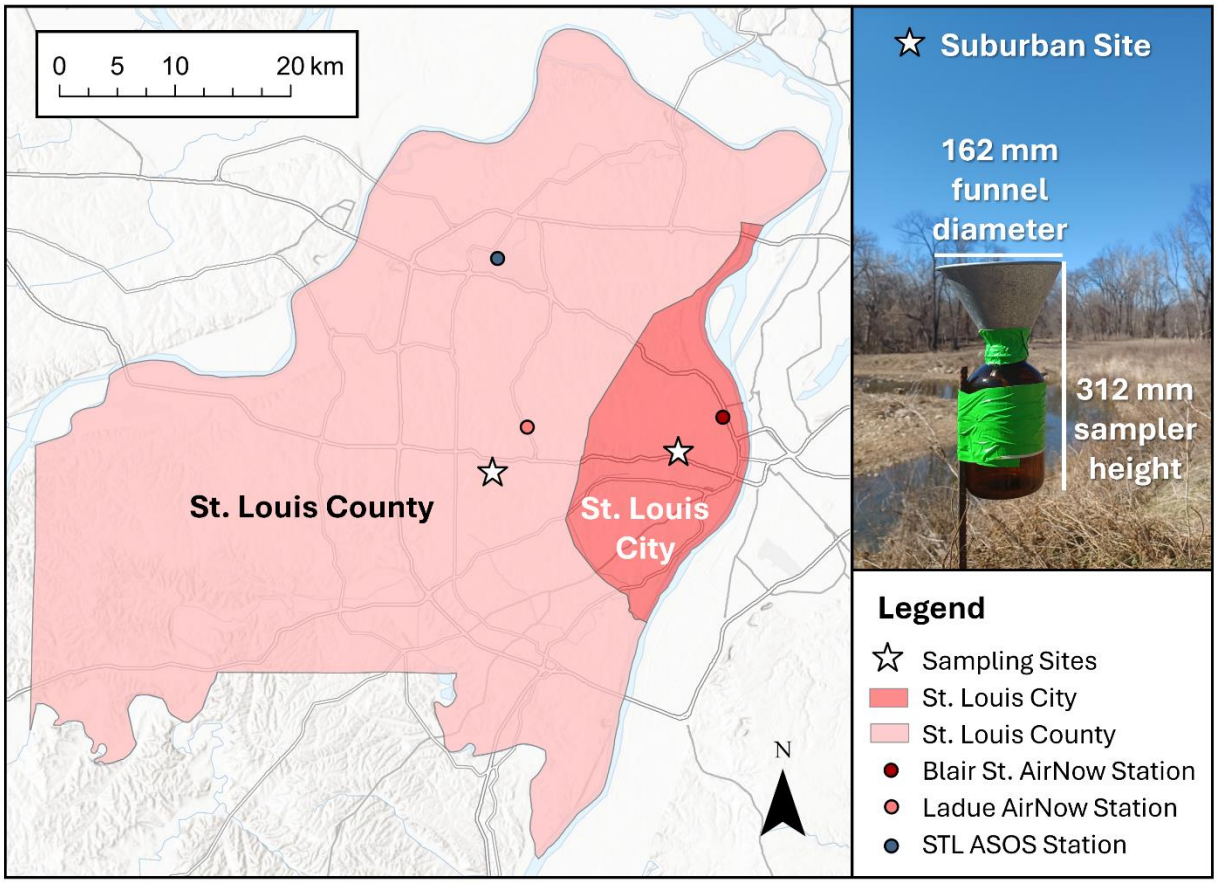

Figure 5.1. *The sampling site locations in St. Louis City and St. Louis County (the basemap is from Esri, 2019), with the locations for atmospheric data collection (i.e., air quality data from the Blair Street and Ladue stations and meteorologic data from the STL ASOS site) as well as an image of the anthropogenic microparticle deposition sampler at the suburban site.*

Table 5.1. *Information about the sampling sites.*

Site	Location	Population[a] (people/km^2)	Elevation above Ground Level[b] (m)
Urban	College campus rooftop	1886.11	158.9
Suburban	Field research station	763.36	146.9

[a]Data are from the United States Census (2020).
[b]Data are from the USGS (2017).

5.3.2. Total Atmospheric Anthropogenic Microparticle Deposition Sampling

Total anthropogenic microparticle atmospheric fallout samples (from both wet and dry deposition) were collected approximately every 8 days (with a range of 3-17 days) from the two sampling sites. The suburban research center site was sampled from April 2023 to April 2024, and the urban campus site was added from June 2023 to April 2024. In total, both sites were simultaneously sampled 33 times between June 2023 and April 2024 (Table 5.S1.). Atmospheric deposition was collected with a stainless-steel funnel connected to a 1-L amber glass bottle at each site (see Fig. 5.1.; Dris et al., 2016). Bright green cotton-vinyl duct tape was used to secure the sampler components in the field (Fig. 5.1.). We selected this distinct color to facilitate the identification of any anthropogenic microparticles released from the tape. On each collection date, 100 mL of filtered distilled deionized (DDI) water was used to thoroughly rinse any anthropogenic microparticles from the funnel into the sample bottle before removing the funnel to store the sample.

5.3.3. Anthropogenic Microparticle Characterization

5.3.3.1. Environmental samples

The atmospheric deposition samples were vacuum-filtered with an all-glass filtration system onto 0.45-µm mixed cellulose ester filters. The resulting filters were visually examined for suspected anthropogenic microparticles (including microplastics, tire and road wear, and modified natural (e.g., cotton) or semi-synthetic (e.g., viscose) fibers) using criteria such as no organic structures, no tapering fibers, and resistance to breakage to identify the microparticles that were likely of human origin (see Hasenmueller et al., 2023, for the full criteria). The visual identification process had a lower size limit of 100 µm. Each suspected anthropogenic microparticle was then photographed, characterized by its color and morphology, and measured for size along its longest axis. The suspected anthropogenic microparticles were next removed from the filter to be stored in filtered 10% ethanol for subsequent material type analysis. The

deposition rate for each sample in particles/m^2/day was calculated following the standard method of dividing the anthropogenic microparticle count for each sample by the area of the opening of the sampler (0.021 m^2) and the sampling interval in days (Zhou et al., 2017; Liu et al., 2022).

The chemical compositions of the suspected anthropogenic microparticles from the atmospheric deposition samples were analyzed with micro-Fourier Transform Infrared (μ-FTIR) spectroscopy using a Thermo Fisher Scientific Nicolet iN5 FTIR instrument. A subset of 7% of the total suspected anthropogenic microparticles (n = 65) were analyzed with μ-FTIR. We sought to analyze ~ 7% of each color-morphology category, though some rare color-morphology combinations were not analyzed (Table 5.S2.). The anthropogenic microparticles were mounted on aluminum foil-covered slides for analysis with the μ-FTIR, which measured attenuated total reflectance across wavenumbers 4000-650 nm with a germanium crystal. Resulting spectra were corrected with atmospheric suppression.

We compared our spectra to both the instrument's default library as well as added libraries for microplastic analysis (e.g., FLOPP from De Frond et al., 2021; Primpke et al., 2018). The μ-FTIR OMNIC software produces a correlation-based match value for each top match within these libraries. We accepted spectra only with matches > 70%, though our goal was a match of > 90% (Lusher et al., 2017; Harris et al., 2021). Our match rate averaged 92%, but a small quantity of the suspected anthropogenic microparticles (n = 4) had no match greater than 70% in the OMNIC software. The spectra for these microparticles were uploaded to Open Specy to check for matches with additional libraries employing automatic preprocessing steps of min-max normalization, smoothing, and wavenumber conformation using linear interpolation (see Cowger et al., 2021). If the Open Specy match value was > 0.8 and the top two matches were for the same material type, these matches were accepted. Despite these efforts, two of the four microparticles remained undefined. When the microparticles matched with cellulosic material,

they were called “anthropogenic” if they were dyed a humanmade color (typically blue) or were called “unknown” if they were not obviously dyed but did not match with plant material.

5.3.3.2. Quality assurance and quality control measures

A series of contamination reduction measures were used during the sample processing steps including wiping down all surfaces, triple rinsing glassware with filtered DDI water, covering containers and equipment with aluminum foil when they were not in use, filtering in a fume hood, and wearing brightly colored 100% cotton attire to allow for the identification of contamination from clothing. We collected blanks for the atmospheric deposition samplers by using the clean steel funnel and glass bottle setup rinsed with 100 mL of filtered DDI water both in the field (n = 2) and laboratory (n = 1). These blanks were subsequently processed alongside our environmental samples. We also collected laboratory filtration blanks (n = 5) by filtering 1 L of prefiltered DDI water during environmental sample processing to check for any contamination caused by the filtration methods.

Similar quantities of anthropogenic microparticles were present in both of our types of blanks (i.e., 3-5 anthropogenic microparticles per individual blank). Thus, the two blank types were combined to calculate a limit of detection (LOD) for our method to blank-correct the atmospheric deposition data. The LOD was calculated as the average of the blank values plus three standard deviations (Table 5.S3.; Dawson et al., 2023). Since the two blank types cannot consistently be reported in the standard units for atmospheric deposition of anthropogenic microparticles (particles/m^2/day), the LOD was applied to the total quantities of each environmental sample before normalizing to the typical sample units and therefore was rounded to a whole number (Table 5.S3.). When the sample anthropogenic microparticle quantities were below the LOD, they were corrected to zero before calculating the deposition rate, which

resulted in deposition rates of zero for these samples. The averages reported for our two sites include these below LOD zero values.

Prior to beginning the analysis of the atmospheric deposition samples from the urban rooftop, we collected two replicate samples at two locations on the roof to determine if the rooftop infrastructure (e.g., exhaust fans) impacted the anthropogenic microparticle deposition rates as well as to concurrently estimate the variability of replicate atmospheric deposition samples (Fig. 5.S1.). The two roof sampling locations included a site far from all the building's infrastructure, which was ultimately chosen for weekly sampling, as well as a site on the opposite side of the building's roof that was near exhaust fans (Fig. 5.S1.).

5.3.4. Landscape, Meteorologic, and Air Quality Data Collection

We assessed the relationships between anthropogenic microparticle deposition and the landscape attributes, meteorologic conditions, and air quality characteristics at our selected sites. Site elevations were obtained from a high-resolution (1 m) digital elevation model (DEM; USGS, 2017). We also assessed differences between typical times of year with leaf cover (defined as April to October) and without leaf cover (defined as November to March). Hourly meteorologic data were collected from an Automated Surface Observing System unit located at St. Louis Lambert International Airport (i.e., the STL site; Iowa Environmental Mesonet (IEM), 2025). Daily or sub-daily air quality data (USEPA, 2024) were collected for PM-2.5 and PM-10 at the Blair Street station (295100085) and PM-2.5 at the Ladue station (291893001). The Ladue station was nearer to our suburban site but lacked other air quality parameters.

The ASOS Network (IEM, 2025) precipitation data for each sampling period were considered with the liquid volume we found in our sampling apparatuses prior to our funnel rinsing step to classify our atmospheric deposition samples as either wet or dry deposition (Table 5.S1.). In detail, when the volume of water in the collected sample was < 15 mL and the total

quantity of the precipitation over the sampling period was < 4 mm, the sample was considered dry deposition. In cases where the sample volume and precipitation data did not both meet these criteria, we used the sample volume to define the deposition type due to the potential for variable weather between the sampling sites and the STL ASOS Network station. Specifically, on the few occasions where the sample volume was < 15 mL but the precipitation was > 4 mm during the monitoring period (n = 4 samples), samples were considered dry deposition. When the sample volume was > 15 mL but the precipitation was < 4 mm during the monitoring period (n = 3 samples), the samples were considered wet deposition.

5.3.5. Data Analysis

Geospatial analyses were conducted using ArcGIS Pro Version 3.0.3. All statistical analyses were performed in R and Microsoft Excel. Microparticle data were non-normal, so non-parametric tests were used to analyzed the datasets (e.g., Spearman's rank correlation coefficient and Wilcoxon signed-rank tests, with $\alpha = 0.05$ for all analyses). Figures were created using ArcGIS Pro Version 3.0.3, R, and Microsoft Excel.

5.4. Results

5.4.1. Quality Assurance and Quality Control Measures

Field and laboratory blanks had 3-5 anthropogenic microparticles identified per individual blank, resulting in a calculated LOD of 5 anthropogenic microparticles (Table 5.S3.). A subset of four anthropogenic microparticles from the blanks (~ 15% of the total 27 anthropogenic microparticles identified within eight blanks) were analyzed with μ-FTIR to determine the common types of materials present in contamination. The identified blank material types included cotton (n = 3) and polyethylene terephthalate (PET; n = 1). The replicates

collected at both the roof subsites (see Fig. 5.S1.) had similar quantities of anthropogenic microparticles deposited during the collection period (i.e., < 20% difference), suggesting that, within a small area (i.e., on one rooftop), the atmospheric deposition sampling procedure is reproducible. However, the anthropogenic microparticle diversity varied somewhat between the two roof subsites (Fig. 5.S1.), with the subsite near the exhaust fans for the building featuring black fibers but no uniquely colored (i.e., red, pink, and orange) fibers compared to the subsite that was away from this building infrastructure. The subsite option farther from the rooftop's exhaust fans was ultimately chosen for our study to avoid the potential influence of the rooftop fans on air circulation. We found that our variable sampling period lengths (3-17 days; see Table 5.S1.) did not influence the key trends in the anthropogenic microparticle data (see Supplemental Information 5.S1.; Fig. 5.S2.).

5.4.2. Anthropogenic Microparticle Content in Atmospheric Deposition

Over the monitoring period, the suburban site had deposition rates from below the LOD (n = 13) to 154.8 particles/m^2/day, with an average and standard deviation of 43.3 ± 42.2 particles/m^2/day (total sample n = 40; Fig. 5.2. (A)). The urban site had deposition rates from below the LOD (n = 4) to 312.9 particles/m^2/day, with an average and standard deviation of 101.7 ± 71.1 particles/m^2/day (total sample n = 37; Fig. 5.2. (A)). The urban site had significantly higher anthropogenic microparticle deposition than the suburban site (Fig. 5.2. (B)). Quantities of anthropogenic microparticles deposited at the two sites for shared sampling dates had a significant and positive correlation (Spearman's ρ = 0.37; Fig. 5.2. (C)).

The anthropogenic microparticle characteristics were similar between the two sites, with the majority of the samples being fibers (> 99%). The most common color-morphology combinations included blue fibers (urban site = 44% and suburban site = 38%) and clear fibers (urban site = 34% and suburban site = 43%; Fig. 5.3. (A)). Cotton and PET were the most

common material types at both sites, but the urban site had a slightly higher percentage of synthetic materials at 49% compared to the suburban site at 41% (Fig. 5.3. (B-C)). Some material types were unique to a given sampling site. For example, only one match to tire wear (i.e., the top spectral matches were polyethylene (PE) – rubber and PE – tire fragment) was found at the urban site, while polypropylene (PP) and styrene acrylonitrile (SAN)/acrylonitrile butadiene styrene (ABS) microparticles were found only at the suburban site. The PET spectral matches included fits to polyester fibers and polyethylene terephthalate fragments, and one microparticle specifically matched with PET shipping label fibers above all other PET types (Fig. 5.3. (C)). The anthropogenic microparticle size averages and standard deviations were 1158.4 ± 742.6 μm at the urban site and 1111.5 ± 823.0 μm at the suburban site. We also observed many small black fragments (< 100 μm) in the samples (see the image backgrounds in Fig. 5.3. (C)) that we were unable to quantify or characterize as natural versus anthropogenic by our visual identification method. Our inability to assess these materials might consequently result in underestimation of atmospheric anthropogenic microparticle deposition.

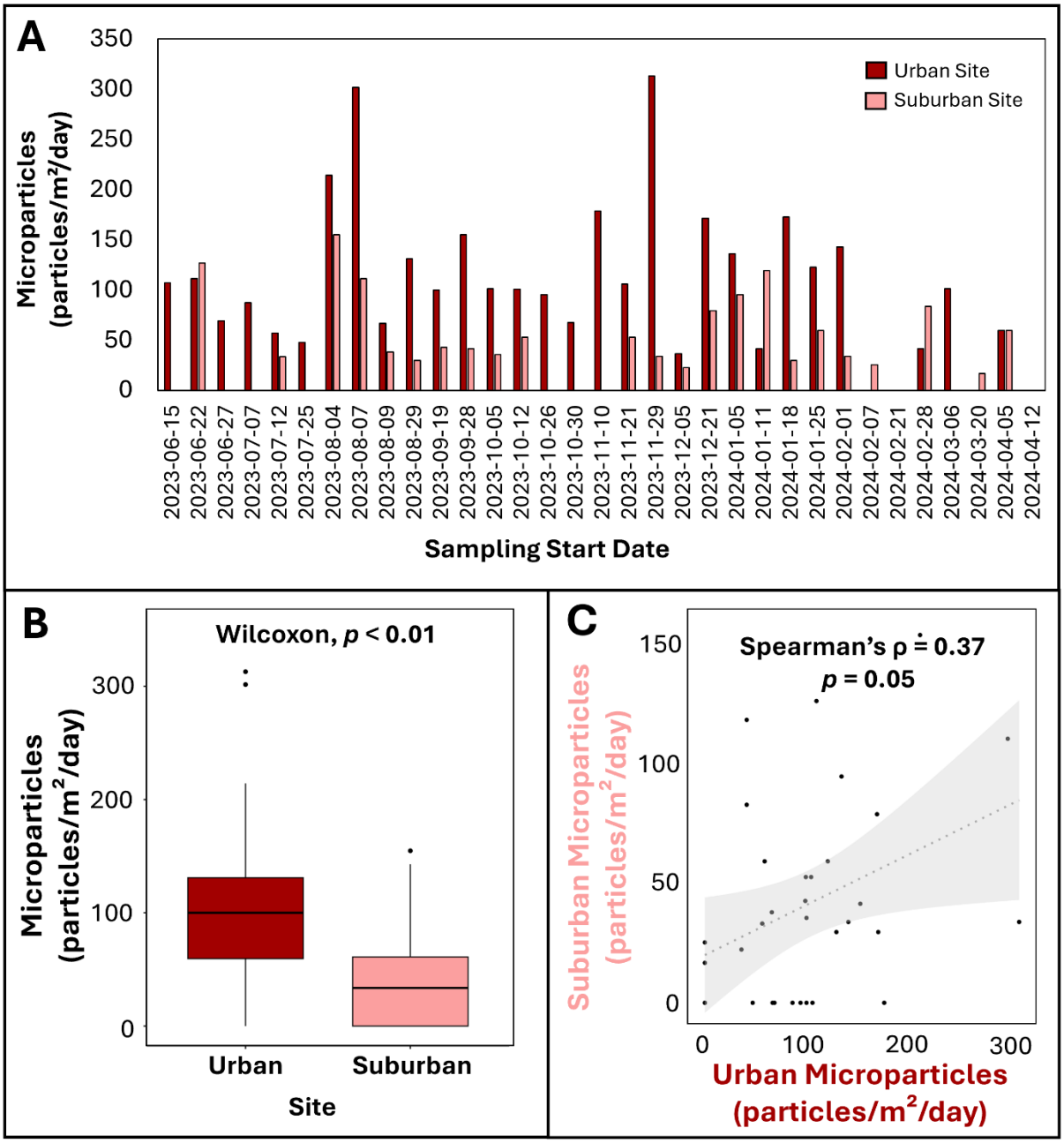

Figure 5.2. *(A) A comparison of atmospheric deposition rates for the shared sampling events at the two sites over time (for additional details about the sampling timesteps, see Fig. 5.S3.). (B) A comparison of all the anthropogenic microparticle deposition data for the urban site and suburban site (see Table 5.S1. for specific details about the sampling dates). (C) The relationship between the atmospheric deposition that was collected concurrently at the two sites.*

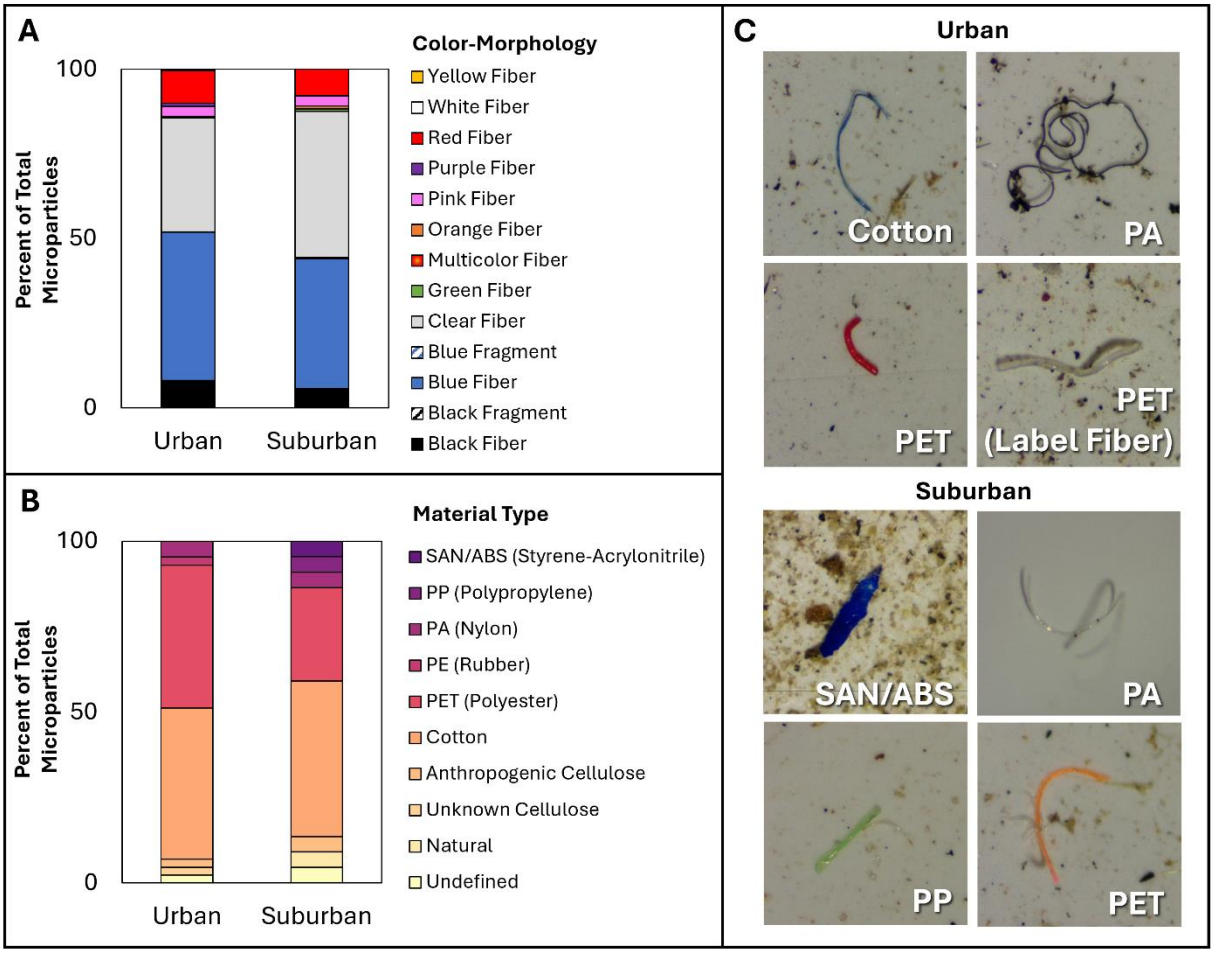

Figure 5.3. *(A) Percentages of each anthropogenic microparticle color-morphology combination, (B) percentages of each anthropogenic microparticle material type analyzed with μ-FTIR, and (C) examples of various anthropogenic microparticle material types identified at the urban and suburban sites (each photograph represents 1 mm by 1 mm in scale).*

5.4.3. The Relationship between Anthropogenic Microparticle Deposition and Atmospheric Conditions

Deposition type (wet versus dry) and leaf cover (leafed versus bare trees) had no impact on anthropogenic microparticle deposition rates (Fig. 5.S4.). Anthropogenic microparticle deposition at the urban site had a significant positive correlation with relative humidity averaged for each sampling interval as well as a significant negative correlation with wind speed similarly averaged for each sampling period (Fig. 5.4.). The suburban anthropogenic microparticle deposition rates did not correlate to wind speed (data not shown), and their strongest significant

correlation was the positive relationship with average relative humidity, which was a trait shared with the urban site (Fig. 5.4.). The suburban site's deposition rate also had a weak, but significant, negative trend with PM-10 (Fig. 5.4.). The only air quality parameter that could be compared using stations near both the urban and suburban sites was the PM-2.5 data, which, like anthropogenic microparticle deposition, was significantly higher at the urban site (Fig. 5.S5.). However, the PM-2.5 values did not correlate with anthropogenic microparticle deposition at either site (data not shown).

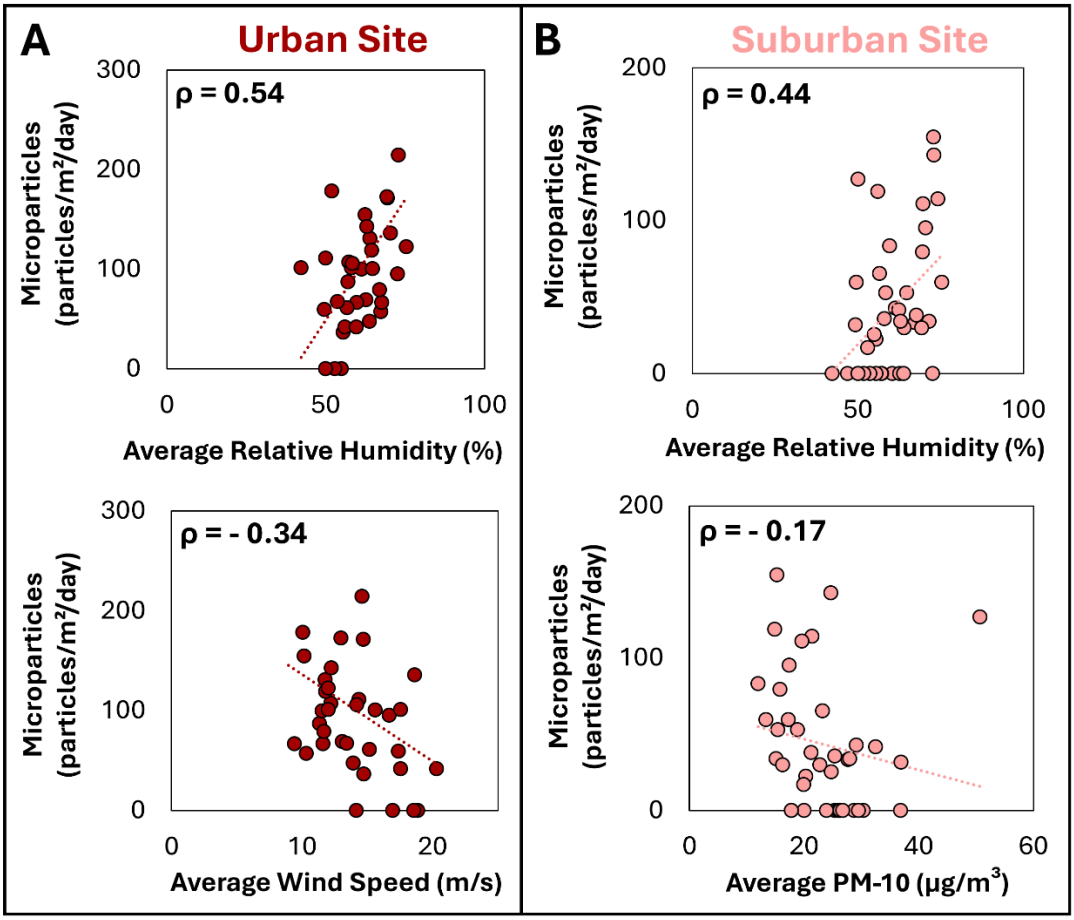

Figure 5.4. *Trends between anthropogenic microparticle deposition and atmospheric condition parameters at the (A) urban site and (B) suburban site. The Spearman's correlation coefficient is shown on each plot and all p values are < 0.05.*

5.5. Discussion

5.5.1. A Global Comparison of Atmospheric Deposition Rates for Anthropogenic Microparticles

The average deposition rate of anthropogenic microparticles at the urban site (101.7 particles/m^2/day) was similar to some urban areas that used comparable methodologies (e.g., up to 110 particles/m^2/day in Paris, France; Dris et al., 2016) but much lower than other cities (e.g., up to 374 particles/m^2/day in Ho Chi Minh City, Vietnam; Truong et al., 2021). These comparisons of the quantities of anthropogenic microparticles in atmospheric deposition among cities globally (see Table 5.S4.) suggest that population size cannot be the sole factor influencing deposition rates. Speculation has arisen recently that climate influences atmospheric anthropogenic microparticle deposition more strongly than population, with higher deposition potentially occurring in tropical climates where wetter conditions may lead to atmospheric moisture adsorbing to the anthropogenic microparticles thereby enhancing their deposition (Leonard et al., 2024).

Indeed, the St. Louis deposition rates are similar to those in other areas that feature a humid subtropical climate (e.g., an average of 114 particles/m^2/day in Guangzhou, China; Huang et al., 2021, and an average of 123 particles/m^2/day in São Paulo, Brazil; Amato-Lourenço et al., 2022), despite the much higher populations in these previously studied megacities (Fig. 5.5.; Table 5.S4.). Arid locations tend to have lower deposition rates (< 100 particles/m^2/day on average; Abbasi and Turner, 2021; Edo et al., 2023), while tropical locations typically have higher deposition rates (> 300 particles/m^2/day; Truong et al., 2021; Winijkul et al., 2024), regardless of population (Fig. 5.5.; Table 5.S4.). Through our comparison with other climates, we found inexplicably broad variation in temperate oceanic climates (specifically, extremely high deposition levels in London, United Kingdom; Wright et al., 2020). For this reason, we visualized global climate and atmospheric anthropogenic microparticle deposition variation both

including (i.e., Fig. 5.5. (A-B)) and excluding (i.e., Fig. 5.5. (C)) temperate oceanic climate data. With temperate oceanic climate anthropogenic microparticle deposition rates excluded, deposition levels globally seem to increase as a given climate's humidity level increases, though we acknowledge that the currently available data are extremely limited across all climates (Fig. 5.5. (C); Table 5.S4.).

Though on the global scale, comparisons like these do not provide evidence for higher anthropogenic microparticle deposition in more densely populated urban areas compared to lower-density urban or remote settings (Table 5.S4.; Leonard et al., 2024), on the local scale, gradients of urbanization sometimes do affect anthropogenic microparticle deposition rates. Other studies with multiple sites within a single urban area have also recorded higher deposition rates at the more densely populated site (e.g., in Paris, France, Dris et al., 2016, and in Hamburg, Germany, Klein et al., 2023), which is much like the gradient we observed for our two sites within the St. Louis region (Fig. 5.2.). Gradients of anthropogenic microparticle deposition related to population might thus be visible on a localized scale within uniform climate zones, even though they may not be evident at the global scale due to the more prominent impacts of climatic variation. St. Louis' atmospheric anthropogenic microparticle deposition rates relative to those found globally therefore seem to be better explained by climate than by population density, though population density might affect localized variation.

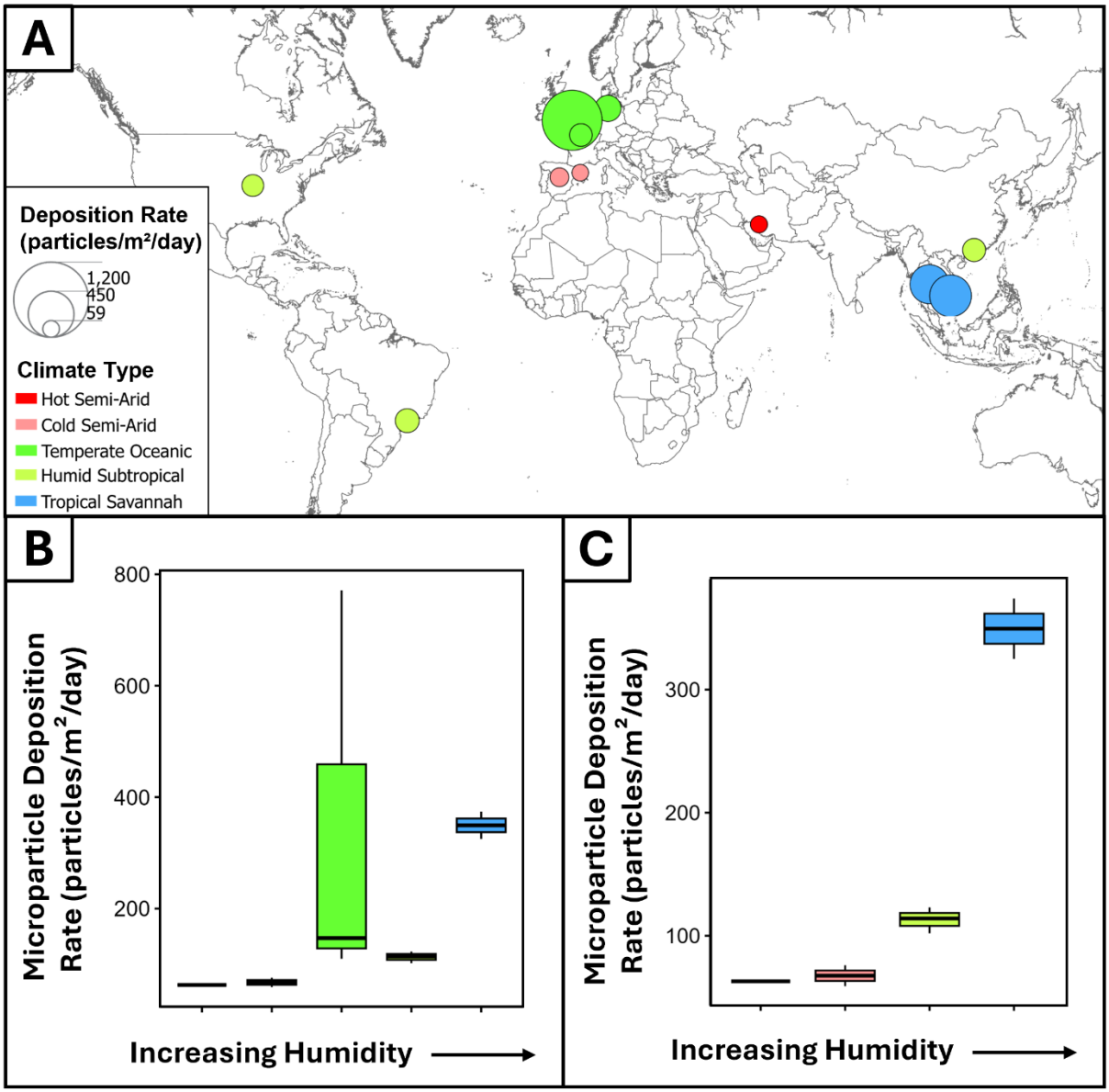

Figure 5.5. *(A) Mapped global data for atmospheric deposition of anthropogenic microparticles (see Table 5.S4. for data sources), with colors representing distinct climate zones (Beck et al., 2023) and circle sizes representing the average anthropogenic microparticle deposition rate for a given location. Also shown are boxplot comparisons of anthropogenic microparticle deposition rates from (B) each climate zone and (C) each climate zone but excluding the highly variable temperate oceanic climate zone.*

5.5.2. The Characteristics of Deposited Atmospheric Anthropogenic Microparticles

The prevalence of microfibers found in our St. Louis atmospheric deposition samples is consistent with the results from most studies (i.e., 10 of the 11 studies in Table 5.S4. find > 70% fibers in atmospheric deposition). Though discussion of microfibers typically focuses on their release from the laundering of textiles, research suggests that wearing textiles generates similar numbers of these microparticles that are released directly to the air (De Falco et al., 2020). A small number of studies have found higher levels of fragments than fibers in atmospheric samples (Allen et al., 2019; Klein and Fischer, 2019), but they all had much lower size limits for detection (≤ 20 μm). Our methodological size limit of 100 μm might accordingly have led to an underestimation of the deposition of small fragments. These smaller anthropogenic microparticles are also the most inhalable (Maurizi et al., 2024), and our study therefore cannot accurately determine risks associated with airborne anthropogenic microparticles in the St. Louis region. Other studies of anthropogenic microparticle deposition in the United States have found a majority of microfibers with high levels in small size ranges (e.g., 70% that were < 25 μm in Brahney et al., 2020). Thus, higher quantities of small-sized microplastics may contaminate St. Louis air more than the larger, less inhalable anthropogenic microparticles that are reported here can convey.

The percentage of synthetic microparticle material types (41% at the suburban site and 49% at the urban site; Fig. 5.3. (B-C)) compared to non-synthetic material is within the range of prior St. Louis area studies of water and sediment and is most like the percentage of synthetic material compared to non-synthetic material from sediment near the suburban site (51%; see Chapter 4). Nearby settings in the region that are in less developed areas have lower proportions of synthetic material in comparison (i.e., 20% synthetic microparticles in Mississippi River samples from Rochman et al., 2022, 23% synthetic microparticles in cave water from Baraza and

Hasenmueller, 2023, and 29% synthetic microparticles in cave sediment from Hasenmueller et al., 2023). Considering this local gradient, our atmospheric deposition samples might therefore have a relatively high proportion of synthetic microparticles due to the proximity of the sampling sites to higher levels of human activity compared to other prior studies in the region.

The prevalence of PET among microplastics has been seen in some prior global atmospheric deposition studies (e.g., Edo et al., 2023; Huang et al., 2021; Amato-Lourenço et al., 2022), though others have seen higher proportions of PP (e.g., Truong et al., 2021). Notably, other studies that found a prominence of PET include previous work in humid subtropical areas, raising the question of whether microplastic material types deposited from the atmosphere could vary across climate zones due to polymer characteristics through density variations, which impact microplastic settling in fluid environments (Waldschläger and Schüttrumpf, 2019), or variable water absorption, which could cause humidity-controlled variation in the material types that are deposited. Though low global data resolution and the common practice of analyzing material types only for a subset of anthropogenic microparticles mean sufficient data is not available to draw conclusions about potential climate-influenced reasons for polymer variation, this question warrants further consideration in future research.

If textiles are assumed to be the primary source of anthropogenic microparticles to St. Louis' atmosphere due to the prominence of fiber morphologies, the prevalence of cotton and PET might also be explained by the higher potential release of fibers from cotton clothing (e.g., due to low durability; Liu et al., 2023) and some types of polyester fabrics (e.g., polyester fleece; Almroth et al., 2017). PET is also the most prevalent microplastic found in sediment and clam samples in the Deer Creek watershed near our suburban atmospheric sampling site (see Chapter 4), supporting the idea that the prevalence of PET is related to sourcing from the populated urban and suburban settings of St. Louis. Interestingly, microplastics in Mississippi River water near

St. Louis were also > 50% PET, which is a finding not explained by other examined sourcing compartments, including agriculture, stormwater, and wastewater inputs (Rochman et al., 2022). Our results therefore suggest both PET predominance among microplastics in the St. Louis region as well as the potential for sourcing of anthropogenic microparticles from atmospheric deposition to waterways.

5.5.3. The Influence of Atmospheric Conditions on Anthropogenic Microparticle Deposition

The only meteorologic and air quality parameters clearly correlated to anthropogenic microparticle deposition over time were relative humidity, wind speed, and PM-10 (Fig. 5.4.). The positive correlation of anthropogenic microparticle deposition with relative humidity aligns with prior global studies that suggest higher humidity might lead to adsorbed moisture and enhanced deposition of these microparticles, which has been observed with other types of atmospheric particles (e.g., biomass; Leonard et al., 2024; Yuan et al., 2023). Humidity may therefore be a more important factor influencing atmospheric deposition of anthropogenic microparticles than previously assumed. Though wind speed had a weak negative correlation that was observed only at the urban site, low wind speed allowing deposition and high wind speed causing suspension is a phenomenon that a prior study comparing deposited and suspended anthropogenic microparticles has identified (Rao et al., 2024). As our study only considers deposited anthropogenic microparticles, these findings lead to further questions regarding whether high levels of breathable anthropogenic microparticles are suspended in the air during low humidity or high wind speed conditions compared to their suspension rates in high humidity or low wind speeds (i.e., due to enhanced deposition).

Several studies suggest that precipitation promotes anthropogenic microparticle deposition (Dris et al., 2016; Rao et al., 2024) or that differences between wet and dry deposition

rates occur (Brahney et al., 2020), though we observed neither in our dataset. Whether anthropogenic microparticle deposition relates to meteorologic factors like rain and wind speed may thus be location-specific (e.g., the relationship to wind speed but not precipitation in Klein et al., 2023, and no relationship to either in Wright et al., 2020, and Truong et al., 2021). Prior research has also suggested that anthropogenic microparticle deposition in urban areas is less driven by meteorologic parameters because point sourcing is more prevalent (Wright et al., 2020). This influence of variable point sourcing across urban spaces could be a reason that even the most apparent correlations we see to meteorologic parameters (e.g., relative humidity) are not particularly strong relationships. Though many intersecting parameters likely affect anthropogenic microparticle deposition rates (e.g., climate, weather, human activity, and point emissions), humidity conditions should be considered in future studies to better determine their impacts on the quantities and types of anthropogenic microparticle suspended in or deposited from the atmosphere.

5.6. Conclusions

This study quantifies and characterizes the deposition rates of larger-sized (> 100 μm) airborne anthropogenic microparticles (including microplastics) in the St. Louis, Missouri, United States, region over a year-long period for the first time. Deposition rates were significantly higher at an urban site (101.7 ± 71.1 particles/m^2/day) compared to a suburban site (43.3 ± 42.2 particles/m^2/day). Both urban and suburban St. Louis had high levels of microfibers that were predominately cotton and PET. Slightly higher fractions of microplastics were found at the urban site (49%) compared to the suburban site (41%). Within the St. Louis region, where weather conditions are typically comparable between the sites, spatial trends in anthropogenic microparticle deposition seem most impacted by differences in population density.

The anthropogenic microparticle deposition rates over time were most strongly influenced by relative humidity, which potentially enhanced the deposition of these microparticles and best explained the temporal fluctuation in the data at both sites. On the global scale, the humid subtropical climate in St. Louis likely also leads to lower anthropogenic microparticle deposition rates in comparison to tropical areas that have more consistent high humidity conditions favoring the deposition of these microparticles. Humidity is thus an influential factor that should be considered in future atmospheric microplastic research. The presence of the most inhalable anthropogenic microparticle sizes (i.e., < 10 μm) could not be assessed in this study. Further investigation of these smaller-sized anthropogenic microparticles is thus warranted as they are likely to be present at much higher levels in the air and may have differing deposition dynamics than the larger anthropogenic microparticles that we assessed.

5.7. Acknowledgements

This work was funded by research grants to Elizabeth A. Hasenmueller from the United States Geological Survey Water Resources Research Act Program (Award: G21AP10582-03) and to Natalie F. Hernandez from the Litzsinger Road Ecology Center Research Grant Program. We greatly appreciate James Faupel's and Adam Rembert's help with coordinating our field sampling and long-term deployment of sampling equipment at the Litzsinger Road Ecology Center as well as Sofie Liang's help coordinating roof access for sampling at Saint Louis University. We thank all the field assistants who helped with sample collection throughout the project. We also appreciate Dr. Susanne Brander and her team who facilitated the use of the μ-FTIR instrumentation at Oregon State University.

5.8. References

Abbasi, S., 2021. Microplastics washout from the atmosphere during a monsoon rain event. J. Hazard. Mater. Adv. 4, 100035.

Abbasi, S., Turner, A., 2021. Dry and wet deposition of microplastics in a semi-arid region (Shiraz, Iran). Sci. Total Environ. 786, 147358.

Abbasi, S., Jaafarzadeh, N., Zahedi, A., Ravanbakhsh, M., Abbaszadeh, S., Turner, A., 2023. Microplastics in the atmosphere of Ahvaz City, Iran. J. Environ. Sci. 126, 95-102.

Allen, D., Allen, S., Abbasi, S., Baker, A., Bergmann, M., Brahney, J., Butler, T., Duce, R.A., Eckhardt, S., Evangeliou, N., Jickells, T., Kanakidou, M., Kershaw, P., Laj, P., Levermore, J., Li, D., Liss, P., Liu, K., Mahowald, N., Masque, P., Materic, D., Mayes, A.G., McGinnity, P., Osvath, I., Prather, K.A., Prospero, J.M., Revell, L.E., Sander, S.G., Shim, W.J., Slade, J., Stein, A., Tarasova, O., Wright, S., 2022. Microplastics and nanoplastics in the marine-atmosphere environment. Nat. Rev. Earth Environ. 3, 393-405.

Allen, S., Allen, D., Baladima, F., Phoenix, V.R., Thomas, J.L., Le Roux, G., Sonke, J.E., 2021. Evidence of free tropospheric and long-range transport of microplastic at Pic du Midi Observatory. Nat. Commun. 12, 7242.

Almroth, B.M.C., Astrom, L., Roslund, S., Petersson, H., Johansson, M., Persson, N., 2017. Quantifying shedding of synthetic fibers from textiles; a source of microplastics released into the environment. Environ. Sci. Pollut. Res. 25, 1191-1199.

Amato-Lourenço, L.F., dos Santos Galvão, L., Wiebeck, H., Carvalho-Oliveira, R., Mauad, T., 2022. Atmospheric microplastic fallout in outdoor and indoor environments in São Paulo megacity. Sci. Total Environ. 821, 153450.

Ankit, Y., Ajay, K., Nischal, S., Kaushal, S., Kataria, V., Dietze, E., Anoop, A., 2024. Atmospheric deposition of microplastics in an urban conglomerate near to the foothills of Indian Himalayas: Investigating the quantity, chemical character, possible sources and transport mechanisms. Environ. Pollut. 361, 124629.

Athey, S.N., Erdle, L.M., 2022. Are we underestimating anthropogenic microfiber pollution? A critical review of occurrence, methods, and reporting. Environ. Toxicol. Chem. 41(4), 822-837.

Baraza, T., Hasenmueller, E.A., 2023. Floods enhance the abundance and diversity of anthropogenic microparticles (including microplastics and treated cellulose) transported through karst systems. Water Res. 242, 120204.

Beaurepaire, M., Gaseperi, J., Tassin, B., Dris, R., 2024. COVID lockdown significantly impacted microplastic bulk atmospheric deposition rates. Environ. Pollut. 344, 123354.

Beck, H.E., McVicar, T.R., Vergopolan, N., Berg, A., Lutsko, N.J., Dufour, A., Zeng, Z., Jiang, X., van Dijk, A.I.J.M., Miralles, D.G., 2023. High-resolution (1 km) Köppen-Geiger maps for 1901–2099 based on constrained CMIP6 projections. Sci. Data, 10, 724.

Brahney, J., Hallerud, M., Heim, E., Hahnenberger, M., Sukumaran, S., 2020. Plastic rain in protected areas of the United States. Science 368, 1257-1260.

Chandrakanthan, K., Fraser, M.P., Herckes, P., 2023. Airborne microplastics in a suburban location in the desert southwest: Occurrence and identification challenges. Atmos. Environ. 298, 119617.

Chen, G., Feng, Q., Wang, J., 2020. Mini-review of microplastics in the atmosphere and their risks to humans. Sci. Total Environ. 703, 135504.

Cowger, W., Steinmetz, Z., Gray, A., Munno, K., Lynch, J., Hapich, H., Primpke, S., De Frond, H., Rochman, C., Herodotou, O., 2021. Microplastic spectral classification needs an open source community: Open Specy to the rescue! Anal. Chem. 93(21), 7543-7548.

Dawson, A.L., Santana, M.F.M., Nelis, J.L.D., Motti, C.A., 2023. Taking control of microplastics data: A comparison of control and blank data correction methods. J. Hazard. Mater. 443A, 130218.

De Falco, F., Cocca, M., Avella, M., Thompson, R.C., 2020. Microfiber release to water, via laundering, and to air, via everyday use: A comparison between polyester clothing with differing textile parameters. Environ. Sci. Technol. 54, 3288-3296.

De Frond, H., Rubinovitz, R., Rochman, C.M., 2021. μATR-FTIR spectral libraries of plastic particles (FLOPP and FLOPP-e) for the analysis of microplastics. Anal. Chem. 93(48), 15878-15885.

Dris, R., Gasperi, J., Rocher, V., Saad, M., Renault, N., Tassin, B., 2015. Microplastic contamination in an urban area: a case study in Greater Paris. Environ. Chem. 12(5), 592-599.

Dris, R., Gasperi, J., Saad, M., Mirande, C., Tassin, B., 2016. Synthetic fibers in atmospheric fallout: A source of microplastics in the environment? Mar. Poll. Bull. 104(1-2), 290-293.

East-West Gateway, 2024. Regional Profile. https://www.ewgateway.org/about-us/who-we-are/regional-profile. Accessed March 01, 2025

Edo, C., Fernandez-Pinas, F., Leganes, F., Gomez, M., Martinez, I., Herrera, A., Hernandez-Sanchez, C., Gonzalez-Salamo, J., Borges, J.H., Lopez-Castellanos, J., Bayo, J., Romera-Castillo, C., Elustondo, D., Santamaria, C., Alonso, R., Garcia-Gomez, H., Gonzalez-Cascon, R., Martinez-Hernandez, V., Landaburu-Aguirre, J., Incera, M., Gago, J., Noya, B., Beiras, R., Muniategui-Lorenzo, S., Rosal, R., Gonzalez-Pleiter, M., 2023. A nationwide monitoring of atmospheric microplastic deposition. Sci. Total Environ. 905, 166923.

Esri, Missouri Dept. of Conservation, Missouri DNR, Tom-Tom, SafeGraph, FAO, METI/NASA, USGS, EPA, NPS, USFWS, NGA, Garmin, 2019. "World Terrain Base" [basemap]. Scale ~1:70k. https://www.arcgis.com/home/item.html?id=c61ad8ab017d49e1a82f580ee1298931. Accessed March 01, 2025.

Evangeliou, N., Grythe, H., Klimont, Z., Heyes, C., Eckhardt, S., Lopez-Aparicio, S., Stohl, A., 2020. Atmospheric transport is a major pathway of microplastics to remote regions. Nat. Commun. 11,3381.

Finnegan, A.M.D., Susserott, R., Gabbott, S.E., Gouramanis, C., 2022. Man-made natural and regenerated cellulosic fibres greatly outnumber microplastic fibres in the atmosphere. Environ. Pollut. 310, 119808.

Geverdt, D., 2019. Education Demographic and Geographic Estimates Program (EDGE): Locale Boundaries File Documentation, 2017 (NCES 2018-115). U.S. Department of Education. Washington, DC: National Center for Education Statistics. https://nces.ed.gov/programs/edge/docs/EDGE_NCES_LOCALE.pdf. Accessed March 01, 2025.

Harris, L.S.T., Beur, L.L., Olsen, A.Y., Smith, A., Eggers, L., Pedersen, E., Van Brocklin, J., Brander, S.M., Larson, S., 2021. Temporal variability of microparticles under the Seattle aquarium, Washington State: Documenting the global Covid-19 pandemic. Environ. Toxicol. Chem. 41(4), 917-930.

Hasenmueller, E.A., Baraza, T., Hernandez, N.F., Finegan, C.R., 2023. Cave sediment sequesters anthropogenic microparticles (including microplastics and modified cellulose) in subsurface environments. Sci. Total Environ. 893, 164690.

Huang, Y., He, T., Yan, M., Yang, L., Gong, H., Wang, W., Qing, X., Wang, J., 2021. Atmospheric transport and deposition of microplastics in a subtropical urban environment. J. Hazard. Mater. 416, 126168.

Illuminati, S., Notarstefano, V., Tinari, C., Fanelli, M., Girolametti, F., Ajdini, B., Scarchilli, C., Ciardini, V., Iaccarino, A., Giorgini, E., Annibaldi, A., Truzzi, C., 2024. Microplastics in bulk atmospheric deposition along the coastal region of Victoria Land, Antarctica. Sci. Total Environ., 949, 175221.

Iowa Environmental Mesonet (IEM), 2025. ASOS Network “ASOS-AWOS-METAR data download”. https://mesonet.agron.iastate.edu/ASOS/. Accessed March 01, 2025.

Jia, Q., Duan, Y., Han, X., Sun, X., Munyanez, J., Ma, J., Xiu, G., 2022. Atmospheric deposition of microplastics in the megalopolis (Shanghai) during rainy season: Characteristics, influence factors, and source. Sci. Total Environ. 847, 157609.

Kernchen, S., Loder, M.G.J., Fischer, F., Fischer, D., Moses, S.R., Georgi, C., Nolscher, A.C., Held, A., Laforsch, C., 2022. Airborne microplastic concentrations and deposition across the Weser River catchment. Sci. Total Environ. 818, 151812.

Kim, L., Kim, S.A., Kim, T.H., Kim, J., An, Y., 2021. Synthetic and natural microfibers induce gut damage in the brine shrimp *Artemia franciscana*. Aquat. Toxicol. 232, 105748.

Klein, M., Fischer, E.K., 2019. Microplastic abundance in atmospheric deposition within the Metropolitan area of Hamburg, Germany. Sci. Total Environ. 685, 96-103.

Klein, M., Bechtel, B., Brecht, T., Fischer, E.K., 2023. Spatial distribution of atmospheric microplastics in bulk-deposition of urban and rural environments – A one-year follow-up study in northern Germany. Sci. Total Environ. 901, 165923.

Leonard, J., Rassi, L.A.E., Samad, M.A., Prehn, S., Mohanty, S.K., 2024. The relative importance of local climate and land use on the deposition rate of airborne microplastics on terrestrial land. Atmos. Environ. 318, 120212.

Liu, Z., Bai, Y., Ma. T., Liu, X., Wei, H., Meng, H., Fu, Y., Ma, Z., Zhang, L., Zhao, J., 2022. Distribution and possible sources of atmospheric microplastic deposition in a valley basin city (Lanzhou, China). Ecotoxicol. Environ. Saf. 233, 113353.

Liu, J., Zhu, B., An, L., Ding, J., Xu, Y., 2023. Atmospheric microfibers dominated by natural and regenerated cellulosic fibers: Explanations from the textile engineering perspective. Environ. Pollut. 317, 120771.

Lusher, A.L., Welden, N.A., Sobral, P., Cole, M., 2017. Sampling, isolating and identifying microplastics ingested by fish and invertebrates. Anal. Methods 9, 1346.

Maurizi, L, Simon-Sanchez, L., Vianello, A., Nielsen, A.H., Vollertsen, J., 2024. Every breath you take: High concentration of breathable microplastics in indoor environments. Chemosphere 361, 142553.

Napper, I.E., Davies, B.F.R., Clifford, H., Elvin, S., Koldewey, H.J., Mayewski, P.A., Miner, K.R., Potocki, M., Elmore, A.C., Gajurel, A.P., Thompson, R.C., 2020. Reaching new heights in plastic pollution—preliminary findings of microplastics on Mount Everest. OE. 3, 621-630.

National Weather Service (NWS), 2024. The climatology of the St. Louis area. https://www.weather.gov/lsx/cli_of_stl. Accessed March 01, 2025.

O'Brien, S., Rauert, C., Ribeiro, F., Okoffo, E.D., Burrows, S.D., O'Brien, J.W., Wang, X., Wright, S.L., Thomas, K.V., 2023. There's something in the air: A review of sources, prevalence and behaviour of microplastics in the atmosphere. Sci. Total Environ. 874, 162193.

Primpke, S., Wirth, M., Lorenz, C., Gerdts, G., 2018. Reference database design for the automated analysis of microplastic samples based on Fourier transform infrared (FTIR) spectroscopy. Anal. Bioanal. Chem. 410, 5131-5141.

Rao, W., Fan, Y., Li, H., Qian, X., Liu, T., 2024. New insights into the long-term dynamics and deposition-suspension distribution of atmospheric microplastics in an urban area. J. Hazard. Mater. 463, 132860.

Rochman, C.M., Grbic, J., Earn, A., Helm, P.A., Hasenmueller, E.A., Trice, M., Munno, K., De Frond, H., Djuric, N., Santoro, S., Kaura, A., Denton, D., Teh, S., 2022., Local monitoring should inform local solutions: Morphological assemblages of microplastics are similar within a pathway, but relative total concentrations vary regionally. Environ. Sci. Technol. 56, 9367-9378.

Shruti, V.C., Kutralam-Muniasamy, G., Perez-Guevara, F., Roy, P.D., Martinez, I.E., 2022. Occurrence and characteristics of atmospheric microplastics in Mexico City. Sci. Total Environ. 847, 157601.

Stanton, T., Johnson, M., Nathanail, P., MacNaughtan, W., Gomes, R.L., 2019. Freshwater and airborne textile fibre populations are dominated by 'natural', not microplastic, fibres. Sci. Total Environ. 666, 377-389.

Trainic, M., Flores, J.M., Pinkas, I., Pedrotti, M.L., Lombard, F., Bourdin, G., Gorsky, G., Boss, E., Rudich, Y., Vardi, A., Koren, I., 2020. Airborne microplastic particles detected in the remote marine atmosphere. Commun. Earth Environ. 1, 64.

Truong, T., Strady, E., Kieu-Le, T., Tran, Q., Le, T., Thuong, Q., 2021. Microplastic in atmospheric fallouts of a developing Southeast Asian megacity under tropical climate. Chemosphere 272, 129874.

United Nations (UN), 2014. World urbanization prospects. Cities, 13-16.

United Nations (UN), Department of Econnomic and Social Affairs, Population Division, 2018. World Urbanisation Prospects 2018. Urban Agglomerations File 12: Population of urban agglomerations with 300,000 inhabitants or more in 2018, by country, 1950-2035 (thousands). https://population.un.org/wup/downloads. Accessed March 01, 2025.

United States of America National Agriculture Imagery Program (USA NAIP), 2024. USA NAIP Imagery: NDVI. USDA Farm Services Agency. https://naip.arcgis.com/arcgis/rest/services/NAIP/ImageServer. Accessed March 04, 2025.

United States Census, 2020. https://www.census.gov/quickfacts/. Accessed December 01, 2024.

United States Environmental Protection Agency (US EPA), 2024. Air Quality System Data Mart. https://www.epa.gov/outdoor-air-quality-data. Accessed December 01, 2024.

United States Geological Survey (USGS), 2017. USGS_OPR_MO_Saint_Louis_Lidar_2017_B17_7283_4277.tif and USGS_OPR_MO_Saint_Louis_Lidar_2017_B17_7403_4278.tif. Missouri Spatial Data Information Service (MSDIS). https://data-msdis.opendata.arcgis.com/pages/lidar. Accessed March 04, 2025

Waldschläger, K., Schüttrumpf, H., 2019. Effects of particle properties on the settling and rise velocities of microplastics in freshwater under laboratory conditions. Environ. Sci. Technol. 53(4), 1958-1966.

Welsh, B., Aherne, J., Paterson, A.M., Yao, H., McConnell, C., 2022. Atmospheric deposition of anthropogenic particles and microplastics in south-central Ontario, Canada. Sci. Total Environ. 835, 155426.

Winijkul, E., Latt, K.Z., Limsiriwong, K., Pussayanavin, T., Prapaspongsa, T., 2024. Depositions of airborne microplastics during the wet and dry seasons in Pathum Thani, Thailand. Atmos. Pollut. Res. 15, 102242.

Wright, S.L., Ulke, J., Font, A., Chan, K.L.A., Kelly, F.J., 2020. Atmospheric microplastic deposition in an urban environment and an evaluation of transport. Environ. Int. 136, 105411.

Yao, Y., Glamoclija, M., Murphy, A., Gao, Y., 2022. Characterization of microplastics in indoor and ambient air in northern New Jersey. Environ. Res. 207, 112142.

Yuan, Y., Li, S., Chen, T., Ren, J., 2023. Effects of ambient temperature and humidity on natural deposition characteristics of airborne biomass particles. Int. J. Environ. Res. Public Health 20(3), 1890.

Zhang, Y., Pu, S., Lv, X., Gao, Y., Ge, L., 2020. Global trends and prospects in microplastics research: A bibliometric analysis. J. Hazard. Mater. 400, 123110.

Zhou, Q., Tian, C., Luo, Y., 2017. Various forms and deposition fluxes of microplastics identified in the coastal urban atmosphere. Sci. Bull. 62(33), 3902-3909.

5.9. Supplementary Materials

5.9.1. Supplemental Information

5.9.1.1. 5.S1. Sample timing

Prior work has suggested that even with comparable sampler setups, shorter time ranges for sampling can lead to an overestimation of anthropogenic microparticle deposition (Leonard et al., 2024). For example, using the same type of sampler while sampling twice per day led to extremely high levels of 462-5346 particles/m^2/day (Ankit et al. 2024; see related discussion Leonard et al., 2024). Differing sampling interval lengths might have also influenced our deposition findings.

Indeed, at the suburban site, samples with anthropogenic microparticle deposition > 100 counts/m^2/day were always during sampling periods of < 10 days. At the urban site, anthropogenic microparticle deposition levels were more consistently > 100 particles/m^2/day during varying sampling periods of up to 15 days, but the highest values we observed (> 200 particles/m^2/day) also occurred during sampling periods of < 10 days. While our samples with shorter sampling intervals might therefore similarly have led to an overestimation of the deposition rate due to higher variability over shorter timescales, when comparing only samples with periods ≥ 10 days (per Leonard et al., 2024), our overarching conclusions of higher deposition at the urban site as well as a significant positive correlation between anthropogenic microparticle deposition rates and relative humidity are maintained (Fig. 5.S2.).

5.9.2. Supplemental Tables

Table 5.S1. *Sampling period dates, the type of deposition collected, when samples were collected at each site (indicated by x), and the deposition rates at each site.*

Start Date	End Date	Time Elapsed (Days)	Deposition Type	Suburban Samples Taken	Urban Samples Taken	Suburban Deposition Rate (particles/m^2/day)	Urban Deposition Rate (particles/m^2/day)
2023-04-20	2023-04-27	8	Dry	X		0.0	
2023-05-04	2023-05-11	8	Wet	X		0.0	
2023-05-11	2023-05-15	5	Wet	X		114.3	
2023-05-15	2023-05-17	3	Wet	X		142.9	
2023-06-07	2023-06-15	9	Wet	X		31.7	
2023-06-15	2023-06-22	8	Wet	X	X	0.0	107.1
2023-06-22	2023-06-27	6	Dry	X	X	127.0	111.1
2023-06-27	2023-06-07	11	Wet	X	X	0.0	69.3
2023-07-07	2023-07-12	6	Dry	X	X	0.0	87.3
2023-07-12	2023-07-21	10	Wet	X	X	33.3	57.1
2023-07-21	2023-07-25	5	Wet		X		66.7
2023-07-25	2023-08-04	10	Wet	X	X	0.0	47.6
2023-08-04	2023-08-07	4	Wet	X	X	154.8	214.3
2023-08-07	2023-08-09	3	Dry	X	X	111.1	301.6
2023-08-09	2023-08-18	10	Wet	X	X	38.1	66.7
2023-08-18	2023-08-29	12	Wet		X		79.4
2023-08-29	2023-08-05	8	Wet	X	X	29.8	131.0
2023-09-05	2023-09-12	8	Dry		X		119.0
2023-09-12	2023-09-19	8	Dry	X		0.0	
2023-09-19	2023-09-28	10	Wet	X	X	42.9	100.0
2023-09-28	2023-09-05	8	Wet	X	X	41.7	154.8
2023-10-05	2023-10-12	8	Wet	X	X	35.7	101.2
2023-10-12	2023-10-20	9	Dry	X	X	52.9	100.5
2023-10-20	2023-10-26	7	Wet		X		61.2
2023-10-26	2023-10-30	5	Wet	X	X	0.0	95.2
2023-10-30	2023-10-10	12	Dry	X	X	0.0	67.5
2023-11-10	2023-11-21	8	Wet	X	X	0.0	178.6

Table 5.S1. *Continued.*

Start Date	End Date	Time Elapsed (Days)	Deposition Type	Suburban Samples Taken	Urban Samples Taken	Suburban Deposition Rate (particles/m^2/day)	Urban Deposition Rate (particles/m^2/day)
2023-11-21	2023-11-29	9	Wet	X	X	52.9	105.8
2023-11-29	2023-11-05	7	Wet	X	X	34.0	312.9
2023-12-05	2023-12-21	17	Wet	X	X	22.4	36.4
2023-12-21	2023-12-05	15	Wet	X	X	79.4	171.4
2024-01-05	2024-01-11	7	Wet	X	X	95.2	136.1
2024-01-11	2024-01-18	8	Wet	X	X	119.0	41.7
2024-01-18	2024-01-25	8	Wet	X	X	29.8	172.6
2024-01-25	2024-01-01	8	Wet	X	X	59.5	122.4
2024-02-01	2024-02-07	7	Dry	X	X	34.0	142.9
2024-02-07	2024-02-21	15	Wet	X	X	25.4	0.0
2024-02-21	2024-02-28	8	Dry	X	X	0.0	0.0
2024-02-28	2024-02-06	8	Dry	X	X	83.3	41.7
2024-03-06	2024-03-13	8	Wet	X		65.5	
2024-03-16	2024-03-20	5	Wet	X	X	0.0	101.2
2024-03-20	2024-03-05	17	Wet	X	X	16.8	0.0
2024-04-05	2024-04-12	8	Wet	X	X	59.5	59.5
2024-04-12	2024-04-18	7	Dry	X	X	0.0	0.0

Table 5.S2. *Quantities of anthropogenic microparticles for each color-morphology category analyzed on µ-FTIR.*

Parameter	Black Fiber	Black Fragment	Blue Fiber	Blue Fragment	Clear Fiber	Green Fiber	Multi-Color Fiber	Orange Fiber	Pink Fiber	Purple Fiber	Red Fiber	White Fiber	Yellow Fiber
Urban (*n* Identified)	50	1	275	1	211	2	1	0	18	6	60	1	2
Suburban (*n* Identified)	15	0	102	1	115	2	0	2	8	0	21	0	0
Total (*n* Identified)	**65**	**1**	**377**	**2**	**326**	**4**	**1**	**2**	**26**	**6**	**81**	**1**	**2**
Quantity Analyzed with µ-FTIR	4	1	27	1	17	1	0	1	4	0	9	0	0
Color-Morphology (% of *n* Analyzed with µ-FTIR)	6	100	7	50	5	25	0	50	15	0	11	0	0
Synthetic Material Identified (% of *n* Analyzed with µ-FTIR)	25	100	41	100	47	100		100	25		56		
Anthropogenic Non-Synthetic Material Identified (% of *n* Analyzed with µ-FTIR)	75	0	59	0	29	0		0	75		44		
Natural/Unknown Material Identified (% of *n* Analyzed with µ-FTIR)	0	0	0	0	24	0		0	0		0		

Table 5.S3. *The data that were used to calculate the limit of detection (LOD) for the atmospheric deposition samples.*

Date	Blank Type	Total Anthropogenic Microparticles (counts)	Clear Fiber (counts)	Blue Fiber (counts)	Black Fiber (counts)	Blue Fragment (counts)
2023-07-21	Sampler Blank (Field)	5	4	1		
2023-06-15	Sampler Blank (Laboratory)	3	3			
2023-09-05	Sampler Blank (Field)	3	2		1	
2024-03-13	Laboratory Filtration Blank	3	2			1
2024-03-13	Laboratory Filtration Blank	3	1	2		
2024-03-27	Laboratory Filtration Blank	4		4		
2024-07-01	Laboratory Filtration Blank	3	2	1		
2024-07-05	Laboratory Filtration Blank	3	3			
	Average	3.38				
	Standard Deviation	0.70				
	LOD	5 counts				

Table 5.S4. *A comparison of anthropogenic microparticle deposition rates from global studies of urban areas using sampling periods of > 24 h. When multiple locations were sampled, the average is reported for sites within the urban area. The table is sorted in order of humidity by the Köppen-Geiger climate classification (Beck et al., 2023), then by population size within a given climate type (UN, 2018).*

Study	Sampling Period	Detection Size Limit	Location	Climate	Population	Average Urban Deposition Rate (particles/m^2/day)
Abbasi and Turner (2021)	30-31 days	20 µm	Shiraz, Iran	Hot Semi-Arid	1.7 million	63[a]
Edo et al. (2023)	30-31 days	25 µm	Barcelona, Spain	Cold Semi-Arid	5.6 million	59[b]
Edo et al. (2023)	30-31 days	25 µm	Madrid, Spain	Cold Semi-Arid	6.6 million	76[b]
Klein et al. (2023)	28 days	10 µm	Hamburg, Germany	Temperate Oceanic	1.8 million	147
Wright et al. (2020)	3-4 days	20 µm	London, United Kingdom	Temperate Oceanic	9.3 million	771
Dris et al. (2016)	Variable, not specified	50 µm	Paris, France	Temperate Oceanic	11.0 million	110
This Chapter	3-17 days	100 µm	St. Louis, Missouri, United States	Humid Subtropical	2.2 million	102
Huang et al. (2021)	22-40 days	50 µm	Guangzhou, China	Humid Subtropical	13.3 million	114
Amato-Lourenço et al. (2022)	15 days	50 µm	São Paulo, Brazil	Humid Subtropical	22.0 million	123
Winijkul et al. (2024)	7 days	44 µm	Pathum Thani, Thailand	Tropical Savannah	914,000	325
Truong et al. (2021)	3-4 days	300 µm	Ho Chi Minh, Vietnam	Tropical Savannah	8.6 million	374

[a]The average deposition rate was converted from a reported monthly average dry deposition rate by dividing the value by 30 days.
[b]Seasonal averages for four seasons were reported but were averaged here for one value.

5.9.3. Supplemental Figures

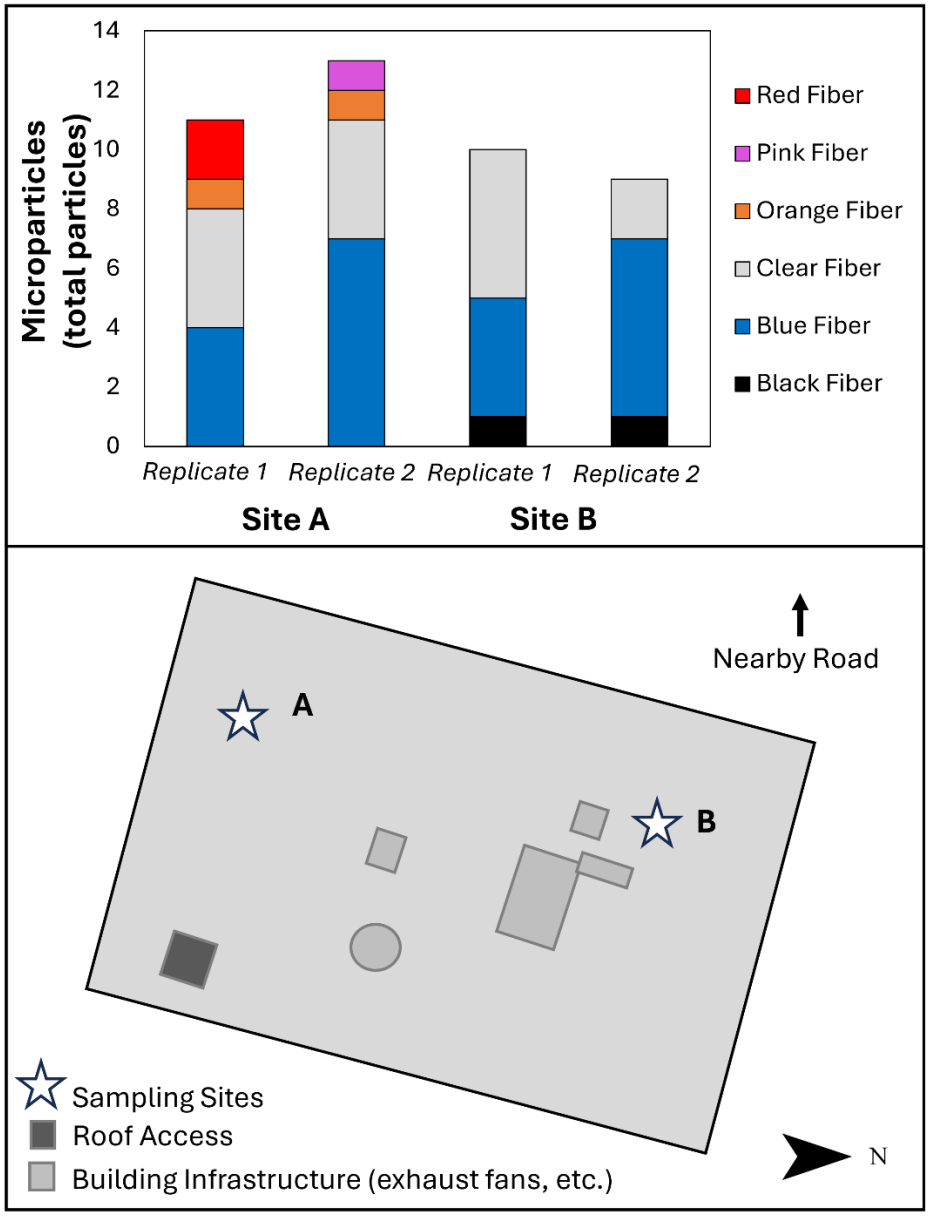

Figure 5.S1. *Results from replicate samples at two subsite locations on the rooftop at the urban site. The lower totals and reduced diversity of the anthropogenic microparticles at subsite B are suspected to be influenced by the proximity of the site to the building's exhaust fans. Subsite A was therefore chosen as the sample collection location for the study.*

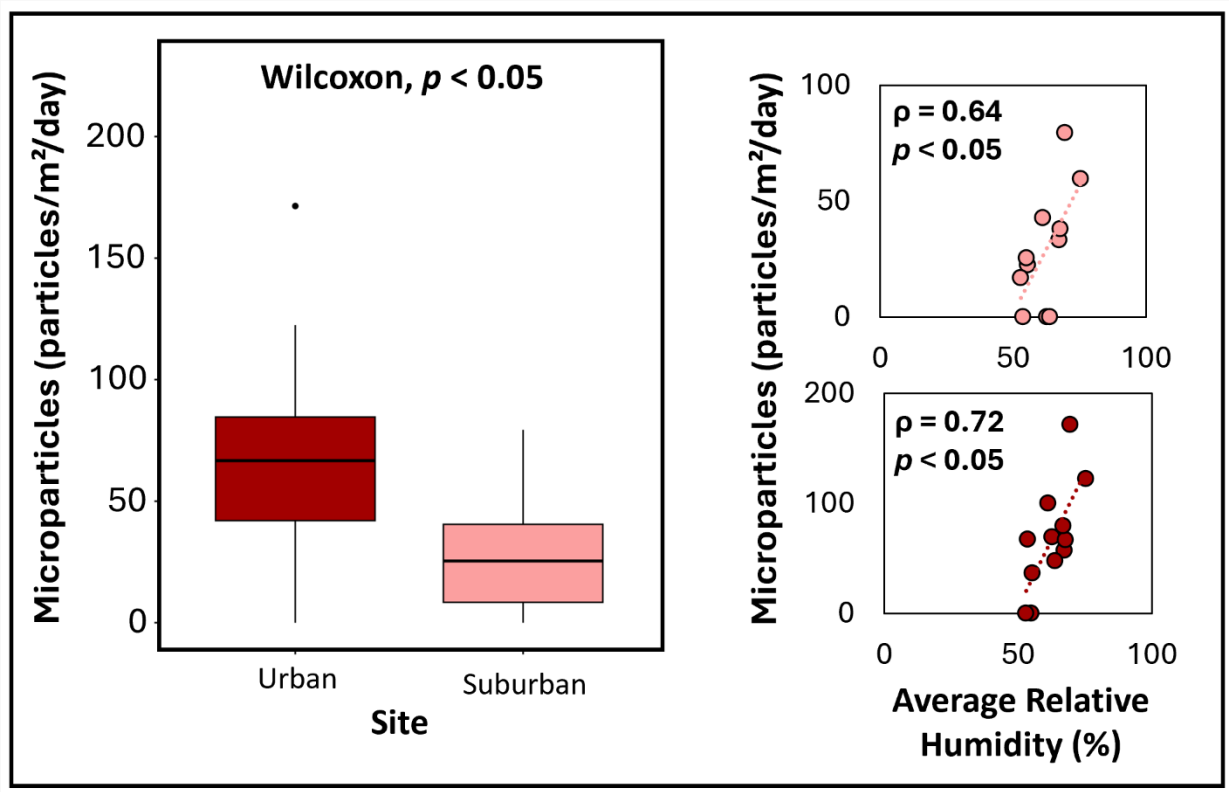

Figure 5.S2. *A comparison of the anthropogenic microparticle deposition rates at the urban and suburban sites for the same dates that feature sampling periods ≥ 10 days (left). We also show the relationships between anthropogenic microparticle deposition rates calculated from samples collected over ≥ 10 days and the corresponding average relative humidity for the suburban (top right) and urban (bottom right) sites.*

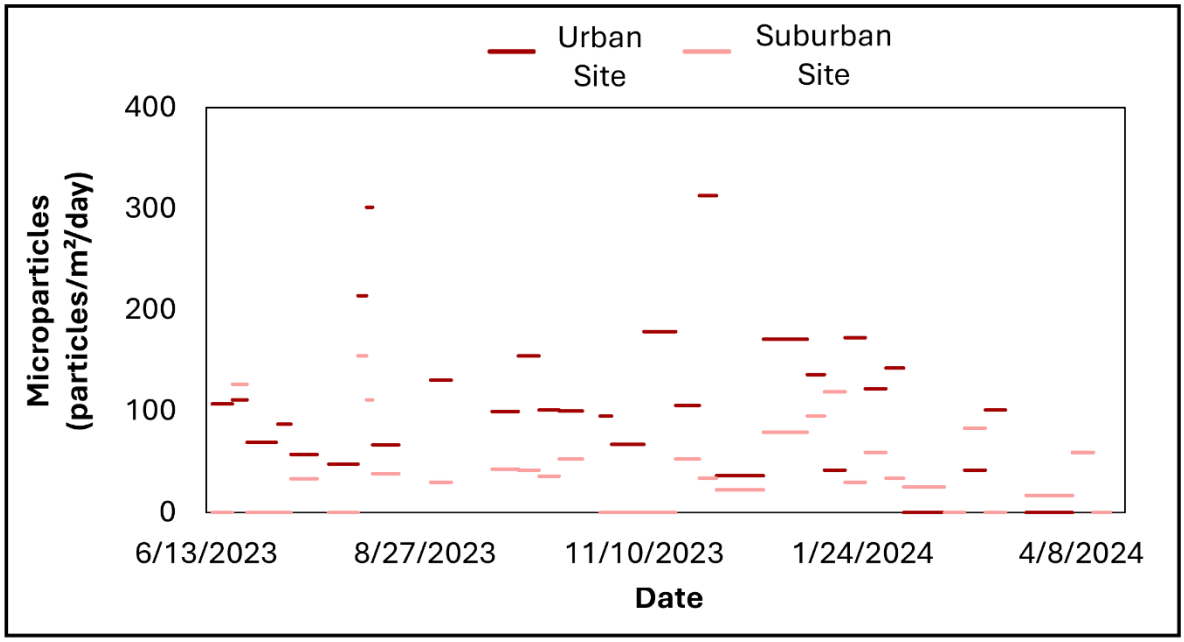

Figure 5.S3. *Anthropogenic microparticle deposition rates at the suburban and urban sites over each co-occurring sampling period using the true timesteps to show the relative lengths of the sampling periods.*

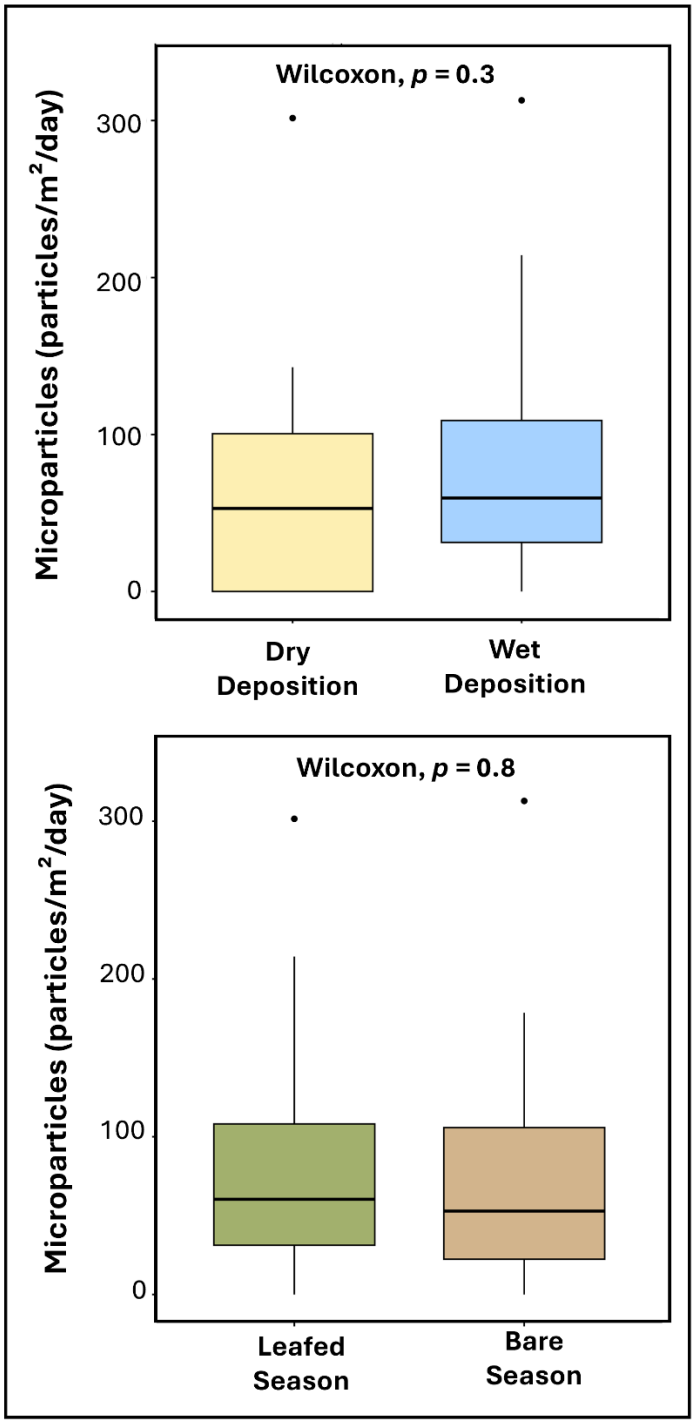

Figure 5.S4. *Comparisons of the anthropogenic microparticle quantities in dry versus wet deposition (top) as well as leafed versus bare tree season deposition (bottom).*

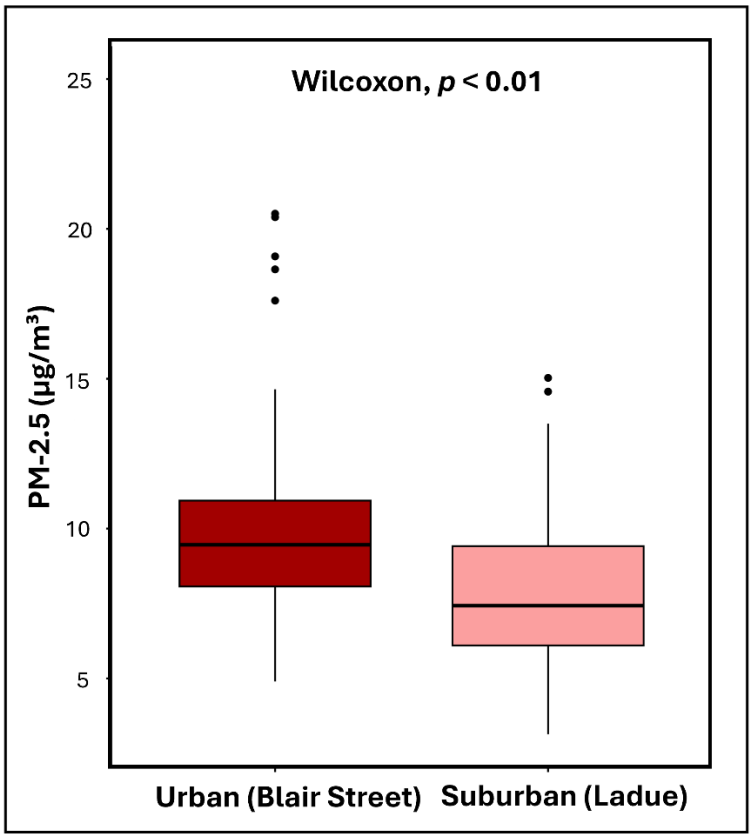

Figure 5.S5. *A comparison of the PM-2.5 values measured at the urban and suburban sites across our study period.*

5.9.4. Supplemental References

Ankit, Y., Ajay, K., Nischal, S., Kaushal, S., Kataria, V., Dietze, E., Anoop, A., 2024. Atmospheric deposition of microplastics in an urban conglomerate near to the foothills of Indian Himalayas: Investigating the quantity, chemical character, possible sources and transport mechanisms. Environ. Pollut. 361, 124629.

Leonard, J., Rassi, L.A.E., Samad, M.A., Prehn, S., Mohanty, S.K., 2024. The relative importance of local climate and land use on the deposition rate of airborne microplastics on terrestrial land. Atmos. Environ. 318, 120212.

CHAPTER 6: CONCLUSIONS AND FUTURE WORK

6.1. Major Findings

This dissertation examined the cycling of microplastics and other anthropogenic microparticles through multiple environmental compartments (i.e., the water, sediment, biota, and atmosphere) across space, time, and varying flow conditions in a small, urban watershed (Deer Creek) near St. Louis, Missouri, United States. Through multiple year-long field sampling campaigns, which included over 750 individual samples, we characterized anthropogenic microparticles in the water and sediment across the watershed's mainstem and tributaries, at high temporal resolution during flood events, inside the potential bioindicator species *C. fluminea*, and in the atmospheric deposition of the surrounding suburb and city. The identified anthropogenic microparticles (> 4300) included microplastics (e.g., polyethylene terephthalate (PET) and polypropylene (PP)), tire wear debris (e.g., polyethylene (PE) rubber), modified fibers (e.g., cotton, cellulose acetate, and dyed cellulose), and microparticles of unknown origins (e.g., undyed cellulose or unidentified material). Our results provide evidence about prevalent types of anthropogenic microparticles in the environment, allowing for the identification of potential common sources and fluxes of these pollutants among compartments. We also identified key points in space and time for the storage or transport of anthropogenic microparticles.

From our long-term (1-year), watershed-scale (10 sites across the mainstem and tributaries) assessment of the water and sediment of our small urban freshwater system in Chapter 2, we found that anthropogenic microparticles were preferentially stored in sediment and typically undetectable in water samples at baseflow conditions. The spatial distribution of anthropogenic microparticle sinks within watershed sediment could vary depending on the season. Generally, this distribution followed the erosion to deposition gradient of the watershed, with the levels of anthropogenic microparticles in sediment increasing from the stream's

headwaters to its outlet. The relationship of sediment anthropogenic microparticle distributions to quantities of nearby point source pollution inputs suggested that improved management of stormwater and wastewater outfalls could reduce further inputs of these microparticles to the system. We did not identify clear controls on the temporal fluctuation of anthropogenic microparticles in the watershed's sediment, demonstrating the complexity of their cycling through the environment.

By examining anthropogenic microparticle levels in water during multiple flow conditions in Chapter 3, we found that flood events can elevate the contaminant to detectable levels in water. These peak moments of water anthropogenic microparticle transport coincided with the highest discharge and suspended sediment levels during the floods. When examining their potential sourcing during flooding, we determined that the levels of anthropogenic microparticles in sediment consistently decreased between pre- and post-flood conditions, suggesting that export from sediment storage is a key input process to the water column. Anthropogenic microparticles were also present at high levels in localized rainfall but very low levels in roadway stormwater runoff. We therefore identified anthropogenic microparticle resuspension from sediment and deposition with rainfall as the most likely sourcing mechanisms to the stream water during flood events.

In Chapter 4, we clarified the challenges associated with using *C. fluminea* as a temporal bioindicator of environmental (i.e., sediment) anthropogenic microparticle contamination in the small, highly variable conditions of the Deer Creek watershed. Sediment anthropogenic microparticle content was related to fluctuations in grain size, while *C. fluminea* exhibited variations in anthropogenic microparticle uptake that seemed to be more influenced by water quality conditions (e.g., low water temperature and/or high salinity in the winter months). Through the comparison of anthropogenic microparticle levels in *C. fluminea* across our work

and other globally distributed studies, we identified that microfiber contamination (including microplastics such as PET and modified fibers such as cotton) is commonly taken up by *C. fluminea*.

We expanded our anthropogenic microparticle assessments to the atmospheric compartment in Chapter 5, in both the study watershed as well as the Midtown neighborhood of St. Louis City, finding the prevalent deposition of microfibers from the atmosphere throughout a year of study. The atmospheric deposition of anthropogenic microparticles was significantly higher at the more urbanized city site compared to the suburban watershed site. We also found that the anthropogenic microparticle deposition rates were enhanced at times when the relative humidity was higher in the atmosphere. The predominance of cotton and PET fibers in the atmospheric deposition samples at both sites was likely the result of sourcing from textile degradation (De Falco, 2020). These fiber types were also commonly present throughout the other types of watershed samples (i.e., water, sediment, and *C. fluminea*) explored in prior chapters. Thus, atmospheric deposition was identified as a key source of environmental anthropogenic microparticle contamination near urban areas.

6.2. Recommendations for Future Work

Our research has provided foundational knowledge on anthropogenic microparticle fluctuations across several environmental compartments over space and time within the watershed of a small, urban headwater stream system. However, further exploration of anthropogenic microparticle dynamics should be prioritized for several key remaining knowledge gaps.

First, the size limitation (100 μm to 5 mm) of our analysis of anthropogenic microparticles prevented our consideration of the presence and movement of smaller microplastics (1 μm to 100 μm) and nanoplastics (< 1 μm) in the various environmental

compartments we explored. When other studies examined these smaller size fractions, higher levels of anthropogenic microparticles were typically found compared to the larger size ranges (Carbery et al., 2024; Faull et al., 2024). Smaller microplastics and nanoplastics might have unique transport mechanisms, higher adsorption capacities for additional contaminants, and greater ecological impacts (Chen et al., 2023). From a human health standpoint, smaller anthropogenic microparticle sizes might move through cell membranes more readily and are more easily inhaled (Maurizi et al., 2024; Shen et al., 2019). In general, incorporating the study of smaller-sized anthropogenic microparticles into future research will clarify how the scale of contamination for these microparticles might differ from the quantities of larger microparticles present. Most pressingly, other atmospheric deposition studies point to the likelihood of high quantities of smaller particle sizes in the air, which could cause direct exposure to organisms from inhalation (Brahney et al., 2020; Chandrakanthan et al., 2023). The recommended method for analysis of environmental nanoparticles is pyrolysis gas chromatography mass spectrometry (Py-GCMS). Because this method provides only mass-based estimates, it might be best used alongside our visual quantification technique to provide more qualitative data about larger anthropogenic microparticles in addition to the quantification of smaller microparticles and nanoparticles of human origin (Seeley and Lynch, 2023).

Second, our ability to determine the movement of anthropogenic microparticles among compartments was hindered by their undetectable levels in most water samples. Our water sample volumes were 1-2 L. Thus, a method capturing higher volumes of water such as pump sampling could improve the estimation of the true quantities of anthropogenic microparticles present at low levels in water samples (Crawford and Quinn, 2017; Razeghi et al., 2021). A published high-volume pump method for water exists (through the American Society for Testing and Materials (ASTM); ASTM D8332), but preliminary attempts at sampling systems following

these criteria do not work effectively in the low flow conditions of small streams (ASTM, 2020; Bryska et al., 2024). The currently designed systems are also not built to function in winter weather and feature extended sample collection times such that they would prevent a study design that includes collecting samples across an entire watershed within the same day (i.e., the design of our study in Chapter 2; Bryska et al., 2024). Further work is therefore needed to adapt the proposed system designs for pump sampling of water, ideally to both meet ASTM criteria and allow holistic sampling of anthropogenic microparticles across all seasons and in small low flow systems.

Overarchingly, questions remain about the drivers of anthropogenic microparticle movement through freshwater systems. In particular, the controls on temporally fluctuating anthropogenic microparticle levels are unclear, and specific questions on this topic have arisen from individual chapters. For example, in Chapter 4, the influence of water temperature and specific conductivity on temporally fluctuating anthropogenic microparticle uptake by *C. fluminea* is an unknown that affects their bioindication potential during winter weather. In Chapter 5, the correlation between anthropogenic microparticle deposition and relative humidity raises the question of whether suspended atmospheric anthropogenic microparticles (i.e., the more inhalable material) exhibit the opposite relationship and therefore are present at higher levels during low humidity conditions. Few studies have considered humidity as an influential factor in atmospheric anthropogenic microparticle suspension and deposition despite the evidence of similar relationships for other particulate matter, and this topic warrants further exploration as an important factor potentially controlling human exposure via inhalation (Kim et al., 2019).

6.3. Conclusions

Overall, this dissertation demonstrated that anthropogenic microparticles (including microplastics) move among environmental compartments in an urban watershed, evidenced by the similarity in anthropogenic microparticle types across the studied compartments. We found that specific distributions of anthropogenic microparticles in each compartment and uptake by biota depended on a complex series of fluctuating spatial and temporal conditions. This research identified a key source of anthropogenic microparticles to the environment (i.e., atmospheric deposition), necessitating further exploration due to the potential human and ecosystem impacts. Our results also highlight key areas where anthropogenic microparticles are concentrated (i.e., the watershed's outlet), key moments in time when anthropogenic microparticle movement is enhanced (i.e., flood events), and the potential impact of legacy pollution (i.e., from point sources like sewer outfalls), which can be concentrated in sediment sinks and subsequently released by flood events. These point outfalls might be strategic locations where filtration technologies can reduce the amount of anthropogenic microparticles entering the watershed. As our global understanding of the threat of anthropogenic microparticle pollution continues to develop, our findings can inform future research directions to better understand and reduce the burden of anthropogenic microparticles (including microplastics) on human and environmental health.

6.4. References

American Society for Testing and Materials (ASTM), 2020. Standard practice for collection of water samples with high, medium, or low suspended solids for identification and quantification of microplastic particles and fibers. 11.02(D8333-20):4.

Brahney, J., Hallerud, M., Heim, E., Hahnenberger, M., Sukumaran, S., 2020. Plastic rain in protected areas of the United States. Science. 368, 1257-1260.

Bryska, J., McGlashan, P., Stelck, N., Wong, J., Anderson-Serson, A., Hart, M., Malcom, T., Battle, B., Mussone, P., 2024. High throughput application of ASTM D8332: Detailed prototype design and operating conditions for microplastic sampling of riverine systems. MethodsX, 12, 102680.

Carbery, M., Herb, F., Reynes, J., Pham, C.K., Fong, W., Lehner, R., 2022. How small is the big problem? Small microplastics <300 μm abundant in marine surface waters of the Great Barrier Reef Marine Park. Mar. Poll. Bull. 184, 114179.

Chandrakanthan, K., Fraser, M.P., Herckes, P., 2023. Airborne microplastics in a suburban location in the desert southwest: Occurrence and identification challenges. Atmos. Environ. 298, 119617.

Chen, Z., Shi, X., Zhang, J., Wu, L., Wei, W., Ni, B., 2023. Nanoplastics are significantly different from microplastics in urban waters. Water Res. X. 19, 100169.

Crawford, C.B., Quinn, B., 2017. Microplastic collection techniques. In: Microplastic Pollutants, 179-202.

De Falco, F., Cocca, M., Avella, M., Thompson, R.C., 2020. Microfiber release to water, via laundering, and to air, via everyday use: A comparison between polyester clothing with differing textile parameters. Environ. Sci. Technol. 54, 3288-3296.

Faull, L.E.M., Zaliznyak, T., Taylor, G.T., 2024. From the Caribbean to the Arctic, the most abundant microplastic particles in the ocean have escaped detection. Mar. Poll. Bull. 202, 116338.

Kim, J.J., Hann, T., Lee, S.J., 2019. Effect of flow and humidity on indoor deposition of particulate matter. Environ. Pollut. 255(2), 113263.

Maurizi, L., Simon-Sánchez, L., Vianello, A., Nielsen, A.H., Vollertsen, J., 2024. Every breath you take: High concentration of breathable microplastics in indoor environments. Chemosphere. 361, 142553.

Razeghi, N., Hamidian, A.H., Wu, C., Zhang, Y., Yang, M., 2021. Microplastic sampling techniques in freshwaters and sediments: a review. Environ. Chem. Lett. 19, 4225-4252.

Seeley, M.E., Lynch, J.M., 2023. Previous successes and untapped potential of pyrolysis–GC/MS for the analysis of plastic pollution. Anal. Bioanal. Chem. 415, 2873-2890.

Shen, M., Zhang, Y., Zhu, Y., Song, B., Zeng, G., Hu, D., Wen, X., Ren, X., 2019. Recent advances in toxicological research of nanoplastics in the environment: A review. Environ. Pollut. 252(A), 511-521.

LIST OF REFERENCES

Abbasi, S., 2021. Microplastics washout from the atmosphere during a monsoon rain event. J. Hazard. Mater. Adv. 4, 100035.

Abbasi, S., Turner, A., 2021. Dry and wet deposition of microplastics in a semi-arid region (Shiraz, Iran). Sci. Total Environ. 786, 147358.

Abbasi, S., Jaafarzadeh, N., Zahedi, A., Ravanbakhsh, M., Abbaszadeh, S., Turner, A., 2023. Microplastics in the atmosphere of Ahvaz City, Iran. J. Environ. Sci. 126, 95-102.

Adams, J.K., Dean, B.Y., Athey, S.N., Jantunen, L.M., Bernstein, S., Stern, G., Diamond, M.L., Finkelstein, S.A., 2021. Anthropogenic particles (including microfibers and microplastics) in marine sediments of the Canadian Arctic. Sci. Total Environ. 784, 147155.

Akanyange, S.N., Zhang, Y., Zhao, X., Adom-Asamoah, G, Ature, A.A., Anning, C., Tianpeng, C., Zhao, H., Lyu, X., Crittenden, J.C., 2022. A holistic assessment of microplastic ubiquitousness: Pathway for source identification in the environment. Sustain. Prod. Consum. 33, 113-145.

Akindele, E.O., Ehlers, S.M., Koop, J.H.E., 2019. First empirical study of freshwater microplastics in West Africa using gastropods from Nigeria as bioindicators. Limnologica 78, 125708.

Alencar, M.V., Gimenez, B.G., Sasahara, C., Elliff, C.I., Rodrigues, L.S., Conti, L.A., Dias, S.L.F.G., Cetrulo, T.B., Scrich, V.M., Turra, A., 2022. How far are we from robust estimates of plastic litter leakage to the environment? J. Environ. Manage. 323, 116195.

Allen, D., Allen, S., Abbasi, S., Baker, A., Bergmann, M., Brahney, J., Butler, T., Duce, R.A., Eckhardt, S., Evangeliou, N., Jickells, T., Kanakidou, M., Kershaw, P., Laj, P., Levermore, J., Li, D., Liss, P., Liu, K., Mahowald, N., Masque, P., Materic, D., Mayes, A.G., McGinnity, P., Osvath, I., Prather, K.A., Prospero, J.M., Revell, L.E., Sander, S.G., Shim, W.J., Slade, J., Stein, A., Tarasova, O., Wright, S., 2022. Microplastics and nanoplastics in the marine-atmosphere environment. Nat. Rev. Earth Environ. 3, 393-405.

Allen, S., Allen, D., Baladima, F., Phoenix, V.R., Thomas, J.L., Le Roux, G., Sonke, J.E., 2021. Evidence of free tropospheric and long-range transport of microplastic at Pic du Midi Observatory. Nat. Commun. 12, 7242.

Almroth, B.M.C., Astrom, L., Roslund, S., Petersson, H., Johansson, M., Persson, N., 2017. Quantifying shedding of synthetic fibers from textiles; a source of microplastics released into the environment. Environ. Sci. Pollut. Res. 25, 1191-1199.

Amato-Lourenço, L.F., dos Santos Galvão, L., Wiebeck, H., Carvalho-Oliveira, R., Mauad, T., 2022. Atmospheric microplastic fallout in outdoor and indoor environments in São Paulo megacity. Sci. Total Environ. 821, 153450.

American Society for Testing and Materials (ASTM), 2020. Standard practice for collection of water samples with high, medium, or low suspended solids for identification and quantification of microplastic particles and fibers. 11.02(D8333-20):4.

Ankit, Y., Ajay, K., Nischal, S., Kaushal, S., Kataria, V., Dietze, E., Anoop, A., 2024. Atmospheric deposition of microplastics in an urban conglomerate near to the foothills of Indian Himalayas: Investigating the quantity, chemical character, possible sources and transport mechanisms. Environ. Pollut. 361, 124629.

Athey, S.N., Erdle, L.M., 2022. Are we underestimating anthropogenic microfiber pollution? A critical review of occurrence, methods, and reporting. Environ. Toxicol. Chem. 41(4), 822-837.

Balestra, V., Galbiati, M., Lapadula, S., Barzaghi, B., Manenti, R., Ficetola, G.F., Bellopede, R., 2024. The problem of anthropogenic microfibres in karst systems: Assessment of water and submerged sediments. Chemosphere. 363, 142811.

Baraza, T., Hasenmueller, E.A., 2023. Floods enhance the abundance and diversity of anthropogenic microparticles (including microplastics and treated cellulose) transported through karst systems. Water Res. 242, 120204.

Baraza, T., Hernandez, N.F., Sebok, J.N., Wu, C., Hasenmueller, E.A., Knouft, J.H., 2022. Integrating land cover, point source pollution, and watershed hydrologic processes data to understand the distribution of microplastics in riverbed sediments. Environ. Pollut. 311, 119852.

Barrett, J., Chase, Z., Zhang, J., Holl, M.M.B., Willis, K., Williams, A., Hardesty, B.D., Wilcox, C., 2020. Microplastic pollution in deep-sea sediments from the Great Australian Bight. Front. Mar. Sci. 7, 576170.

Beaurepaire, M., Gaseperi, J., Tassin, B., Dris, R., 2024. COVID lockdown significantly impacted microplastic bulk atmospheric deposition rates. Environ. Pollut. 344, 123354.

Beaver, J.R., Crisman, T.L., Brock, R.J., 1991. Grazing effects of an exotic bivalve (*Corbicula fluminea)* on hypereutrophic lake water. LRM 7(1).

Beck, H.E., McVicar, T.R., Vergopolan, N., Berg, A., Lutsko, N.J., Dufour, A., Zeng, Z., Jiang, X., van Dijk, A.I.J.M., Miralles, D.G., 2023. High-resolution (1 km) Köppen-Geiger maps for 1901–2099 based on constrained CMIP6 projections. Sci. Data, 10, 724.

Bergmann, M., Mutzel, S., Primpke, S., Tekman, M.B., Trachsel, J., Gerdts, G., 2019. White and wonderful? Microplastics prevail in snow from the Alps to the Arctic. Sci. Adv. 5(8).

Brahney, J., Hallerud, M., Heim, E., Hahnenberger, M., Sukumaran, S., 2020. Plastic rain in protected areas of the United States. Science. 368, 1257-1260.

Bryska, J., McGlashan, P., Stelck, N., Wong, J., Anderson-Serson, A., Hart, M., Malcom, T., Battle, B., Mussone, P., 2024. High throughput application of ASTM D8332: Detailed

prototype design and operating conditions for microplastic sampling of riverine systems. MethodsX, 12, 102680.

Büngener, L., Schäffer, S., Schwarz, A., Shwalb, A., 2024. Microplastics in a small river: Occurrence and influencing factors along the river Oker, Northern Germany. J. Contam. Hydrol. 264, 104366.

Carbery, M., Herb, F., Reynes, J., Pham, C.K., Fong, W., Lehner, R., 2022. How small is the big problem? Small microplastics <300 μm abundant in marine surface waters of the Great Barrier Reef Marine Park. Mar. Poll. Bull. 184, 114179.

Carpenter, E.J., Smith, K.L., 1972. Plastics on the Sargasso Sea surface. Science. 175(4027), 1240-1241.

Chand, R., Putna-Nimane, I., Vecmane, E., Lykkemark, J., Dencker, J., Nielsen, A.H., Vollertsen, J., Liu, F., 2024. Snow dumping station – A considerable source of tyre wear, microplastics, and heavy metal pollution. Environ. Int. 188, 108782.

Chandrakanthan, K., Fraser, M.P., Herckes, P., 2023. Airborne microplastics in a suburban location in the desert southwest: Occurrence and identification challenges. Atmos. Environ. 298, 119617.

Chen, G., Feng, Q., Wang, J., 2020. Mini-review of microplastics in the atmosphere and their risks to humans. Sci. Total Environ. 703, 135504.

Chen, Z., Shi, X., Zhang, J., Wu, L., Wei, W., Ni, B., 2023. Nanoplastics are significantly different from microplastics in urban waters. Water Res. X. 19, 100169.

Cowger, W., Steinmetz, Z., Gray, A., Munno, K., Lynch, J., Hapich, H., Primpke, S., De Frond, H., Rochman, C., Herodotou, O., 2021. Microplastic spectral classification needs an open source community: Open Specy to the rescue! Anal. Chem. 93(21), 7543-7548.

Cox, K.D., Covernton, G.A., Davies, H.L., Dower, J.F., Juanes, F., Dudas, S.E., 2019. Human consumption of microplastics. Environ. Sci. Technol. 53, 7068-7074.

Crawford, C.B., Quinn, B., 2017. Microplastic collection techniques. In: Microplastic Pollutants, 179-202.

Criss, R.E., Stein, E.M., Nelson, D.L., 2022. Generation and propagation of an urban flash flood and our collective responsibilities. J. Earth Sci. 33(6), 1624-1628.

Cunningham, E.M., Seijo, N.R., Altieri, K.E., Audh, R.R., Burger, J.M., Bornman, T.G., Fawcett, S., Gwinnett, C.M.B., Osborne, A.O., Woodall, L.C., 2022. The transport and fate of microplastic fibres in the Antarctic: The role of multiple global processes. Front. Mar. Sci. 9:1056081.

Dahms, H.F.J., van Rensburg, G.J., Greenfield, R., 2020. The microplastic profile of an urban African stream. Sci. Total Environ. 731, 138893.

Dawson, A.L., Santana, M.F.M., Nelis, J.L.D., Motti, C.A., 2023. Taking control of microplastics data: A comparison of control and blank data correction methods. J. Hazard. Mater. 443A, 130218.

De Arbeloa, N.P., Marzadri, A., 2024. Modeling the transport of microplastics along river networks. Sci. Total Environ. 911, 168227.

De Carvalho, A.R., Garcia, F., Riem-Galliano, L., Tudesque, L., Albignac, M., ter Halle, A., Cucherousset, J., 2021. Urbanization and hydrological conditions drive the spatial and temporal variability of microplastic pollution in the Garonne River. Sci. Total Environ. 769, 144479.

De Carvalho, A.R., Riem-Galliano, L., ter Halle, A., Cucherousset, J., 2022. Interactive effect of urbanization and flood in modulating microplastic pollution in rivers. Environ. Pollut. 309, 119760.

De Falco, F., Cocca, M., Avella, M., Thompson, R.C., 2020. Microfiber release to water, via laundering, and to air, via everyday use: A comparison between polyester clothing with differing textile parameters. Environ. Sci. Technol. 54, 3288-3296.

De Frond, H., Rubinovitz, R., Rochman, C.M., 2021. μATR-FTIR spectral libraries of plastic particles (FLOPP and FLOPP-e) for the analysis of microplastics. Anal. Chem. 93(48), 15878-15885.

Della Torre, C., Riccardi, N., Magni, S., Modesto, V., Fossati, M., Binelli, A., 2023. First comparative assessment of contamination by plastics and non-synthetic particles in three bivalve species from an Italian sub-alpine lake. Environ. Pollut. 330, 121752.

Dewitz, J., 2021. National Land Cover Database (NLCD) 2019 Impervious Products: U.S. Geological Survey data release.

Dewitz, J., 2023. National Land Cover Database (NLCD) 2021 Products: U.S. Geological Survey data release.

Dikareva, N., Simon, K.S., 2019. Microplastic pollution in streams spanning an urbanization gradient. Environ. Pollut. 250, 292-299.

Ditlhakanyane, B.C., Ultra Jr., V.U., Mokgosi, M.S., Mokopasetso, T., 2023. Microplastic abundance in the surface water, clams (*Corbicula fluminea*) and fish species (*Oreochromis niloticus* and *Coregonus kiyi*) from the Gaborone Dam, Botswana. Water Air Soil Pollut. 234:602.

Dris, R., Gasperi, J., Rocher, V., Saad, M., Renault, N., Tassin, B., 2015. Microplastic contamination in an urban area: a case study in Greater Paris. Environ. Chem. 12(5), 592-599.

Dris, R., Gasperi, J., Saad, M., Mirande, C., Tassin, B., 2016. Synthetic fibers in atmospheric fallout: A source of microplastics in the environment? Mar. Poll. Bull. 104(1-2), 290-293.

Drummond, J.D., Schneidewind, U., Li, A., Hoellein, T.J., Krause, S., Packman, A.I., 2022. Microplastic accumulation in riverbed sediment via hyporheic exchange from headwaters to mainstems. Sci. Adv. 8, eabi9305.

East-West Gateway, 2024. Regional Profile. https://www.ewgateway.org/about-us/who-we-are/regional-profile. Accessed March 01, 2025

Edo, C., Fernandez-Pinas, F., Leganes, F., Gomez, M., Martinez, I., Herrera, A., Hernandez-Sanchez, C., Gonzalez-Salamo, J., Borges, J.H., Lopez-Castellanos, J., Bayo, J., Romera-Castillo, C., Elustondo, D., Santamaria, C., Alonso, R., Garcia-Gomez, H., Gonzalez-Cascon, R., Martinez-Hernandez, V., Landaburu-Aguirre, J., Incera, M., Gago, J., Noya, B., Beiras, R., Muniategui-Lorenzo, S., Rosal, R., Gonzalez-Pleiter, M., 2023. A nationwide monitoring of atmospheric microplastic deposition. Sci. Total Environ. 905, 166923.

Esri., 2024. "World Imagery" [basemap]. https://www.arcgis.com/home/item.html?id=10df2279f9684e4a9f6a7f08febac2a9. Accessed January 03, 2025.

Esri, DigitalGlobe, GeoEye, i-cubed, USDA FSA, USGS, AEX, Getmapping, Aerogrid, IGN, IGP, swisstopo, GIS User Community, 2025a. “World Imagery” [basemap]. https://services.arcgisonline.com/ArcGIS/rest/services/World_Imagery/MapServer. Accessed February 20, 2025.

Esri, TomTom, FAO, NOAA, USGS, 2025b. “World Street Map” [basemap]. https://basemaps.arcgis.com/arcgis/rest/services/World_Basemap_v2/VectorTileServer. Accessed February 24, 2025.

Esri, Missouri Dept. of Conservation, Missouri DNR, Tom-Tom, SafeGraph, FAO, METI/NASA, USGS, EPA, NPS, USFWS, NGA, Garmin, 2019. "World Terrain Base" [basemap]. Scale ~1:70k. https://www.arcgis.com/home/item.html?id=c61ad8ab017d49e1a82f580ee1298931. Accessed March 01, 2025.

Evangeliou, N., Grythe, H., Klimont, Z., Heyes, C., Eckhardt, S., Lopez-Aparicio, S., Stohl, A., 2020. Atmospheric transport is a major pathway of microplastics to remote regions. Nat. Commun. 11,3381.

Faull, L.E.M., Zaliznyak, T., Taylor, G.T., 2024. From the Caribbean to the Arctic, the most abundant microplastic particles in the ocean have escaped detection. Mar. Poll. Bull. 202, 116338.

Feng, S., Lu, H., Xue, Y., Yan, P., Sun, T., 2024. Fate, transport, and source of microplastics in the headwaters of the Yangtze River on the Tibetan Plateau. J. Hazard. Mater. 455, 131526.

Finegan-Dronchi, C.R., Hasenmueller, E.A., 2023. Winter road salt retention is enhanced in watersheds dominated by silicate rocks compared to carbonate rocks. AGU Fall Meeting Abstracts, 2057, H33U-2057.

Finegan-Dronchi, C.R., Hasenmueller, E.A., 2024. Municipal water exchanges between surface water and groundwater resources in an urban catchment. Geological Society of America Abstracts, 56, 402924.

Finnegan, A.M.D., Susserott, R., Gabbott, S.E., Gouramanis, C., 2022. Man-made natural and regenerated cellulosic fibres greatly outnumber microplastic fibres in the atmosphere. Environ. Pollut. 310, 119808.

Frias, J., Nash, R., 2019. Microplastics: Finding a consensus on the definition. Mar. Poll. Bull. 138, 145-147.

Fu, L., Xi, M., Nicholaus, R., Wang, Z., Wang, X., Kong, F., Yu, Z., 2022. Behaviors and biochemical responses of macroinvertebrate *Corbicula fluminea* to polystyrene microplastics. Sci. Total Environ. 813, 152617.

Geverdt, D., 2019. Education Demographic and Geographic Estimates Program (EDGE): Locale Boundaries File Documentation, 2017 (NCES 2018-115). U.S. Department of Education. Washington, DC: National Center for Education Statistics. https://nces.ed.gov/programs/edge/docs/EDGE_NCES_LOCALE.pdf. Accessed March 01, 2025.

Giarratano, E., Trovant, B., Hernandez-Moresino, R.D., 2024. Asian clam *Corbicula fluminea* as potential bioindicator of microplastics and metal(oid)s in a Patagonian River. Mar. Environ. Res. 198, 106548.

Goehler, L.O., Moruzzi, R.B., Da Conceiçao, F.T., Júnior, A.A.C., Speranza, L.G., Busquets, R., Campos, L.C., 2022. Relevance of tyre wear particles to the total content of microplastics transported by runoff in a high-imperviousness and intense vehicle traffic urban area. Environ. Pollut. 314, 120200.

González-Aravena, M., Rotunno, C., Cárdenas, C.A., Torres, M., Morley, S.A., Hurley, J., Caro-Lara, L., Pozo, K., Galban, C., Rondon, R., 2024. Detection of plastic, cellulosic micro-fragments and microfibers in *Laternula elliptica* from King George Island (Maritime Antarctica). Mar. Poll. Bull. 201, 116257.

Gonzalez-Inca, C., Valkama, P., Lill, J., Slotte, J., Hietaharju, E., Uusitalo, R., 2018. Spatial modeling of sediment transfer and identification of sediment sources during snowmelt in an agricultural watershed in boreal climate. Sci. Total Environ. 612, 303-312.

Guilhermino, L., Vieira, L.R., Riveiro, D., Tavares, A.S., Cardoso, V., Alves, A., Almeida, J.M., 2018. Uptake and effects of the antimicrobial florfenicol, microplastics and their mixtures on freshwater exotic invasive bivalve *Corbicula fluminea*. Sci. Total Environ. 622-623, 1131-1142.

Gündogdu, S., Cevik, C., Ayat, B., Aydogan, B., Karaka, S., 2018. How microplastics quantities increase with flood events? An example from Mersin Bay NE Levantine coast of Turkey. Environ. Pollut. 239, 342-350.

Guo, X., Cai, Y., Ma, C., Han, L., Yang, Z., 2021. Combined toxicity of micro/nano scale polystyrene plastics and ciprofloxacin to *Corbicula fluminea* in freshwater sediments. Sci. Total Environ. 789, 147887.

Harris, L.S.T., Beur, L.L., Olsen, A.Y., Smith, A., Eggers, L., Pedersen, E., Van Brocklin, J., Brander, S.M., Larson, S., 2021. Temporal variability of microparticles under the Seattle aquarium, Washington State: Documenting the global Covid-19 pandemic. Environ. Toxicol. Chem. 41(4), 917-930.

Hasenmueller, E.A., Baraza, T., Hernandez, N.F., Finegan, C.R., 2023. Cave sediment sequesters anthropogenic microparticles (including microplastics and modified cellulose) in subsurface environments. Sci. Total Environ. 893, 164690.

Hasenmueller, E.A., Criss, R.E., Winston, W.E., Shaughnessy, A.R., 2017. Stream hydrology and geochemistry along a rural to urban land use gradient. Appl. Geochem. 83, 136-149.

Hasenmueller, E.A., Ritter, A.N. 2024. Microplastic chemostasis and homogeneity during a historic flood on the Mississippi River. Environ. Eng. Sci. 41(12), 563-573.

He, B., Goonetilleke, A., Ayoko, G., Rintoul, L., 2019. Abundance, distribution patterns, and identification of microplastics in Brisbane River sediments, Australia. Sci. Total Environ. 700, 134467.

He, B., Wijesiri, B., Ayoko, G.A., Egodawatta, P., Rintoul, L., Goonetilleke, A., 2020. Influential factors on microplastics occurrence in river sediments. Sci. Total Environ. 738, 139901.

Hernandez, E., Nowack, B., Mitrano, D.M., 2017. Polyester textiles as a source of microplastics from households: A mechanistic study to understand microfiber release during washing. Environ. Sci. Technol. 51, 7036-7046.

Hernandez, N.F., Hasenmueller, E.A., 2024. Anthropogenic macroscale and microscale debris (including plastics) have differing spatial distributions across a small urban watershed. Environ. Eng. Sci. 41(12), 509-519.

Hitchcock, J.N., 2020. Storm events as key moments of microplastic contamination in aquatic ecosystems. Sci. Total Environ. 734, 139436.

Huang, Y., He, T., Yan, M., Yang, L., Gong, H., Wang, W., Qing, X., Wang, J., 2021. Atmospheric transport and deposition of microplastics in a subtropical urban environment. J. Hazard. Mater. 416, 126168.

Hurley, R., Woodward, J., Rothwell, J.J., 2018. Microplastic contamination of river beds significantly reduced by catchment-wide flooding. Nat. Geosci. 11, 251-257.

Illuminati, S., Notarstefano, V., Tinari, C., Fanelli, M., Girolametti, F., Ajdini, B., Scarchilli, C., Ciardini, V., Iaccarino, A., Giorgini, E., Annibaldi, A., Truzzi, C., 2024. Microplastics in

bulk atmospheric deposition along the coastal region of Victoria Land, Antarctica. Sci. Total Environ., 949, 175221.

Iowa Environmental Mesonet (IEM), 2025. ASOS Network "ASOS-AWOS-METAR data download". https://mesonet.agron.iastate.edu/ASOS/. Accessed March 01, 2025.

Jia, Q., Duan, Y., Han, X., Sun, X., Munyanez, J., Ma, J., Xiu, G., 2022. Atmospheric deposition of microplastics in the megalopolis (Shanghai) during rainy season: Characteristics, influence factors, and source. Sci. Total Environ. 847, 157609.

Jeong, E., Lee, J., Redwan, M., 2024. Animal exposure to microplastics and health effects: A review. Emerg. Contam. 10(4), 100369.

Kabir, A.H.M.E., Sekine, M., Imai, T., Yamamoto, K., Kanno, A., Higuchi, T., 2022. Microplastics in the sediments of small-scale Japanese rivers: Abundance and distribution, characterization, sources-to-sink, and ecological risks. Sci. Total Environ. 812, 152590.

Karapetrova, A., Cowger, W., Michell, A., Braun, A., Bair, E., Gray, A., Gan, J., 2024. Exploring microplastic distribution in Western North American snow. J. Hazard. Mater. 480, 136126.

Kernchen, S., Loder, M.G.J., Fischer, F., Fischer, D., Moses, S.R., Georgi, C., Nolscher, A.C., Held, A., Laforsch, C., 2022. Airborne microplastic concentrations and deposition across the Weser River catchment. Sci. Total Environ. 818, 151812.

Kim, J.J., Hann, T., Lee, S.J., 2019. Effect of flow and humidity on indoor deposition of particulate matter. Environ. Pollut. 255(2), 113263.

Kim, L., Kim, S.A., Kim, T.H., Kim, J., An, Y., 2021. Synthetic and natural microfibers induce gut damage in the brine shrimp *Artemia franciscana*. Aquat. Toxicol. 232, 105748.

Klein, M., Fischer, E.K., 2019. Microplastic abundance in atmospheric deposition within the Metropolitan area of Hamburg, Germany. Sci. Total Environ. 685, 96-103.

Klein, M., Bechtel, B., Brecht, T., Fischer, E.K., 2023. Spatial distribution of atmospheric microplastics in bulk-deposition of urban and rural environments – A one-year follow-up study in northern Germany. Sci. Total Environ. 901, 165923.

Koban, L.A., King, T., Huff, T.B., Furst, K.E., Nelson, T.R., Pfluger, A.R., Kuppa, M.M., Fowler, A.E., 2024. Passive biomonitoring for per- and polyfluoroalkyl substances using invasive clams, *C. fluminea.* J. Hazard. Mater. 472, 134463.

Koutnik, V.S., Leonard, J.L., Alkidim, S., DePrima, F.J., Ravi, S., Hoek, E.M.V., Mohanty, S.K., 2021. Distribution of microplastics in soil and freshwater environments: Global analysis and framework for transport modeling. Environ. Pollut. 274, 116552.

Koutsikos, N., Koi, A.M., Zeri, C., Tsangaris, C., Dimitriou, Kalantzi, O., 2023. Exploring microplastic pollution in a Mediterranean river: The role of introduced species as bioindicators. Heliyon 9(4), e15069.

Lahon, J., Handique, S., 2024. Flood-induced variation and source apportionment of microplastics in Jia Bharali River of mid-Brahmaputra Valley, India. Environ. Monit. Assess. 196:1236.

Lauritsen, D.D., 1986. Filter-Feeding in *Corbicula fluminea* and its effect on seston removal. J. N. Am. Benthol. Soc. 5(3).

Leonard, J., Rassi, L.A.E., Samad, M.A., Prehn, S., Mohanty, S.K., 2024. The relative importance of local climate and land use on the deposition rate of airborne microplastics on terrestrial land. Atmos. Environ. 318, 120212.

Li, L., Frey, M., Browning, K.J., 2010. Biodegradability study on cotton and polyester fabrics. J. Eng. Fiber. Fabr. 5(4).

Li, L., Su, L., Cai, H., Rochman, C.M., Li, Q., Kolandhasamy, P., Peng, J., Shi, H., 2019. The uptake of microfibers by freshwater Asian clams (*Corbicula fluminea*) varies based upon physicochemical properties. Chemosphere 221, 107-114.

Li, W., Brunetti, G., Zafiu, C., Kunaschk, M., Debreczeby, M., Stumpp, C., 2024. Experimental and simulated microplastics transport in saturated natural sediments: Impact of grain size and particle size. J. Hazard. Mater. 468, 133772.

Liu, Z., Bai, Y., Ma. T., Liu, X., Wei, H., Meng, H., Fu, Y., Ma, Z., Zhang, L., Zhao, J., 2022. Distribution and possible sources of atmospheric microplastic deposition in a valley basin city (Lanzhou, China). Ecotoxicol. Environ. Saf. 233, 113353.

Liu, J., Zhu, B., An, L., Ding, J., Xu, Y., 2023. Atmospheric microfibers dominated by natural and regenerated cellulosic fibers: Explanations from the textile engineering perspective. Environ. Pollut. 317, 120771.

Lockmiller, K.A., Wang, K., Fike, D.A., Shaughnessy, A.R., Hasenmueller, E.A., 2019. Using multiple tracers (F^-,B, $\delta^{11}B$, and optical brighteners) to distinguish between municipal drinking water and wastewater inputs to urban streams. Sci. Total Environ. 671, 1245-1256.

Luo, W., Fu, H., Lu, Q., Li, B., Cao, X., Chen, S., Liu, R., Tang, B., Yan, X., Zheng, J., 2024. Microplastic pollution differences in freshwater river according to stream order: Insights from spatial distribution, annual load, and ecological assessment. J. Environ. Manage. 366, 121836.

Lusher, A.L., Welden, N.A., Sobral, P., Cole, M., 2017. Sampling, isolating and identifying microplastics ingested by fish and invertebrates. Anal. Methods 9, 1346.

Macieira, R.M., Oliveira, L.A.S., Cardozo-Ferreira, G.C., Pimental, C.R., Andrades, R., Gasparini, J.L., Sarti, F., Chelazzi, D., Cincinelli, A., Gomes, L.C., Giarrizzo, T., 2021.

Microplastic and artificial cellulose microfibers ingestion by reef fishes in the Guarapari Islands, southwestern Atlantic. Mar. Poll. Bull. 167, 112371.

Mancini, M., Serra, T., Colomer, J., Solari, L., 2023. Suspended sediments mediate microplastic sedimentation in unidirectional flows. Sci. Total Environ. 890, 164363.

Matjašič, T., Mori, N., Hostnik, I., Bajt, O., Viršek, M.K., 2022. Microplastic pollution in small rivers along rural–urban gradients: Variations across catchments and between water column and sediments. Sci. Total Environ. 858(3), 160043.

Mattsson, K., Da Silva, V.H., Deonarine, A., Louie, S.M., Gondikas, A., 2021. Monitoring anthropogenic particles in the environment: Recent developments and remaining challenges at the forefront of analytical methods. Curr. Opin. Colloid Interface Sci. 56, 101513.

Maurizi, L., Simon-Sánchez, L., Vianello, A., Nielsen, A.H., Vollertsen, J., 2024. Every breath you take: High concentration of breathable microplastics in indoor environments. Chemosphere. 361, 142553.

McCoy, K.A., Hodgson, D.J., Clark, P.F., Morritt, D., 2020. The effects of wet wipe pollution on the Asian clam, *Corbicula fluminea* (Mollusca: Bivalvia) in the River Thames, London. Environ. Pollut. 264, 114577.

Metropolitan Saint Louis Sewer District (MSD), 2024. Sewer Overflows, MSD Project Clear Web page. https://msdprojectclear.org/customers/problems-tips/sewer-overflows/. Accessed February 01, 2025.

Metropolitan St. Louis Sewer District (MSD)., 2025a. Deer Creek Sanitary Tunnel. Project Clear. https://msdprojectclear.org/projects/tunnels/deer-creek-sanitary-tunnel/. Accessed March 01, 2025.

Metropolitan St. Louis Sewer District (MSD)., 2025b. Sewer overflow locations map ‘sewer overflow locations as of June 30, 2018’. https://msdprojectclear.org/customers/problems-tips/sewer-overflows/. Accessed March 01, 2025.

Miller, W.A., Atwill, E.R., Gardner, I.A., Miller, M.A., Fritz, H.M., Hedrick, R.P., Melli, A.C., Barnes, N.M., Conrad, P.A., 2005. Clams (*Corbicula fluminea*) as bioindicators of fecal contamination with Cryptosporidium and Giardia spp. in freshwater ecosystems in California. IJP-PAW 35(6), 673-684.

Missouri Department of Natural Resources (MoDNR), 2020. Bedrock 24k. https://gis.dnr.mo.gov/host/rest/services/geology/bedrock_24k/MapServer/1. Accessed March 01, 2025.

Missouri Department of Natural Resources (MoDNR), 2021. MO NPDES Outfalls. https://services2.arcgis.com/kNS2ppBA4rwAQQZy/arcgis/rest/services/MO_NPDES_Outfalls/FeatureServer. Accessed March 01, 2025.

Missouri Department of Natural Resources (MoDNR), 2022. 2022 Section 303(d) listed waters: proposed list for public notice on October 13, 2022. https://dnr.mo.gov/document-search/2022-epa-approved-section-303d-listed-waters. Accessed April 03, 2025.

Missouri Spatial Data Information Service (MSDIS), 2019. MO 2018 Sinkholes. https://services2.arcgis.com/kNS2ppBA4rwAQQZy/arcgis/rest/services/MO_2018_Sinkholes/FeatureServer/0. Accessed March 01, 2025.

Muller, M., Murphy, B., Burghammer, M., Riekel, C., Pantos, E., Gunneweg, J., 2007. Ageing of native cellulose fibres under archaeological conditions: textiles from the Dead Sea region studied using synchrotron X-ray microdiffraction. Appl. Phys. A – Mater. 89, 877-881.

Nan, G., Peigang, W., Chao, W., Jun, H., Jin, Q., Lingzhan, M., 2016. Mechanisms of cadmium accumulation (adsorption and absorption) by the freshwater bivalve *Corbicula fluminea* under hydrodynamic conditions. Environ. Pollut. 212, 550-558.

Napper, I.E., Davies, B.F.R., Clifford, H., Elvin, S., Koldewey, H.J., Mayewski, P.A., Miner, K.R., Potocki, M., Elmore, A.C., Gajurel, A.P., Thompson, R.C., 2020. Reaching new heights in plastic pollution—Preliminary findings of microplastics on Mount Everest. One Earth. 3, 621-630.

National Weather Service (NWS), 2024. The climatology of the St. Louis area. https://www.weather.gov/lsx/cli_of_stl. Accessed March 01, 2025.

O'Brien, S., Rauert, C., Ribeiro, F., Okoffo, E.D., Burrows, S.D., O'Brien, J.W., Wang, X., Wright, S.L., Thomas, K.V., 2023. There's something in the air: A review of sources, prevalence and behaviour of microplastics in the atmosphere. Sci. Total Environ. 874, 162193.

O'Driscoll, M., Clinton, S., Jefferson, A., Manda, A., McMillan, S., 2010. Urbanization effects on watershed hydrology and in-stream processes in the Southern United States. Water, 2(3), 605-648.

Park, C.H., Kang, Y.K., Im, S.S. Biodegradability of cellulose fabrics., 2004. J. Appl. Polym. Sci. 94(1), 248-253.

Pastorino, P., Anselmi, S., Zanoli, A., Esposito, G., Bondavalli, F., Dondo, A., Pucci, A., Pizzul, E., Faggio, C., Barcelo, D., Renzi, M., Prearo, M., 2023. The invasive red swamp crayfish (*Procambarus clarkii*) as a bioindicator of microplastic pollution: Insights from Lake Candia (northwestern Italy). Ecol. Indic. 150, 110200.

Primpke, S., Wirth, M., Lorenz, C., Gerdts, G., 2018. Reference database design for the automated analysis of microplastic samples based on Fourier transform infrared (FTIR) spectroscopy. Anal. Bioanal. Chem. 410, 5131-5141.

Range, D., Scherer, C., Stock. F., Ternes, T.A., Hoffmann, T.O., 2023. Hydro-geomorphic perspectives on microplastic distribution in freshwater river systems: A critical review. Water Res. 245, 120567.

Rao, W., Fan, Y., Li, H., Qian, X., Liu, T., 2024. New insights into the long-term dynamics and deposition-suspension distribution of atmospheric microplastics in an urban area. J. Hazard. Mater. 463, 132860.

Razeghi, N., Hamidian, A.H., Wu, C., Zhang, Y., Yang, M., 2021. Microplastic sampling techniques in freshwaters and sediments: a review. Environ. Chem. Lett. 19, 4225-4252.

Rinasti, A.N., Ibrahim, I.F., Gunasekara, K., Kottatep, T., Winijkul, E., 2022. Fate identification and management strategies of non-recyclable plastic waste through the integration of material flow analysis and leakage hotspot modeling. Nat. Sci. Rep. 12, 16298.

Rochman, C.M., 2018. Microplastics research — From source to sink in freshwater systems. Science, 360(6384), 28-29.

Rochman, C.M., Brookson, C., Bikker, J., Djuric, N., Earn, A., Bucci, K., Athey, S., Huntington, A., McIlwraith, H., Munno, K., De Frond, H., Kolomijeca, A., Erdle, L., Grbic, J., Bayoumi, M., Borrelle, S.B., Wu, T., Santoro, S., Werbowski, L.M., Zhu, X., Giles, R.K., Hamilton, B.M., Thaysen, C., Kaura, A., Klasios, N., Ead, L., Kim, J., Sherlock, C., Ho, A., Hung, C., 2019. Rethinking microplastics as a diverse contaminant suite. Environ. Toxicol. Chem. 38(4), 703-711.

Rochman, C.M., Grbic, J., Earn, A., Helm, P.A., Hasenmueller, E.A., Trice, M., Munno, K., De Frond, H., Djuric, N., Santoro, S., Kaura, A., Denton, D., Teh, S., 2022., Local monitoring should inform local solutions: Morphological assemblages of microplastics are similar within a pathway, but relative total concentrations vary regionally. Environ. Sci. Technol. 56, 9367-9378.

Rochman, C.M., Hentschel, B.T., Teh, S.J., 2014. Long-term sorption of metals is similar among plastic types: Implications for plastic debris in aquatic environments. PLOS One 9(1), e85433.

Roden, J., 2018. Determining the physiological and behavioral aspects of salinity tolerance in the Asian clam, *Corbicula fluminea*. Undergraduate Honors Theses, 443.

Rong, Y., Tang, Y., Ren, L., Taylor, W.D., Razlutskij, V., Naselli-Flores, L., Liu, Z., Zhang, X., 2021. Effects of the filter-feeding benthic bivalve *Corbicula fluminea* on plankton community and water quality in aquatic ecosystems: A mesocosm study. Water 13(13), 1827.

Saint Louis County GIS Service Center and St. Louis County Assessor's Office, 2021. Parcels "Parcel Data Jurisdictions". https://www.arcgis.com/apps/webappviewer/index.html?id=4ac4f88eb26543afb04e643b9cba868c. Accessed March 01, 2025.

Sait, S.T.L., Sorensen, L., Kubowicz, S., Vike-Jonas, K., Gonzalez, S.V., Asimakopoulos, A.G., Booth, A.M., 2021. Microplastic fibres from synthetic textiles: Environmental degradation and additive chemical content. Environ. Pollut. 268, 115745.

Sanchez-Vidal, A., Thompson, R.C., Canals, M., de Haan, W.P., 2018. The imprint of microfibres in southern European deep seas. PLoS ONE 13(11), e0207033.

Scherer, C., Weber, A., Stock, F., Vurusic, S., Egerci, H., Kochleus, C., Arendt, N., Foeldi, C., Dierkes, G., Wagner, M., Brennholt, N., Reifferscheid, G., 2020. Comparative assessment of microplastics in water and sediment of a large European river. Sci. Total Environ. 738, 139866.

Scircle, A., Cizdziel, J.V., Tisinger, L., Anumol, T., Robey, D., 2020. Occurrence of microplastic pollution at oyster reefs and other coastal sites in the Mississippi Sound, USA: Impacts of freshwater inflows from flooding. Toxics 8(2), 35.

Seeley, M.E., Lynch, J.M., 2023. Previous successes and untapped potential of pyrolysis–GC/MS for the analysis of plastic pollution. Anal. Bioanal. Chem. 415, 2873-2890.

Sewwandi, M., Kumar, A., Pallewatta, S., Vithanage, M., 2024. Microplastics in urban stormwater sediments and runoff: An essential component in the microplastic cycle. Trends Anal. Chem. 178, 117824.

Shen, M., Zhang, Y., Zhu, Y., Song, B., Zeng, G., Hu, D., Wen, X., Ren, X., 2019. Recent advances in toxicological research of nanoplastics in the environment: A review. Environ. Pollut. 252(A), 511-521.

Shruti, V.C., Kutralam-Muniasamy, G., Perez-Guevara, F., Roy, P.D., Martinez, I.E., 2022. Occurrence and characteristics of atmospheric microplastics in Mexico City. Sci. Total Environ. 847, 157601.

Skalska, K., Ockelford, A., Ebdon, J.E., Cundy, A.B., 2020. Riverine microplastics: Behaviour, spatio-temporal variability, and recommendations for standardised sampling and monitoring. J. Water Process Eng. 38, 101600.

Soler, M., Colomer, J., Pohl, F., Serra, T., 2025. Transport and sedimentation of microplastics by turbidity currents: Dependence on suspended sediment concentration and grain size. Environ. Int. 195, 109271.

Soininen, T., Uurasjärvi, E., Sorvari, J., Saarni, S., Koistinen, A., 2024. Microplastic accumulation in one-year freshwater ice: A four-year monitoring study reveals winter dynamics of microplastics. Sci. Total Environ. 957, 177602.

Sousa, R., Antunes, C., Fuilhermino, L., 2008. Ecology of the invasive Asian clam *Corbicula fluminea* (Müller, 1774) in aquatic ecosystems: an overview. Ann. Limnol.-Int. J. 44 (2), 85-94.

Stankovic, J., Milosevic, D., Paunovic, M., Jovanovic, B., Popovic, N., Tomovic, J., Atanackovic, A., Radulovic, K., Loncarevic, D., Rakovic, M., 2024. Microplastics in the Danube River and its main tributaries—ingestion by freshwater macroinvertebrates. Water 16, 962.

Stanton, T., Johnson, M., Nathanail, P., MacNaughtan, W., Gomes, R., 2019. Freshwater and airborne textile fibre populations are dominated by 'natural', not microplastic, fibres. Sci. Total Environ. 666, 377-389.

Su, L., Xue, Y., Li, L., Yang, D., Kolandhasamy, P., Li, D., Shi, H., 2016. Microplastics in Taihu Lake, China. Env. Pollut., 216, 711-719.

Su, L., Huiwen, C., Kolandhasamy, P., Wu, C., Rochman, C.M., Shi, H., 2018. Using the Asian clam as an indicator of microplastic pollution in freshwater ecosystems. Environ. Pollut. 234, 347-355.

Talbot, R., Chang, H., 2022. Microplastics in freshwater: A global review of factors affecting spatial and temporal variations. Environ. Pollut. 292(B), 118393.

Thompson, R.C., Courtene-Jones, W., Boucher, J., Pahl, S., Raubenheimer, K., Koelmans, A.A., 2024. Twenty years of microplastic pollution research—What have we learned? Science, 386: eadl2746.

Trainic, M., Flores, J.M., Pinkas, I., Pedrotti, M.L., Lombard, F., Bourdin, G., Gorsky, G., Boss, E., Rudich, Y., Vardi, A., Koren, I., 2020. Airborne microplastic particles detected in the remote marine atmosphere. Commun. Earth Environ. 1, 64.

Treilles, R., Gasperi, J., Tramoy, R., Dris, R., Gallard, A., Partibane, C., Tassin, B., 2022. Microplastic and microfiber fluxes in the Seine River: Flood events versus dry periods. Sci. Total Environ. 805, 150123.

Truong, T., Strady, E., Kieu-Le, T., Tran, Q., Le, T., Thuong, Q., 2021. Microplastic in atmospheric fallouts of a developing Southeast Asian megacity under tropical climate. Chemosphere 272, 129874.

Turner, A., 2021. Paint particles in the marine environment: An overlooked component of microplastics. Water Res. X. 12, 100110.

United Nations (UN), 2014. World urbanization prospects. Cities, 13-16.

United Nations (UN), Department of Econnomic and Social Affairs, Population Division, 2018. World Urbanisation Prospects 2018. Urban Agglomerations File 12: Population of urban agglomerations with 300,000 inhabitants or more in 2018, by country, 1950-2035 (thousands). https://population.un.org/wup/downloads. Accessed March 01, 2025.

United States of America National Agriculture Imagery Program (USA NAIP), 2024. USA NAIP Imagery: NDVI. USDA Farm Services Agency. https://naip.arcgis.com/arcgis/rest/services/NAIP/ImageServer. Accessed March 04, 2025.

United States Census, 2020. https://www.census.gov/quickfacts/. Accessed December 01, 2024.

United States Environmental Protection Agency (US EPA), 2024. Air Quality System Data Mart. https://www.epa.gov/outdoor-air-quality-data. Accessed December 01, 2024.

United States Geological Survey (USGS), 2017. USGS_OPR_MO_Saint_Louis_Lidar_2017_B17_7283_4277.tif and USGS_OPR_MO_Saint_Louis_Lidar_2017_B17_7403_4278.tif. Missouri Spatial Data Information Service (MSDIS). https://data-msdis.opendata.arcgis.com/pages/lidar. Accessed March 04, 2025

United States Geological Survey (USGS), 2025. National Water Information System data available on the World Wide Web "USGS water data for the nation". https://waterdata.usgs.gov/. Accessed February 19, 2025.

Van Daele, M., Van Bastelaere, B., De Clercq, J., Meyer, I., Vercauteren, M., Asselman, J., 2024. Mud and organic content are strongly correlated with microplastic contamination in a meandering riverbed. Commun. Earth Environ. 5, 453.

Van Emmerik, T., Mellink, Y., Hauk, R., Waldschlager, K., Schreyers, L., 2022. Rivers as plastic reservoirs. Front. Water 3, 786936.

Veerasingan, S., Mugilarasan, M., Venkatachalapathy, R., Vethamony, P., 2016. Influence of 2015 flood on the distribution and occurrence of microplastic pellets along the Chennai coast, India. Mar. Poll. Bull. 109(1), 196-204.

Vidal, A., Phuong, N., Metais, I., Gasperi, J., Chatel, A., 2023. Assessment of microplastic contamination in the Loire River (France) throughout analysis of different biotic and abiotic freshwater matrices. Environ. Pollut. 334, 122167.

Waldschläger, K., Schüttrumpf, H., 2019. Effects of particle properties on the settling and rise velocities of microplastics in freshwater under laboratory conditions. Environ. Sci. Technol. 53(4), 1958-1966.

Wei, Q., Zhu, G., Wu, P., Cui, L., Zhang, K., Zhou, J., Zhang, W., 2010. Distributions of typical contaminant species in urban short-term storm runoff and their fates during rain events: A case of Xiamen City. J. Environ. Sci. 22(4), 533-539.

Welsh, B., Aherne, J., Paterson, A.M., Yao, H., McConnell, C., 2022. Atmospheric deposition of anthropogenic particles and microplastics in south-central Ontario, Canada. Sci. Total Environ. 835, 155426.

Wesch, C., Bredimus, K., Paulus, M., Klein, R., 2016. Towards the suitable monitoring of ingestion of microplastics by marine biota: A review. Environ. Pollut. 218, 1200-1208.

Winijkul, E., Latt, K.Z., Limsiriwong, K., Pussayanavin, T., Prapaspongsa, T., 2024. Depositions of airborne microplastics during the wet and dry seasons in Pathum Thani, Thailand. Atmos. Pollut. Res. 15, 102242.

Wright, S.L., Ulke, J., Font, A., Chan, K.L.A., Kelly, F.J., 2020. Atmospheric microplastic deposition in an urban environment and an evaluation of transport. Environ. Int. 136, 105411.

Wu, P., Tang, Y., Dang, M., Wang, S., Jin, H., Liu, Y., Jing, H., Zheng, C., Yi, S., Cai, Z., 2019. Spatial-temporal distribution of microplastics in surface water and sediments of Maozhou River within Guangdong-Hong Kong-Macao Greater Bay Area. Sci. Total Environ. 717, 135187.

Wu, Y., Yang, J., Li, Z., He, H., Wang, Y., Wu, H., Xie, L., Chen, D., Wang, L., 2022. How does bivalve size influence microplastics accumulation? Environ. Res. 113847.

Yao, Y., Glamoclija, M., Murphy, A., Gao, Y., 2022. Characterization of microplastics in indoor and ambient air in northern New Jersey. Environ. Res. 207, 112142.

Yuan, Y., Li, S., Chen, T., Ren, J., 2023. Effects of ambient temperature and humidity on natural deposition characteristics of airborne biomass particles. Int. J. Environ. Res. Public Health 20(3), 1890.

Zhang, Y., Pu, S., Lv, X., Gao, Y., Ge, L., 2020. Global trends and prospects in microplastics research: A bibliometric analysis. J. Hazard. Mater. 400, 123110.

Zhou, Q., Tian, C., Luo, Y., 2017. Various forms and deposition fluxes of microplastics identified in the coastal urban atmosphere. Sci. Bull. 62(33), 3902-3909.

Zhou, Y., Li, Y., Yan, Z., Wang, H., Chen, H., Zhao, S., Zhong, N., Cheng, Y., Acharya, K., 2023. Microplastics discharged from urban drainage system: Prominent contribution of sewer overflow pollution. Water Res. 236, 119976.

VITA AUCTORIS

Natalie Faith Hernandez was born in Germantown, Tennessee, and earned a B.S. in Environmental Science from Baylor University in Waco, Texas, in 2019. Natalie is currently a Ph.D. candidate in the Department of Earth, Environmental, and Geospatial Science at Saint Louis University (formerly the Department of Earth and Atmospheric Sciences). Natalie anticipates earning a Ph.D. in Geoscience with a concentration in Environmental Geoscience in May 2025, and plans to continue their research career as a Postdoctoral Researcher at the Saint Louis University WATER Institute after Ph.D. completion.